Tandem Transesterification in Polymer Synthesis:

Gradient and Pinpoint-Functionalized Polymers

Yusuke Ogura

2017

CONTENTS

GENERAL INTRODUCTION 1

PART I Concurrent Tandem Catalysis with Monomer-Selective Transesterification for Functional Gradient Copolymers

Chapter 1 Hard/Soft MMA/DMA Gradient Copolymers: Gradient Sequence Control via Tandem Transesterification and Extremely Broad Glass Transition Temperature 27

Chapter 2 Amphiphilic PEG-Functionalized Gradient Copolymers: From Modular Synthesis to Sequence-Dependent Self-Assembly and Thermoresponsive Properties 41

Chapter 3 Hydrogen-Bonding Gradient Copolymers: Effects of Supramolecular Unit Sequence on Single-Chain Folding and Self-Assembly 65

Chapter 4 Fluorinated Gradient Copolymers: Tandem Transesterification with Fluoroalcohols 83

Chapter 5 Fluorous, Perfluorinated Gradient Copolymers: Tandem Transesterification with a Perfluorinated Methacrylate and Physical Properties 103

PART II Sequential/Iterative Tandem Catalysis and Functionalization with Terminal and Acrylate-Selective Transesterification for Telechelic or Pinpoint-Functionalized Polymers

Chapter 6 Telechelic and Pinpoint-Functionalized Polymers via Terminal-Selective Transesterifcation of Chlorine-Capped Poly(methyl methacrylate)s 123

Chapter 7 Telechelic Polymers from Bromine-Capped Poly(methyl methacrylate)s via Terminal-Selective Transesterification and Cyclization 141

Chapter 8 Post-Functionalization of Methacrylate/Acrylate Copolymers via Acrylate-Selective Transesterification: A New Avenue in Polymer Reactions 157

LIST OF PUBLICATIONS 169

ACKNOWLEDGMENTS 173

GENERAL INTRODUCTION

Background

1. Organic Chemistry in Polymer Chemistry: the Essence of Design and Synthesis

Organic chemistry is deeply related to polymer chemistry: organic reactions and catalysis are the "essence" to design and synthesize organic polymers and macromolecules. In general, synthetic organic polymers [e.g., poly(methyl methacrylate), polyester], as well as natural biopolymers, consist of monomer units that are consecutively connected through covalent bonds. The characteristics of polymers thus depend on the primary structure (e.g., molecular weight, terminal, stereoregularity, repeat-unit sequence), monomer units and functional groups, and three-dimensional architectures (e.g., random coil, branched, cyclic, globular, and rod-like). These factors are programmed into polymers as information to express the inherent properties and functions. Thus, a goal in synthetic polymer chemistry is directed toward the precision control of primary and three-dimensional structures via selective and site-specific functionalization.

In polymer synthesis, organic reactions assume important roles in "molecular design", "polymerization", and "functionalization": (1) design and functionalization of monomers, initiators, and terminators; (2) polymerization of monomers into polymers; (3) post-functionalization of polymers (Figure 1).

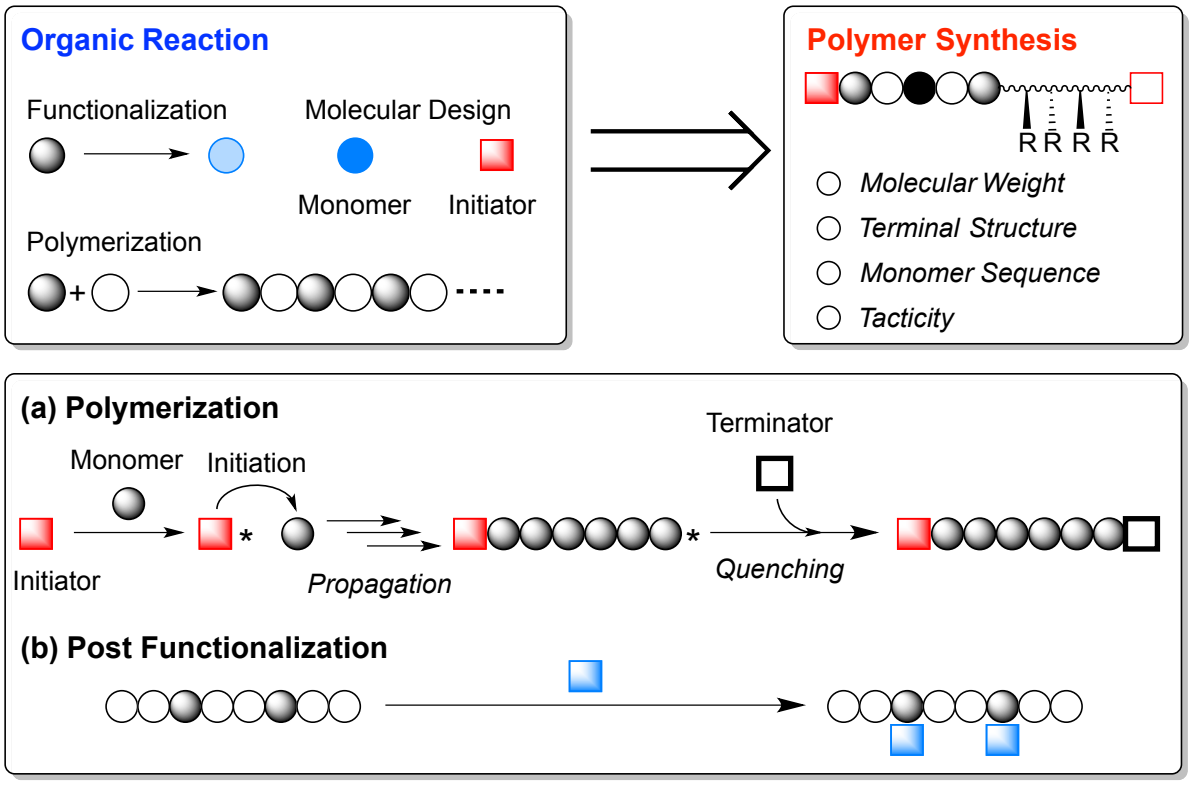

Figure 1. Organic reactions for polymer synthesis.

Various precision polymerization systems including living and/or stereospecific polymerizations have recently been developed, to allow fine control of the primary structure of polymers: e.g., molecular weight, composition, terminal structure, and stereoregularity.[1-4] Herein, the prerequisite is selective and efficient organic reactions to connect monomers into high molecular weight polymers. In chain polymerization, for instance, monomers repeatedly react with a growing active species over several hundred or thousand times virtually without failure. Monomers, initiators, and terminators turn to be structural elements of polymers. The molecular design thus affects the physical properties of resulting polymers.

Post-functionalization of polymers is useful in both laboratory scale and industrial production to convert polymeric precursors into desired functional polymers.[5-7] This is particularly effective to introduce functional groups that potentially interfere polymerization and often deactivate the growing species. In another aspect, post-functionalization is intriguing as a modular synthetic approach to various functional polymers from an identical precursor. Since polymer pendants are sterically hindered by the neighboring monomer units and condensed environments, the modification of polymers are generally less efficient than that of the corresponding monomers. Thus, harsh reactions and conditions have been often employed for efficient conversion but in turn led to less site-selective transformation. To overcome these issues, efficient post-functionalization systems have been developed, via selective organic reactions such as click reactions (azide-alkyne, thiol-ene, etc.)[8-10] or with selectively convertible units like activated esters (pentafluoro phenyl units and alcohols, *N*-hydroxysuccinimide esters and amines, etc.).[11]

Though precision polymerization and post-functionalization systems have been developed, monomer-sequence control and site-selective functionalization of polymers are still difficult and remaining issues in polymer chemistry. For these, synergetic combination of selective organic reactions with precision polymerizations would open a new avenue.

2. Tandem Catalysis of Precision Polymerizations and Organic Reactions

Tandem catalysis is one-pot synthetic methodology where two or several different reactions are sequentially or concurrently conducted in single vessels (Figure 2).[12,13] Such a tandem system directly gives final products from starting materials through multiple catalysis, more efficiently and conveniently than a convensional multistep synthesis involving isolation and purification of the intermediates. Thus, the tandem catalysis combined with precision polymerization and selective organic reactions would be promising as an efficient and versatile approach to functional polymers with precision primary structure.

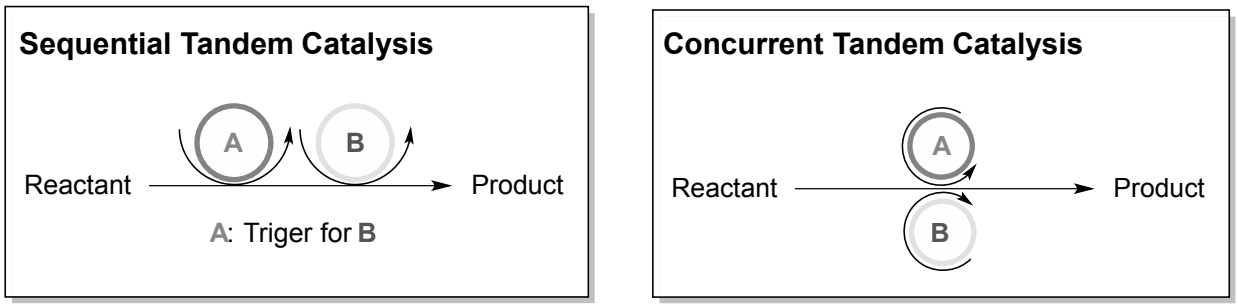

Figure 2. Sequential or concurrent tandem catalysis.

Tandem catalysis and tandem reactions include some variants. In sequential tandem catalysis, for example, multiple reactions "sequentially" take place, typically via the direct addition of chemical reagents for next reactions into the reaction mixtures.[14] One-pot cascade or domino reactions, which automatically induce multistep reactions, are also developed as efficient synthetic systems in organic synthesis. In concurrent tandem catalysis, several different reactions proceed "simultaneously" in single vessels to directly give final products.[15] Importantly, the concurrent system requires high compatibility of the active species and intermediates of the different catalytic cycles; if one catalysis deactivates another, concurrent tandem catalysis is impossible.

Various tandem catalytic systems have been developed for organic reactions, polymerization, and polymer synthesis.[16] In tandem polymerizations coupled with organic reactions, living and/or controlled polymerization is often utilized to regulate primary structure (e.g., uniform chain length and terminal structure), while selective organic reactions like hydrogenation, nucleophilic attack, click reaction and transesterification are employed as site-selective functionalization techniques of polymers.[17] By sequentially or concurrently conducting these different catalyses in one-pot, tandem polymerization affords modular design and high throughput synthesis of functional polymers with multiple-controlled primary structures (Figure 3). This is more efficient than multistep procedures combining precision polymerization and post-functionalization.

(1) Sequential Tandem Polymerization with Functionalization

The sequential tandem polymerization is useful for the one-pot synthesis of block, star, or end-functionalized (co)polymers. Living polymerizations are often used as precision polymerization systems. In living anionic polymerization, for instance, a pair of monomers [e.g. *n*-butyl acrylate and methyl methacrylate] with highly different reactivity undergo domino-type block copolymerization to give block copolymers.[18] Star polymers can also be obtained by a sequential tandem polymerization of monomers for arms, followed by the crosslinking of the arms with a divinyl monomer.[19] The sequential catalysis of different polymerizations with a single initiator (e.g. ROMP and ATRP) is also effective to produce block copolymers that cannot be obtained by a sequential polymerization of a single mechanism.[20]

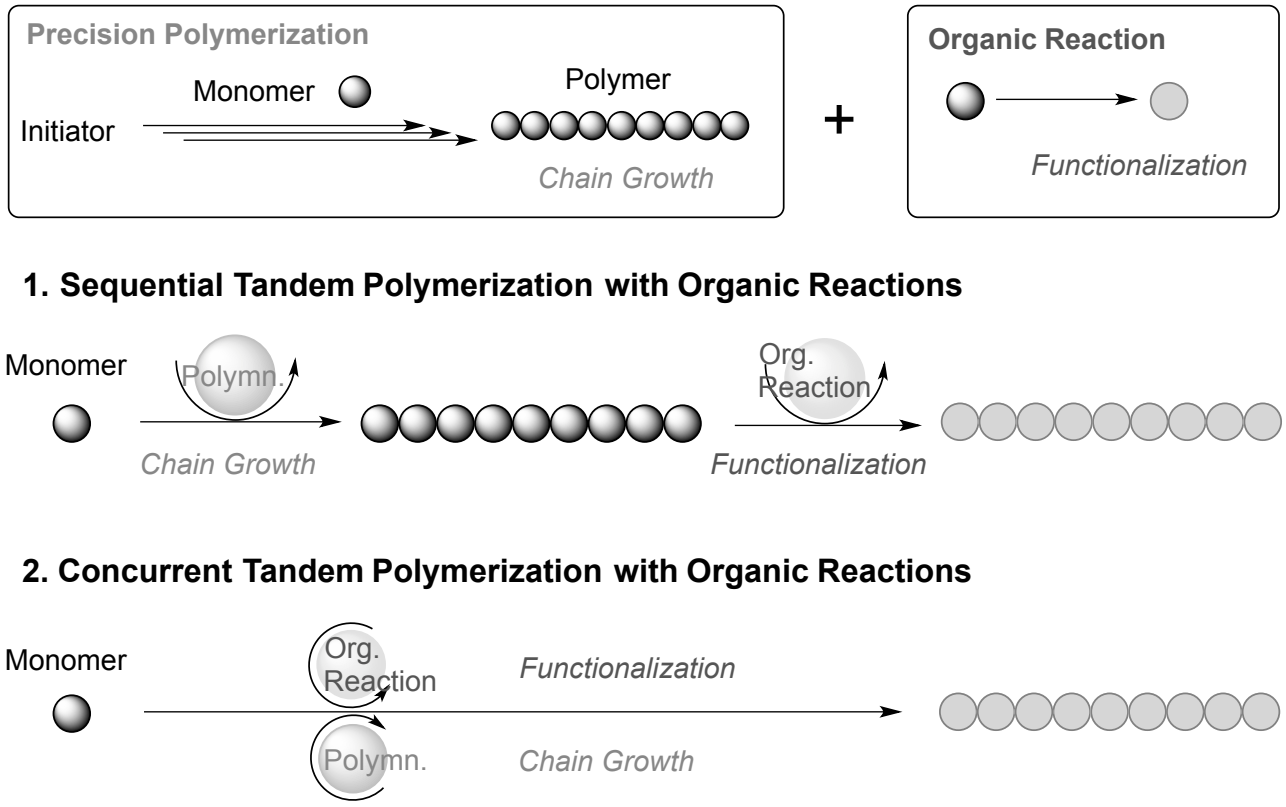

Figure 3. Tandem catalysis of precision polymerization and selective organic reactions for well-controlled functional polymers.

Terminal-selective hydrogenation of a chlorine-capped poly(methyl methacrylate) (PMMA-Cl) into a hydrogen capped version (PMMA-H) is achieved via the sequential tandem catalysis of ruthenium [$RuCl_2(PPh_3)_3$]-catalyzed LRP of MMA with a chloride initiator and the in-situ hydrogenation of the chlorine terminal of the resulting PMMA-Cl.[21] The ruthenium complex plays a dual role of polymerization catalyst and hydrogenation counterpart, where the ruthenium chloride for polymerization is subsequently transformed into a ruthenium hydride [$RuH_2(PPh_3)_3$] via the direct addition of 2-propanol and K_2CO_3. Perrier et al. reported the sequential catalysis of RAFT (reversible addition-fragmentation chain-transfer) polymerization and Curtius rearrangement for poly(methyl acrylate), polystyrene and poly(acryl amide) with alkyne group at their terminals.[22] An iterative process of different catalytic systems is also effective to create novel chiral polymers: Meijer et al. reported the synthesis of enantio-pure chiral polyesters via the iterative tandem catalysis of lipase-catalyzed ring-opening polymerization (ROP) and Ru-catalyzed racemization of the polymer terminals.[23]

(2) Concurrent Tandem Polymerization with Functionalization

Concurrent tandem polymerization with organic reactions is employed for the synthesis of unique block copolymers. For example, a concurrent tandem catalysis of LRP of MMA and ring-opening metathesis polymerization (ROMP) of cyclooctadiene (COD) was achieved with a designed ruthenium catalyst, to give unique block copolymers comprising PMMA and PCOD segments.[24] A ruthenium complex further catalyzes hydrogenation of the internal olefin of the block copolymers.

Concurrent tandem catalysis is further effective for the in-situ functionalization and transformation of monomers via organic reactions. Cu-catalyzed LRP (ATRP) of propargyl methacrylate is compatible with Cu-mediated click reaction of the alkyne units and azide compounds.[25] The simultaneous catalysis of the two reactions successfully provides various pendant-functionalized polymers. In author's group, concurrent tandem catalysis of LRP and in-situ transesterification of methacrylates with alcohols was developed as a versatile synthetic strategy of methacrylate-based gradient copolymers.[26] This system affords the catalytic control of gradient sequence by tuning the kinetic balance of polymerization for chain growth and monomer-selective transesterification for gradient composition. The details are described later.

3. Transesterification in Polymer Chemistry

Transesterification is an efficient and simple reaction to produce ester compounds (R^1COOR^3) with other ester compounds (R^1COOR^2) and alcohols (R^3OH). The diversity of final products is one of the most attractive features of transesterification; i.e., various esters and alcohols can be utilized and combined to virtually allow the design and synthesis of unlimited kinds of ester compounds. Thus, transesterification has been actually employed as a synthetic tool for not only ester compounds but also ester-based polymers in laboratory and industry. Transesterification plays an important role in polymer chemistry (Figure 4).

For example, derivatives of methacrylates and acrylates are industrially produced by transesterification with alcohols. Transesterification also functions as a key reaction in step-growth polymerization or ring-opening polymerization for polyesters. Poly(ethylene terephthalate) (PET) is manufactured via the transesterification of dimethyl terephthalate with ethylene glycol. Needless to say, it is used as materials for bottles and indispensable in daily life. Other common and commercial polymers including polycarbonate, polylactide and polycaprolactone are also similarly obtained via transesterification.

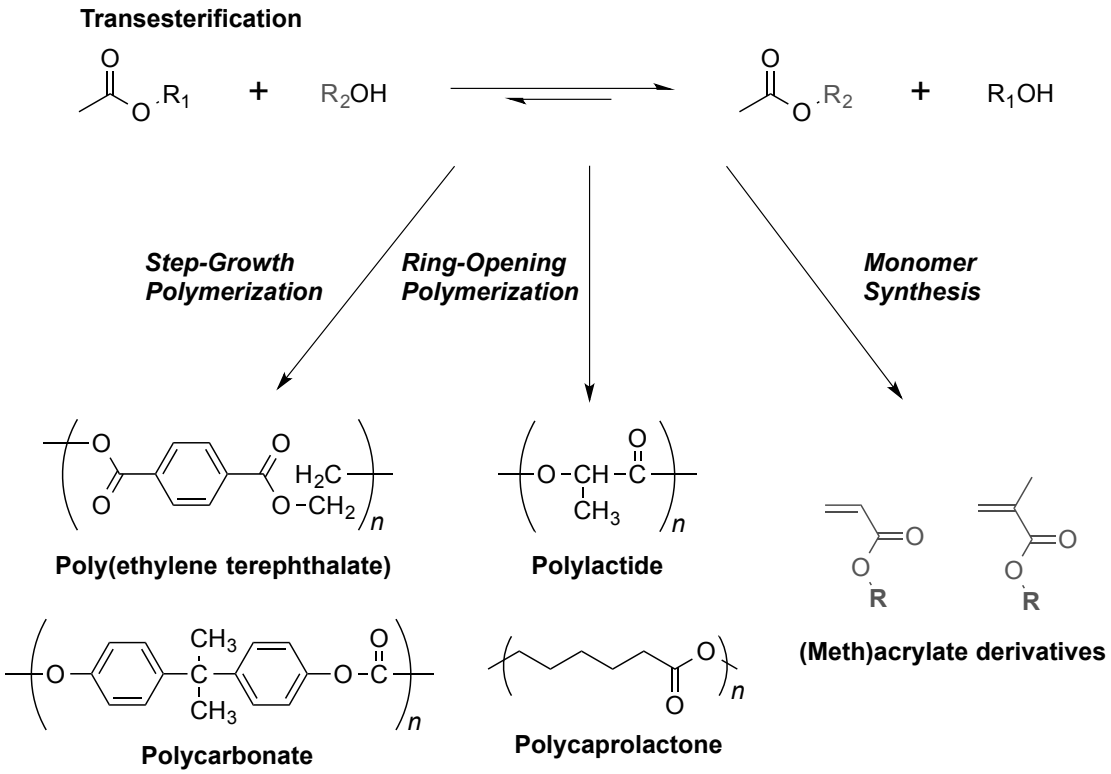

Figure 4. Transesterification in polymer chemistry.

Transesterification is catalyzed by strong acids (e.g., sulfuric acid), strong or organic bases (e.g., DMAP), Lewis acids and metal alkoxides (e.g., Zn, Al, Ti, La, Yb, La) and enzyme (e.g., lipase).[27-32] Various Lewis acids and metal alkoxides are developed for efficient and selective transesterification with alcohols under mild conditions. Because transesterification is an equilibrium reaction, the removal of volatile alcohols generating from starting esters is critical to promote the reaction. The reactivity of esters and/or alcohols are highly dependent on the steric hindrance and electronic factors.[33] In metal-mediated transesterification, the activity depends on alcohols and decreases in this order: primary > secondary > tertiary alcohols (e.g., *tert*-butanol). Transesterification is compatible with the other chemical reactions such as living radical polymerization. Due to high selectivity and compatibility, transesterification is applicable to tandem catalysis and polymerization to create functional polymeric materials.[26,34,35]

4. Living Radical Polymerization for Functional Polymers

Radical polymerization is widely used in industry to produce various polymeric materials such as rubber, resin, plastics, fibers and films. Advantages of radical polymerization are wide applicability of diverse monomers, high yield synthesis, and tolerance to polar functional groups and solvents (e.g., water and alcohols). In 1990s, the concept of dormant/active equilibrium is introduced into radical polymerization to accomplish living radical polymerization (LRP).[36,37]

Various LRP systems via different mechanisms have been developed so far: nitroxide-mediated polymerization (NMP), metal-catalyzed LRP (atom transfer radical polymerization: ATRP), reversible addition-fragmentation chain-transfer (RAFT) polymerization, tellurium-mediated radical polymerization (TERP), and organometallic mediated radical polymerization (OMRP).[38-41]

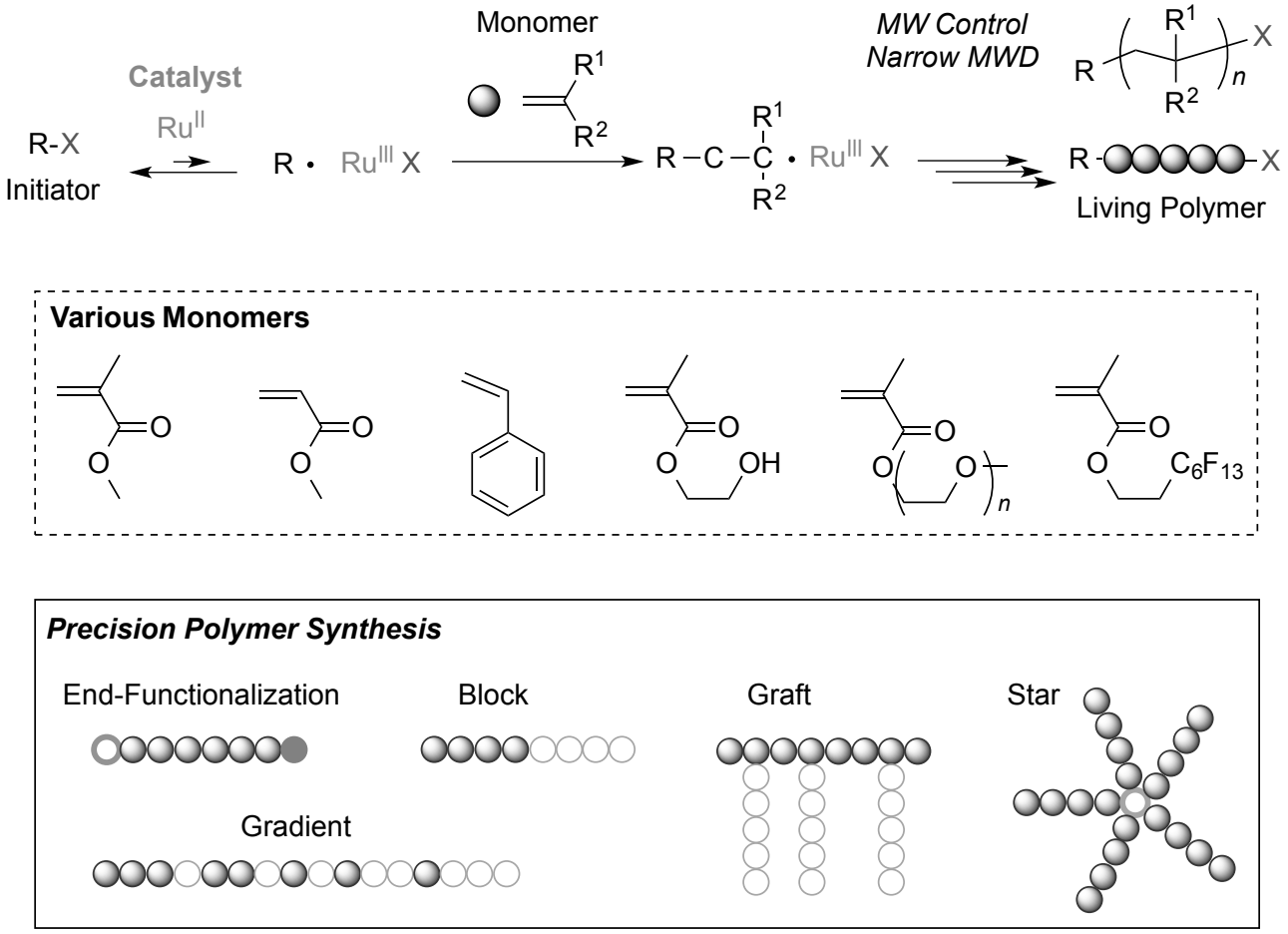

Figure 5. Ru-catalyzed living radical polymerization for functional polymers.

Among them, ruthenium-catalyzed LRP is effective to design methacrylate-based functional polymers (Figure 5).[42] Thanks to the high functionality tolerance, ruthenium catalysts efficiently catalyze LRP in alcohols and water.[43,44] In ruthenium-catalyzed LRP, the selection of cocatalysts (amines, aminoalcohols, and metal alkoxides) are also important to achieve high controllability; for example, aluminum or titanium alkoxides [Ti(O*i*-Pr)$_4$, Al(O*i*-Pr)$_3$] are typically effective for methacrylates.[45] A series of LRP systems now affords the precision control of molecular weight, terminal structure, monomer sequence distribution, and branched structures. In particular, gradient, sequence-controlled, telechelic, and pinpoint-functionalized polymers are intriguing as well-defined functional polymers with unique properties.

(1) Gradient Copolymers

Gradient copolymers are one class of sequence-regulated copolymers where monomer sequence distribution continuously changes from α-end to ω-end along a chain (Figure 6). Owing to the unique sequence distribution, gradient copolymers often show solid and solution properties distinct from corresponding random or block counterparts: *e.g.*, phase segregation behavior, thermal/rheological properties, compatibility, contact angle, micellization, and lower critical solution temperature.[46-50] A/B gradient copolymers have unlimited possibilities of gradient sequence: e.g., gradual and linear composition change from A to B; sudden composition change from A to B at the middle point between two A/B-blocky segments; A/B gradient from α-end to the middle point and A/B random to ω-end (Figure 6). Given these features, functional gradient copolymers are expected to show novel physical properties and functions that cannot be achieved with random and block counterparts.

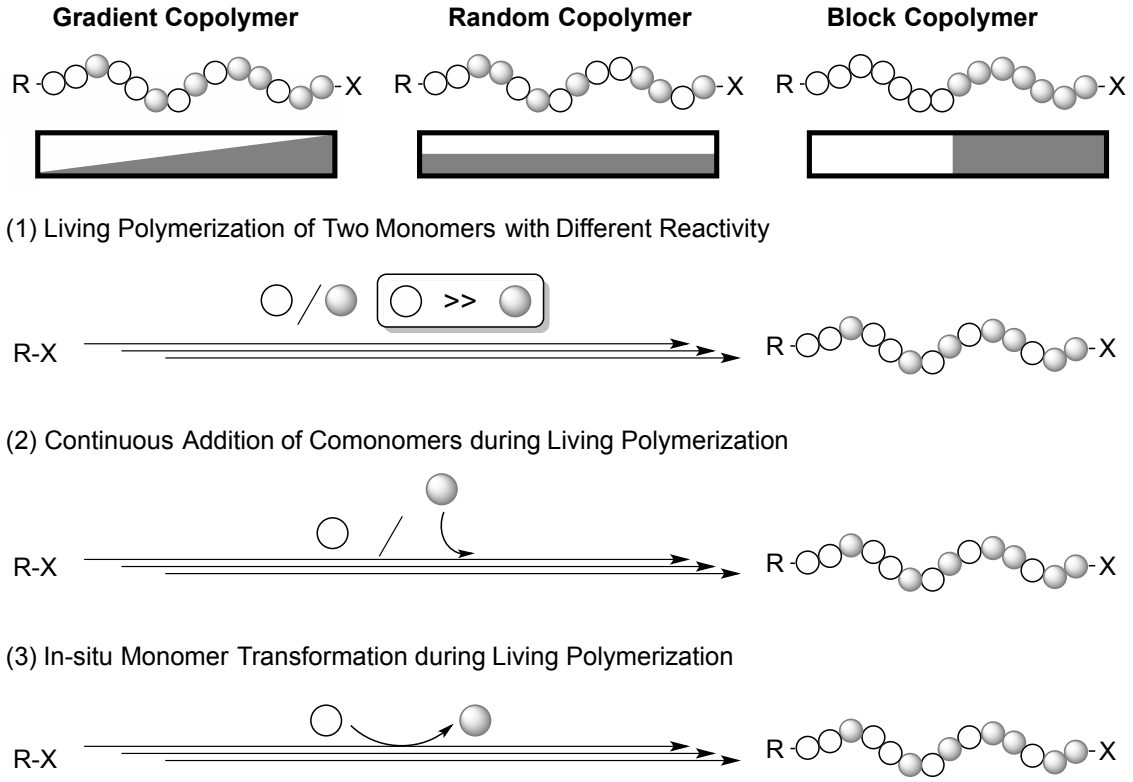

Figure 6. Synthetic strategies and features of gradient copolymers.

A/B gradient copolymers are generally obtained by living polymerization as follows: 1) "spontaneous gradient" via copolymerization of two monomers with different reactivity [A > B, e.g., copolymerization of methacrylate (A) and acrylate (B)], 2) "forced gradient" via continuous addition of a comonomer (B) into living polymerization of a starting monomer (A), and 3) "catalytic gradient" via concurrent tandem LRP with in-situ transformation of a starting monomer (A) to a comonomer (B).[51] The third method was originally developed in the author's group

(Figure 7).[26] Here, a methacrylate comonomer (B: R_2MA) is directly produced via the transesterification of a starting methacrylate (A: R_1MA) with alcohols (R_2OH) during LRP; i.e., monomer composition in polymerization solutions changes concurrently with copolymerization of the resulting two monomers. Thus, the instantaneous composition of monomers in polymerization solutions is reflected to the instantaneous gradient sequence of resulting copolymers. The transesterification of monomers is efficiently catalyzed by metal alkoxides [$Ti(O\textit{i}\text{-}Pr)_4$, $Al(O\textit{i}\text{-}Pr)_3$] that are originally employed as cocatalysts for Ru-catalyzed LRP of methacrylates. Thus, the transesterification does not interfere with Ru-catalyzed LRP. The gradient sequence can be catalytically controlled by tuning the kinetic balance of polymerization and transesterification. By applying various methacrylates and alcohols, the tandem catalytic polymerization would make it possible to design and synthesize functional gradient copolymers for intriguing properties and functions.

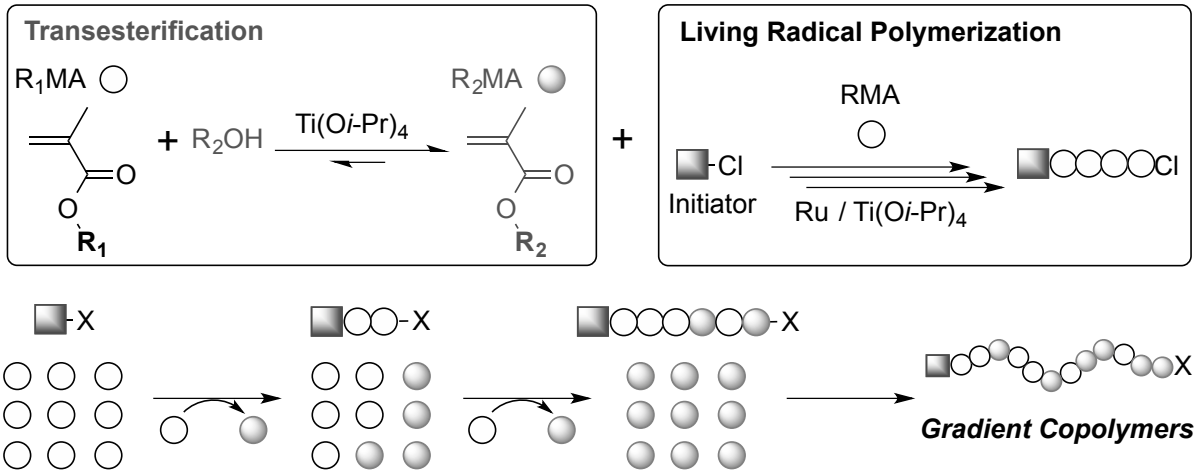

Figure 7. Concurrent tandem catalysis of transesterification and living radical polymerization.

(2) End-Functionalized and Telechelic Polymers

End-functionalized and telechelic polymers are important functional materials for wide variety of applications. α-End-functionalized polymers are efficiently synthesized by LRP with functional initiators (Figure 8a). Telechelic polymers bearing α,ω-end-functional groups are prepared by LRP with mono- or bi-functional initiators, followed by the subsequent transformation of the ω-end halogen terminal (Figure 8b). The ω-end halogen of polystyrenes, polymethacrylates, and polyacrylates obtained from LRP can be transformed into various groups including hydrogen, amine, hydroxyl groups. Typically, a chlorine-capped α-methoxystyrene terminal reacts with alcohols by nucleophilic attack[52]. Telechelic polymers can be utilized as precursors for di- or triblock copolymers and cyclic polymers.[53-56] Acrylic diene metathesis polymerization (ADMET) of telechelic oligomers also affords sequence-controlled polymers with repetitive monomer sequence.[57]

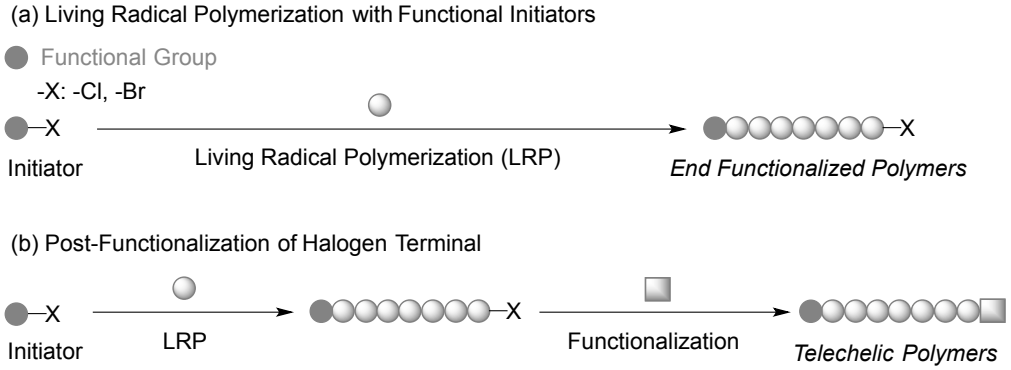

Figure 8. Synthetic routes for Terminal Functionalization.

(3) Pinpoint-Functionalized and Sequence-Controlled Polymers

Monomer-sequence control of synthetic polymers is one of the most challenging issues in polymer chemistry, while the technique is essential in order to create polymeric materials with sequence-dependent functions like natural biopolymers such as proteins and enzymes. For sequence-controlled polymers, several synthetic strategies and concepts have been developed so far: 1) alternating living copolymerization of two monomers (e.g., styrene and maleimide derivatives);[58] 2) living radical cyclopolymerization of multi-functional template monomers with programmed sequence (Figure 9a);[59] 3) polyaddition of sequence-regulated oligomers;[60] 4) periodical sequence control by the direct addition of small amount of maleimide derivatives into LRP of styrene derivatives;[61] and 5) iterative addition (or reactions) of single monomers (Figure 9b).[62] Selective pinpoint-functionalization of desired sites of polymers are effective for periodically sequence-controlled polymers.

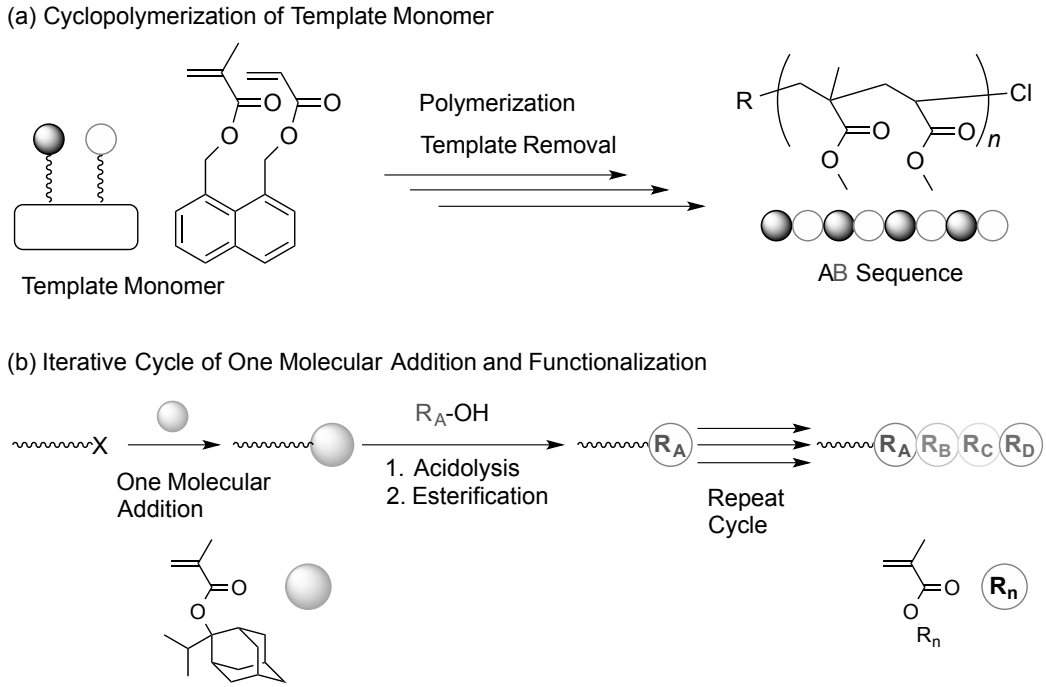

Figure 9. Typical strategies for the synthesis of sequence-controlled polymers.

Objectives in This Study

Given these backgrounds, the author aimed to create novel efficient approaches to well-controlled functional polymers via metal-catalyzed living radical polymerization (LRP) coupled with metal alkoxide-mediated transesterification. Owing to high versatility and functionality tolerance, metal-catalyzed LRP is applicable to various methacrylates and alcohols as monomers and solvents, respectively. Importantly, metal alkoxides [$Ti(O\textit{i}\text{-}Pr)_4$, $Al(O\textit{i}\text{-}Pr)_3$] not only serve as cocatalysts for the LRP but also work as catalysts for transesterification. Radical active species of polymers generating from LRP should never interfere the active intermediates formed in transesterification; thereby, metal alkoxide-mediated transesterification can be compatible with LRP. Transesterification further exhibits highly selective reactivity to ester compounds, dependent on the steric hindrance and electronic factors around the carbonyl groups.

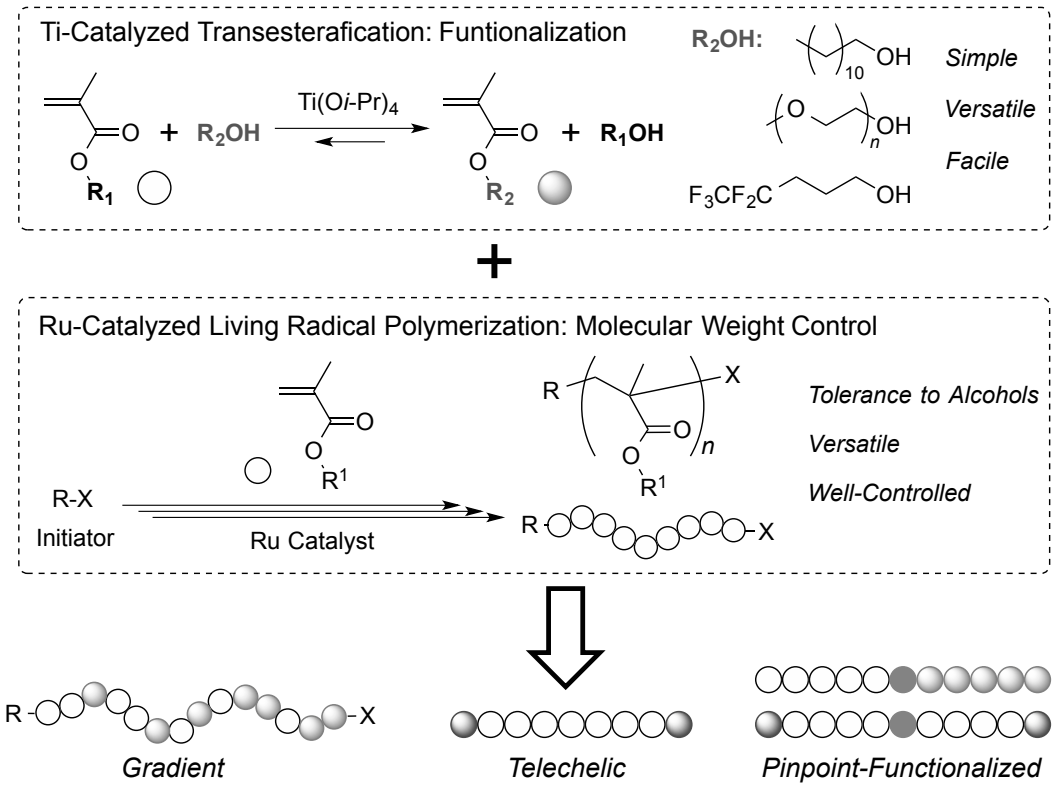

Figure 10. Tandem catalysis of transesterification and LRP for gradient sequence control and site-selective functionalization.

Thus, transesterification was concurrently or sequentially combined with LRP to prepare functional gradient, telechelic, pinpoint-functionalized, and related sequence-controlled (co)polymers (Figure 10). Site-specific modification of ester units is particularly important for the efficient and selective synthesis of their functional polymers. Objectives in this thesis were focused on the following aspects.

1. Development of novel synthetic systems with site-selective transesterification and LRP
2. Precision synthesis of functional polymers with well-defined primary structure: functional gradient, telechelic, pinpoint-functionalized, and sequence-controlled (co)polymers
3. Evaluation of the physical properties of their functional polymers

For this, this doctoral thesis consists of the two parts:

1. ***Concurrent Monomer-Selective Transesterification with LRP for Functional Gradient Copolymers***
2. ***Terminal and Acrylate-Selective Transesterification with LRP for Telechelic, Pinpoint-Functionalized, and Sequence-Controlled Polymers***

1. Concurrent Monomer-Selective Transesterification with LRP for Functional Gradient Copolymers

The first part in this thesis is to synthesize functional gradient and sequence-regulated copolymers via tandem catalysis where transesterification of monomers simultaneously proceeds during LRP.

For this, various methacrylates (methyl methacrylate: MMA, 2-ethylhexyl methacrylate: EHMA, *1H*,*1H*,*2H*,*2H*-perfluorooctyl methacrylate: 13FOMA) and alcohols [e.g., 1-dodecanol; hydrophobic, poly(ethylene glycol) methyl ether: PEG-OH; hydrophilic and thermoresponsive, fluoroalcohols, and a 1,3,5-tricarboxamide (BTA)-bearing alcohol; hydrogen bonding] were employed as starting monomers and solvents, respectively. $Ti(O\textit{i}\text{-}Pr)_4$ efficiently catalyzed concurrent transesterification of the methacrylates with the alcohols (ROH) to in-situ form second functional monomers. Molecular sieves 4A (MS 4A) efficiently promotes the transesterification of MMA into corresponding methacrylates (RMA) up to high yield by suppressing the reverse reaction via the removal of methanol generating therefrom. The diverse combination of methacrylates and alcohols allowed to produce various functional gradient copolymers: hard/soft MMA/dodecyl methacrylate (DMA) gradient, amphiphilic MMA/poly(ethylene glycol) methyl ether methacrylate (PEGMA) gradient, fluorinated and/or fluorous gradient, and hydrogen-bonding EHMA/BTA-functionalized methacrylate (BTAMA) gradient (Scheme 1). The gradient sequence was catalytically controlled by the Ti catalyst concentration and/or the amount of MS 4A.

Gradient sequence distribution of monomers with opposite and/or distinct nature is expected to provide novel and intriguing functions. The physical properties of functional gradient copolymers obtained herein were thus evaluated by differential scanning calorimetry (DSC), dynamic light scattering (DLS), ultraviolet visible absorption spectroscopy (UV-vis). A series of gradient copolymers actually showed solid and solution properties distinct from corresponding

random or block copolymers. The effects of sequence distribution (gradient, random, block) on their properties were discussed in detail.

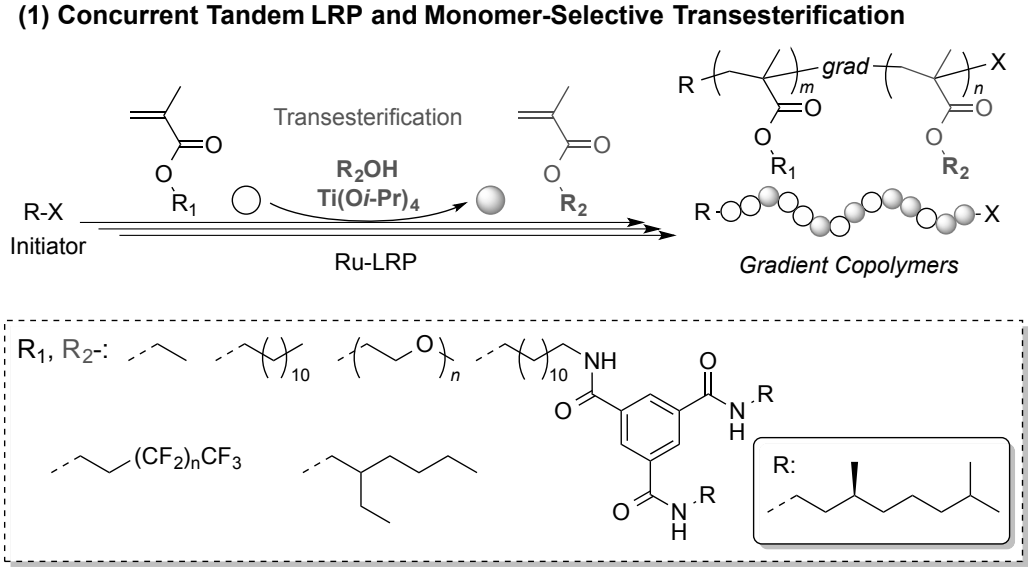

Scheme 1. Concurrent Tandem Catalysis of LRP and Monomer-Selective Transesterification for Functional Gradient Copolymers

2. *Terminal and Acrylate-Selective Transesterification with LRP for Telechelic, Pinpoint-Functionalized, and Sequence-Controlled Polymers*

The second part of this thesis is directed to the site-selective functionalization of polymers via terminal or acrylate-selective transesterification for telechelic, pinpoint-functionalized, and sequence-controlled polymers.

Finding of selective transesterification in the previous Part I encouraged the author to utilize the reaction for selective post-functionalization of halogen-capped poly(methyl methacrylate)s (PMMA-X) and the related copolymers (Scheme 2). A chlorine-capped PMMA (PMMA-Cl) has α- and ω-end esters that are less sterically hindered and/or more activated with an electron-withdrawing chlorine terminal than the other pendant esters (Scheme 2a). The inherent environment of the both terminals allowed terminal-selective transesterification with Ti(O*i*-Pr)$_4$ and alcohols (ROH), providing various chlorine-capped telechelic PMMAs (R-PMMA-RMA-Cl). It should be noted that the telechelic polymers still carry a chlorine terminal and thereby work as a macroinitiator for LRP. Thus, iterative cycles of LRP with the telechelic polymer as a macroinitiator and terminal-selective transesterification gave pinpoint-functionalized polymers and joint-functionalized block copolymers, into which single monomer units were periodically or site-specifically introduced. In contrast, Ti-mediated transesterification of bromine-capped PMMAs (PMMA-Br) with alcohols led to halogen free telechelic polymers (Scheme 2b).

(2) Post-Functionalization with Terminal or Acrylate Selective Transesterification

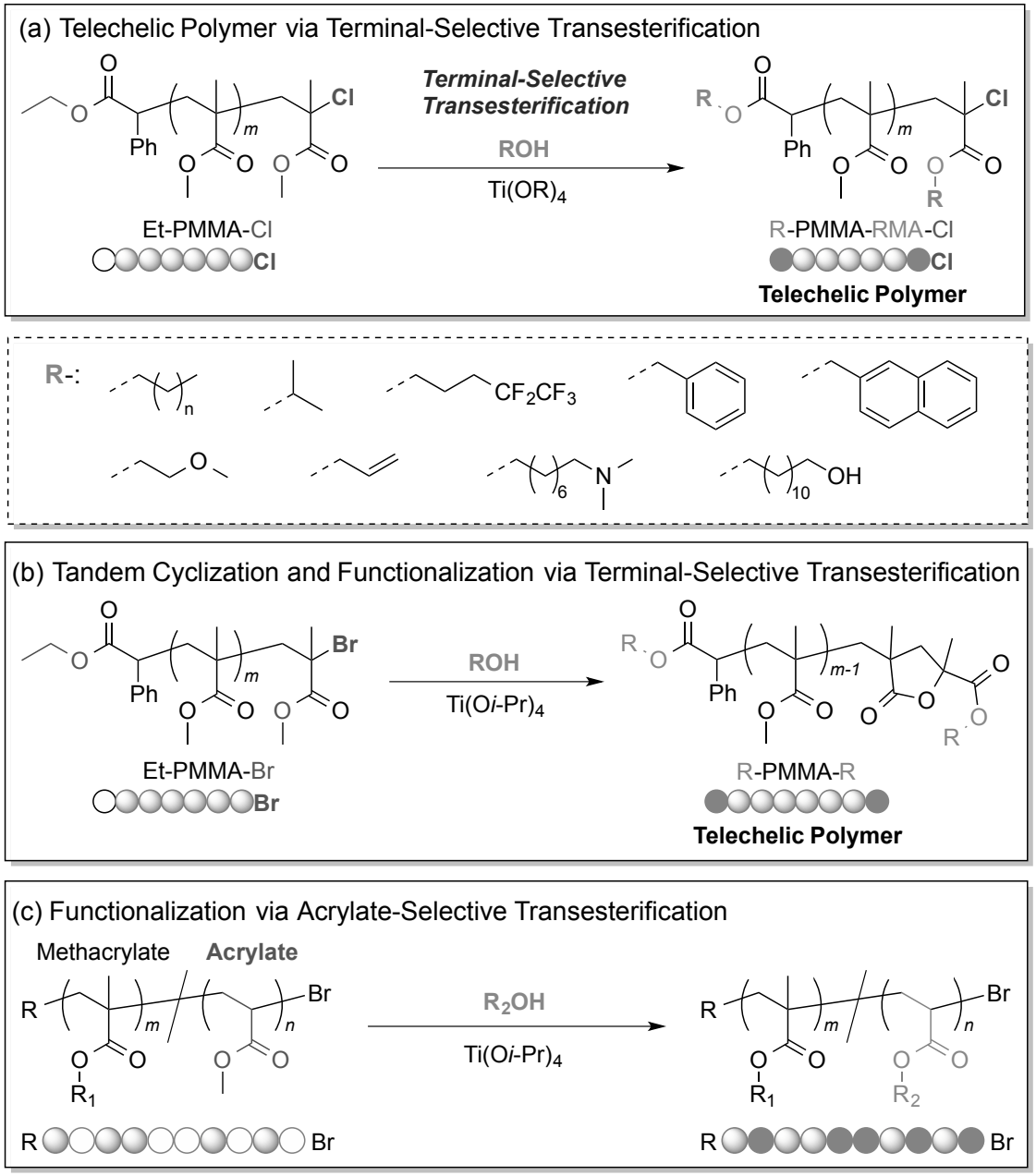

Scheme 2. Terminal or Acrylate-Selective Transesterification for Telechelic and Pinpoint-Functionalized Polymers

Finally, transesterification of methacrylate and methyl acrylate (RMA/MA) random copolymers was also investigated with Ti(O*i*-Pr)$_4$ and alcohols (R'OH) (Scheme 2c). Owing to the less steric hindrance, the methyl acrylate (MA) units were selectively transesterified into corresponding acrylate counterparts (R'A) to give RMA/R'A random copolymers. Importantly, MA, a common monomer, can serve as a selective transformation segment for efficient post-functionalization via transesterification without using activated esters.

Outline of This Study

This thesis consists of two parts including 8 chapters:

Part I (Chapters 1 – 5) deals with the synthesis and characterization of functional gradient copolymers via concurrent tandem catalysis of LRP and transesterification. The polymer design is focused on the precision and on-demand control of the gradient sequence by tuning the kinetic balance of the two reactions and gradient functionalization with various methacrylates and alcohols (*e.g.*, hydrophobic, hydrophilic, fluorous, and hydrogen-bonding). Solid and solution properties of gradient copolymers were also evaluated by differential scanning calorimetry (DSC), dynamic light scattering (DLS), and UV-vis and circular dichroism (CD) spectroscopy, compared with random and block counterparts.

Part II (Chapters 6 – 8) is related to the development of selective post-functionalization systems of poly(methacrylate)s and the related copolymers with transesterification. Chlorine-capped or end-cyclized telechelic poly(methyl methacrylate)s were synthesized by terminal-selective transesterification. The polymers were characterized by ^{1}H nuclear magnetic resonance (NMR) spectroscopy and matrix-assisted laser desorption ionization time-of-flight mass spectrometry (MALDI-TOF-MS). Iterative catalysis of LRP and the terminal-selective transesterification of chlorine-capped telechelic poly(methyl methacrylate)s afforded pinpoint-functionalized or periodically sequence-controlled polymers. Transesterification was further applied to the selective functionalization of methyl acrylate units in methacrylate/methyl acrylate random copolymers.

In part I, **Chapter 1** focuses on the synthesis of MMA/DMA gradient copolymers via concurrent tandem catalysis of ruthenium-catalyzed LRP and in situ transesterification of MMA with 1-dodecanol and titanium isopropoxide [Ti(O*i*-Pr)$_4$] (Scheme 3). Perfect synchronization of LRP and transesterification was achieved via the optimization of the Ti catalyst concentration and the use of molecular sieves 4A (MS 4A). In particular, MS 4A effectively removed methanol generating from the transesterification of MMA to increase the content of DMA in monomers without disturbing LRP. As a result, well-controlled MMA/DMA gradient copolymers were obtained where DMA composition gradually and linearly increased from the initiating terminal (α-end) to the growing Cl terminal (ω-end) along a chain. Analyzed by differential scanning calorimetry (DSC), the gradient copolymer showed extremely broad glass transition temperature (T_g) spreading from -50 ^{o}C to 100 ^{o}C. This feature is specific to the gradient copolymer and clearly different from random or block counterparts indicating T_g at 6 ^{o}C or two T_g's at -52 ^{o}C and 116 ^{o}C, respectively.

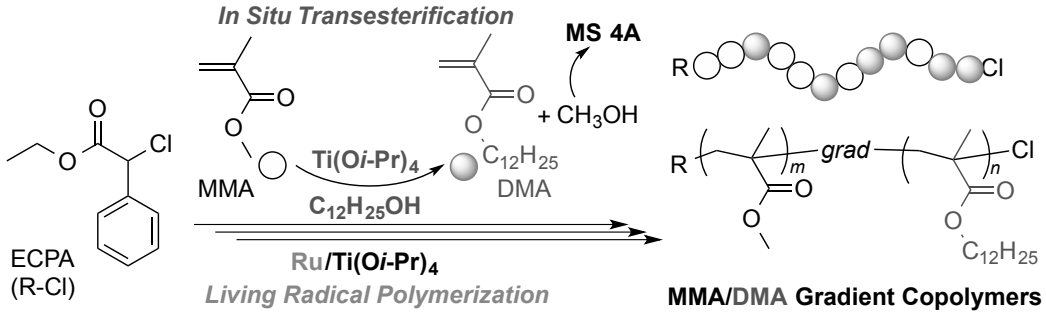

Scheme 3. MMA/DMA Gradient Copolymers via Concurrent Tandem Catalysis of LRP and In-Situ Transesterification of MMA with 1-Dodecanol

Chapter 2 deals with the synthesis of amphiphilic gradient copolymers whose sequence distribution gradually changes from hydrophobic MMA alone to hydrophilic and thermosensitive poly(ethylene glycol) methyl ether methacrylate (PEGMA) (Scheme 4). Gradient sequence was catalytically controlled by adjusting the rate of transesterification with Ti(O*i*-Pr)$_4$ (catalyst) and MS 4A. Various PEGs with different oxyethylene unit number [$CH_3(OCH_2CH_2)_nOH$: n = 1 ~ 11.8] were employed to control the hydrophilicity of amphiphilic gradient copolymers. Confirmed by DLS, MMA/PEGMA [n = 7.2 (average)] gradient copolymers induced self-assembly to form nanoaggregates in water and methanol; the size and aggregation properties are different from those random and block counterparts. Furthermore, MMA/PEGMA copolymers also showed lower critical solution temperature (LCST)-type phase separation in water and upper critical solution temperature (UCST) in alcohols (*i*PrOH, methanol). The thermoresponsive properties depended on the PEG length and/or sequence distribution.

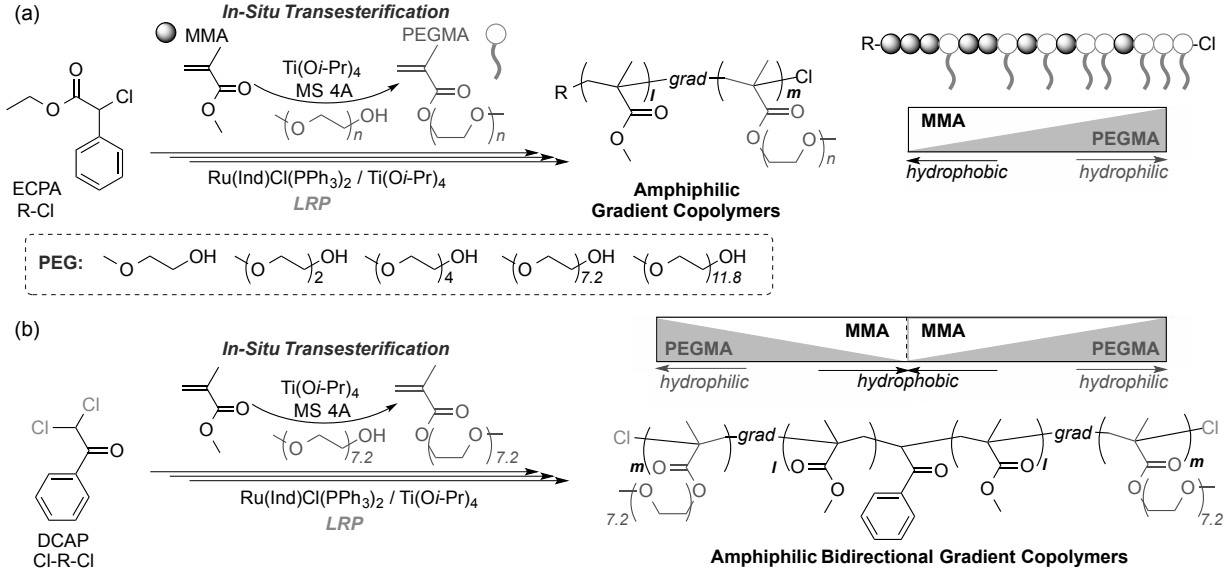

Scheme 4. Synthesis of Amphiphilic Gradient Copolymers via Concurrent Tandem Catalysis of LRP and Transesterification with MMA and Hydrophilic PEGs

Chapter 3 presents the synthesis and self-assembly of chiral 1,3,5-tricarboxamide (BTA)-functionalized copolymers with gradient, bidirectional gradient, and random sequence distributions. The sequence control was efficiently achieved by the tandem catalysis of LRP and in-situ transesterification of 2-ethylexyl methacrylate (EHMA) in the presence of a BTA alcohol (BTA-OH) and Ti(O*i*-Pr)$_4$ (Scheme 5). By tuning the Ti concentration and the timing of the Ti addition, synchronized tandem catalysis took place to afford EHMA/BTA-functionalized methacrylate (BTAMA) gradient copolymers. The folding/self-assembly properties of the BTA sequence-controlled copolymers were examined in 1,2-dichloroethane (DCE), methylcyclohexane (MCH), and the mixture by temperature-dependent CD spectroscopy and DLS. Typically, the gradient copolymer induced intermolecular self-assembly in MCH to form nanoaggregates that are larger than the random counterpart.

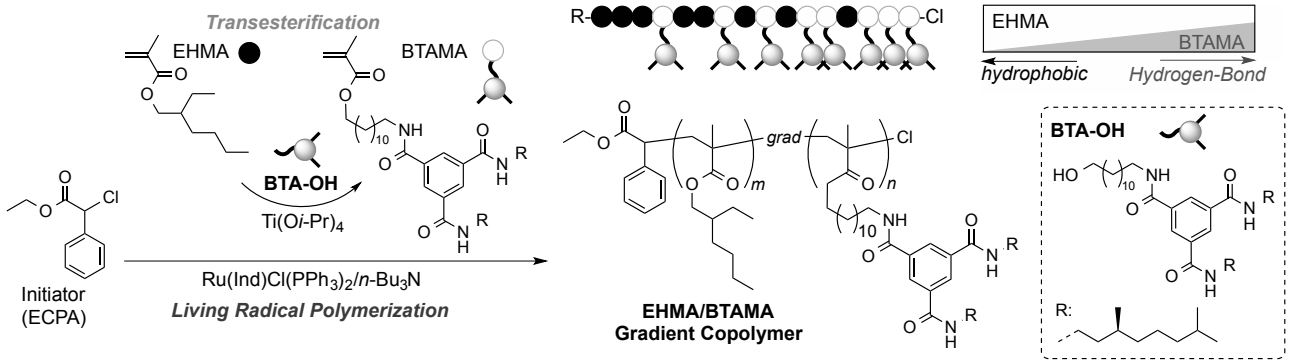

Scheme 5. Synthesis of Hydrogen-Bonding Gradient Copolymers via Concurrent Tandem Catalysis of LRP and Transesterification with BTA-OH for Self-Folding/Self-Assembly in Organic Media

Chapter 4 concerns the synthesis of fluorinated gradient copolymers via tandem polymerization of MMA in fluoroalcohols (R_FOH). Though it is generally difficult due to the high acidity and low nucleophilicity of fluoroalcohols, transesterification of MMA with $CF_3CF_2CH_2CH_2CH_2OH$ (5FPOH), $CF_3CF_2CF_2CF_2CH_2CH_2OH$ (9FHOH), and $CF_3CF_2CF_2CH_2OH$ (7FBOH) were efficiently catalyzed with Ti(O*i*-Pr)$_4$ and MS 4A to give corresponding fluorinated methacrylates (R_FMA: 5FPMA, 9FHMA, and 7FBMA). Thus, tandem polymerization of MMA with the Ti catalyst, MS 4A, and their fluoroalcohols successfully produced corresponding gradient copolymers (Scheme 6). The key is to use MS 4A to promote transesterification by removing methanol generating therefrom.

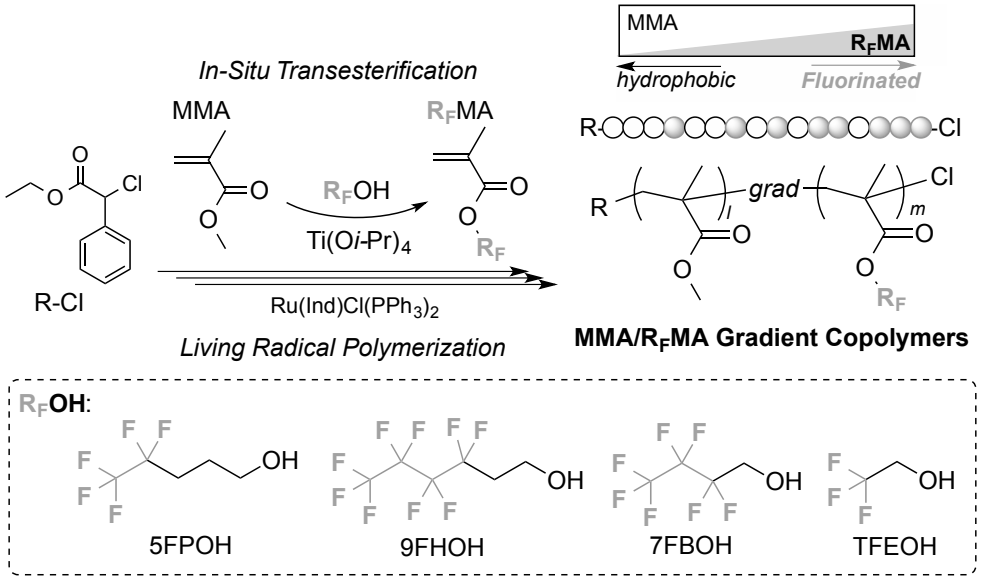

Scheme 6. Synthesis of Fluorinated Gradient Copolymers via Concurrent Tandem Catalysis of LRP and Transesterification with Fluoroalcohols.

Chapter 5 focuses on the synthesis and physical properties of fluorous, perfluorinated gradient copolymers via tandem LRP of *1H,1H,2H,2H*-perfluorooctyl methacrylate (13FOMA) with hydrophobic or hydrophilic alcohols (e.g., 1-dodecanol, PEG-OH) and a Ti(O*i*-Pr)$_4$ catalyst. Owing to the electron-withdrawing perfluorinated segment and less nucleophilic properties of generating *1H,1H,2H,2H*-perfluorooctanol, 13FOMA was efficiently transesterified with alcohols into various methacrylates during tandem LRP. As a result, this system provided various 13FOMA-based fluorous gradient copolymers with dodecyl methacrylate (DMA; soft and hydrophobic), octadecyl methacrylate (ODMA; crystalline), and PEGMA (hydrophilic, thermosensitive) (Scheme 7). Solution and physical properties (micellization, surface tension, phase separation, glass transition temperature, and contact angle) of 13FOMA/DMA gradient copolymer was evaluated, compared with the random or block counterparts.

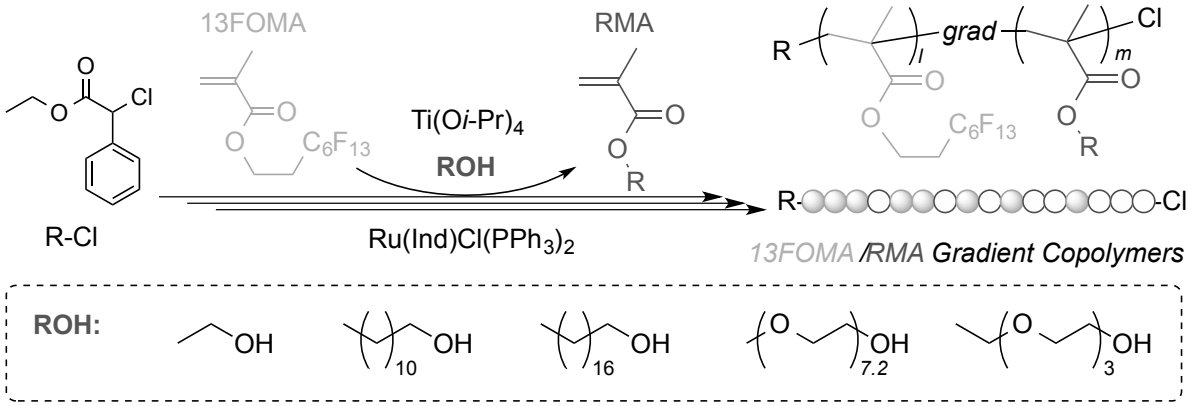

Scheme 7. Synthesis of Fluorous Gradient Copolymers via Concurrent Tandem Catalysis of LRP and Transesterification with a Perfluoroalkyl Methacrylate.

In Part II, **Chapter 6** concerns terminal-selective transesterification of chlorine-capped poly(methyl methacrylate)s (Et-PMMA-Cl) with various alcohols (ROH) and Ti(O*i*-Pr)$_4$ as a novel approach to chlorine-capped telechelic polymers (R-PMMA-RMA-Cl) (Scheme 8a). Highly selective transesterification of the both terminal esters was attributed to the less steric hindrance of the carbonyl groups and/or the activation by the electron-withdrawing Cl terminal. A wide variety of functional groups such as alkene, naphthalene and amine were successfully introduced into the polymer terminals. Joint-functionalized block and pinpoint- functionalized (co)polymers were also efficiently synthesized via the iterative tandem catalysis of LRP and terminal-selective transesterification with a chlorine-capped telechelic PMMA as macroinitiator (Scheme 8b,c).

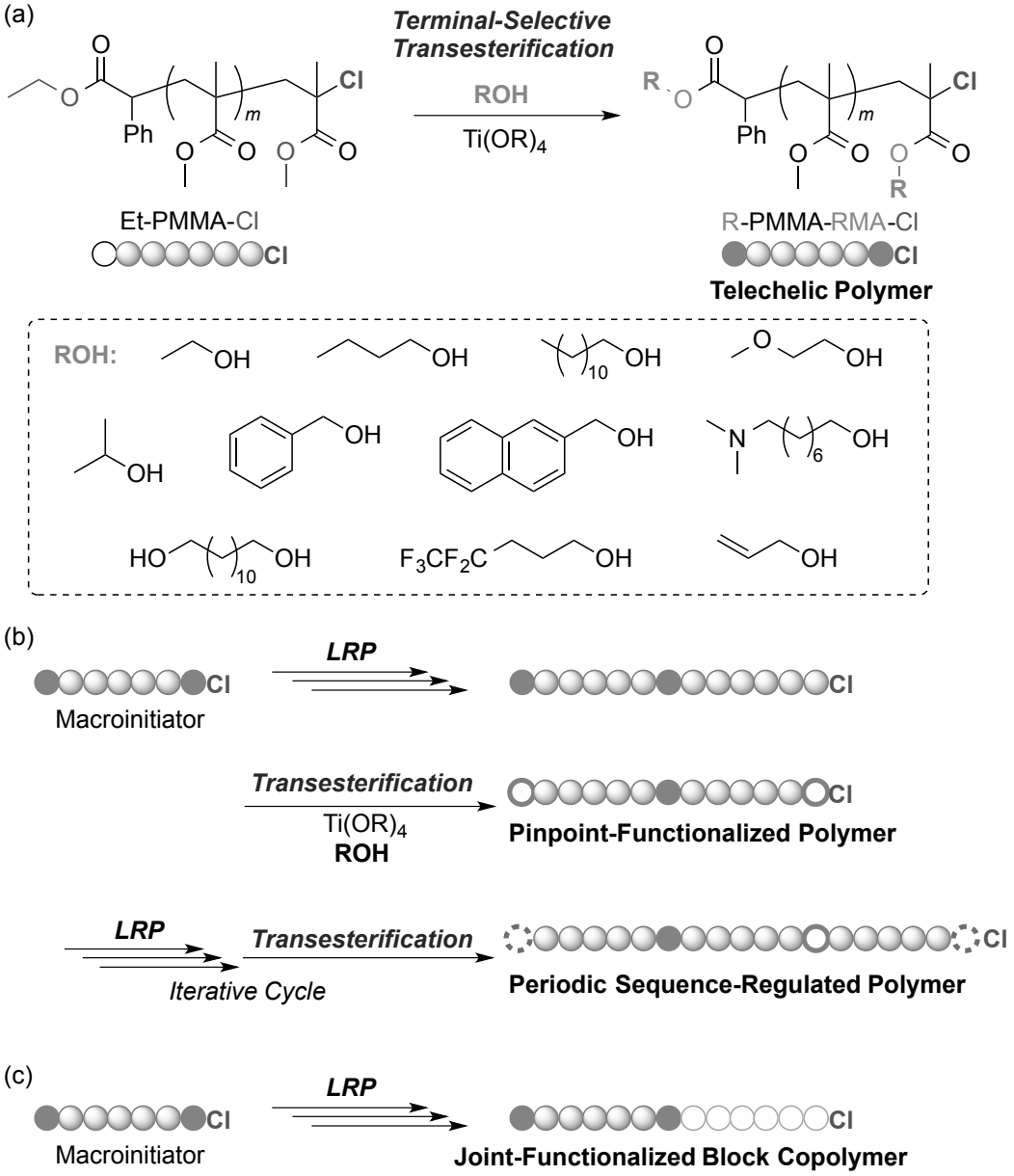

Scheme 8. Synthesis of (a) Telechelic, (b) Pinpoint-Functionalized, and (c) Joint-Functionalized Block (Co)polymers via Terminal-Selective Transesterification of Chlorine-Capped Poly(methyl methacrylate)s.

Chapter 7 deals with a versatile strategy to synthesize halogen-free *ω*-end-cyclized telechelic polymers via terminal-selective transesterification and *ω*-end cyclization of bromine-capped poly(methyl methacrylate)s (PMMA-Br) with various alcohols (ROH) and Ti(O*i*-Pr)$_4$ (Scheme 9). Mechanism of the cyclization was examined by model experiments with a bromine-capped MMA dimer [H-(MMA)$_2$-Br]. The telechelic polymers were also directly obtained from the sequential tandem catalysis of iron-catalyzed LRP of MMA with a bromide initiator, followed by the transesterification and cyclization of the resulting PMMA-Br with alcohols.

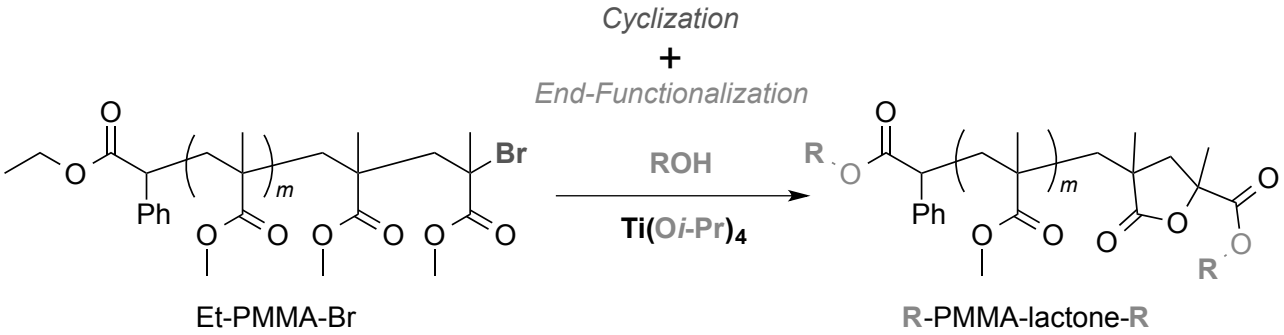

Scheme 9. Synthesis of *ω*-End-Cyclized Telechelic Polymers via One-Pot Terminal-Selective Transesterification and *ω*-End Cyclization of PMMA-Br with Alcohols.

Chapter 8 focuses on acrylate-selective transesterification of methacrylate (R_1MA)/methyl acrylate (MA) random copolymers with alcohols (R_2OH) and Ti(O*i*-Pr)$_4$ for R_1MA/R_2A copolymers (Scheme 10). This method allows efficient post-functionalization of the polymers using MA units as selectively transforming monomers. Various methacrylates and alcohols were applied to produce functional random copolymers.

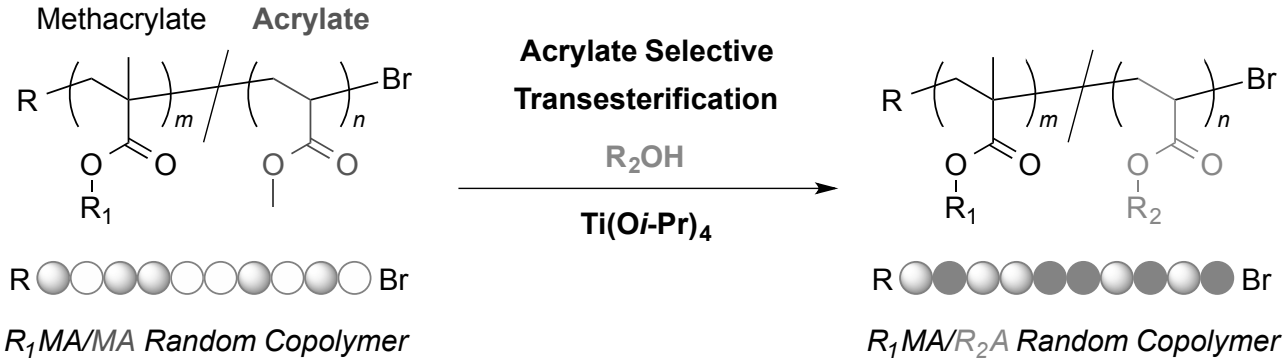

Scheme 10. Post-Functionalization of Methacrylate/Acrylate Random Copolymers with Alcohols via Acrylate-Selective Transesterification

In conclusion, the author achieved the precision synthesis of functional gradient, telechelic, and related sequence-controlled copolymers via selective-transesterification coupled with LRP. In Part I, functional gradient copolymers were efficiently prepared by concurrent tandem catalysis of LRP and monomer-selective transesterification. In Part II, telechelic and pinpoint-functionalized polymers were successfully obtained from post-functionalization of chlorine or bromine-capped PMMAs or methacrylate/acrylate random copolymers via terminal or acrylate-selective transesterification. The key is incomparable selectivity of transesterification for site-specific functionalization. Transesterification with LRP created new avenues to produce unprecedented functional polymers with well-controlled primary structure and functional sequences. The synthetic systems developed in this thesis are thereby beyond traditional methodologies by simple combination of polymerization and organic reactions.

References

(1) Ouchi,M.; Terashima, T.; Sawamoto, M. *Chem. Rev*. **2009**, *109*, 4963-5050.

(2) Matyjaszewski, K.; Tsarevsky, N. V. *Nat. Chem*. **2009**, *1*, 276-288.

(3) Satoh, K.; Kamigaito, M. *Chem. Rev*. **2009**, *109*, 5120-5156.

(4) Aoshima, S.; Kanaoka, S. *Chem. Rev*. **2009**, *109*, 5245-5287.

(5) Breed, D. R.; Thibault, R.; Xie, F.; Wang, Q.; Hawker, C. J.; Pine, D. J. *Langmuir* **2009**, *25*, 4370-4376.

(6) Campos, L. M.; Killops, K. L.; Sakai, R.; Paulusse, J. M. J.; Damiron, D.; Drockenmuller, E.; Messmore, B. W.; Hawker, C. J. *Macromolecules* **2008**, *41*, 7063-7070.

(7) Zheng, J.; Hua, G.; Yu, J.; Lin, F.; Wade, M. B.; Reneker, D. H.; Becker, M. L. *ACS Macro Lett*. **2015**, *4*, 207-213.

(8) Iha, R. K.; Wooley, K. L.; Nyström, A. M.; Burke, D. J.; Kade, M. J.; Hawker, C. J. *Chem. Rev*. **2009**, *109*, 5620-5686.

(9) Hoyle, C. E.; Bowman, C. N. *Angew. Chem. Int. Ed*. **2010**, *49*, 1540-1573.

(10) Lowe, A. B. *Polym. Chem*. **2010**, *1*, 17-36.

(11) (a) Das, A.; Theato, P. *Chem. Rev*. **2016**, *116*, 1434-1495. (b) Theato, P. *J. Polym. Sci. Part A: Polym. Chem.* **2008**, *46*, 6677–6686. (c) Das, A.; Theato, P. *Macromolecules* **2015**, *48*, 8695-8707.

(12) Nicolaou, K. C.; Edmonds, D. J.; Bulger, P. G. *Angew. Chem. Int. Ed*. **2006**, *45*, 7134-7186.

(13) Filice, M.; Palomo, J. M. *ACS Catal*. **2014**, *4*, 1588-1598.

(14) Tietze, L. F. *Chem. Rev*. **1996**, *96*, 115-136.

(15) Wasilke, J-C.; Obrey, S. J.; Baker, R. T.; Bazan, G. C. *Chem. Rev*. **2005**, *105*, 1001-1020.

(16) Doran, S.; Yilmaz, G.; Yagci, Y. *Macromolecules* **2015**, *48*, 7446-7452.

(17) Wu, G-P.; Darensbourg, D. J. *Macromolecules* **2016**, *49*, 807-814.

(18) Kitayama, T.; Tabuchi, M.; Kawauchi, T.; Hatada, K. *Polym. J.* **2002**, *34*, 370-375.

(19) Kanaoka, S.; Yamada, M.; Ashida, J.; Kanazawa, A.; Aoshima, S. *J. Polym. Sci. Part A: Polym. Chem.* **2012**, *50*, 4594–4598.

(20) Matson, J. B.; Grubbs, R. H. *Macromolecules* **2008**, *41*, 5626-5631.

(21) Terashima, T.; Ouchi, M.; Ando, T.; Sawamoto, M. *J. Am. Chem. Soc.* **2006**, *128*, 11014−11015.

(22) Gody, G.; Rossner, C.; Moraes, J.; Vana, P.; Maschmeyer, T.; Perrier, S. *J. Am. Chem. Soc.* **2012**, *134*, 12596−12603.

(23) (a) van As, B. A. C.; van Buijtenen, J.; Heise, A.; Broxterman, Q. B.; Verzijl, G. K. M.; Palmans, A. R. A.; Meijer, E. W. *J. Am. Chem. Soc.* **2005**, *127*, 9964−9965. (b) van Buijtenen, J.; Bart A. C. van As, B. A. C.; Meuldijk, J.; Palmans, A. R. A.; Vekemans, J. A. J. M.;

Hulshof, L. A.; Meijer, E. W. *Chem. Commun*. **2006**, 3169-3171.

(24) Bielawski, C. W.; Louie, J.; Grubbs, R. H. *J. Am. Chem. Soc.* **2000**, *122*, 12872−12873.

(25) Geng, J.; Lindqvist, J.; Mantovani, G.; Haddleton, D. M. *Angew. Chem. Int. Ed*. **2008**, *47*, 4180-4183.

(26) (a) Nakatani, K.; Terashima, T.; Sawamoto, M. *J. Am. Chem. Soc.* **2009**, *131*, 13600−13601. (b) Nakatani, K.; Ogura, Y.; Koda, Y.; Terashima, T.; Sawamoto, M. *J. Am. Chem. Soc.* **2012**, *134*, 4373−4383.

(27) Otera, J. *Chem. Rev*. **1993**, *93*, 1449-1470.

(28) Enders, D.; Niemeier, O.; Henseler, A. *Chem. Rev*. **2007**, *107*, 5606-5655.

(29) Ishihara, K.; Nakayama, M.; Ohara, S.; Yamamoto, H. *Tetrahedron*, **2002**, *58*, 8179-8188.

(30) Ohshima, T.; Iwasaki, T.; Mashima, K. *Chem. Commun*. **2006**, 2711-2713.

(31) Hatano, M.; Kamiya, S.; Ishihara, K. *Chem. Commun*. **2012**, *48*, 9465-9467.

(32) Kirchner, G.; Scollar, M. P.; Klibanov, A. M. *J. Am. Chem. Soc.* **1985**, *107*, 7072−7076.

(33) Krasik, P. *Tetrahedron Lett*. **1998**, *39*, 4223-4226.

(34) (a) Wang, S.; Fu, C.; Zhang, Y.; Tao, L.; Li, S.; Wei, Y. *ACS Macro Lett.* **2012**, *1*, 1224−1227. (b) Fu, C.; Xu, J.; Tao, L.; Boyer, C. *ACS Macro Lett.* **2014**, *3*, 633−638.

(35) Wu, G-P.; Darensbourg, D. J.; Lu, X-B. *J. Am. Chem. Soc.* **2012**, *134*, 17739−17745.

(36) Kato, M.; Kamigaito, M.; Sawamoto, M.; Higashimura, T. *Macromolecules* **1996**, *28*, 1721-1723.

(37) Wang, J-S.; Matyjaszewski, K. *J. Am. Chem. Soc.* **1995**, *117*, 5614−5615.

(38) Hawker, C. J.; Bosman, A. W.; Harth, E. *Chem. Rev*. **2001**, *101*, 3661-3688.

(39) Matyjaszewski, K.; Tsarevsky, N. V. *J. Am. Chem. Soc.* **2014**, *136*, 6513−6533.

(40) Moad, G.; Rizzardo, E.; Thang, S. H. *Aust. J. Chem*. **2012**, *65*, 985-1076.

(41) Yamago, S. *Chem. Rev*. **2009**, *109*, 5051-5068.

(42) Kamigaito, M.; Ando, T.; Sawamoto, M. *Chem. Rev*. **2001**, *101*, 3689-3745.

(43) Yoda, H.; Nakatani, K.; Terashima, T.; Ouchi, M.; Sawamoto, M. *Macromolecules* **2010**, *43*, 5595-5601.

(44) Nishizawa, K.; Ouchi, M.; Sawamoto, M. *RSC Adv*. **2016**, *6*, 6577-6582.

(45) (a) Ando, T.; Kato, M.; Kamigaito, M.; Sawamoto, M. *Macromolecules* **1996**, *29*, 1070-1072. (b) Ando, T.; Kamigaito, M.; Sawamoto, M. *Macromolecules* **2000**, *33*, 6732-6737.

(46) Seno, K.; Tsujimoto, I.; Kanaoka, S.; Aoshima, S. *J. Polym. Sci. Part A: Polym. Chem.* **2008**, *46*, 6444–6454.

(47) Kim, J.; Mok, M. M.; Sandoval, R. W.; Woo, D. J.; Torkelson, J. M. *Macromolecules* **2006**, *39*, 6152-6160.

(48) Mok, M. M.; Ellison, C. J.; Torkelson, J. M. *Macromolecules* **2011**, *44*, 6220-6226.

(49) Kim, J.; Gray, M. K.; Zhou, H.; Nguyen, S. T.; Torkelson J. M. *Macromolecules* **2005**, *38*, 1037-1040.

(50) Karaky, K.; Billon, L.; Pouchan, C.; Desbriéres, J. *Macromolecules* **2007**, *40*, 458-464.

(51) Matyjaszewski, K.; Ziegler, M. J.; Arehart, S. V.; Greszta, D.; Pakula, T. *J. Phys. Org. Chem.* **2000**, *13*, 775−786.

(52) Nakatani, K.; Terashima, T.; Ouchi, M.; Sawamoto, M. *Macromolecules* **2010**, *43*, 8910-8916.

(53) Urien, M.; Erothu, H.; Cloutet, E.; Hiorns, R. C.; Vignau, L.; Cramail, H. *Macromolecules* **2008**, *41*, 7033-7040.

(54) Zhang, M.; Rupar, P. A.; Feng, C.; Lin, K.; Lunn, D. J.; Oliver, A.; Nunns, A.; Whittell, G. R.; Manners, I.; Winnik, M. A. *Macromolecules* **2013**, *46*, 1296-1304.

(55) Laurent, B. A.; Grayson, S. M. *J. Am. Chem. Soc.* **2006**, *128*, 4238−4239.

(56) Kubo, M.; Nishigawa, T.; Uno, T.; Itoh, T.; Sato, H. *Macromolecules* **2003**, *36*, 9264-9266.

(57) Li, Z-L.; Li, L.; Deng, X-X.; Zhang, L-J.; Dong, B-T.; Du, F-S.; Li, Z-C. *Macromolecules* **2012**, *45*, 4590-4598.

(58) Hutchings, L. R.; Brooks, P. P.; Parker, D.; Mosely, J. A.; Sevinc, S. *Macromolecules* **2015**, *48*, 610-628.

(59) (a) Hibi, Y.; Tokuoka, S.; Terashima, T.; Ouchi, M.; Sawamoto, M. *Polym. Chem*. **2011**, *2*, 341-347. (b) Hibi, Y.; Ouchi, M.; Sawamoto, M. *Angew. Chem. Int. Ed*. **2011**, *50*, 7434-7437.

(60) Satoh, K.; Ozawa, S.; Mizutani, M.; Nagai, K.; Kamigaito, M. *Nat. Commun.* **2010**, *1*.

(61) Pfeifer, S.; Lutz, J-F. *J. Am. Chem. Soc.* **2007**, *129*, 9542−9543.

(62) Oh, D.; Ouchi, M.; Nakanishi, T.; Ono, H.; Sawamoto, M. *ACS Macro Lett*. **2016**, *5*, 745-749.

PART I

Concurrent Tandem Catalysis with Monomer-Selective Transesterification for Functional Gradient Copolymers

Chapter 1

Hard/Soft MMA/DMA Gradient Copolymers: Gradient Sequence Control via Tandem Transesterification and Extremely Broad Glass Transition Temperature

Abstract

Gradient copolymers with differential sequences linearly changing from methyl methacrylate (MMA) to dodecyl methacrylate (DMA) were efficiently synthesized by a concurrent tandem catalysis in the ruthenium-catalyzed living radical (co)polymerization coupled with the in situ transesterification of MMA with 1-dodecanol assisted by titanium isopropoxide [Ti(O*i*-Pr)$_4$]. The key is to perfectly synchronize the two reactions throughout the tandem catalysis by using molecular sieves (MS), which facilitates the MMA transesterification into DMA by removing the resulting methanol. The MMA/DMA gradient copolymers had an extremely broad glass transition temperature range [i.e., hardly detectable by differential scanning calorimetry (DSC)], in sharp contrast to the random and the block counterparts of similar compositions.

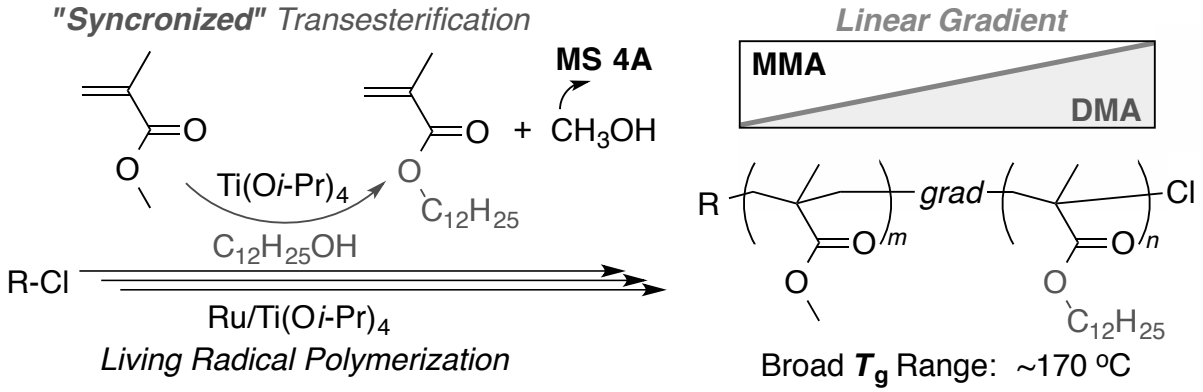

Introduction

Gradient copolymers are a class of sequence-regulated copolymers where the differential comonomer composition along the backbone gradually and continuously changes from one terminal to the other.[1-16] Owing to this particular sequence distribution, gradient copolymers often exhibit intriguing physical properties in solid state and/or in solution and thus differ from the corresponding random and block copolymers.[1,2,6-15] Typically, A-B gradient copolymers often exhibit broad grass transition temperature (T_g) for monomer pairs whose homopolymers have very different T_g.[2,10-12] The breadth of the T_g range is dependent on not only comonomer combination but also their sequence distribution and the degree of polymerization (*DP*). Such polymeric materials with broad T_g range would be quite effective for vibration or acoustic damping.[17,18]

In general, gradient copolymers have been obtained in living polymerization by the following two methods: the "spontaneous" gradient formation from two monomers with different reactivity;[4,7,8] and the "forced" gradient formation via a continuous feed of a second monomer into a living polymerization system of another (first) monomer.[3,5,6,9-14] In radical polymerization, in particular, the two methodologies are often combined[19-26] by taking the advantage of facile cross-propagation, but this approach involves drawbacks such as limited monomer combinations and cumbersome procedures, sometimes spoiling the versatility of radical polymerization where a wide variety of monomers is applicable.

As a new, efficient, and versatile strategy for gradient copolymers, the author has recently developed the concurrent tandem catalysis that combines the ruthenium-catalyzed living radical polymerization with the in-situ transformation of an initially fed methacrylate (R_1MA) into another (R_2MA) via transesterification with an alcohol (R_2OH) and a metal alkoxide [$Al(O\textit{i}\text{-}Pr)_3$, $Ti(O\textit{i}\text{-}Pr)_4$, etc.] (Scheme 1).[15,16] In this system, these metal alkoxides, originally employed as polymerization cocatalysts (additives),[27,28] concurrently catalyze the transesterification[29] from R_1MA into R_2MA. The instantaneous comonomer composition thereby continuously changes from R_1MA alone to an R_2MA rich mixture. The seamless change of the monomer composition is directly reflected onto the instantaneous monomer-unit composition (gradient sequence distribution), because methacrylates usually have similar reactivity independent of the pendent ester alkyl group, and because the transesterification takes place specifically for monomers and not for polymers.

Owing to the diversity of alcohols and methacrylates along with the catalytic control of monomer sequence, the tandem catalysis can potentially provide tailor-made gradient copolymers with wide comonomer combinations, as well as interesting sequences, from such common reagents as alcohols for polymeric functional materials.

Herein, the author focuses on the design of gradient copolymers via a perfectly synchronized

tandem catalysis of living radical polymerization and the Ti(O*i*-Pr)$_4$-catalyzed in-situ transesterification of MMA into dodecyl methacrylate (DMA) with 1-dodecanol (Scheme 1). The synchronized system is of vital importance in achieving a linearly shifting sequence distribution from MMA into DMA along the backbone. Given a large difference in T_g between PMMA and PDMA (+116 ^oC and –52 ^oC, respectively), MMA/DMA gradient copolymers are expected to have quite broad T_g range.[2] In fact, it was found that, in sharp contrast to random and block counterparts of the same composition, MMA/DMA gradient copolymers with a linear sequence change have an extremely broad transition breadth (ΔT_g), showing virtually no detectable DSC transition signals.

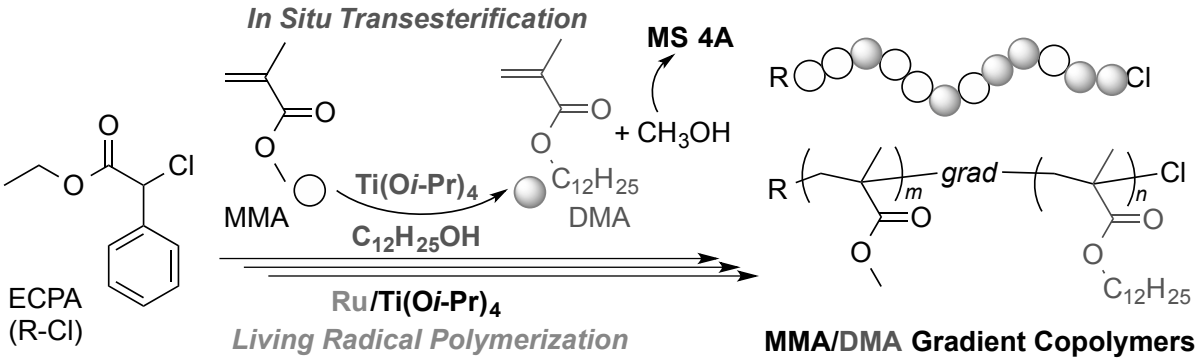

Scheme 1. MMA/DMA Gradient Copolymers via Synchronized Tandem Catalysis of Living Radical Polymerization and Transesterification

Experimental Section

Materials

Methyl methacrylate (MMA: TCI; purity >99.8%) and tetralin (1,2,3,4-tetrahydronaphthalene: Kishida Chemical; purity >98%; an internal standard for ^{1}H NMR analysis) were dried overnight over calcium chloride and distilled from calcium hydride under reduced pressure before use. Dodecyl methacrylate (DMA: Wako, purity >95%) was purified by an inhibitor removal column (Aldrich) and was degassed by triple vacuum-argon purge cycles before use. 1-Dodecanol (TCI, purity >99%), Ti(O*i*-Pr)$_4$ (Aldrich, purity >97%), and *n*-Bu$_3$N (TCI, purity >98%) was degassed by triple vacuum-argon purge cycles before use. Ethyl 2-chloro-2-phenylacetate (ECPA: Aldrich; purity >97%) was distilled under reduced pressure before use. Ru(Ind)Cl(PPh$_3$)$_2$ (Aldrich) were used as received and handled in a glove box under moisture- and oxygen-free argon (H_2O <1 ppm; O_2 <1 ppm). Toluene (solvent) was purified before use; pashing it through a purification column (Glass Contour Solvent Systems: SG Water USA). Molecular sieves (MS) 4A and 3A (Wako) were baked with heat gun under reduced pressure before use.

Characterization

The molecular weight distribution (MWD) curves, M_n, and M_w/M_n ratio of the polymers were measured by SEC in $CHCl_3$ at 40 °C (flow rate: 1 mL/min) on three linear-type polystyrene gel columns (Shodex K-805L: exclusion limit = 4×10^6; particle size = 10 mm; pore size = 5000 Å; 0.8 cm i.d. × 30 cm) that were connected to a Jasco PU-980 precision pump, a Jasco RI-1530 refractive index detector, and a Jasco UV-980 UV/vis detector set at 250 nm. The columns were calibrated against 10 standard poly(MMA) samples (Polymer Laboratories; M_n = 1000–1200000; M_w/M_n = 1.06–1.22). ^{1}H NMR spectra were recorded in $CDCl_3$ and CD_2Cl_2 on a JEOL JNM-ECA500 spectrometer operating at 500.16 MHz. Differential scanning calorimetry (DSC) was performed for polymer samples (ca. 4 mg weighed into an aluminum pan) under a dry nitrogen flow on a DSC Q200 calorimeter (TA Instruments) equipped with a RCS 90 electric freezing machine. The heating and cooling rates were performed at 10 °C/min and -10 °C/min, respectively, between -80 °C and 150 °C. Polymer samples for DSC analysis were fractionated by preparative SEC [column: Shodex K-5002; particle size = 15 mm; 5.0 cm i.d. × 30 cm; exclusion limit = 5×10^3 g/mol; flow rate = 10 mL/min].

Transesterification

The reaction was carried out by the syringe technique under dry argon in baked glass tubes equipped with a three-way stopcock. A procedure for Ti(O*i*-Pr)$_4$-catalyzed transesterification of MMA in toluene/1-dodecanol (1/1, v/v) with MS 4A was given: Into a glass tube, MS 4A (1.0 g) was charged in a glass tube. Then, toluene (1.02 mL), tetralin (0.08 mL), a toluene solution of Ti(O*i*-Pr)$_4$ (500 mM, 0.12 mL, Ti(O*i*-Pr)$_4$ = 0.06 mmol), MMA (0.642 mL, 6 mmol), and 1-dodecanol (1.14 mL) were added at room temperature under dry argon. The total volume of the reaction mixture was thus 3.0 mL. The glass tube was immediately placed in an oil bath kept at 80 °C. At predetermined intervals, a small portion of the mixture was sampled with a syringe under dry argon and cooled to –78 °C to terminate the reaction. Then, the conversion was determined by ^{1}H NMR with tetralin as an internal standard in $CDCl_3$ at r.t..

Polymerization

The synthesis of MMA/DMA copolymers (gradient, random, block) was carried out by syringe technique under argon in baked glass tubes equipped with a three-way stopcock.

MMA/DMA gradient copolymer (*DP* = 400: entry 12 in Table 1 main text)**.** A typical procedure for a gradient copolymer with MS 4A was given: MS 4A (1.0 g) was first placed and dried in a 30 mL glass tube under reduced pressure with heat gun. Into the tube, Ru(Ind)Cl(PPh$_3$)$_2$ (0.0025 mmol, 1.94 mg) was then charged, and toluene (1.85 mL), 1-dodecanol (1.89 mL), tetralin

(0.10 mL), a toluene solution of Ti(O*i*-Pr)$_4$ (500 mM, 0.05 mL, Ti(O*i*-Pr)$_4$ = 0.025 mmol), MMA (10 mmol, 1.07 mL), and ECPA (656 mM, 0.038 mL, ECPA = 0.025 mmol) were added sequentially in that order at 25 °C under argon. The total volume of the reaction mixture was thus 5.0 mL. The glass tube was placed in an oil bath kept at 80 °C. At predetermined intervals, the mixture was sampled with a syringe under dry argon and cooled to –78 °C to terminate the reaction. The total monomer conversion, DMA content in monomer, and cumulative DMA content in polymer ($F_{cum,DMA}$) were directly determined by ^{1}H NMR measurements of the terminated reaction solution in $CDCl_3$ at r.t. with tetralin as an internal standard. Instantaneous DMA content in polymer ($F_{inst,DMA}$) was estimated according to the following equation: $F_{inst,DMA}$ = [Conv.$_{total,\ i}$ x $F_{cum,DMA,\ i}$ - Conv.$_{total,\ i-1}$ x $F_{cum,DMA,\ i-1}$]/[Conv.$_{total,\ i}$ - Conv.$_{total,\ i-1}$], where Conv.$_{total}$ is the total conversion of both monomers. The quenched reaction solutions were evaporated to dryness to give the crude product. The product was fractionated by preparative SEC for DSC analysis. SEC ($CHCl_3$, PMMA std.): M_n = 68,500 g/mol; M_w/M_n = 1.38. ^{1}H NMR [500 MHz, CD_2Cl_2, 25 °C, δ = 5.33 CH_2Cl_2] δ 7.30–7.15 (aromatic), 4.04–3.82 (-COOC<u>H</u>$_2$CH$_2$-), 3.69–3.47 (-COOC<u>H</u>$_3$), 2.10–1.71 (-C<u>H</u>$_2$C(CH$_3$)-), 1.71–1.57 (-COOCH$_2$C<u>H</u>$_2$-), 1.57–1.14 (-CH$_2$(C<u>H</u>$_2$)$_9$CH$_3$), 1.25–0.68 (-CH$_2$C<u>H</u>$_3$, -CH$_2$C(C<u>H</u>$_3$)-). M_n (NMR, α) = 76600; DP_{MMA}/DP_{DMA} = 191/225; $F_{cum,DMA}$ = 54%.

MMA/DMA (200/200) random copolymer. In a 30 mL glass tube, Ru(Ind)Cl(PPh$_3$)$_2$ (0.0025 mmol, 1.94 mg) was placed. Then, toluene (2.78 mL), tetralin (0.10 mL), a toluene solution of Ti(O*i*-Pr)$_4$ (500 mM, 0.10 mL, Ti(O*i*-Pr)$_4$ = 0.050 mmol), MMA (5.0 mmol, 0.53 mL), DMA (5.0 mmol, 1.46 mL), and ECPA (656 mM, 0.038 mL, ECPA = 0.025 mmol) were added sequentially in that order into the tube at 25 °C under argon (The total volume: 5.0 mL). The glass tube was placed in an oil bath kept at 80 °C. After 95 h, the solution was cooled to –78 °C to terminate the reaction. The conversion of MMA and DMA was determined as 94% and 94%, respectively, by ^{1}H NMR in $CDCl_3$ at r.t. with tetralin as an internal standard. The quenched solution was evaporated to dryness to give the crude product. The product was further fractionated by preparative SEC for DSC analysis. SEC ($CHCl_3$, PMMA std.): M_n = 56,800 g/mol; M_w/M_n = 1.19. ^{1}H NMR [500 MHz, CD_2Cl_2, 25 °C, δ = 5.33 CH_2Cl_2] δ 7.30–7.15 (aromatic), 4.03–3.85 (-COOC<u>H</u>$_2$CH$_2$-), 3.66–3.50 (-COOC<u>H</u>$_3$), 2.08–1.71 (-C<u>H</u>$_2$C(CH$_3$)-), 1.71–1.54 (-COOCH$_2$C<u>H</u>$_2$-), 1.52–1.18 (-CH$_2$(C<u>H</u>$_2$)$_9$CH$_3$), 1.26–0.71 (-CH$_2$C<u>H</u>$_3$, -CH$_2$C(C<u>H</u>$_3$)-). M_n (NMR, α) = 70300: DP_{MMA}/DP_{DMA} = 192/200; $F_{cum,DMA}$ = 51%.

MMA/DMA (200/200) block copolymer. In a 30 mL glass tube, Ru(Ind)Cl(PPh$_3$)$_2$ (0.0025 mmol, 1.94 mg) was placed. Then, toluene (2.78 mL), tetralin (0.10 mL), a toluene solution of Ti(O*i*-Pr)$_4$ (500 mM, 0.10 mL, Ti(O*i*-Pr)$_4$ = 0.050 mmol), MMA (5.0 mmol, 0.53 mL), and ECPA (656 mM, 0.038 mL, ECPA = 0.025 mmol) were added sequentially in that order into the tube at 25

°C under argon (The total volume: 3.54 mL). The glass tube was placed in an oil bath kept at 80 °C. After 137 h, the polymerization reached 87% conversion (determined by ^{1}H NMR) to give PMMA-Cl (M_n = 25200 g/mol; M_w/M_n = 1.20, by SEC in $CHCl_3$ with PMMA std.). Into the polymerization mixture, DMA (5.0 mmol, 1.46 mL) was directly added under argon. After 90 h, the reaction solution was cooled to –78 °C to terminate the reaction (93% conversion: determined by ^{1}H NMR). The quenched reaction solution was evaporated to dryness and the resulting crude product was fractionated by preparative SEC for DSC analysis. SEC ($CHCl_3$, PMMA std.): M_n = 64,400 g/mol; M_w/M_n = 1.36. ^{1}H NMR [500 MHz, CD_2Cl_2, 25 °C, δ = 5.33 CH_2Cl_2]: δ 7.30–7.15 (aromatic), 4.00–3.87 (-COOC<u>H</u>$_2$CH$_2$-), 3.64–3.53 (-COOC<u>H</u>$_3$), 2.07–1.71 (-C<u>H</u>$_2$C(CH$_3$)-), 1.71–1.58 (-COOCH$_2$C<u>H</u>$_2$-), 1.58–1.16 (-CH$_2$(C<u>H</u>$_2$)$_9$CH$_3$), 1.27–0.75 (-CH$_2$C<u>H</u>$_3$, -CH$_2$C(C<u>H</u>$_3$)-). M_n (NMR, α) = 72900: DP_{MMA}/DP_{DMA} = 205/205; $F_{cum,DMA}$ = 50%.

Results and Discussion

1. MMA/DMA Gradient Copolymers via Tandem Catalysis

For MMA/DMA gradient copolymers, concurrent tandem polymerization of MMA (2.0 M) was examined with Ru(Ind)Cl(PPh$_3$)$_2$, Ti(O*i*-Pr)$_4$, and ethyl 2-chloro-2-phenylacetate (ECPA) in toluene/1-dodecanol (1/1 v/v, [1-dodecanol]$_0$ = 1.7 M) at 80 °C (Figures 1 and 2, and Table 1). Polymerization efficiently proceeded in high yield to give a well-controlled polymer with narrow molecular weight distribution (a typical result with Ti of 20 mM: total conversion = 95 %; 25 h; M_n = 15000 and M_w/M_n = 1.25 by size-exclusion chromatography (SEC) in $CHCl_3$; Figure 1e, Table 1, entry 7).

In situ transesterification and the gradient sequence in polymer were analyzed by proton nuclear magnetic resonance (^{1}H NMR) spectroscopy. The DMA content in the polymerization solution gradually increased (Figure 1a: blue symbols). The cumulative and the instantaneous DMA content in polymer ($F_{cum,DMA}$ and $F_{inst,DMA}$, respectively) increased with the normalized chain length, while virtually identical to total conversion (Figure 1c), where the normalized chain length is defined as DP_t/DP_{final} for living copolymers; DP_t = [MMA]$_0$ x (total conversion/100)/[ECPA]$_0$; DP_{final} = [MMA]$_0$ x (total final conversion/100)/[ECPA]$_0$;. Thus, a gradient copolymer from MMA to DMA was obtained.

It turned out, however, that the instantaneous composition ($F_{inst,DMA}$) does not change linearly along the polymer backbone; i.e., $F_{inst,DMA}$ increases sharply at the beginning of the reaction [or at the vicinity of the initiating terminal (α-end)] but more moderately as the reaction was retarded at about 60 % conversion. This sequence-distribution shift along the backbone directly reflects time-dependent changes in the instantaneous comonomer composition in the reaction mixture.

Namely, the in situ transesterification of MMA into DMA was faster than the copolymerization of the monomers during the early phases (total conversion below 40 %), but sharply slowed down and almost stopped beyond conversion over 50 % (Figure 1a: black versus blue plots).

Table 1. MMA/DMA Gradient Copolymers Obtained from Concurrent Tandem Living Radical Polymerization[a]

Entry	*DP*	$[Ti(O\textit{i}\text{-}Pr)_4]_0$ (mM)	$[1\text{-dodecanol}]_0$ (M)	MS	MS (g/ml)	Time (h)	Conv.[b] (%)	M_n[c]	M_w/M_n[c]	$F_{cum.DMA}$[d]	$F_{inst.DMA}$[d]
1	100	5.0	1.72	4A	0.33	19	92	19000	1.36	50	77
2	100	10	1.72	4A	0.33	25	95	17700	1.45	61	80
3	100	20	1.72	4A	0.33	14	95	17900	1.42	68	85
4	100	40	1.72	4A	0.33	22	98	23100	1.37	72	82
5	100	5.0	1.72	-	-	22	90	14500	1.27	7	13
6	100	10	1.72	-	-	25	95	14300	1.26	35	44
7	100	20	1.72	-	-	25	95	15000	1.25	45	59
8	100	40	1.72		-	34	94	18700	1.22	48	53
9	100	20	1.0	4A	0.33	33	89	18200	1.28	51	59
10	100	10	1.72	4A	0.17	24	93	16900	1.30	45	66
11	100	10	1.72	3A	0.33	22	90	18500	1.38	56	77
12	400	5.0	1.72	4A	0.33	19	91	68500	1.38	54	80
13	400	20	1.72	-	0.33	24	93	84800	1.38	41	52

[a] $[MMA]_0/[ECPA]_0/[Ru(Ind)Cl(PPh_3)_2]_0/[Ti(O\textit{i}\text{-}Pr)_4]_0$ = 2000/20/2.0 (entries 1-11) or 0.5 (entries 12,13)/5.0 - 20 mM with or without MS 4A (or 3A) in toluene/1-dodecanol at 80 °C. [b] Total monomer conversion: determined by ^1H NMR with an internal standard. [c] Determined by SEC in $CHCl_3$ with a PMMA standard calibration. [d] Cumulative DMA content ($F_{cum,DMA}$) and instantaneous DMA content ($F_{inst,DMA}$) in products.

Though the final $F_{cum,DMA}$ and the initial $F_{inst,DMA}$ indeed increased with increasing concentration of $Ti(O\textit{i}\text{-}Pr)_4$ (from 5.0 mM to 40 mM; Table 1, entries 5-8), the retardation of $F_{inst,DMA}$ beyond the middle reaction stage was inevitable (Figure 2b), indicating that the increased $Ti(O\textit{i}\text{-}Pr)_4$ concentration could accelerate the transesterification just in the early phases of polymerization alone. This is because, under these conditions, the transesterification is reversible and soon reaches equilibrium well before the MMA-DMA copolymerization has been completed.

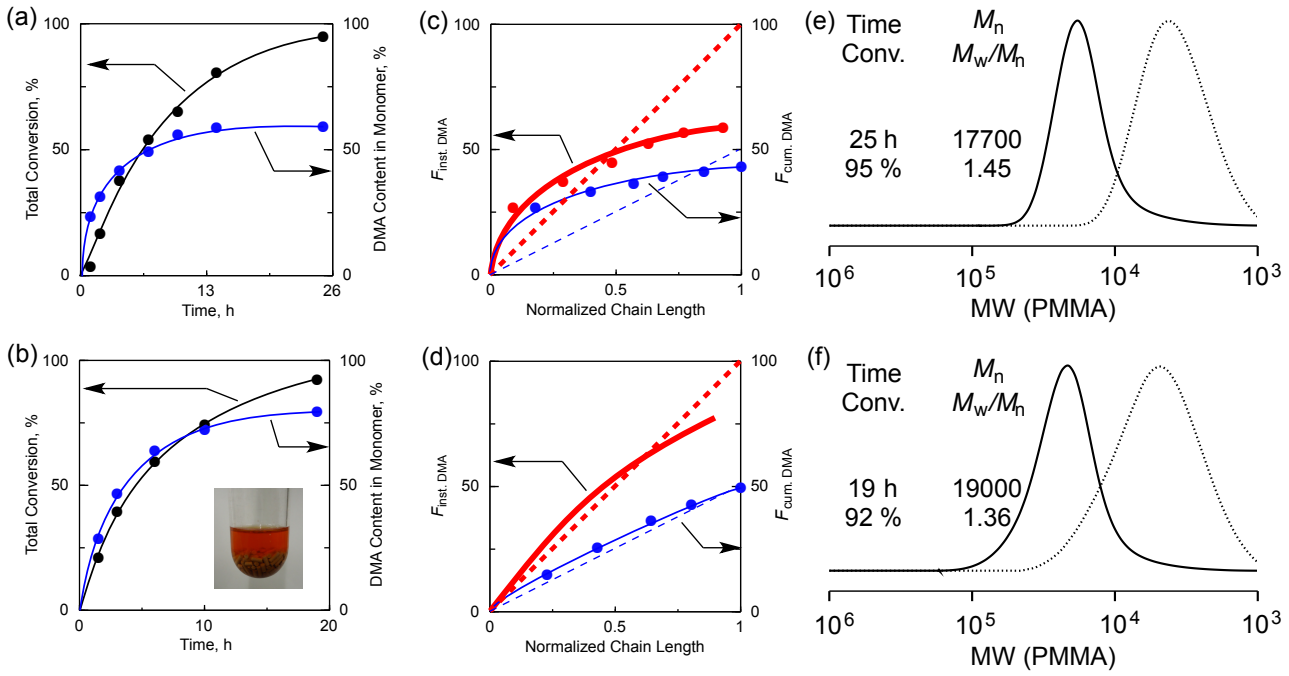

Figure 1. Effects of MS 4A on concurrent tandem living radical polymerization for MMA/DMA gradient copolymers: (a, b) total monomer conversion and DMA content in monomer; (c, d) cumulative ($F_{cum,DMA}$) and instantaneous ($F_{inst,DMA}$) DMA content in products; SEC of the products; $[MMA]_0/[ECPA]_0/[Ru(Ind)Cl(PPh_3)_2]_0/[Ti(O\textit{i}\text{-}Pr)_4]_0$ = 2000/20/2.0/5.0 (b, d, f) or 20 (a, c, e) mM (b, d, f) with or (a, c, e) without MS 4A (0.33 mg/mL) in toluene/1-dodecanol (1/1 v/v, $[1\text{-dodecanol}]_0$ = 1.7 M) at 80 °C. In-set picture in (b): tandem polymerization with MS 4A.

2. Effects of Molecular Sieves on Polymer Composition in Tandem Catalysis

To enhance DMA formation, or to shift the MMA-DMA transformation equilibrium far to the latter monomer, the author employed molecular sieves (MS 4A or 3A) that would remove the resulting methanol by absorption during the transesterification.[30,31] In fact, separate experiments showed that MS 4A efficiently accelerated the transesterification of MMA into DMA (Figure 3). Thus, for example, the concurrent tandem polymerization starting from MMA with $Ru(Ind)Cl(PPh_3)_2$, $Ti(O\textit{i}\text{-}Pr)_4$, and 1-dodecanol was examined in the presence of MS 4A (nominal concentration 0.33 g/mL) (see the in-set picture in Figure 1 b); note that herein the alkoxide concentration was kept rather low (5 mM) relative to the standard conditions (20 mM; see above).

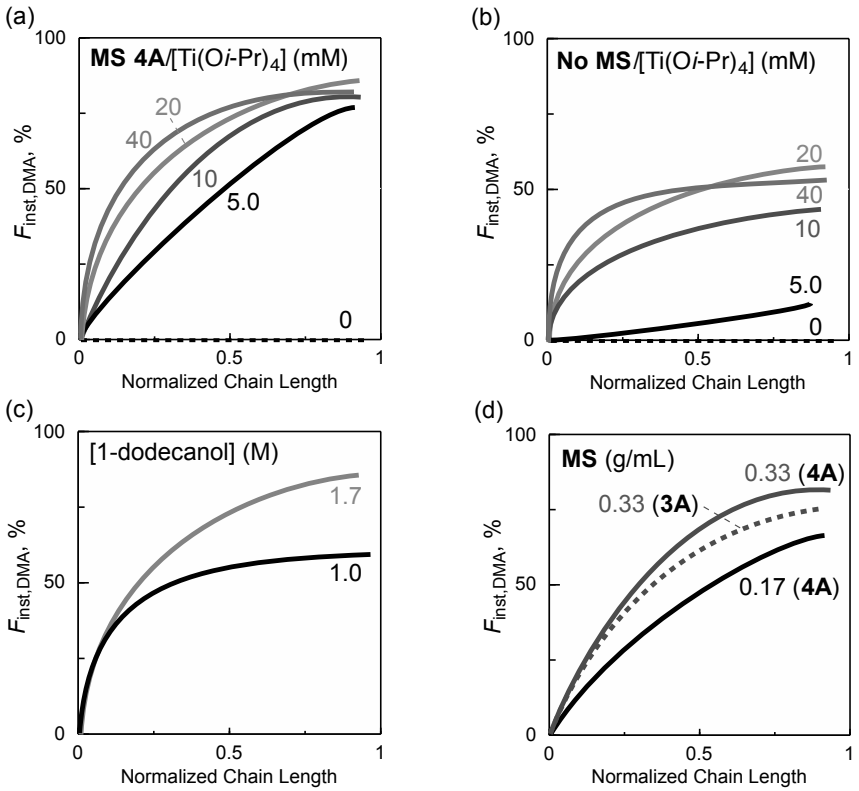

Figure 2. Effects of reaction conditions on MMA/DMA gradient copolymers (*DP* = 100). (a) Ti(O*i*-Pr)$_4$ (0, 5, 10, 20, 40 mM), 1-dodecanol (1720 mM) with MS 4A (0.33 mg/mL). (b) Ti(O*i*-Pr)$_4$ (0, 5, 10, 20, 40 mM), 1-dodecanol (1.7 M) without MS 4A. (c) Ti(O*i*-Pr)$_4$ (20 mM), 1-dodecanol (1.7, 1.0 mM) with MS 4A (0.33 mg/mL). (d) Ti(O*i*-Pr)$_4$ (10 mM), 1-dodecanol (1.7 M) with MS 4A (0.33, 0.17 mg/mL) or MS 3A (0.33 mg/mL).

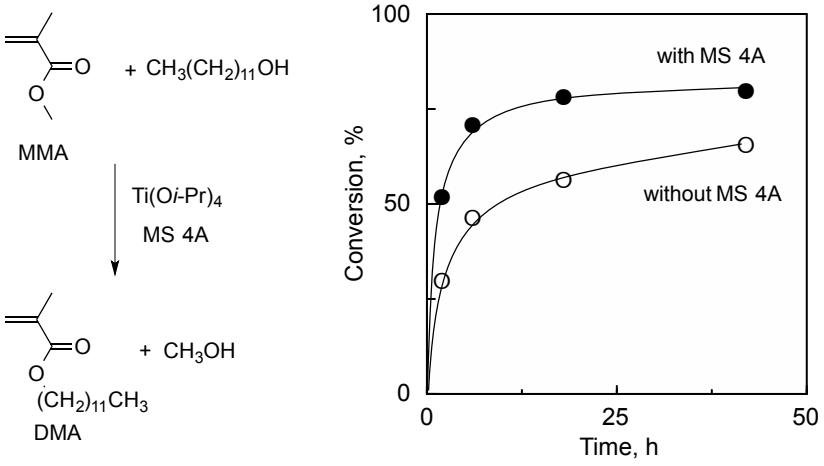

Figure 3. Ti(O*i*-Pr)$_4$-mediated transesterification of MMA into DMA with (filled circle) or without (open circle) MS 4A in 1-dodecanol: $[MMA]_0/[Ti(Oi\text{-}Pr)_4]_0$ = 2000/20 mM, $[MS\ 4A]_0$ = 0.33 g/mL in toluene/1-dodecanol (1/1 v/v, $[1\text{-dodecanol}]_0$ = 1720 mM) at 80 ^{o}C. The final conversion at 42 h was the followings: 80% (with MS 4A); 65% (without MS 4A).

The use of MS 4A at a low Ti(O*i*-Pr)$_4$ concentration perfectly synchronized polymerization and transesterification throughout the tandem catalysis (Figure 1b), to produce a well-controlled gradient copolymer with sequence distribution linearly changing from MMA to DMA (Figure 1d, f and Table 1, entry 1; total conversion = 92 %; 19 h; M_n = 19000; M_w/M_n = 1.36; $F_{cum,DMA}$ = 50%; $F_{inst,DMA}$ = 77%). Without the methanol-absorbent, in contrast, in-situ transesterification hardly proceeded with such a low Ti(O*i*-Pr)$_4$ concentration (Figure 2b, Table 1 entry 5). Another finding with the use of molecular sieves was that gradient copolymers rich in DMA content from the initiating terminal ($F_{cum,DMA}$ = ~70 %; $F_{inst,DMA}$ = ~85%) can be obtained by increasing Ti(O*i*-Pr)$_4$ concentration from 10 to 40 mM, where 82 % of 1-dodecanol was incorporated into DMA (Figure 2a; Table 1, entries 2-4).

3. Sequence Distribution Control by Changing Polymerization Condition

The gradient sequence can also be controlled by the amount of MS 4A or 3A. For example, decreasing MS 4A from 0.33 g/mL to 0.17 g/mL reduced $F_{inst,DMA}$ (Figure 2d, Table 1 entries 10,11). These results demonstrate that molecular sieves efficiently and selectively entrap methanol in the presence of various chemical reagents in this tandem catalysis.

The gradient monomer sequence could be also controlled by decreasing the amount of 1-dodecanol from 1.72 M to 1 M (Figure 2c; Table 1, entry 9; with MS 4A). In this case, the in situ transesterification into DMA hardly proceeded beyond the middle stages of the tandem catalysis; thus $F_{inst,DMA}$ remained unchanged with normalized chain length above 0.5, where 1-dodecanol was converted into DMA almost completely (~91%). The product was therefore a virtual block copolymer consisting of a gradient-sequence segment from the α-end to the middle point and a random-sequence segment from the middle to the ω-end (Figure 2c).

4. Thermal Property of MMA/DMA Gradient Copolymer

To investigate effects of gradient sequence distribution on copolymers' thermal properties, MMA/DMA gradient copolymers were analyzed by DSC, in comparison to the random and the block counterparts (Figure 4). For this, the author prepared two samples of MMA/DMA copolymers with total *DP* of 400: One sample had a sequence distribution linearly changing from MMA to DMA over the backbone from the α-end to the ω-end, obtained from the perfectly synchronized catalysis with MS 4A as discussed above (**Gradient 1**: M_n = 68500; M_w/M_n = 1.38; $F_{cum,DMA}$ = 54%; $F_{inst,DMA}$ = 80%; Table 1, entry 12). The second sample had a retarded DMA distribution obtained without MS 4A, where the DMA content in the segment closer to the ω-end is

smaller than in the first sample and richer near the α-end (**Gradient 2**: M_n = 84800; M_w/M_n = 1.38; $F_{cum,DMA}$ = 41%; $F_{inst,DMA}$ = 52%; Table 1, entry 13).

As seen in the heat flow charts (heating rate 10 °C/min, Figure 4c, black lines), **Gradient 1** did not show a clear T_g, whereas **Gradient 2** seemed to have a broad T_g range. In contrast, the corresponding random copolymer (**Random**: M_n = 56800; M_w/M_n = 1.19; $F_{cum,DMA}$ = 51%) had one T_g at 6 °C, and the block counterpart (**Block**: M_n = 64400; M_w/M_n = 1.36; $F_{cum,DMA}$ = 50%) showed two T_g's at -52 °C for DMA and 116 °C for MMA (Figure 4b), both identical to those for their homopolymers.

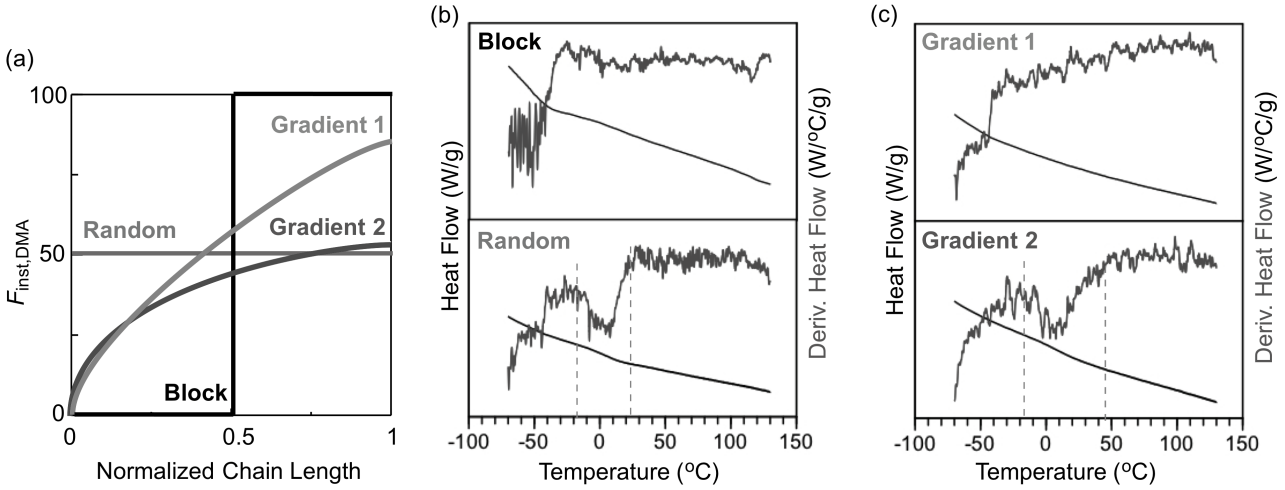

Figure 4. (a) Sequence distribution of MMA/DMA copolymers employed for DSC measurements (*DP* = 400, Block, Random, Gradient 1: entry 12, Gradient 2: entry 13). DSC heating curves and the first derivatives of DSC heating curves with temperature for (b) Block and Random and (c) Gradient 1 and Gradient 2.

The difference in thermal properties was more visible in the first derivatives of heating curves (the blue lines in Figures 4b and 4c). **Gradient 2** clearly showed a signal originating from glass transition, and the width (ΔT_g = ~65 °C) was larger than that for **Random** (ΔT_g = ~40 °C). **Gradient 1** in turn hardly showed glass transition. However, the T_g range for **Gradient 1** apparently spread over 170 degrees, due to the difference in T_g between MMA (116 °C) and DMA (-52 °C) homopolymers. Therefore, "perfect" or "synchronized" gradient MMA/DMA copolymers afforded unique polymeric materials with an extremely broad T_g range resulting from a sequence distribution linearly changing along the backbone from α- to ω-ends.

Conclusion

The author has successfully achieved sequence control of MMA/DMA gradient copolymers via concurrent tandem catalysis of the ruthenium-catalyzed living radical polymerization and the in-situ transesterification of MMA with Ti(O*i*-Pr)$_4$ and 1-dodecanol. Importantly, the combination of molecular sieves and a small amount of Ti(O*i*-Pr)$_4$ induced perfectly synchronized catalysis, to give MMA/DMA gradient copolymers with the sequence distribution linearly changing from MMA to DMA along the backbone. These gradient copolymers turned out to have an extremely large breadth of T_g and thus would be potentially attractive as vibration or acoustic damping materials.

References

(1) Matyjaszewski, K.; Ziegler, M. J.; Arehart, S. V.; Greszta, D.; Pakula, T. *J. Phys. Org. Chem.* **2000**, *13*, 775-786.

(2) Lefebvre, M. D.; de la Cruz, M. O.; Shull, K. R. *Macromolecules* **2004**, *37*, 1118-1123.

(3) Börner, H. G.; Duran, D.; D.; Matyjaszewski, K.; da Silva, M.; Sheiko, S. S. *Macromolecules* **2002**, *35*, 3387-3394.

(4) Qin, S.; Saget, J.; Pyun, J.; Jia, S.; Kowalewski, T.; Matyjaszewski, K. *Macromolecules* **2003**, *36*, 8969-8977.

(5) Min, K.; Oh, J. K.; Matyjaszewski, K. *J. Polym. Sci. Part A: Polym. Chem.* **2007**, *45*, 1413-1423.

(6) Karaky, K.; Billon, L.; Pouchan, C.; Desbrières, J. *Macromolecules* **2007**, *40*, 458-464.

(7) Phan, T. N. T.; Maiez-Tribut, S.; Pascault, J.-P. Bonnet, A.; Gerard, P.; Guerret, O.; Bertin, D. *Macromolecules* **2007**, *40*, 4516-4523.

(8) Park, J.-S.; Kataoka, K. *Macromolecules* **2006**, *39*, 6622-6630.

(9) Kim, J.; Gray, M. K.; Zhou, H.; Nguyen, S. T.; Torkelson, J. M. *Macromolecules* **2005**, *38*, 1037-1040.

(10) Kim, J.; Mok, M. M.; Sandoval, R. W.; Woo, D. J.; Torkelson, J. M. *Macromolecules* **2006**, *39*, 6152-6160.

(11) Wong, C. L. H.; Kim, J.; Torkelson, J. M. *J. Polym. Sci. Part A: Polym. Chem.* **2007**, *45*, 2842-2849.

(12) Mok, M. M.; Pujari, S.; Burghardt, W. R.; Dettmer, C. M.; Nguyen, S. T.; Ellison, C. J.; Torkelson, J. M. *Macromolecules* **2008**, *41*, 5818-5829.

(13) Mok, M. M.; Ellison, C. J.; Torkelson, J. M. *Macromolecules* **2011**, *44*, 6220-6226.

(14) Zhou, Y.-N.; Li, J.-J.; Luo, Z.-H. *J. Polym. Sci. Part A: Polym. Sci.* **2012**, *50*, 3052-3066.

(15) Nakatani, K.; Terashima, T.; Sawamoto, M. *J. Am. Chem. Soc.* **2009**, *131*, 13600-13601.

(16) Nakatani, K.; Ogura, Y.; Koda, Y.; Terashima, T.; Sawamoto, M. *J. Am. Chem. Soc.* **2012**, *134*, 4373-4383.

(17) Agari, Y.; Shiada, M.; Ueda, A.; Nagai, S. *Macromol. Chem. Phys.* **1996**, *197*, 2017-2033.

(18) Qin, C. L.; Zhao, D. Y.; Bai, X. D. Zhang, X. G.; Zhang, B.; Jin, Z.; Niu, H. J. *Mater. Chem. Phys.* **2006**, *97*, 517-524.

(19) Ouchi, M.; Terashima, T.; Sawamoto, M. *Acc. Chem. Res.* **2008**, *41*, 1120-1132.

(20) Ouchi, M.; Terashima, T.; Sawamoto, M. *Chem. Rev.* **2009**, *109*, 4963-5050.

(21) Tsarevsky, N. V.; Matyjaszewski, K. *Chem. Rev.* **2007**, *107*, 2270-2299.

(22) Matyjaszewski, K,. Tsarevsky, N. V. *Nature Chem.* **2009**, *1*, 276-288.

(23) Matyjaszewski, K. *Macromolecules.* **2012**, *45*, 4015-4039.

(24) Hawker, C. J.; Bosman, A. W.; Harth, E. *Chem. Rev.* **2001**, *101*, 3661-3688.

(25) Moad, G.; Rizzardo, E.; Thang, S. H. *Polymer* **2008**, *49*, 1079-1131.

(26) Yamago, S. *Chem. Rev.* **2009**, *109*, 5051-5068.

(27) Ando, T.; Kato, M.; Kamigaito, M.; Sawamoto, M. *Macromolecules* **1996**, *29*, 1070-1072.

(28) Ando, T.; Kamigaito, M.; Sawamoto, M. *Macromolecules* **2000**, *33*, 6732-6737.

(29) Otera, J. *Chem. Rev*. **1993**, *93*, 1449-1470.

(30) Grasa, G. A.; Güveli, T.; Singh, R.; Nolan, S. P. *J. Org. Chem.* **2003**, *68*, 2812-2819.

(31) Hatano, M.; Furuya, Y.; Shimmura, T.; Moriyama, K.; Kamiya, S.; Maki, T.; Ishihara, K. *Org. Lett.* **2011**, *13*, 426-429.

Chapter 2

Amphiphilic PEG-Functionalized Gradient Copolymers: From Modular Synthesis to Sequence-Dependent Self-Assembly and Thermoresponsive Properties

Abstract

Amphiphilic gradient copolymers with poly(ethylene glycol) pendants were synthesized via tandem catalysis of ruthenium-catalyzed living radical polymerization (LRP) and titanium alkoxide-mediated transesterification. The gradient sequence can be catalytically controlled by tuning the kinetic balance of the two reactions. The tandem catalysis is one of the most efficient and versatile systems to produce amphiphilic gradient and sequence-controlled copolymers. Typically, methyl methacrylate (MMA) was polymerized as a starting monomer with a ruthenium catalyst and a chloride initiator in the presence of Ti(O*i*-Pr)$_4$ and molecular sieves (MS 4A) in poly(ethylene glycol) methyl ether (PEG-OH) as a solvent at 80 ^{o}C. Hydrophobic MMA was concurrently transesterified into hydrophilic PEG methacrylate (PEGMA) during LRP to give MMA/PEGMA gradient copolymers. The gradient sequence is directly determined by the instantaneous monomer composition changing from MMA alone to PEGMA-rich mixture in solution. Synchronized catalysis of LRP and transesterification thus affords gradient copolymers whose composition linearly changes from an initiating terminal to growing counterpart. Additionally, amphiphilic MMA/PEGMA gradient copolymers showed self-assembly, thermoresponsive, and thermal properties specific to the gradient sequence, distinct from amphiphilic random or block counterparts.

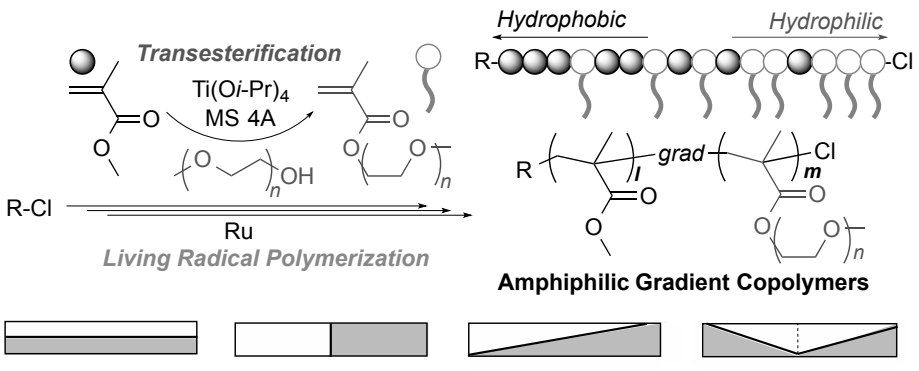

Introduction

Sequence of monomers and functional groups in polymers takes an important role to determine physical properties of functional polymeric materials. Gradient copolymers[1] are one class of sequence-controlled copolymers, where monomer composition continuously and gradually changes from an initiating terminal (α-end) to a growing counterpart (ω-end) along a polymer chain. Given such peculiar sequence distribution, gradient copolymers often show solid and solution properties distinct from corresponding random or block counterparts: *e.g.*, phase segregation behavior,[2] thermal/rheological properties,[3-5] compatibility,[6] contact angle,[7] micellization,[8-11] and lower critical solution temperature.[9,12] In particular, amphiphilic gradient copolymers consisting of hydrophobic and hydrophilic (and/or thermosensitive) monomers have continuous change of hydrophobic or hydrophilic properties, *i.e.*, local solvent affinity, along a chain, in contrast to amphiphilic segregated block or statistically distributed random copolymers. Thus, amphiphilic gradient sequence-controlled copolymers are expected to exhibit self-assembly behavior and thermoresponsive properties that are specific to the functional monomer sequences.[9-11,13-17]

For such functional gradient copolymers, the author has developed concurrent tandem catalysis of ruthenium-catalyzed living radical polymerization (LRP) and metal alkoxide [*e.g.,* $Al(O\textit{i}\text{-}Pr)_3$, $Ti(O\textit{i}\text{-}Pr)_4$]-catalyzed transesterification with methacrylates as monomers and alcohols as solvents.[18,19] This is a novel versatile system to synthesize gradient sequence-controlled copolymers, different from the conventional counterparts: 1) living copolymerization of two monomers with different reactivity (e.g., copolymerization of methacrylate and acrylate); 2) living copolymerization via continuous addition of a second monomer.[1,3,8,9] Compared with these, tandem system described above allows not only efficient and catalytic control of gradient monomer sequence but also easy process just using a single reaction vessel without monomer feed set-up (normally required in the latter method). More importantly, diverse alcohols and common methacrylates are applicable; this feature affords unlimited design of methacrylate-based gradient copolymers of different monomer combination and sequence for desired physical properties and functions.

The key in the tandem catalysis is in-situ generation of second monomers (R^2MA) via transesterification of an initially fed methacrylate (R^1MA) with alcohols (R^2OH, solvent) during LRP. Monomer composition in solution gradually changes from R^1MA to R^2MA-rich mixture; the instantaneous monomer composition in solution is directly reflected to the instantaneous composition of generating gradient copolymers. Perfectly synchronized catalysis of LRP (chain growth) and transesterification (monomer transformation; gradient composition) results in R^1MA/R^2MA gradient copolymers whose composition linearly changes from R^1MA (at α-end) to R^2MA (at ω-end). Importantly, transesterification takes place selectively for monomer esters

(R^1MA), while it does not occur for the copolymers [poly(R^1MA/R^2MA)] owing to steric hindrance around the pendant carbonyl groups. The formation of gradient copolymers requires such monomer selective transesterification. The author have already produced several gradient copolymers with unique properties. Typically, synchronized tandem catalysis with methyl methacrylate (MMA) and 1-dodecanol gave MMA/dodecyl methacrylate (DMA) gradient copolymers with very broad glass transition temperature range (T_g range: ~150 ^oC).[19] These polymers are expected to be useful for vibration or acoustic damping materials.[20,21] Owing to high functionality tolerance of LRP,[22,23] hydrophilic alcohols such as poly(ethylene glycol) methyl ether (PEG-OH) can be also employed in tandem catalysis.[18a] Thus, the combination of MMA and various PEG-OH (different oxyethylene unit number) would allow the diverse design and synthesis of amphiphilic gradient and sequence-controlled copolymers, revealing association and thermoresponsive properties dependent on the monomer sequence.

Given these features, in this chapter, the author deal with the precision synthesis of amphiphilic PEG-functionalized gradient copolymers via tandem catalysis of ruthenium-catalyzed LRP and titanium alkoxide-mediated transesterification with MMA and PEG-OH [$(CH_3(OCH_2CH_2)_nOH$; n = 1, 2, 4, 7.2 (average); M_n = 350, 11.8 (average); M_n = 550 (Scheme 1). Discussion is especially focused on the catalytic control of gradient sequence and sequence-dependent solution/solid properties. Importantly, MMA/PEGMA gradient copolymers have unique amphiphilic sequence: hydrophilic PEG pendant density gradually increased from the α-end to ω-end in a chain.

The author first investigated the control of kinetic balance between transesterification of MMA into PEGMA and LRP of the two monomers by tuning the concentration of Ti(O*i*-Pr)$_4$ with or without molecular sieves (MS) 4A. As a result, the author successfully produced various MMA/PEGMA gradient copolymers with different composition and sequence distribution. Perfectly synchronized catalysis of LRP and transesterification gave MMA/PEGMA gradient copolymers with linear composition change. PEG-OH derivatives with different oxyethylene number (n) were effective to control the hydrophilicity of gradient copolymers (Scheme 1a). A bifunctional initiator affords a MMA/PEGMA bidirectional gradient copolymer (Scheme 1b); the middle segment is more hydrophobic and hydrophilicity increased from the middle to both terminals. Sequential tandem catalysis of quantitative Ti-mediated transesterification, followed by ruthenium-catalyzed LRP, in turn allows the synthesis of MMA/PEGMA random or block copolymers (Scheme 1c).

Then, association properties of MMA/PEGMA gradient and related copolymers were evaluated in methanol or aqueous solutions by dynamic light scattering (DLS), focused on the effects of monomer sequence (random, random-gradient, gradient, block, bidirectional gradient). A series of MMA/PEGMA copolymers showed thermoresponsive solubility in aqueous media and

alcohols (2-propanol, methanol). The cloud points depended on composition and monomer sequence. The gradient copolymers further had broad glass transition temperature, where T_g was dependent on pendant oxyethylene units.

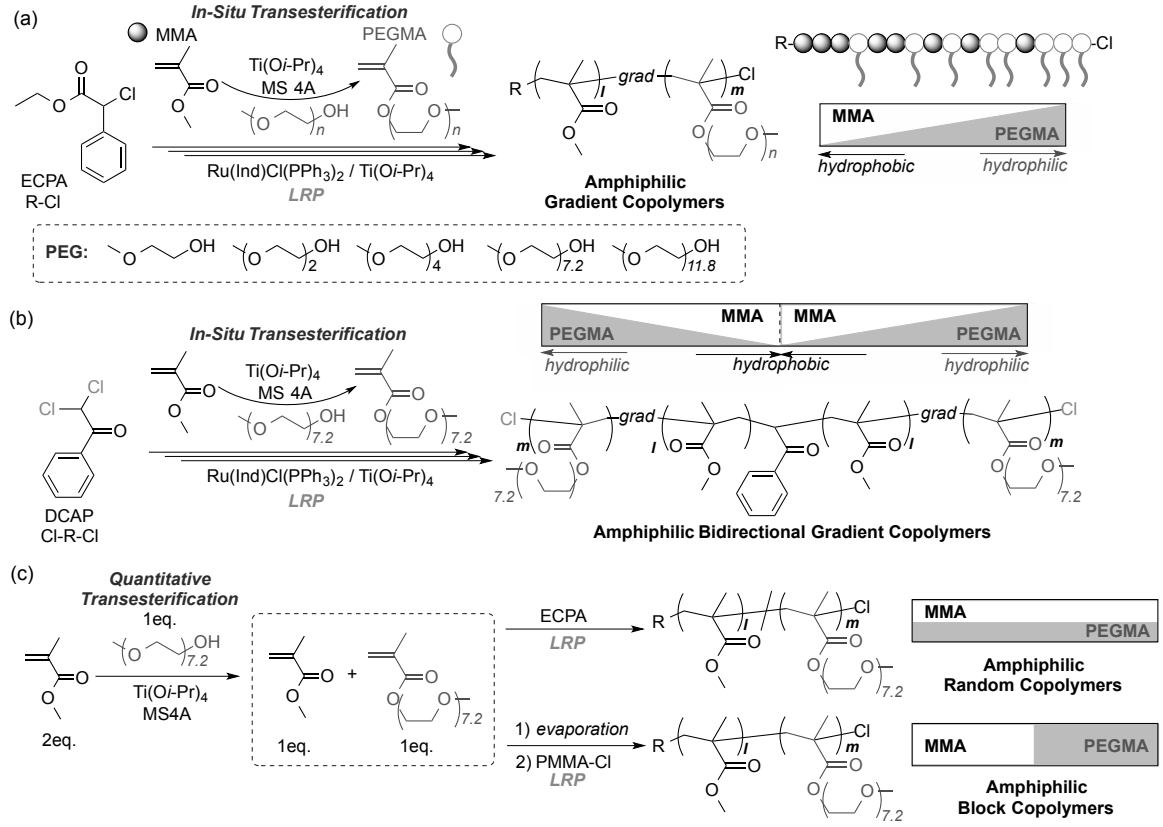

Scheme 1. Synthesis of MMA/PEGMA Amphiphilic (a) Gradient, (b) Bidirectional Gradient, (c) Random, and Block Copolymers via Tandem Catalysis of Living Radical Polymerization and Transesterification.

Experimental Section

Materials. Methyl methacrylate (MMA: TCI; purity >99.8%) and tetralin (1,2,3,4-tetrahydronaphthalene: Kishida Chemical; purity >98%; an internal standard for ^{1}H NMR analysis) were dried overnight with calcium chloride and distilled from calcium hydride under reduced pressure before use. Polyethylene glycol methyl ether (PEG-OH) (Aldrich, M_n = 350, 550), 2-methoxyethanol (MEG-OH) (Wako, purity >99%), 2-(2-methoxyethoxy)ethanol (DEG-OH) (Wako, purity >98%), tetra(ethylene glycol) monomethyl ether (TEG-OH) (TCI, purity >98%), Ti(O*i*-Pr)$_4$ (Aldrich, purity >97%), and *n*-Bu$_3$N (TCI, purity >98%) were degassed by triple vacuum-argon purge cycles before use. Ethyl 2-chloro-2-phenylacetate (ECPA: Aldrich; purity >97%) and 2,2-dichloroacetophenone (DCAP: TCI; purity >96%) were distilled under reduced pressure before use. Ru(Ind)Cl(PPh$_3$)$_2$ (Aldrich) was used as received and handled in a glove box under moisture- and oxygen-free argon (H_2O <1 ppm; O_2 <1 ppm). Toluene (solvent) was

purified by pashing it through a purification column (Glass Contour Solvent Systems: SG Water USA). Molecular sieves (MS) 4A (Wako) were baked with heat gun under reduced pressure before use.

Characterization. Molecular weight distribution (MWD) curves, M_n, and M_w/M_n ratio of polymers were measured by SEC in DMF containing 10 mM LiBr at 40 ^oC (flow rate: 1 mL/min) on three linear-type polystyrene gel columns (Shodex KF-805L: exclusion limit = 4×10^6; particle size = 10 mm; pore size = 5000 Å; 0.8 cm i.d. × 30 cm) that were connected to a Jasco PU-2080 precision pump, a Jasco RI-2031 refractive index detector, and a Jasco UV-2075 UV/vis detector set at 270 nm. The columns were calibrated against 10 standard poly(MMA) samples (Polymer Laboratories; M_n = 1000–1200000; M_w/M_n = 1.06–1.22). To remove unreacted monomers, PEG-OH, and catalyst residues, polymer samples for the evaluation of solution/solid properties were purified by preparative SEC [TOSOH TSKgel α-3000: particle size = 13 mm; 5.5 cm i.d. × 30 cm; exclusion limit = 9×10^4 g/mol; flow rate = 15 mL/min] connected to a Jasco PU-2086 precision pump, a Jasco RI-2013 refractive index detector, and a Jasco UV-2075 ultraviolet detector. ^1H NMR spectra were recorded in $CDCl_3$ and CD_2Cl_2 on a JEOL JNM-ECA500 spectrometer operating at 500.16 MHz. Dynamic light scattering (DLS) was measured on Otsuka Photal ELSZ-0 equipped with a semiconductor laser (wavelength: 658 nm) at 25 ^oC: [Polymer] = 10 mg/mL in methanol or acetone/H_2O (1/9, v/v). The measuring angle was 165° and the data was analyzed by CONTIN fitting method. Turbidity measurements of polymer solutions were conducted with Shimadzu UV-1800 in methanol, H_2O, and 2-propanol at 25 ^oC (optical path length = 1.0 cm). Differential scanning calorimetry (DSC) was performed for samples (ca. 5 mg weighed into an aluminum pan) under dry nitrogen flow on a DSC Q200 calorimeter (TA Instruments) equipped with a RCS 90 electric freezing machine. The polymer samples were heated to 150 ^oC at the rate of 10 ^oC/min and held at the temperature for 10 min to erase thermal history. Then, the samples were cooled to -80 ^oC at the rate of -10 ^oC/min and held at the temperature for 10 min, and again heated to 150 ^oC at the rate of 10 ^oC/min. The second heating runs were used for the thermal analysis of polymers in Figure 9 in result and discussion.

Polymerization. The synthesis of MMA/PEGMA copolymers was carried out by syringe technique under argon in baked glass tubes equipped with a three-way stopcock.

MMA/PEGMA gradient copolymer (entry 7 in Table 1)**.** A typical procedure for a gradient copolymer with MS 4A was given: MS 4A (1.0 g) was first placed and dried in a 30 mL glass tube under reduced pressure with heat gun. Into the tube, $Ru(Ind)Cl(PPh_3)_2$ (0.003 mmol, 2.33 mg) was charged, and toluene (1.15 mL), PEG-OH (M_n = 350) (1.32 mL), tetralin (0.04 mL), a 500 mM

toluene solution of Ti(O*i*-Pr)$_4$ (0.12 mL, Ti(O*i*-Pr)$_4$ = 0.06 mmol), MMA (3 mmol, 0.32 mL), and a 274 mM toluene solution of ECPA (0.05 mL, ECPA = 0.015 mmol) were added sequentially in that order at 25 °C under argon (the total volume of the reaction mixture: 3.0 mL). The glass tube was then placed in an oil bath kept at 80 °C. At predetermined intervals, the mixture was sampled with a syringe under argon, and the sampled solutions were cooled to –78 °C to terminate the reaction. The total monomer conversion, PEGMA content in monomer, and cumulative PEGMA content in polymer ($F_{cum,PEGMA}$) were directly determined by ^{1}H NMR measurements of the terminated reaction solution in $CDCl_3$ at 25 °C with tetralin as an internal standard. Instantaneous PEGMA content in polymer ($F_{inst,PEGMA}$) was estimated according to the following equation: $F_{inst,PEGMA}$ = [Conv.$_{total,\,i}$ x $F_{cum,PEGMA,\,i}$ - Conv.$_{total,\,i-1}$ x $F_{cum,PEGMA,\,i-1}$]/[Conv.$_{total,\,i}$ - Conv.$_{total,\,i-1}$], where Conv.$_{total}$ is the total conversion of both monomers. The quenched solutions were evaporated to dryness to give the crude product. To remove unreacted monomers, solvents, and catalyst residue, the product was purified by preparative SEC before characterization (^{1}H NMR, physical properties). SEC (DMF, PMMA std.): M_n = 51,700 g/mol; M_w/M_n = 1.46. ^{1}H NMR [500 MHz, CD_2Cl_2, 25 °C, δ = 5.33 $CDHCl_2$] δ 7.30–7.15 (aromatic), 4.18–3.98 (-COOC<u>H$_2$</u>CH$_2$O-), 3.75–3.62 (-COOCH$_2$C<u>H$_2$</u>O-), 3.62–3.38 (-OC<u>H$_2$</u>C<u>H$_2$</u>O-), 3.38–3.27 (-OC<u>H$_3$</u>), 2.08−1.68 (-C<u>H$_2$</u>C(CH$_3$)-), 1.25–0.68 (-CH$_2$C(C<u>H$_3$</u>)-). M_n (NMR, α) = 51400; DP_{MMA}/DP_{PEGMA} = 102/98; $F_{cum,PEGMA}$ = 49%.

MMA/PEGMA bidirectional gradient copolymer (entry 14 in Table 1)**.** SEC (DMF, PMMA std.): M_n = 41,700 g/mol; M_w/M_n = 1.36. ^{1}H NMR [500 MHz, CD_2Cl_2, 25 °C, δ = 5.33 $CDHCl_2$] δ 7.63–7.41 (aromatic), 4.20–3.96 (-COOC<u>H$_2$</u>CH$_2$O-), 3.75–3.62 (-COOCH$_2$C<u>H$_2$</u>O-), 3.62–3.38 (-OC<u>H$_2$</u>C<u>H$_2$</u>O-), 3.38–3.27 (-OC<u>H$_3$</u>), 2.08−1.68 (-C<u>H$_2$</u>C(CH$_3$)-), 1.25–0.68 (-CH$_2$C(C<u>H$_3$</u>)-). M_n (NMR, α) = 52100; DP_{MMA}/DP_{PEGMA} = 84/104; $F_{cum,PEGMA}$ = 54%.

MMA/PEGMA gradient random copolymer (entry 12 in Table 1)**.** SEC (DMF, PMMA std.): M_n = 40,400 g/mol; M_w/M_n = 1.35. ^{1}H NMR [500 MHz, CD_2Cl_2, 25 °C, δ = 5.33 $CDHCl_2$] δ 7.30–7.15 (aromatic), 4.87–4.77 (-COOC<u>H</u>(CH$_3$)$_2$), 4.18–3.98 (-COOC<u>H$_2$</u>CH$_2$O-), 3.75–3.62 (-COOCH$_2$C<u>H$_2$</u>O-), 3.62–3.38 (-OC<u>H$_2$</u>C<u>H$_2$</u>O-), 3.38–3.27 (-OC<u>H$_3$</u>), 2.08−1.67 (-C<u>H$_2$</u>C(CH$_3$)-), 1.26–0.68 (-CH$_2$C(C<u>H$_3$</u>)-). M_n (NMR, α) = 37000; $DP_{MMA}/DP_{PEGMA}/DP_{iPrMA}$ = 92/63/10; $F_{cum,PEGMA}$ = 38%.

MMA/DEGMA (PEGMA: n = 2) **gradient copolymer** (entry 3 in Table 1)**.** SEC (DMF, PMMA std.): M_n = 33,200 g/mol; M_w/M_n = 1.44. ^{1}H NMR [500 MHz, CD_2Cl_2, 25 °C, δ = 5.33 $CDHCl_2$] δ 7.30–7.15 (aromatic), 4.17–3.98 (-COOC<u>H$_2$</u>CH$_2$O-), 3.72–3.61 (-COOCH$_2$C<u>H$_2$</u>O-), 3.61–3.45 (-OC<u>H$_2$</u>C<u>H$_2$</u>O-), 3.38–3.28 (-OC<u>H$_3$</u>), 2.08−1.70 (-C<u>H$_2$</u>C(CH$_3$)-), 1.27–0.68 (-CH$_2$C(C<u>H$_3$</u>)-). M_n (NMR, α) = 29800; DP_{MMA}/DP_{DEGMA} = 119/94; $F_{cum,DEGMA}$ = 44%.

MMA/TEGMA (PEGMA: n = 4) **gradient copolymer** (entry 5 in Table 1)**.** SEC (DMF, PMMA std.): M_n = 25,600 g/mol; M_w/M_n = 1.39. ^{1}H NMR [500 MHz, CD_2Cl_2, 25 °C, δ = 5.33

$CDHCl_2$] δ 7.31–7.15 (aromatic), 4.90–4.75 (-COOC<u>H</u>$(CH_3)_2$), 4.18–3.98 (-COOC<u>H</u>$_2$$CH_2$O-), 3.75–3.62 (-$COOCH_2$C<u>H</u>$_2$O-), 3.62–3.38 (-OC<u>H</u>$_2$C<u>H</u>$_2$O-), 3.38–3.27 (-OC<u>H</u>$_3$), 2.08−1.68 (-C<u>H</u>$_2$C(CH_3)-), 1.25–0.68 (-CH_2C(C<u>H</u>$_3$)-). M_n (NMR, α) = 24000; $DP_{MMA}/DP_{TEGMA}/DP_{i\text{PrMA}}$ = 84/56/1; $F_{cum,TEGMA}$ = 39%.

MMA/PEGMA random copolymer. MS 4A (1.0 g) was first placed and dried in a 30 mL glass tube under reduced pressure with heat gun. In a 30 mL glass tube, Ru(Ind)Cl$(PPh_3)_2$ (0.003 mmol, 2.33 mg) was charged, and toluene (2.006 mL), PEG-OH (M_n = 350) (1.5 mmol, 0.49 mL), tetralin (0.04 mL), a 500 mM toluene solution of Ti(O*i*-Pr)$_4$ (0.12 mL, Ti(O*i*-Pr)$_4$ = 0.06 mmol) and MMA (3 mmol, 0.32 mL) were added sequentially in that order at 25 °C under argon (the total volume: 2.976 mL). The glass tube was placed in an oil bath kept at 80 °C. After 23 h, the solutions were cooled to –78 °C to terminate transesterification (yield: MMA/PEGMA/*i*PrMA = 45%/49%/6%, by ^{1}H NMR in $CDCl_3$ at r.t. with tetralin as an internal standard). Into the solution, a toluene solution of ECPA (622 mM, 0.024 mL, ECPA = 0.015 mmol) was then added at 25 °C under argon (the total volume: 3.0 mL). The glass tube was placed in an oil bath kept at 80 °C. After 66 h, the mixture was cooled to –78 °C to terminate the copolymerization (conv. MMA/PEGMA = 90%/90%). The quenched solution was evaporated to dryness to give the crude product. To remove unreacted monomers, solvents, and catalyst residue, the product was purified by preparative SEC. SEC (DMF, PMMA std.): M_n = 95400 g/mol; M_w/M_n = 1.51. ^{1}H NMR [500 MHz, CD_2Cl_2, 25 °C, δ = 5.33 $CDHCl_2$] δ 7.30–7.15 (aromatic), 4.90–4.75 (-COOC<u>H</u>$(CH_3)_2$), 4.15–3.99 (-COOC<u>H</u>$_2$$CH_2$O-), 3.75–3.62 (-$COOCH_2$C<u>H</u>$_2$O-), 3.62–3.38 (-OC<u>H</u>$_2$C<u>H</u>$_2$O-), 3.36–3.28 (-OC<u>H</u>$_3$), 2.08−1.68 (-C<u>H</u>$_2$C(CH_3)-), 1.25–0.68 (-CH_2C(C<u>H</u>$_3$)-). M_n (NMR, α) = 59100: $DP_{MMA}/DP_{PEGMA}/DP_{i\text{PrMA}}$ = 108/106/16; $F_{cum,PEGMA}$ = 46%.

MMA/PEGMA block copolymer. Into a 30 mL glass tube (A), Ru(Ind)Cl$(PPh_3)_2$ (0.003 mmol, 2.33 mg) was then charged, and toluene (0.955 mL), tetralin (0.04 mL), MMA (3 mmol, 0.32 mL), a 400 mM toluene solution of *n*-Bu_3N (0.075 mL, *n*-Bu_3N = 0.03 mmol), and a 274 mM toluene solution of ECPA (0.11 mL, ECPA = 0.03 mmol) were added sequentially in that order at 25 °C under argon (the total volume: 1.5 mL). The glass tube was placed in an oil bath kept at 80 °C. After 123 h, the polymerization reached 95% conversion (determined by ^{1}H NMR) to give PMMA-Cl (M_n = 13,500 g/mol; M_w/M_n = 1.09, by SEC in DMF with PMMA std.).

Into another 30 mL glass tube (B), MS 4A (1.0 g) was first placed and dried under reduced pressure with heat gun. Into the tube, toluene (4.06 mL), tetralin (0.08 mL), PEG-OH (M_n = 350) (3 mmol, 0.98 mL), MMA (6 mmol, 0.32 mL), and a 500 mM toluene solution of Ti(O*i*-Pr)$_4$ (0.24 mL, Ti(O*i*-Pr)$_4$ = 0.12 mmol) were added sequentially in that order at 25 °C under argon (the total volume: 6.0 mL). After 35h, MMA was transesterified into PEGMA and *i*PrMA (yield: MMA/PEGMA/*i*PrMA = 45%/49%/6%, determined by ^{1}H NMR). Then, the solution was

evaporated to remove volatile MMA and *i*PrMA. Into the tube including non-volatile PEGMA, toluene (3.2 mL) was added to make a toluene solution of PEGMA (PEGMA = 2.9 mmol, total volume: 4.5 mL).

Into the tube (A), the toluene solution of PEGMA (4.5 mL, PEGMA = 2.9 mmol) was added under argon. The mixture was placed at 80 ^{o}C. After 30 h, the solution was cooled to –78 °C to terminate the reaction (conv. 93%, determined by ^{1}H NMR). The quenched solution was evaporated to dryness. To remove unreacted monomers, solvents, and catalyst residue, the resulting crude was purified by preparative SEC. SEC (DMF, PMMA std.): M_n = 46,800 g/mol; M_w/M_n = 1.34. ^{1}H NMR [500 MHz, CD_2Cl_2, 25 ^{o}C, δ = 5.33 $CDHCl_2$] δ 7.30–7.15 (aromatic), 4.15–4.00 (-COOC$\underline{H}_2$CH_2O-), 3.73–3.62 (-COOCH_2C$\underline{H}_2$O-), 3.62–3.39 (-OC$\underline{H}_2$C$\underline{H}_2$O-), 3.37–3.28 (-OC$\underline{H}_3$), 2.07−1.68 (-C$\underline{H}_2$C(CH_3)-), 1.25–0.68 (-CH_2C(C$\underline{H}_3$)-). M_n (NMR, α) = 43900: DP_{MMA}/DP_{PEGMA} = 99/81; $F_{cum,PEGMA}$ = 45%.

Results and Discussion

1. Amphiphilic MMA/PEGMA Gradient Copolymers via Synchronized Tandem Catalysis

The author investigated the synthesis of amphiphilic gradient copolymers via synchronized tandem catalysis of ruthenium-catalyzed living radical polymerization (LRP) and in-situ transesterification of hydrophobic methyl methacrylate (MMA) with hydrophilic poly(ethylene glycol) methyl ether [PEG-OH: ($CH_3(OCH_2CH_2)_n$OH; n = 7.2 (average); M_n = 350) (Scheme 1). Ti(O*i*-Pr)$_4$ was employed as a catalyst for transesterification because of its high activity and compatibility (as co-catalyst) in ruthenium-catalyzed LRP.[24] The author further utilized molecular sieves 4A (MS 4A) to remove methanol generating from in-situ transesterification of MMA; this technique is effective to induce transesterification up to high conversion.[19] Ideally, hydrophobic MMA is transformed into hydrophilic PEGMA during LRP, where monomer composition in solution gradually changes from MMA alone to PEGMA-rich mixture. Transesterification synchronized with LRP is thus important to produce MMA/EGMA gradient copolymers. In order to control the kinetic balance of LRP and transesterification, the author examined various concentration of Ti(O*i*-Pr)$_4$ (10, 20, 30, and 40 mM) coupled with MS 4A (Table 1, entries 6-9). As a result, 20 mM of Ti(O*i*-Pr)$_4$ with MS 4A allowed perfect synchronization of LRP and transesterification (entry 7).

MMA (2 M) was polymerized with a Ru(Ind)Cl(PPh_3)$_2$ catalyst and a chloride initiator (ethyl 2-chloro-2-phenylacetate: ECPA) in the presence of Ti(O*i*-Pr)$_4$ (20 mM) and MS 4A (0.33 g/mL) in a toluene/PEG-OH (M_n = 350, 1.4 M) (1/1, v/v) mixed solvent at 80 ^{o}C (Table 1, entry 7, Figure 1). The total monomer conversion and PEGMA content in monomer (100 x $[PEGMA]_t/[MMA$ +

PEGMA]$_t$) were analyzed by ^{1}H NMR measurements of polymerization mixtures that were sampled at predetermined periods. PEGMA content in monomer was determined from the area ratio of the methylene protons of PEGMA adjacent to ester (4.3 ppm) to all olefin protons of MMA and in-situ generating PEGMA (5.6, 6.1 ppm). As shown in Figure 1a (dash line), MMA was efficiently transesterified into PEGMA during polymerization: PEGMA content in monomer increased from 0% to almost 100%. The transesterification of MMA into PEGMA was perfectly synchronized with the consumption of both MMA and generating PEGMA for polymerization (total conversion: solid line). PEGMA content in monomer thus proportionally increased with total conversion (Figure 1b). Copolymerization of the two monomers smoothly reached to 94% in 35 h to give well-controlled polymers with relatively narrow molecular weight distribution (M_n = 51700, M_w/M_n = 1.46, Figure 1d), confirmed by size exclusion chromatography (SEC). The SEC curves of products clearly shifted to high molecular weight with increasing conversion, demonstrating that Ti-mediated transesterification of MMA with PEG-OH does not interfere with controllability of LRP.

Table 1. Synthesis of MMA/PEGMA Gradient Copolymers via Concurrent Tandem Living Radical Polymerization[a]

Entry	PEG-OH (n)	MS (g/mL)	[Ti(O*i*-Pr)$_4$] (mM)	Time (h)	Conv[b] (%)	M_n[c] (GPC)	M_w/M_n[c]	M_n[d] (NMR)	$F_{cum,\ PEGMA}$[e] (%)
1	1	0.33	20	38	95	28000	1.58	-	38
2	1	0.33	30	21	92	29700	1.45	-	49
3	2	0.33	20	38	96	33200	1.44	29800	44
4	4	0.33	20	27	92	34600	1.49	-	30
5	4	0.33	40	23	96	25600	1.39	24000	39
6	*7.2*	0.33	10	48	94	42400	1.36	-	16
7	*7.2*	0.33	20	35	94	51700	1.46	51400	49
8	*7.2*	0.33	30	24	90	64900	1.42	-	59
9	*7.2*	0.33	40	24	92	68000	1.44	-	63
10	*7.2*	-	40	21	89	35600	1.35	-	36
11	*7.2*	-	60	23	96	34500	1.38	-	38
12	*7.2*	-	80	23	88	40400	1.35	37000	38
13	*11.8*	0.33	40	11	79	60100	1.51	-	45
14	*7.2*	0.33	20	23	89	41700	1.36	52100	54

[a][MMA]/[ECPA (entries 1-13) or DCAP (entry 14)]/[Ru(Ind)Cl(PPh$_3$)$_2$]/[Ti(O*i*-Pr)$_4$] = 1000/5/1/10-80 mM with or without MS 4A in toluene/PEG-OH [CH$_3$(OCH$_2$CH$_2$)$_n$OH: n = 1, 2, 4, *7.2*, and *11.8*] (1/1, v/v) at 80 °C. [b]Total monomer conversion determined by ^{1}H NMR with an internal standard (tetralin). [c]Determined by SEC in DMF with a PMMA standard calibration. [d]Number average molecular weight determined by ^{1}H NMR. [e]Cumulative PEGMA content ($F_{cum,PEGMA}$) determined by ^{1}H NMR.

Cumulative PEGMA content in polymers ($F_{cum,PEGMA}$) was analyzed by ^{1}H NMR measurements of polymerization mixtures that were sampled at predetermined periods. $F_{cum,PEGMA}$ against total monomer conversion was first determined with methylene protons of polymerized PEGMA adjacent to the ester units (4.2 – 4.0 ppm). $F_{cum,PEGMA}$ values were then plotted as a function of normalized chain length (Figure 1c, blue). The normalized chain length is defined as DP_t/DP_{final} for living copolymers: DP_t = $[MMA]_0$ × (total conversion/100)/$[ECPA]_0$; DP_{final} = $[MMA]_0$ × (total final conversion/100)/$[ECPA]_0$. Both $F_{cum,PEGMA}$ and the instantaneous PEGMA content ($F_{inst.PEGMA}$) calculated therefrom[1,18,19] linearly increased with normalized chain length (Figures 1c). $F_{inst.PEGMA}$ is consistent with PEGMA content in monomer against monomer conversion (Figures 1c and 1b). This indicates that the gradient copolymer composition is directly determined by the instantaneous monomer composition in polymerization solution, which further indicates that MMA and PEGMA have close monomer reactivity in living radical copolymerization.

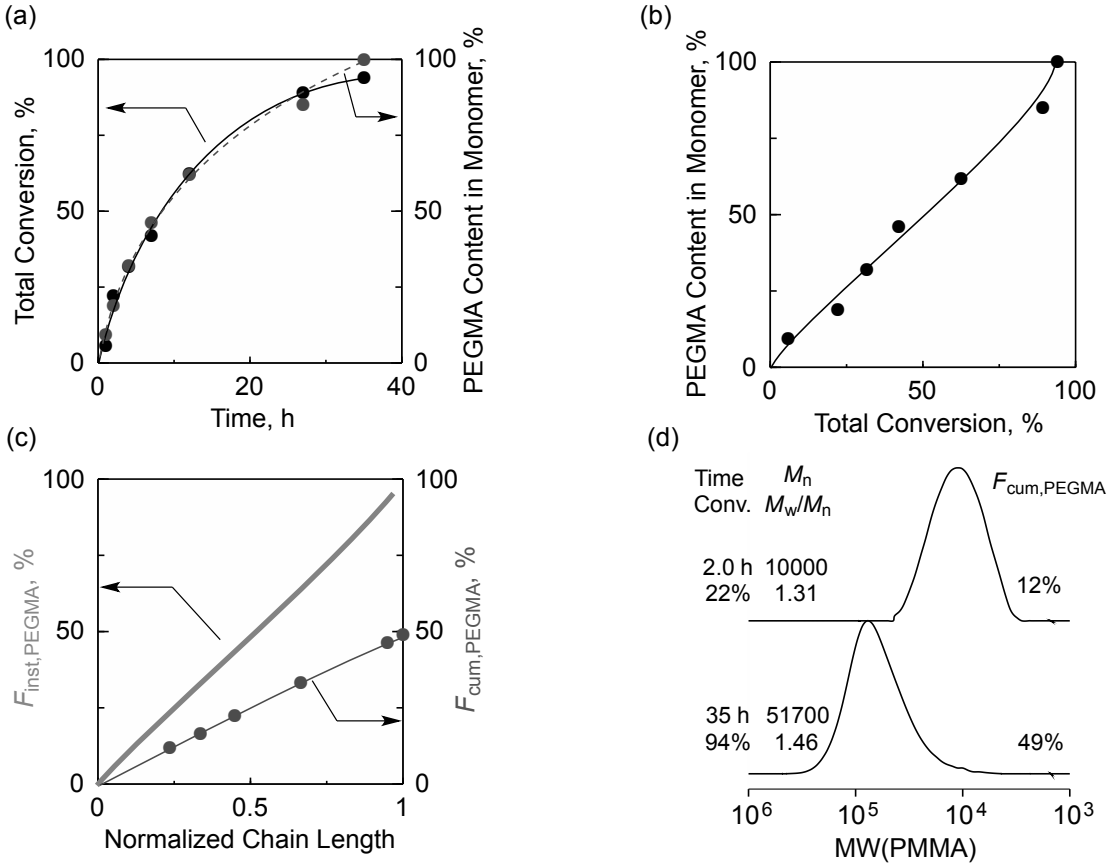

Figure 1. Synthesis of MMA/PEGMA gradient copolymers via concurrent tandem catalysis: [MMA]/[ECPA]/[Ru(Ind)Cl(PPh_3)$_2$]/[Ti(O*i*-Pr)$_4$] = 1000/5/1/20 mM in toluene/PEG-OH (M_n = 350) (1/1, v/v) with MS 4A (0.33 g/mL) at 80 °C. (a) total monomer conversion and PEGMA content in monomer. (b) PEGMA content in monomer as a function of total conversion. (c) cumulative ($F_{cum,PEGMA}$) and instantaneous ($F_{inst,PEGMA}$) PEGMA content in products. (d) SEC curves of products.

After purification by preparative SEC (for removal of monomer, alcohol and catalyst residue), the gradient copolymer was analyzed by ^{1}H NMR spectroscopy (Figure 2). The polymer consisted of MMA, PEGMA ($F_{cum,PEGMA}$ = 49%), and a tiny amount of *i*-PrMA (< 1 %) that arose from the transesterification of MMA with isopropanol from Ti(O*i*-Pr)$_4$. The number average molecular weight [M_n(NMR)] was determined to be 51400, from the area ratio of methylene protons of PEG pendants (*d*: 4.2 – 4.0 ppm), methylene and methyl protons of all pendants (*e*, *c*, *f*, *g*: 3.7 – 3.3 ppm), and the aromatic protons of the ECPA initiating terminal (*i*: 7.3 – 7.1 ppm, α-end).

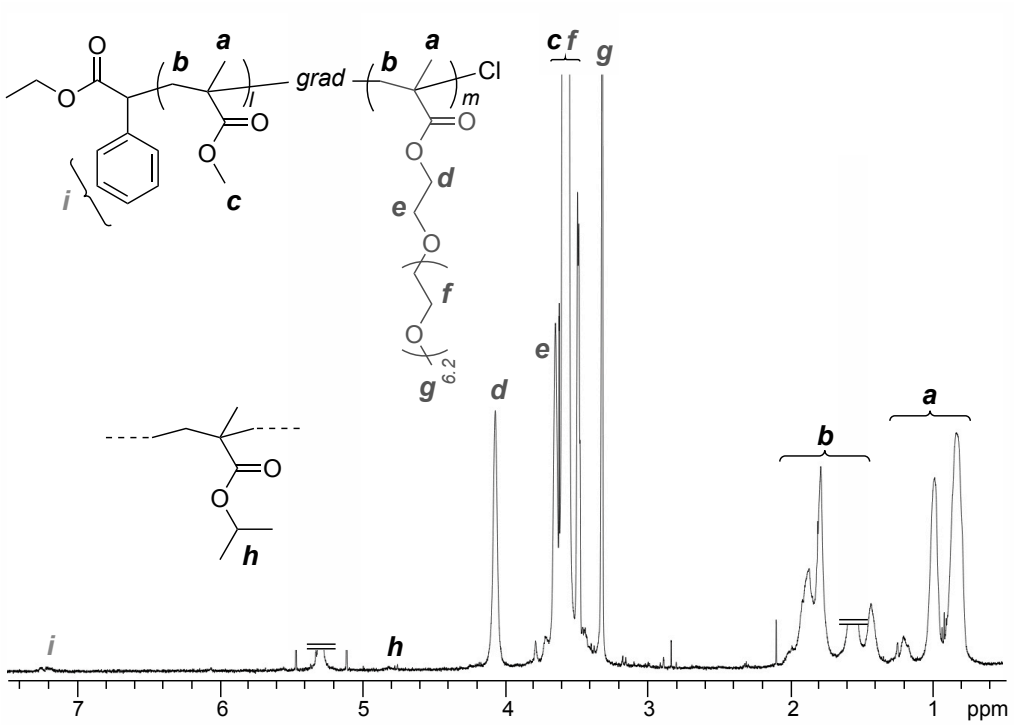

Figure 2. ^{1}H NMR spectrum of a MMA/PEGMA gradient copolymer (entry 7, Table 1) in CD_2Cl_2 at 25 ^oC.

2. Catalytic Control of Gradient Sequence

As described above, the combination of 20 mM Ti(O*i*-Pr)$_4$ with MS 4A induced perfectly synchronized transesterification with LRP to give a MMA/PEGMA gradient copolymer with linear composition change (entry 7). In contrast, the tandem catalysis of slower or faster transesterification than LRP is also effective to modulate gradient sequence of copolymers. Thus, The author analyzed PEGMA content in monomer (transesterification) and gradient sequence of copolymers ($F_{inst,PEGMA}$) obtained from the other conditions: 10, 30, and 40 mM Ti with MS 4A (entries 6, 8, 9, Figure 3a-c). In all cases, well-controlled polymers were obtained (Table 1, Figure S1). Ti(O*i*-Pr)$_4$ of 10 mM (low Ti concentration) induced slower transesterification than LRP (Figure 3a) to give a MMA/PEGMA gradient copolymer whose PEGMA composition ($F_{inst,PEGMA}$) more gently increased than that with Ti of 20 mM (Figure 3c). In contrast, higher Ti(O*i*-Pr)$_4$ concentration systems (30 or 40 mM) accelerated transesterification against LRP (Figures 3b) to

produce MMA/PEGMA gradient copolymers with high PEGMA content even around the initiating terminal (Figure 3c). The cumulative PEGMA contents in final gradient copolymers increased with Ti(O*i*-Pr)$_4$ concentration from 10 to 40 mM ($F_{cum,PEGMA}$ = 16, 49, 59, and 63 %). Importantly, the Ti concentration mainly affects the kinetics and yield of transesterification and is almost independent of kinetics and controllability of LRP. Thus, adjusting Ti(O*i*-Pr)$_4$ concentration allows conveniently control of the gradient sequence of MMA/PEGMA copolymers.

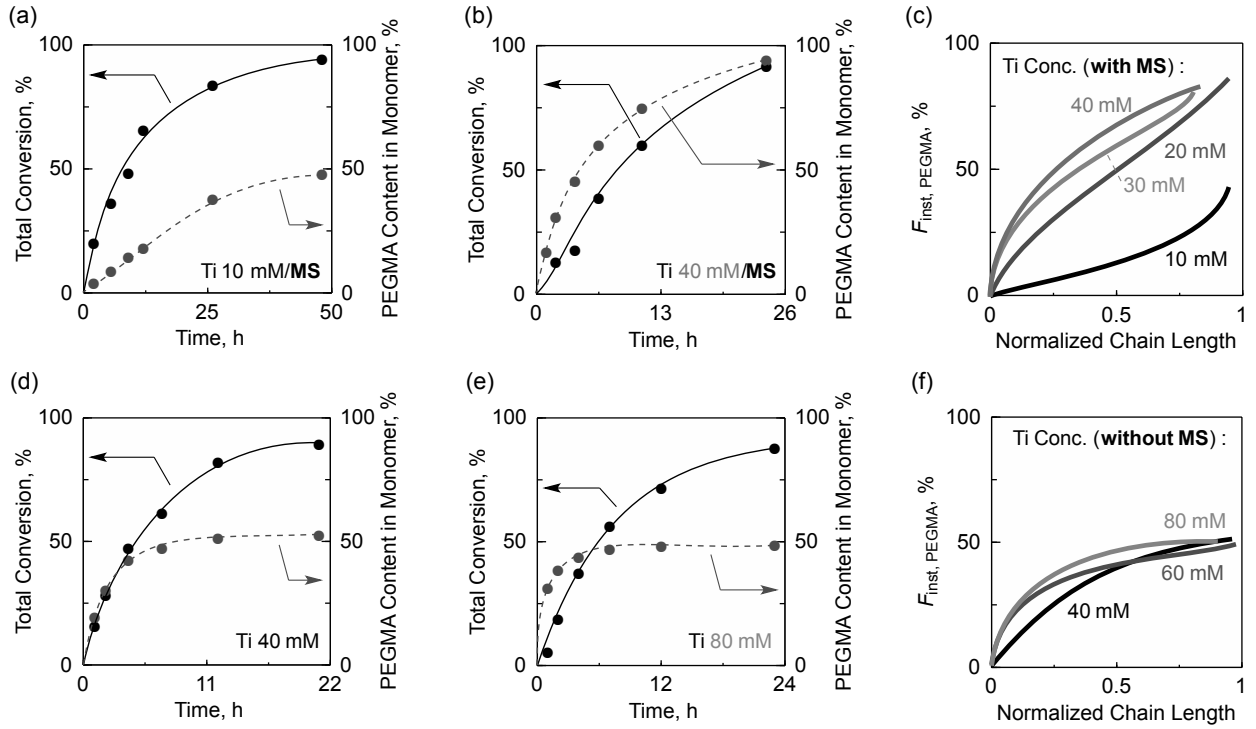

Figure 3. Effects of Ti(O*i*-Pr)$_4$ catalyst concentration and molecular sieves (MS 4A) on the gradient sequence of copolymers obtained from concurrent tandem LRP with in-situ transesterification: [MMA]/[ECPA]/[Ru(Ind)Cl(PPh$_3$)$_2$]/[Ti(O*i*-Pr)$_4$] = 1000/5/1/10 - 80 mM in toluene/PEG-OH (M_n = 350) (1/1, v/v) with or without MS 4A (0.33 g/mL) at 80 ^oC. Total monomer conversion and PEGMA content in monomer as a function of time: (a) 10 mM or (b) 40 mM Ti with MS 4A; (d) 40 mM or (e) 80 mM Ti without MS 4A. Instantaneous PEGMA composition in copolymers obtained (c) with or (f) without MS 4A as a function of normalized chain length.

In contrast, Ti-catalyzed transesterification of MMA into PEGMA in the absence of MS 4A was always saturated at around 50% PEGMA content in monomer after the middle stage of polymerization even using high Ti concentration (40 - 80 mM) (Figures 3d,e, Table 1 entries 10-12). The cumulative PEGMA content ($F_{cum,PEGMA}$) in final products was almost constant (36 – 38%) independent of Ti concentration. The constant PEGMA content is owing to the equilibrium of transesterification; in this stage, generating MeOH from MMA is almost the same amount of

remaining PEG-OH because of no use of MS 4A. Typically with 80 mM Ti, $F_{inst,PEGMA}$ (PEGMA composition in polymer) smoothly increased to approximately 50% until the middle point of the polymer chain and then virtually kept constant at 50% until Cl terminal (Figure 3f). Interestingly, this means the one-pot formation of a block copolymer consisting of a MMA/PEGMA gradient segment (from the α-end to the middle) and random counterpart (from the middle to the ω-end). Thus, this tandem catalysis is versatile to design MMA/PEGMA amphiphilic gradient copolymers with different gradient sequence and composition.

3. Amphiphilicity Control with PEG-OH

Amphiphilic properties of MMA/PEGMA gradient copolymers can be controlled not only by the composition but also with hydrophilic PEG length (oxyethylene number: n). Thus, various PEG-OH derivatives [$CH_3(OCH_2CH_2)_nOH$: n = 1, 2, 4, and 11.8 (average; M_n = 550)] were used as co-solvent in ruthenium-catalyzed tandem polymerization of MMA with Ti(O*i*-Pr)$_4$ (20-40 mM) and MS 4A in toluene/PEG-OH (1/1, v/v) (Table 1, entries 1-5, 13, Figures 4). In all PEG-OH [n = 1, 2, 4, and 11.8 (average)], transesterification of MMA into corresponding PEGMA was synchronized with LRP to give well-controlled MMA/PEGMA gradient copolymers (Figure 4). Here, Ti(O*i*-Pr)$_4$ concentration was optimized because the kinetics of LRP and transesterification were dependent on PEG-OH species.

Using Ti(O*i*-Pr)$_4$ of 20 mM, 2-(2-methoxyethoxy) ethanol (PEG-OH: n = 2) induced transesterification perfectly synchronized with LRP (Figure 4b) as well as PEG-OH (n = *7.2*) to produce a MMA/PEGMA (n = 2) gradient copolymer with linear composition change (Figure 4e). In contrast, transesterification of MMA with 2-methoxyethanol (PEG-OH: n = 1) or tetraethylene glycol monomethyl ether (PEG-OH: n = 4) is slightly slower than LRP (Figure 4a, c), resulting in corresponding gradient copolymers with smaller $F_{inst,PEGMA}$ than those obtained from PEG-OH (n = 2, *7.2*) (Figure 4e). We estimated half-life period of MMA ($T_{1/2}$: reaction time for 50% yield of PEGMA) in in-situ transesterification of MMA with PEG-OH (n = 1, 2, 4, and 7.2). The initial volume of PEG-OH was constant in mixed solvents (toluene/PEG-OH = 1/1, v/v), while the molar concentration is different [n = 1 (5.6 M), 2 (3.7 M), 4 (2.3 M), 7.2 (1.4 M)]. The half-life period of MMA depended on the oxyethylene number (n) and increased in this order: $T_{1/2}$ (n) = 8.3 h (7.2) < 9.7 h (2) < 12 h (4) < 13 h (1). Full synchronization of transesterification and LRP with PEG-OH (n = 1, 4) was achieved with increased Ti concentration (30 or 40 mM) (Table 1 entries 2 and 5). A longer PEG-OH [n = *11.8* (average)] required high concentration Ti (40 mM) for synchronized transesterification because LRP was faster than that with other PEG-OH derivatives (Table 1 entry 13, Figure 4d). Independent of PEG chain length (n), $F_{inst,PEGMA}$ well corresponds to PEGMA content in monomers that is estimated from time-conversion plots (Figure 4). Thus,

the gradient sequence distribution of copolymers is determined by PEGMA content in monomer that seamlessly changes during tandem catalytic polymerization.

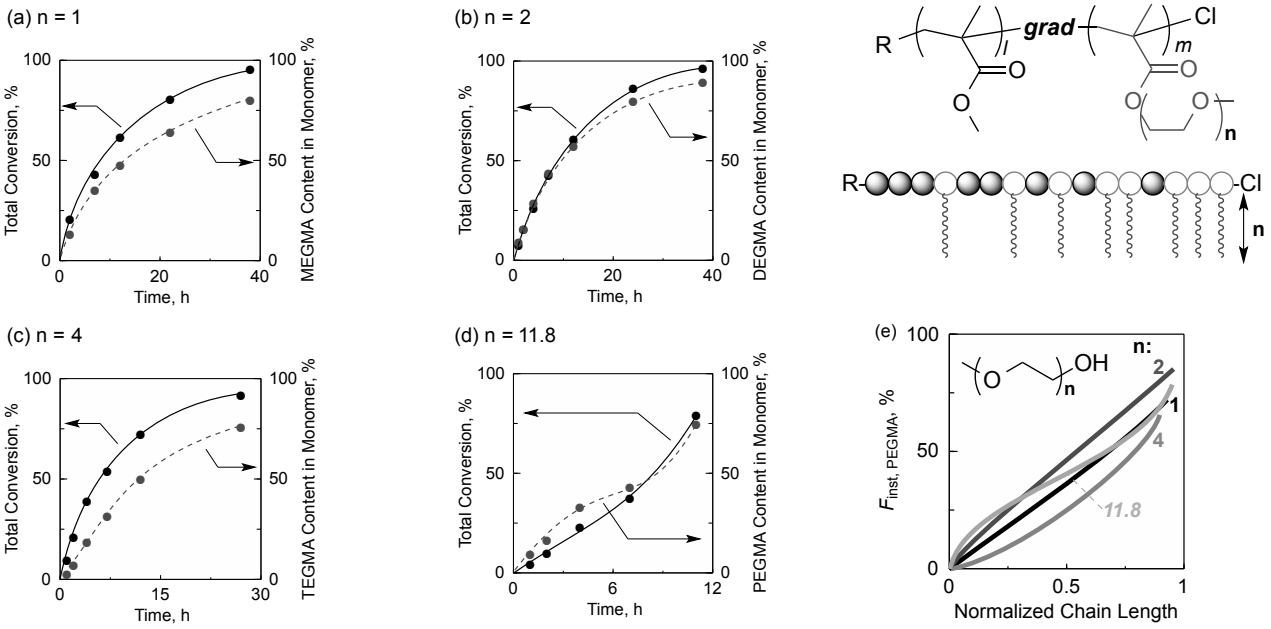

Figure 4. Synthesis of MMA/PEGMA gradient copolymers via concurrent tandem catalysis with various PEG-OH [$CH_3(OCH_2CH_2)_nOH$: n = 1, 2, 4, *11.8* (M_n = 550)]: [MMA]/[ECPA]/[Ru(Ind)Cl(PPh_3)$_2$]/[Ti(O*i*-Pr)$_4$] = 1000/5/1/20 (n = 1, 2, 4) or 40 (n = *11.8*) mM in toluene/PEG-OH (1/1, v/v) with MS 4A (0.33 g/mL) at 80 ^oC. (a)-(d) total monomer conversion and PEGMA content in monomer as a function of time: (a) n = 1 (b) 2 (c) 4 (d) *11.8*. (e) Instantaneous PEGMA composition in copolymers obtained with each alcohol.

4. Amphiphilic Bidirectional Gradient Copolymers

Amphiphilic bidirectional gradient copolymers were designed by tandem LRP of MMA with a bifunctional chloride initiator (2,2-dichloroacetophenone: DCAP) and PEG-OH (*n* = 7.2) (Figures 5). The copolymers have unique gradient sequence: hydrophilic PEGMA content gradually increased from the middle point of the polymer chain to both Cl (growing) terminals. Thus, the central part is more hydrophobic, while the both terminal segments are more hydrophilic. For this, MMA was polymerized with Ru(Ind)Cl(PPh_3)$_2$ and DCAP in the presence of Ti(O*i*-Pr)$_4$ (20 mM) in toluene/PEG-OH (*n* = 7.2, M_n = 350) with MS 4A at 80 ^oC. Transesterification was fully synchronized with LRP of MMA and in-situ generating PEGMA to provide a well-controlled MMA/PEGMA bidirectional gradient copolymer in high yield (Total conversion = 89%, M_n = 41700, M_n/M_w = 1.36, $F_{cum,PEGMA}$ = 54%, Table 1, entry14).

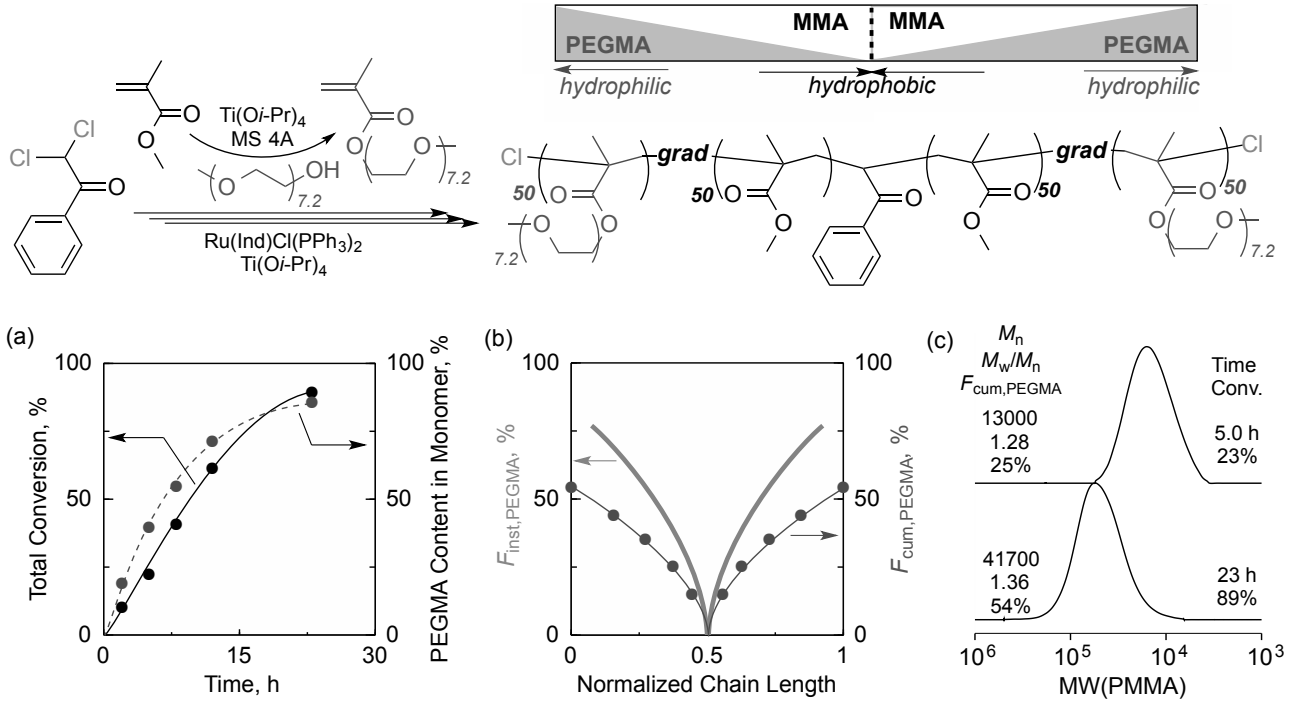

Figure 5. Synthesis of a MMA/PEGMA bidirectional gradient copolymer via concurrent tandem catalysis with 2,2-dichloroacetophenone (DCAP): [MMA]/[DCAP]/[Ru(Ind)Cl(PPh_3)$_2$]/[Ti(O*i*-Pr)$_4$] = 1000/5/1/20 mM in toluene/PEG-OH (M_n = 350) (1/1, v/v) with MS 4A (0.33 g/mL) at 80 ^oC.

6. Amphiphilic Random or Block Copolymers via Sequential Tandem Catalysis

Tandem catalysis of transesterification and LRP is effective to synthesize wide range of sequence-controlled copolymers including not only gradient but also random and block monomer sequence.[18] Thus, synthesis of amphiphilic random or block copolymers was examined by sequential tandem catalysis of quantitative transesterification of MMA with PEG-OH and LRP of the generating monomers (Scheme 2, experimental section).

For this, transesterification of MMA with PEG-OH (n = *7.2*) was conducted in the presence of Ti(O*i*-Pr)$_4$ (20 mM), MS 4A (0.33 g/mL), and Ru(Ind)Cl(PPh_3)$_2$ (a catalyst for subsequent LRP) at 80 ^oC. The molar ratio of MMA and PEG-OH was set as 2/1 ([MMA]$_0$/[PEG-OH]$_0$). MMA was transformed into PEGMA to give a mixture of MMA/PEGMA/*i*PrMA (45%/49%/6%, determined by ^1H NMR). It should be noted that the fed PEG-OH was quantitatively consumed to form PEGMA. The formation of a small amount of *i*PrMA is due to transesterification of MMA with isopropanol from the Ti catalyst. Into the monomer mixture, a chloride initiator (ECPA) was directly added to start random copolymerization (Scheme 2b), giving a MMA/PEGMA random copolymer (**R1**: M_n = 95400, M_w/M_n = 1.51, M_n (NMR) = 59100, $DP_{MMA}/DP_{PEGMA}/DP_{iPrMA}$ = 108/106/16, $F_{cum,PEGMA}$ = 46%), while the random copolymer partially included *i*PrMA units.

For block copolymerization, a monomer mixture of MMA/PEGMA/*i*PrMA obtained from with quantitative transesterification was evaporated to remove volatile MMA and *i*PrMA (Scheme 2a). The resulting PEGMA was directly utilized as a monomer for block copolymerization with a chlorine-capped poly(methyl methacrylate) (PMMA-Cl: M_n = 13500, M_w/M_n = 1.09) to produce a well-controlled MMA/PEGMA block copolymer (**B1**: M_n = 46800, M_w/M_n = 1.34, M_n (NMR) = 43900, DP_{MMA}/DP_{PEGMA} = 99/81, $F_{cum,PEGMA}$ = 45%, Scheme 2c).

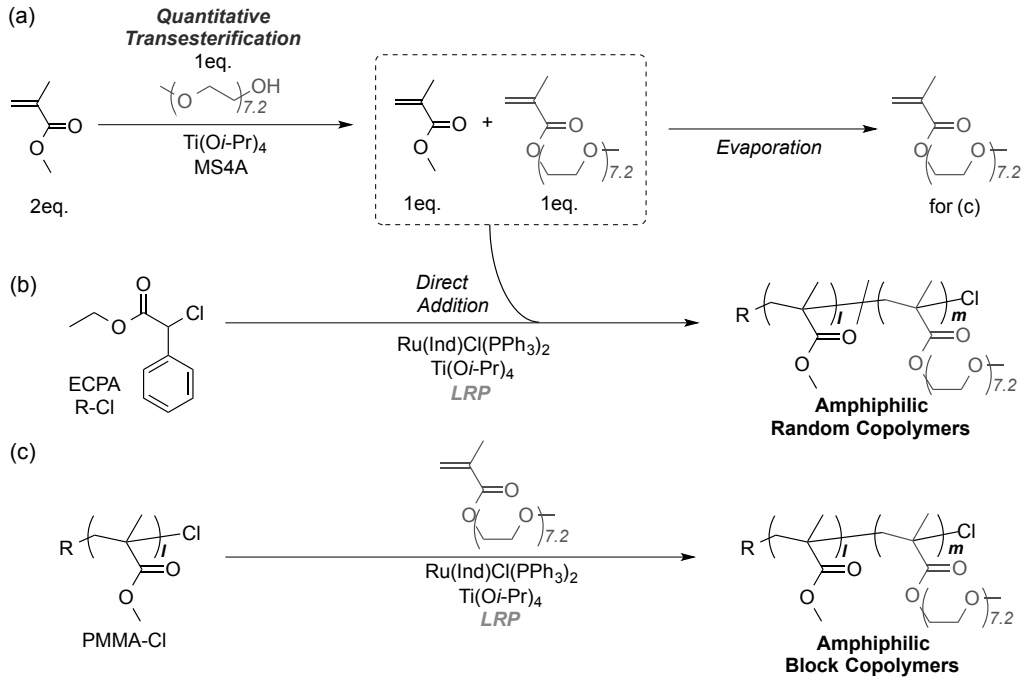

Scheme 2. Synthesis of Amphiphilic (b) Random or (c) Block Copolymers via Sequential Tandem Catalysis of (a) Quantitative Transesterification and LRP.

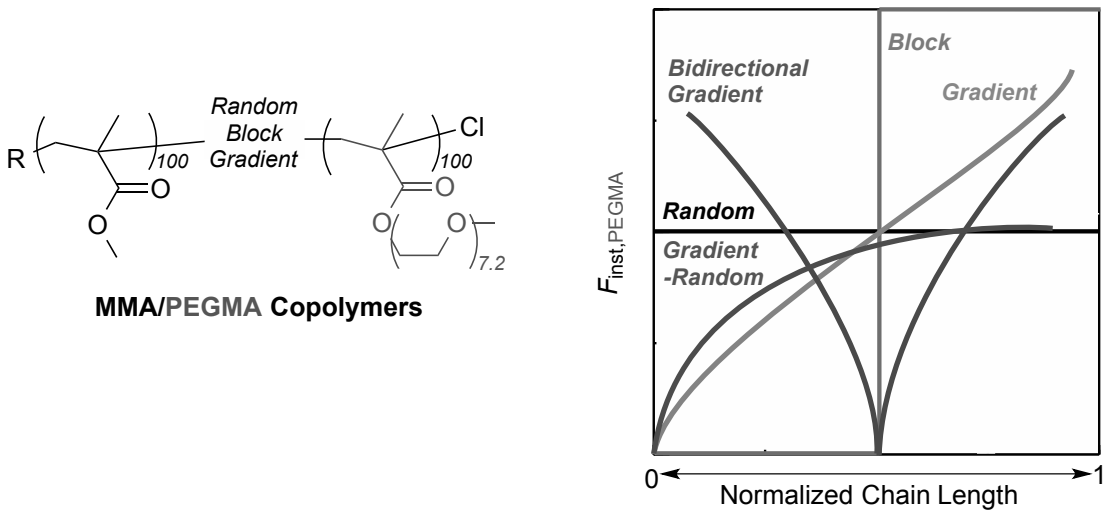

Figure 6. PEGMA sequence distribution of MMA/PEGMA random, gradient random, gradient, block, and bifunctional gradient copolymers.

7. Self-Assembly of Amphiphilic Copolymers

Various amphiphilic copolymers with different monomer sequence were successfully obtained from tandem catalysis of LRP and transesterification. Figure 6 summarized the sequence distribution of PEGMA ($F_{inst,PEGMA}$) against normalized chain length for the following copolymers: gradient (entry 7 Table 1), gradient-random (entry 12, Table 1), bidirectional gradient (entry 14, Table 1), random (**R1**), and block (**B1**). The five samples have almost constant DP (~200) and PEGMA composition ($F_{cum,PEGMA}$ = ~50). The monomer sequence would affect self-assembly (micellization) and thermoresponsive properties in solution and thermal properties in bulk.

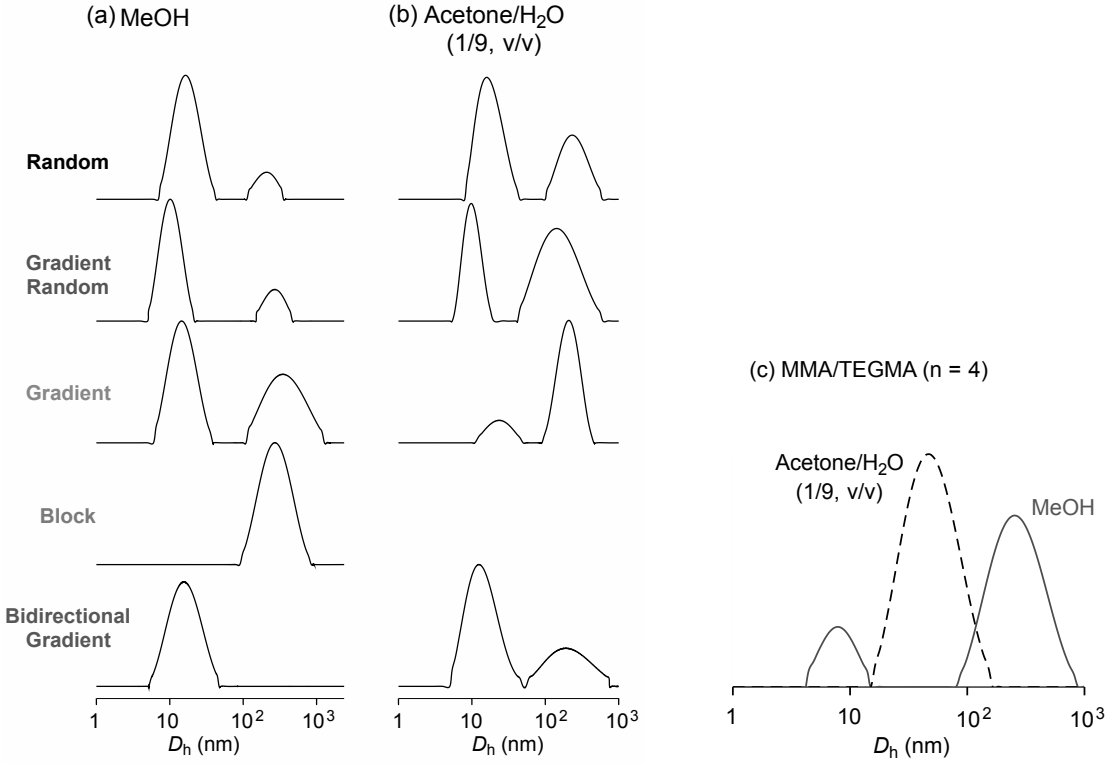

Figure 7. DLS intensity size distribution of MMA/PEGMA copolymers (random, gradient random, gradient, block, and bidirectional) in (a) methanol or (b) acetone/H_2O (1/9, v/v) (c) MMA/TEGMA gradient copolymers (Table 1, entry 5) in methanol or acetone/H_2O (1/9, v/v) at 25 ^oC: [Polymer] = 10 mg/mL.

The author evaluated the self-assembly behavior of the five amphiphilic copolymers in methanol or acetone/H_2O (1/9, v/v) mixture (Figure 7). The solutions were analyzed by dynamic light scattering (DLS). Methanol is a good solvent for poly(PEGMA) segment but a poor solvent for poly(MMA) counterpart. In order to investigate the effects of sequence distribution on self-assembly in organic media, methanol was utilized at first. All of the copolymers are easily soluble in methanol (10 mg/mL) at 25 ^oC. As shown in Figure 7a, random, gradient-random, gradient, and bidirectional gradient copolymers, mainly or only, had small size distribution of

hydrodynamic radius (R_h) below 10 nm (the volume fraction: random >99%; gradient-random 99%; gradient 96%, Table 2) though the three samples showed bimodal light scattering intensity size distribution. This suggests that these four samples should be unimolecularly solubilized in methanol or form self-folding unimer micelles or small nanoaggregates via the self-assembly of MMA-rich segments.[17] In contrast, the MMA/PEGMA block copolymer formed large micelles (R_h = 150 nm) via the aggregation of the PMMA homo-segment. These results indicate that, in methanol, MMA/PEGMA gradient sequence copolymers (gradient, gradient-random, and bidirectional gradient) have properties similar to a corresponding random counterpart.[11] A more hydrophobic MMA/PEGMA (n = 4) gradient copolymer with a shorter hydrophilic pendants clearly include large size aggregates (R_h = 146 nm, volume fraction: 37%, Table 2, Figure 7c), compared with MMA/PEGMA (n = *7.2*) counterpart.

Table 2. Solution Properties of Amphiphilic Copolymers

entry	sequence (sample code)	PEG (n)	R_h in MeOH[a] (nm)	R_h in H_2O[a] (nm)	Cp in H_2O[b] (^oC)	Cp in *i*PrOH[b] (^oC)	Cp in MeOH[b] (^oC)
1	random (**R1**)	*7.2*	9.0 (>99%)	9.2 (92%), 129 (8%)	58	33	n.d.
2	gradient random (entry 12, Table 1)	*7.2*	5.4 (99%)	5.2 (76%), 87 (24%)	52	35	n.d.
3	gradient (entry 7, Table 1)	*7.2*	7.9 (96%)	12 (24%), 87 (76%)	65	37	n.d.
4	block (**B1**)	*7.2*	150	-	insoluble	40	n.d.
5	bidirectional gradient (entry 14, Table 1)	*7.2*	8.8	7.6 (89%), 123 (11%)	66	30	n.d.
6	gradient (entry 5, Table 1)	4	4.1 (63 %), 146 (37 %)	27	43	41	14
7	gradient (entry 3, Table 1)	2	-	-	insoluble	50	23

[a]Hydrodynamic radius (R_h) of the samples determined by dynamic light scattering in methanol or H_2O [acetone/H_2O (1/9, v/v)] at 25 ^oC: [polymer] = 10 mg/mL. Values in parentheses mean the volume fraction of the portion. [b]Cloud point (Cp) of the aqueous, 2-propanol, and methanol solutions of the samples: [polymer] = 10 mg/mL. Cp: defined as the temperature at which the transmittance of the solution becomes 90%. n.d.: the samples of PEGMA (n = *7.2*) do not show Cp at 0 ^oC.

Owing to hydrophilic PEG pendants, MMA/PEGMA random, gradient, gradient-random, and bidirectional gradient copolymers are fully soluble in water. However, the block counterpart was not soluble in water due to long hydrophobic PMMA segment. Thus, self-assembly of the soluble four samples was investigated in aqueous media at 25 ^oC. Here, water was slowly added into the acetone solution of the polymers (100 mg/mL) to make homogeneous aqueous solutions (10 mg/mL) in acetone/water (1/9, v/v). Analyzed by DLS, all of the solutions exhibited bimodal light scattering intensity size distributions of small R_h (5 ~12 nm) and large R_h (~100 nm). The large

size portion increased as volume fraction in this order: random (8%) < bidirectional gradient (11%) < gradient-random (24%) < gradient (76%). The high content of large aggregates in the gradient copolymer would be attributed to the fact that the locally accumulated hydrophobic MMA segment effectively induces intermolecular self-assembly of the polymer chains. In contrast, random or bidirectional gradient counterparts preferentially self-fold or self-assemble into unimer micelles or small nanoaggregates even in water. Similar tendency was already reported on self-assembly of PEGMA/alkyl methacrylate random copolymers in water.[17] These results suggest that the delicate sequence control of hydrophobic and hydrophilic monomers such as gradient sequence also allows to modulate the self-assembling properties of amphiphilic copolymers.

8. Thermoresponsive Properties

PEG-based polymers often show lower critical solution temperature (LCST)-type phase separation in water[11,17,25-27] and upper critical solution temperature (UCST)-type phase separation in 2-propanol.[28,29] To investigate the effects of monomer sequence on phase separation in water, the author conducted the temperature-dependent turbidity measurements of the aqueous solutions of MMA/PEGMA random, random-gradient, gradient, and bidirectional gradient copolymers at the temperature range between 40 and 80 ^{o}C ([polymer] = 10 mg/mL, heating/cooling speed = 1 ^{o}C/min, λ = 670nm). The cloud point (Cp) was defined as the temperature at which the transmittance of the solution becomes 90%. All of the copolymers sharply induced LCST-type phase separation in water upon heating. Cp of gradient copolymers (gradient: 65 ^{o}C, bidirectional gradient: 66 ^{o}C) is higher than that of random counterpart (random: 58 ^{o}C) (Figure 8a, Table 2). Such higher cloud point is probably because gradient copolymers stably form unimer or multichain micelles in water that are effectively covered by condensed PEG pendants. The preforming micellization of our gradient copolymers may be also attributed to the relatively sharp phase separation, distinct from some thermoresponsive gradient copolymers with gradual phase separation.[9] A random-gradient copolymer showed lower Cp (52 ^{o}C) than a random counterpart (Figure 8e). This is probably due to the relatively low content of PEGMA in copolymer (F_{cum} = 42 mol%) compared with the others.

In 2-propanol, all MMA/PEGMA random, gradient, bidirectional gradient, and block copolymers are fully soluble over 50 ^{o}C ([polymer] = 10 mg/mL). By cooling the solutions, they showed UCST-type phase separation in 2-propanol (Figures 8b). Dependent on the monomer sequence, Cp decreased in this order (Table 2): block (40 ^{o}C) > gradient (37 ^{o}C) > random-gradient (35 ^{o}C) > random (33 ^{o}C) > bidirectional gradient (30 ^{o}C). This order suggests that Cp decreases with increasing the unimolecular solubility. Namely, the bidirectional gradient copolymer would unimolecularly dissolve to effectively cover the central MMA rich segment by both PEGMA rich segments.

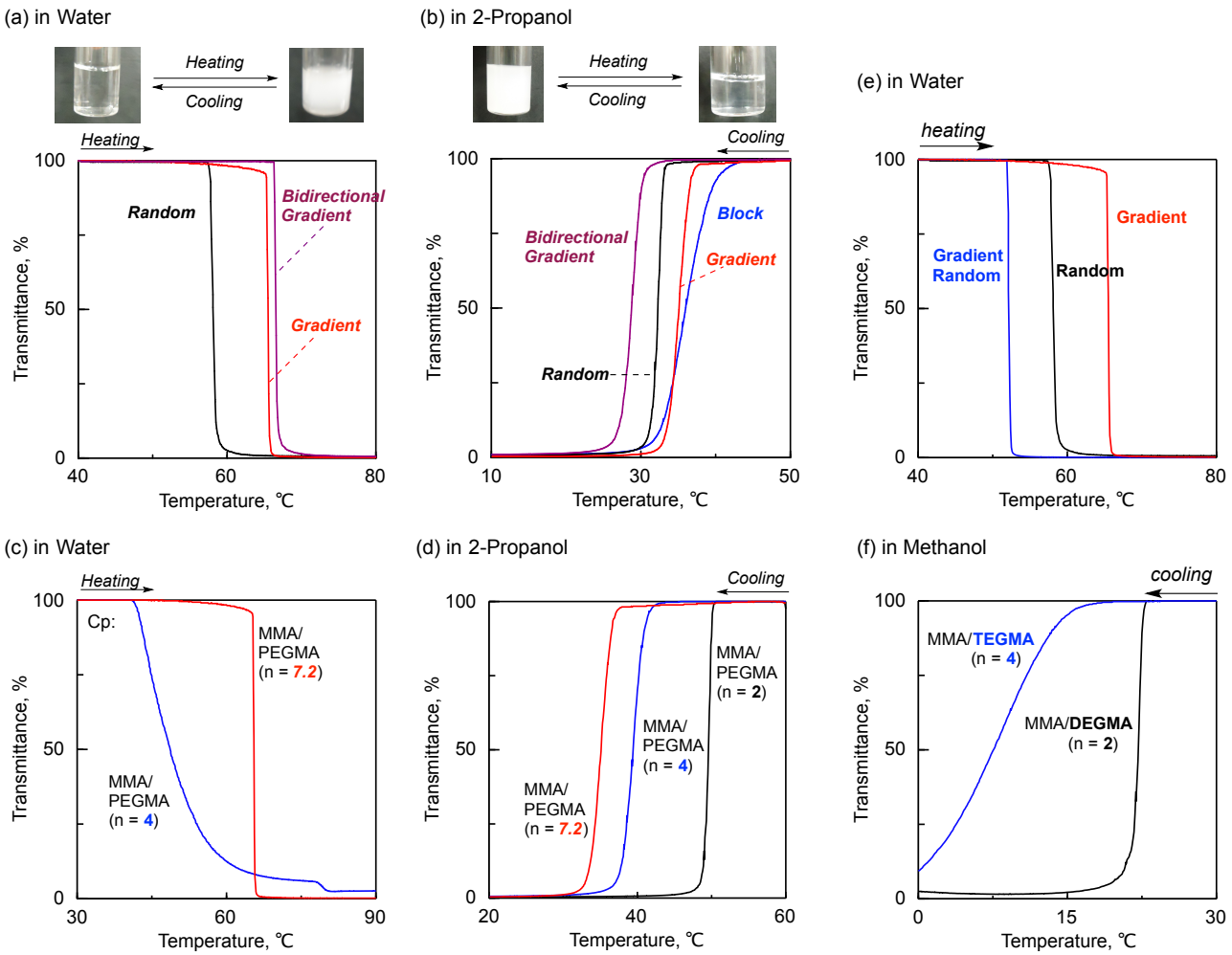

Figure 8. Turbidity measurements of the aqueous solutions of (a)(e) MMA/PEGMA (n = *7.2*) random, gradient random, gradient, and bidirectional copolymers (upon heating with 1 °C/min from 40 to 80 °C) and (c) a MMA/PEGMA (n = 4) gradient copolymer (upon heating with 1 °C/min from 30 to 90 °C): [polymer] = 10 mg/mL. Turbidity measurements of the 2-propanol solutions of (b) MMA/PEGMA (n = *7.2*) random, gradient, bidirectional, and block copolymers (by cooling with 1 °C/min from 50 to 10 °C) and (d) MMA/PEGMA gradient copolymers with different PEG pendant length (n = 2, 4, *7.2*, by cooling with 1 °C/min from 60 to 20 °C): [Polymer] = 10 mg/mL. (f) Turbidity measurements of the methanol solutions of MMA/PEGMA gradient copolymers with different PEG pendant length (n = 2, 4, by cooling with 1 °C/min from 30 to 0 °C): [Polymer] = 10 mg/mL.

Cp of MMA/PEGMA gradient copolymers in water or 2-propanol is also dependent on the pendant PEG length (oxyethylene number: n = 2, 4, *7.2*). Cp in water decreased with PEG length (Figure 8c, n = 4: Cp = 43 °C), while that in 2-propanol increased with decreasing PEG length (Figure 8d, n = 4: Cp = 41 °C, n = 2: 50 °C). Similarly, short PEG pendant gradient copolymers showed UCST-type phase separation in methanol (n = 4: Cp = 14 °C, n = 2: Cp = 23 °C, Figure 8f)

but a long PEG gradient copolymer (n = 7.2) was transparent even at 0 °C. These results support that longer PEG chains enhance the solubility of the copolymers in both water and 2-propanol.

9. Thermal Properties

Glass transition temperature (T_g) of MMA/PEGMA gradient copolymers with different PEG pendant length (n = 2, 4, *7.2*) was analyzed by differential scanning calorimetry (DSC, temperature range: -80~150 °C, heating rate: 10 °C/min) (Figure 9). All the samples clearly exhibited endothermic peaks at different temperature. T_g decreased with increasing PEG pendant length (n) (n = *7.2*: T_g = -56 °C, n = 4: T_g = -37 °C, n = 2: T_g = 26 °C) (Figure 9a). From the first derivatives of the heat flow signals (Figure 9b), the two samples (n = 4, 2) had broad T_g range between high T_g of PMMA and low T_g of corresponding poly(PEGMA) (*e.g.*, n = 2: T_g = -30 °C - 50 °C). Such broad T_g range is characteristic of gradient copolymers.[3,19] Thus, thermal properties of MMA/PEGMA gradient copolymers in solid state are also controlled by the PEG pendant length.

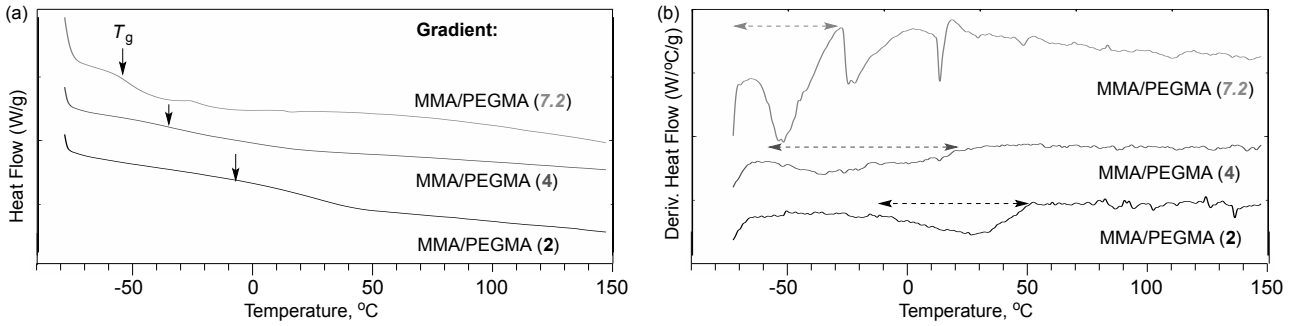

Figure 9. DSC measurements of MMA/PEGMA (n) gradient copolymers (n = *7.2*, 4, 2): (a) heat flow and (b) first derivative heat flow (lower); heating = 10 °C/min.

Conclusion

Amphiphilic MMA/PEGMA gradient and sequence-controlled copolymers were successfully synthesized via tandem catalysis of Ru-catalyzed LRP and Ti-mediated transesterification. Here, the author utilized MMA as a starting monomer, Ti(O*i*-Pr)$_4$ as a catalyst for transesterification, and PEG-OH as a co-solvent in Ru-catalyzed LRP systems. Hydrophobic MMA is smoothly transesterified into hydrophilic PEGMA during LRP, resulting in the formation of MMA/PEGMA gradient copolymers. The gradient sequence is attributed to the monomer composition change in solution, meaning that the monomer sequence can be effectively controlled by the kinetic balance of two reactions. A bifunctional initiator directly afforded amphiphilic bidirectional gradient copolymers. In contrast, sequential tandem catalysis of transesterification of MMA with PEG-OH

into PEGMA, followed by LRP of the monomers, provided amphiphilic random or block copolymers. This tandem catalysis is thus one of the most versatile systems to produce amphiphilic copolymers with designed monomer sequence. Amphiphilic gradient copolymers had solution (self-assembly, thermoresponsive) and solid (thermal) properties distinct from corresponding random or block counterparts. This importantly suggests that gradient monomer sequence is promising to control the physical and amphiphilic properties of polymers. Thus, tandem catalytic system in this chapter and amphiphilic gradient sequence-controlled copolymers would open new vistas in the design and functions of amphiphilic polymeric materials.

References

(1) Matyjaszewski, K.; Ziegler, M. J.; Arehart, S. V.; Greszta, D.; Pakula, T. *J. Phys. Org. Chem.* **2000**, *13*, 775−786.

(2) Mok, M. M.; Ellison, C. J.; Torkelson, J. M. *Macromolecules* **2011**, *44*, 6220-6226.

(3) Kim, J.; Mok, M. M.; Sandoval, R. W.; Woo, D. J.; Torkelson, J. M. *Macromolecules* **2006**, *39*, 6152-6160.

(4) Zhang, J.; Li, J.; Huang, L.; Liu, Z. *Polym. Chem.* **2013**, *4*, 4639-4647.

(5) Karaky, K.; Péré, E.; Pouchan, C.; Desbriéres, J.; Dérail, C.; Billon, L. *Soft Matter.* **2006**, *2*, 770-778.

(6) Kim, J.; Gray, M. K.; Zhou, H.; Nguyen, S. T.; Torkelson J. M. *Macromolecules* **2005**, *38*, 1037-1040.

(7) Karaky, K.; Billon, L.; Pouchan, C.; Desbriéres, J. *Macromolecules* **2007**, *40*, 458-464.

(8) Wong, C. L. H.; Kim, J.; Roth, C. B.; Torkelson, J. M. *Macromolecules* **2007**, *40*, 5631-5633.

(9) Seno, K.; Tsujimoto, I.; Kanaoka, S.; Aoshima, S. *J. Polym. Sci. Part A: Polym. Chem.* **2008**, *46*, 6444–6454.

(10) Lee, S. B.; Russell, A. J.; Matyjaszewski, K. *Biomacromolecules* **2003**, *4*, 1386-1393.

(11) Matsumoto, K.; Terashima, T.; Sugita, T.; Takenaka, M.; Sawamoto, M. *Macromolecules* **2016**, *49*, 7917-7927.

(12) Park, J-S.; Kataoka, K. *Macromolecules* **2006**, *39*, 6622-6630.

(13) Liu, R. C. W.; Pallier, A.; Brestaz, M.; Pantoustier, N.; Tribet, C. *Macromolecules* **2007**, *40*, 4276−4286.

(14) Steinhauer, W.; Hoogenboom, R.; Keul, H.; Moeller, M. *Macromolecules* **2013**, *46*, 1447−1460.

(15) Borisova, O.; Billon, L.; Zaremski, M.; Grassl, B.; Bakaeva, Z.; Lapp, A.; Stepanek, P.; Borisov, O. *Soft Matter* **2011**, *7*, 10824-10833.

(16) Li, L.; Raghupathi, K.; Song, C.; Prasad, P.; Thayumanavan, S. *Chem. Commun.* **2014**, *50*, 13417-13432.

(17) (a) Terashima, T.; Sugita, T.; Fukae, K.; Sawamoto, M. *Macromolecules* **2014**, *47*, 589−600. (b) Hirai, Y.; Terashima, T.; Takenaka, M.; Sawamoto, M. *Macromolecules* **2016**, *49*, 5084-5091.

(18) (a) Nakatani, K.; Terashima, T.; Sawamoto, M. *J. Am. Chem. Soc.* **2009**, *131*, 13600−13601. (b) Nakatani, K.; Ogura, Y.; Koda, Y.; Terashima, T.; Sawamoto, M. *J. Am. Chem. Soc.* **2012**, *134*, 4373−4383.

(19) Ogura, Y.; Terashima, T.; Sawamoto, M. *ACS Macro Lett.* **2013**, *2*, 985−989.

(20) Agari, Y.; Shimada, M.; Ueda, A.; Nagai, S. *Macromol. Chem. Phys.* **1996**, *197*, 2017−2033.

(21) Qin, C. L.; Zhao, D. Y.; Bai, X. D.; Zhang, X. G.; Zhang, B.; Jin, Z.; Niu, H. J. *J. Mater. Chem. Phys.* **2006**, *97*, 517−524.

(22) Ouchi, M.; Terashima, T.; Sawamoto, M. *Chem. Rev.* **2009**, *109*, 4963−5050.

(23) Matyjaszewski, K.; Tsarevsky, N. V. *J. Am. Chem. Soc.* **2014**, *136*, 6513-6533.

(24) (a) Ando, T.; Kato, M.; Kamigaito, M.; Sawamoto, M. *Macromolecules* **1996**, *29*, 1070−1072. (b) Ando, T.; Kamigaito, M.; Sawamoto, M. *Macromolecules* **2000**, *33*, 6732−6737.

(25) Neugebauer, D. *Polym. Int.* **2007**, *56*, 1469-1498.

(26) Lutz, J.-F. *J. Polym. Sci. Part A: Polym. Chem.* **2008**, *46*, 3459-3470.

(27) Han, S.; Hagiwara, M.; Ishizone, T. *Macromolecules* **2003**, *36*, 8312−8319.

(28) Terashima, T.; Ouchi, M.; Ando, T.; Kamigaito, M.; Sawamoto, M. *Macromolecules* **2007**, *40*, 3581-3588.

(29) Zhu, M.; Liu, W.; Xiao, J.; Ling, Y.; Tang, H. *J. Polym. Sci. Part A: Polym. Chem.* **2016**, *54*, 3444-3453.

Chapter 3

Hydrogen-Bonding Gradient Copolymers: Effects of Supramolecular Unit Sequence on Single-Chain Folding and Self-Assembly

Abstract

Chiral 1,3,5-tricarboxamide (BTA)-functionalized copolymers with gradient, bidirectional gradient, and random sequence distributions were synthesized via tandem living radical polymerization (LRP) with in-situ monomer transesterification to investigate the effects of the BTA sequence on self-folding/aggregation properties in organic media. Here, 2-ethylhexyl methacrylate (EHMA) as a starting monomer was polymerized with a ruthenium catalytic system in the presence of a chiral BTA-bearing alcohol (BTA-OH) and Ti(O*i*-Pr)$_4$. By tuning the concentration and time of addition of the Ti catalyst, the transesterification rate of EHMA into a chiral BTA-functionalized methacrylate (BTAMA) was synchronized with LRP to produce EHMA/BTAMA gradient or bidirectional gradient copolymers. In contrast, faster transesterification than LRP gave the corresponding random copolymer. Circular dichroism spectroscopy and dynamic light scattering performed on solutions of all BTA-functionalized copolymers indicated that the chiral BTA pendants helically self-assemble via hydrogen-bonding interaction in 1,2-dichloroethane, methylcyclohexane (MCH), and their mixtures to form single-chain or multi-chain polymeric nanoparticles. The temperature-dependent self-assembly behavior of the BTA pendants was virtually independent of the sequence distribution, whereas the size of the resultant nanoparticles depended on the sequence as follows: random < gradient < bidirectional gradient in MCH.

Introduction

The marriage of precision polymerization and supramolecular self-assembly creates new avenues to obtain functional polymeric materials with well-defined three-dimensional architectures. Single-chain polymeric nanoparticles (SCPNs) and related unimolecular micelles and nanoaggregates[1-35] are attracting increasing attention as these compartmentalized polymers show promise in mimicking functions of natural biopolymers such as proteins and enzymes.[16-18,23] SCPNs are often constructed by the self-folding of functional and/or amphiphilic "random" copolymers via physical interaction. Hereby, they dynamically and reversibly form globular structures that are responsive to stimuli or environmental changes.[10-29] The intramolecular folding process is triggered by the site-specific self-assembly of the functional pendants via non-covalent interactions (e.g. hydrogen-bond, coordination, host-guest)[10-24] and/or autonomous self-assembly of the amphiphilic main chains or pendants in water or specific solvents.[15-18,25-29] Thus, selective formation of desired SCPNs requires the precision control of the primary structure (*e.g.*, molecular weight: chain length, composition, monomer sequence) by living polymerization,[15,16,25-29] in addition to the design of the functional pendants.

Among them, chiral benzene-1,3,5-tricarboxamide (BTA)-functionalized random copolymers are promising scaffolds to self-fold or self-assemble into SCPNs in organic or aqueous media.[11-18] Similar to "free" BTA derivatives,[36-43] the chiral BTA pendants induce helical self-assembly via strong three-fold hydrogen bonding interaction. Resultant SCPNs contain helical secondary structures within their globular tertiary structure; this feature has encouraged the author to design enzyme-like polymer catalysts with well-defined nanospaces.[16-18] To understand the internal structure of BTA-based SCPNs, the BTA helical stacking process in chain folding was investigated by temperature-dependent circular dichroism (CD) spectroscopy.[11-18] The elongation temperature of the pendant BTA units is dependent on the local concentration along a chain, *i.e.*, BTA composition, while it is independent of the total concentration of the BTA in solutions.[11-16] This is characteristic of the intramolecular self-assembly of the BTA units within a single macromolecule. The BTA pendants do not undergo cooperative self-assembly, in contrast to "free" (non polymer-supported) BTA derivatives. Such non-cooperative self-assembly is attributed to the formation of segregated and multiple helical stacks of the pendant BTAs within SCPNs, as inferred from "Sergeant-and-Soldiers" experiments with BTA-functionalized random block copolymers.[13] However, to date the folding and self-assembly processes have always been studied using BTA pendants "randomly" distributed along the polymer chain. The question remains if the BTA-sequence distribution along a polymer chain has an effect on the degree of BTA self-assembly and polymer chain folding/aggregation.

In previous chapter, the author introduced the concept of gradient copolymerization using the tandem catalysis of ruthenium-catalyzed living radical polymerization (LRP)[44,45] and metal alkoxide-mediated transesterification of methacrylates with alcohols.[46-49] This system is effective to design various gradient copolymers because the gradient sequence and composition can be catalytically controlled by tuning the synchronization efficiency of LRP and in-situ transesterification of monomers. Thus, the controllability of sequence distribution is better than the conventional two methods: 1) living polymerization of two monomers with different reactivity and 2) living polymerization via continuous addition of a second monomer.[50-53] Additionally, diverse primary and secondary alcohols and common methacrylates can be utilized to functionalize gradient copolymers, where unlimited functionalization is possible in one-pot for gradient copolymers.

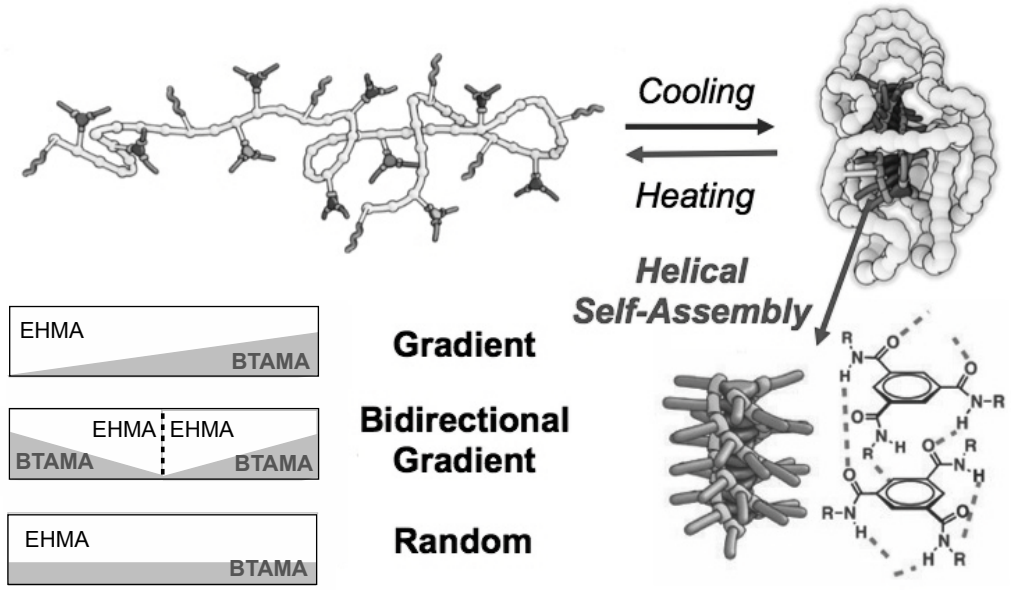

Scheme 1. Self-folding and self-assembly of BTA-functionalized copolymers with different sequence distribution.

In this chapter, the author concerns the precision synthesis of BTA-functionalized copolymers which differ in monomer sequence distributions, namely gradient, bidirectional gradient, and randomly distributed, and investigate the consequences of the BTA sequence on self-folding/aggregation properties in organic media (Scheme 1). BTA-functionalized gradient copolymers are of particular interest because the local concentration of BTA pendants gradually increases from one terminal to another along a polymer chain. Such a biased sequence distribution of BTA units may lead to polymer chain folding and/or BTA self-assembly that differs from its random counterpart. A series of BTA sequence-controlled copolymers was prepared by this tandem polymerization system (Scheme 2).

2-Ethylhexyl methacrylate (EHMA) as a starting monomer was polymerized with a ruthenium catalytic system [Ru(Ind)Cl(PPh_3)$_2$/*n*-Bu_3N] and a chloride initiator in the presence of a chiral BTA-functionalized alcohol (BTA-OH), and Ti(O*i*-Pr)$_4$. The selection of EHMA is due to the high solubility of resulting copolymers in organic media such as 1,2-dichroloethane (DCE) or methyl cyclohexane (MCH). EHMA was concurrently transesterified with BTA-OH and the Ti catalyst into a chiral BTA-functionalized methacrylate (BTAMA) during LRP by modulating concentration and additional timing of the Ti catalyst. As a result, a synchronized transesterification with polymerization occurred to give a EHMA/BTAMA gradient copolymer whose BTA composition gradually increased from the initiating terminal to the growing counterpart. Synchronized tandem catalysis using a bifunctional initiator further led to a EHMA/BTAMA bidirectional gradient copolymer, where BTA composition gradually increased from the center of the chain to both terminals. In contrast, faster transesterification than LRP provided a EHMA/BTAMA random copolymer. The self-folding and self-assembly properties of EHMA/BTAMA gradient, bidirectional gradient, and random copolymers were further evaluated by temperature-dependent CD measurement and dynamic light scattering (DLS).

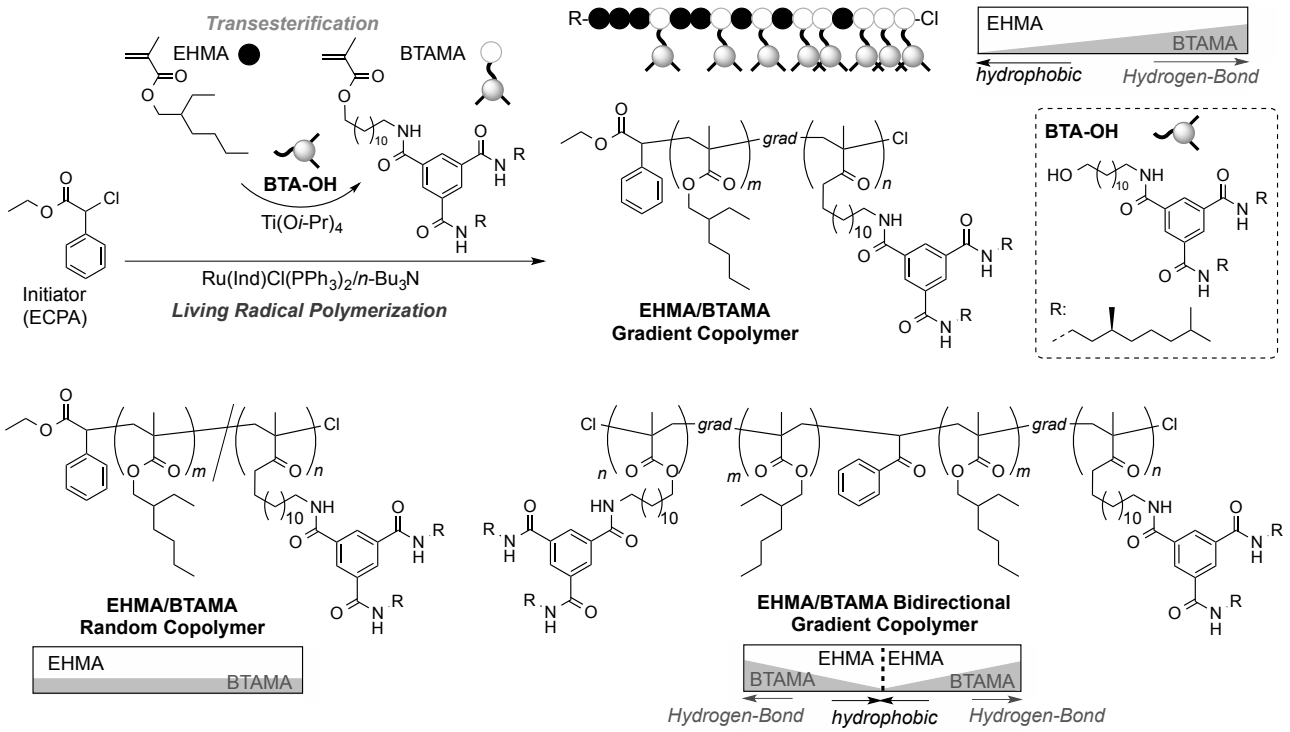

Scheme 2. EHMA/BTAMA gradient, random, and bidirectional gradient copolymers via concurrent tandem catalysis of ruthenium-catalyzed living radical polymerization and in-situ monomer transesterification.

Experimental Section

Materials. 2-Ethylhexyl methacrylate (EHMA: TCI, purity >99%) were purified with inhibitor remover (Aldrich) and purged by argon before use. BTA-OH was prepared according to the following literature.[16] Tetralin (1,2,3,4-tetrahydronaphthalene: TCI; purity >97%; an internal standard for ^{1}H NMR analysis) were dried overnight with calcium chloride and distilled from calcium hydride under reduced pressure before use. Ti(O*i*-Pr)$_4$ (Aldrich, purity >97%), 2,2-dichloroacetophenone (DCAP: TCI; purity >96%), and *n*-Bu$_3$N (TCI, purity >98%) were degassed by triple vacuum-argon purge cycles before use. Ethyl 2-chloro-2-phenylacetate (ECPA: Aldrich; purity >97%) was distilled under reduced pressure before use. Ru(Ind)Cl(PPh$_3$)$_2$ (Aldrich) were used as received and handled in a glove box under moisture- and oxygen-free argon (H_2O <1 ppm; O_2 <1 ppm). Toluene (solvent) was purified before use by pashing it through a purification column (Glass Contour Solvent Systems: SG Water USA). 1,4-Dioxane (Wako; purity >99.5%) was dehydrated with molecular sieves (4A) and degassed before use. 1,2-dichroloethane (DCE: TCI; purity >99.5%) and methylcyclohexane (MCH: TCI; purity >99%) were used as received.

Characterization. The molecular weight distribution (MWD) curves, M_n, and M_w/M_n ratio of the polymers were measured by SEC in THF as an eluent at 40 ^{o}C on three polystyrene-gel columns (Shodex LF-404: exclusion limit = 2×10^6 g/mol; particle size = 6 μm; pore size = 3000 Å; 0.46 cm i.d. × 25 cm; flow rate, 0.3 mL/min) connected to a DU-H2000 pump, a RI-74S refractive index detector, and a UV-41 ultraviolet detector (all from Shodex; Shodex GPC-104). The columns were calibrated against 13 standard poly(MMA) samples (Polymer Laboratories; M_n = 620−1200000; M_w/M_n = 1.06−1.22). ^{1}H NMR spectra were recorded in $CDCl_3$ and CD_2Cl_2 on a JEOL JNM-ECA500 spectrometer operating at 500.16 MHz. Dynamic light scattering (DLS) was measured on Otsuka Photal ELSZ-0 equipped with a semiconductor laser (wavelength: 658 nm) at 25 ^{o}C ([Polymer] = 1 mg/mL in DCE, MCH, DCE/MCH mixture). The measuring angle was 165° and the data was analyzed by CONTIN fitting method. Circular dichroism (CD) measurement of polymers was performed on a Jasco J-1500 spectrometer in DCE, MCH and DCE/MCH mixtures (optical path length = 0.5 cm, sensitivity: standard, response: 1.0 s, band width: 1.0 nm, data pitch: 0.1 nm, scanning speed: 20 nm/min). Temperature-dependent CD measurements were performed at the temperature range between 0 °C and 80 °C with a Jasco PFD-425S/15 Peltier temperature controller (cooling rate: 1K/min, data pitch: 0.1 °C, l = 223 nm). To remove residue of catalysts and BTA-OH, polymer samples for analysis were fractionated by preparative SEC in THF and $CHCl_3$ [column (THF): Shodex K-2003; particle size = 6 μm; 2.0 cm i.d. × 30 cm; exclusion limit = 7×10^4 g/mol; flow rate = 3 mL/min], column ($CHCl_3$): Shodex K-5002; particle size = 15 μm; 5.0

cm i.d. × 30 cm; exclusion limit = 5×10^3 g/mol; flow rate = 10 mL/min]. Sample solutions for DLS and CD measurements were prepared according to the following: the polymers and corresponding organic solvents were charged into 6 mL or 11 mL vials, and the mixtures were sonicated for 5 hours at room temperature with BRANSONIC 510 (BRANSON) to give homogenous solutions of polymers. The resultant solutions were immediately used for DLS and CD measurements.

Polymerization. The synthesis of EHMA/BTAMA copolymers were carried out by syringe technique under argon in baked glass tubes equipped with a three-way stopcock.

EHMA/BTAMA gradient copolymer (**P1**). Into glass tube, $Ru(Ind)Cl(PPh_3)_2$ (0.0024 mmol, 1.86 mg) and BTA-OH (0.144 mmol, 0.1 g) were charged, and 1,4-dioxane (0.51 mL), tetralin (0.04 mL), EHMA (1.2 mmol, 0.27 mL), and a 40 mM 1,4-dioxane solution of ECPA (0.15 mL, ECPA = 0.0060 mmol) were added sequentially in that order at 25 °C under argon (total volume: 1.0 mL). The glass tube was placed in an oil bath kept at 80 °C. After 4h, a 50 mM 1,4-dioxane solution of $Ti(O\textit{i}\text{-}Pr)_4$ (0.20 mL, $Ti(O\textit{i}\text{-}Pr)_4$ = 0.01 mmol) was directly added into the polymerization solution under argon (total volume: 1.2 mL). At predetermined intervals, the mixture was sampled with a syringe under argon. The sampled solutions were cooled to –78 °C to terminate the reaction. The total monomer conversion and BTAMA content in monomer were determined by ^{1}H NMR measurement of the terminated reaction solution in $CDCl_3$ at r.t. with tetralin as an internal standard. The quenched reaction solutions were evaporated to dryness to give the crude product. The product was purified by preparative SEC. SEC (THF, PMMA std.): M_n = 45000 g/mol; M_w/M_n = 1.34. ^{1}H NMR [500 MHz, CD_2Cl_2, 25 °C, δ = 5.33 CH_2Cl_2] δ 8.3 (BTA: aromatic), 7.3–7.1 (ECPA: aromatic), 4.9–4.7 (-COOC<u>H</u>$(CH_3)_2$), 4.1–3.5 (-COOC<u>H</u>$_2$CH(CH_2CH_3)-, -COOC<u>H</u>$_2$CH$_2$-), 3.5–3.0 (-CH_2C<u>H</u>$_2$NHCO-), 2.1−1.7 (-C<u>H</u>$_2$C(CH_3)-), 1.7−1.2 (-CH_2(C<u>H</u>$_2$)$_{10}$$CH_2$-, -$CH_2$C<u>H</u>$(CH_2CH_3)$C<u>H</u>$_2$C<u>H</u>$_2$C<u>H</u>$_2$C<u>H</u>$_3$), 1.20–0.65 (-$CH_2$C(C<u>H</u>$_3$)-). M_n (NMR, α) = 52700; $DP_{MMA}/DP_{BTAMA}/DP_{\textit{i}PrMA}$ = 202/17/1; Cumulative BTAMA content in polymer ($F_{cum,BTAMA}$) = 7.5%.

EHMA/BTAMA bidirectional gradient copolymer (**P4**). SEC (THF, PMMA std.): M_n = 43700 g/mol; M_w/M_n = 1.35. ^{1}H NMR [500 MHz, CD_2Cl_2, 25 °C, δ = 5.33 CH_2Cl_2] δ 8.3 (BTA: aromatic), 7.7–7.4 (DCAP: aromatic), 4.9–4.7 (-COOC<u>H</u>$(CH_3)_2$), 4.1–3.5 (-COOC<u>H</u>$_2$CH(CH_2CH_3)-, -COOC<u>H</u>$_2$CH$_2$-), 3.6–3.0 (-CH_2C<u>H</u>$_2$NHCO-), 2.1−1.7 (-C<u>H</u>$_2$C(CH_3)-), 1.7−1.2 (-CH_2(C<u>H</u>$_2$)$_{10}$$CH_2$-, -$CH_2$C<u>H</u>$(CH_2CH_3)$C<u>H</u>$_2$C<u>H</u>$_2$C<u>H</u>$_2$C<u>H</u>$_3$), 1.2–0.6 (-$CH_2$C(C<u>H</u>$_3$)-). M_n (NMR, α) = 49400; $DP_{MMA}/DP_{BTAMA}/DP_{\textit{i}PrMA}$ = 189/16/1; $F_{cum,BTAMA}$ = 7.7%.

EHMA/BTAMA random copolymer (**P3**). SEC (THF, PMMA std.): M_n = 36200 g/mol; M_w/M_n = 1.43. ^{1}H NMR [500 MHz, CD_2Cl_2, 25 °C, δ = 5.33 CH_2Cl_2] δ 8.3 (BTA: aromatic), 7.3–7.1

(ECPA: aromatic), 4.9–4.7 (-COOC<u>H</u>(CH_3)$_2$), 4.1–3.5 (-COOC<u>H_2</u>CH(CH_2CH_3)-, -COOC<u>H_2</u>CH_2-), 3.6–3.0 (-CH_2C<u>H_2</u>NHCO-), 2.1−1.7 (-C<u>H_2</u>C(CH_3)-), 1.7−1.2 (-CH_2(C<u>H_2</u>)$_{10}$$CH_2$-, -$CH_2$C<u>H</u>(C<u>$H_2$</u>C<u>$H_3$</u>)C<u>$H_2$</u>C<u>$H_2$</u>C<u>$H_2$</u>C<u>$H_3$</u>), 1.2–0.5 (-$CH_2$C(C<u>$H_3$</u>)-). M_n (NMR, α) = 47600; $DP_{MMA}/DP_{BTAMA}/DP_{iPrMA}$ = 168/18/8; $F_{cum,BTAMA}$ = 9.3%.

Results and Discussion

1. Synthesis of EHMA/BTAMA Gradient and Random Copolymers by Tandem LRP

To begin with, the transesterification of EHMA (1000 mM) was investigated with Ti(O*i*-Pr)$_4$ (20 mM) and *N*-(6-hydroxyhexyl)benzamide (250 mM) as a model alcohol of BTA-OH in 1,4-dioxane at 80 ^oC (Scheme 3). 1,4-Dioxane was employed to efficiently solubilize the amide-bearing alcohol. EHMA was efficiently transesterified into a corresponding methacrylate. The conversion of EHMA reached 10 % in 17 h, giving 100 mM of the product (confirmed by ^1H NMR). This indicates that Ti-mediated transesterification is compatible with EHMA and amide-functionalized alcohols and products.[54,55]

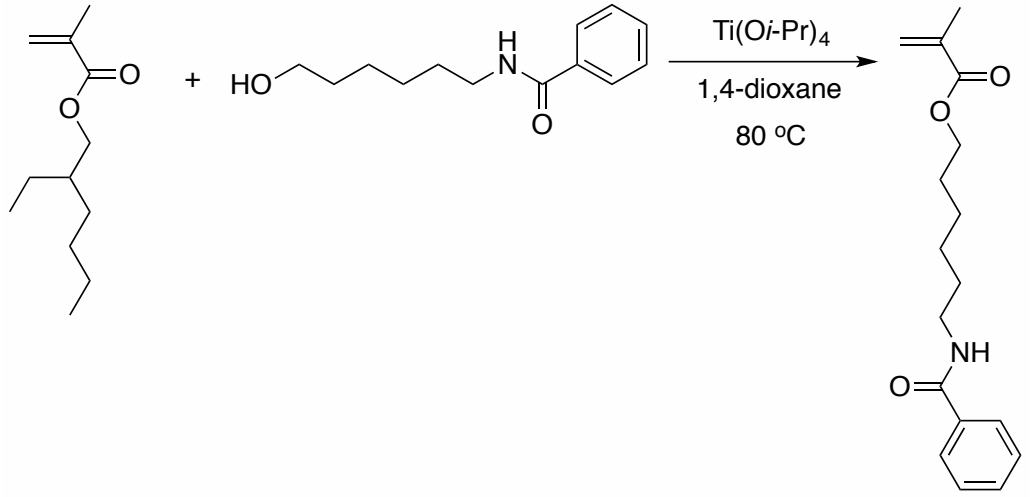

Scheme 3. Transesterification of EHMA with *N*-(6-hydroxyhexyl)benzamide in 1,4-dioxane.

Given the model study, the author examined the synthesis of EHMA/BTAMA gradient and random copolymers via concurrent tandem catalysis of LRP and in-situ transesterification. The target BTAMA content was set at around 10 mol% because 10 mol% BTAMA-functionalized random copolymers have been often utilized to investigate self-folding properties in aqueous and organic media.[11-18] The formation of gradient copolymers requires kinetic synchronization of LRP and transesterification.[46-49] We thus carried out tandem polymerization of EHMA with BTA-OH by changing the concentration of Ti(O*i*-Pr)$_4$ catalyst between 8 and 20 mM, and by changing the time of catalyst addition (immediately, after 2 h or after 4 h) (Figure 1, Table 1).

EHMA was polymerized with $Ru(Ind)Cl(PPh_3)_2$ catalyst and a chloride initiator (ECPA) in the presence of *n*-Bu_3N co-catalyst (for LRP), Ti(O*i*-Pr)$_4$ catalyst (for transesterification), and BTA-OH as alcohol in 1,4-dioxane at 80 ^oC (Figure 1c). Aiming at the formation of about 10 mol% BTAMA, the author used a relatively small amount of BTA-OH (120 mM) with EHMA (1000 mM). The in-situ generation of BTAMA was monitored by ^1H NMR measurement of the polymerization solutions that were sampled at predetermined periods. The conversion of total monomers (all methacrylate bonds: EHMA and generating BTAMA) and the BTAMA content in the monomer [BTAMA/(EHMA+BTAMA)] are plotted as a function of reaction time (Figure 1c).

Table 1. Synthesis of MMA/BTAMA Copolymers via Concurrent Tandem Living Radical Polymerization[a]

Code	[Ti(O*i*-Pr)$_4$] (mM)	Time (h)	Conv[b] (%)	M_n[c] (GPC)	M_w/M_n[c]	M_n[d] (NMR)	EHMA/BTAMA/*i*-PrMA[e] (%)
P1	8	23	74	45000	1.34	52700	92.1/7.5/0.4
P2	15	24	80	36800	1.52	48800	88.6/8.8/2.6
P3	20	23	76	36200	1.43	47600	86.6/9.3/4.1
P4	8	28	83	43700	1.35	49400	91.8/7.7/0.5

[a][EHMA]/[ECPA (**P1**-**P3**) or DCAP (**P4**)]/[$Ru(Ind)Cl(PPh_3)_2$]/[Ti(O*i*-Pr)$_4$]/[*n*-Bu_3N]/[BTA-OH] = 1000/5/1/8, 15, and 20/20/120 mM in 1,4-dioxane at 80 ^oC. Ti(O*i*-Pr)$_4$ catalyst was pre-loaded before polymerization (**P3**) or added to the polymerization solutions after 2 h (**P2**) or 4 h (**P1**, **P4**). [b]Total monomer conversion determined by ^1H NMR using an internal standard (tetralin). [c]Determined by SEC in THF with PMMA standard calibration. [d]Number-average molecular weight determined by ^1H NMR. [e]Copolymer composition (mol %) determined by ^1H NMR.

To synchronize in-situ transesterification with LRP for gradient copolymers, the author added Ti(O*i*-Pr)$_4$ into polymerization solutions after starting LRP of EHMA. The Ti catalyst concentration was set as 8 or 15 mM (Figure 1a,b). A delay in the addition of Ti(O*i*-Pr)$_4$ allows skipping the induction period of LRP. In fact, synchronized transesterification with LRP was successfully achieved by adding 8 mM Ti catalyst at 4 h after starting LRP (Figure 1a). The BTAMA content in the monomer linearly increased with increasing monomer conversion (Figure 1d). The synchronized catalysis efficiently produced well-controlled EHMA/BTAMA gradient copolymers with narrow molecular weight distribution (**P1**: M_n = 45000, M_w/M_n = 1.34). Instantaneous BTAMA content in polymer ($F_{inst,BTAMA}$) was estimated with BTAMA composition in monomer (Figure 1d), assuming that EHMA and BTAMA have similar reactivities in the copolymerization. $F_{inst,BTAMA}$ gradually increased from 0% to 16% along the polymer chain (Figure 1e). Delayed addition of 15 mM Ti catalyst at 2 h also gave a EHMA/BTAMA gradient copolymer (**P2**), whereas $F_{inst,BTAMA}$ quickly increased from 0 to 10 % after addition of Ti and then slowly increased to 16% (Figure 1e). This is because the fast transesterification takes place even if the addition of the Ti catalyst is delayed.

Isolated EHMA/BTAMA gradient copolymers, **P1** and the intermediate (conv. = 39%), were further analyzed by ^{1}H NMR (Figure 2). Both samples exhibited methylene protons adjacent to BTA amide group (*c*: 3.6 – 3.0 ppm), aromatic protons of BTA units (*d*: 8.3 ppm), and methylene protons adjacent to ester pendants (*a*, *b*: 4.1 – 3.6 ppm), in addition to aromatic protons of the initiator fragment (*e*: 7.3 – 7.1 ppm), methylene and methyl protons of methacrylate backbone and BTAMA alkyl pendants. Cumulative BTAMA content in polymer ($F_{\text{cum. BTAMA}}$) was estimated from the area ratio of peak *c* and peak *a*+*b* [$c/3(a + b)$]. $F_{\text{cum,BTAMA}}$ of **P1** and the intermediate was determined to be 7.5 % and 4%, respectively. $F_{\text{cum,BTAMA}}$ actually increased with conversion, i.e., chain length, in sharp contrast to that of **P3**. This result supports that **P1** is a gradient copolymer whose BTAMA composition gradually increased from the initiating terminal to growing counterpart.

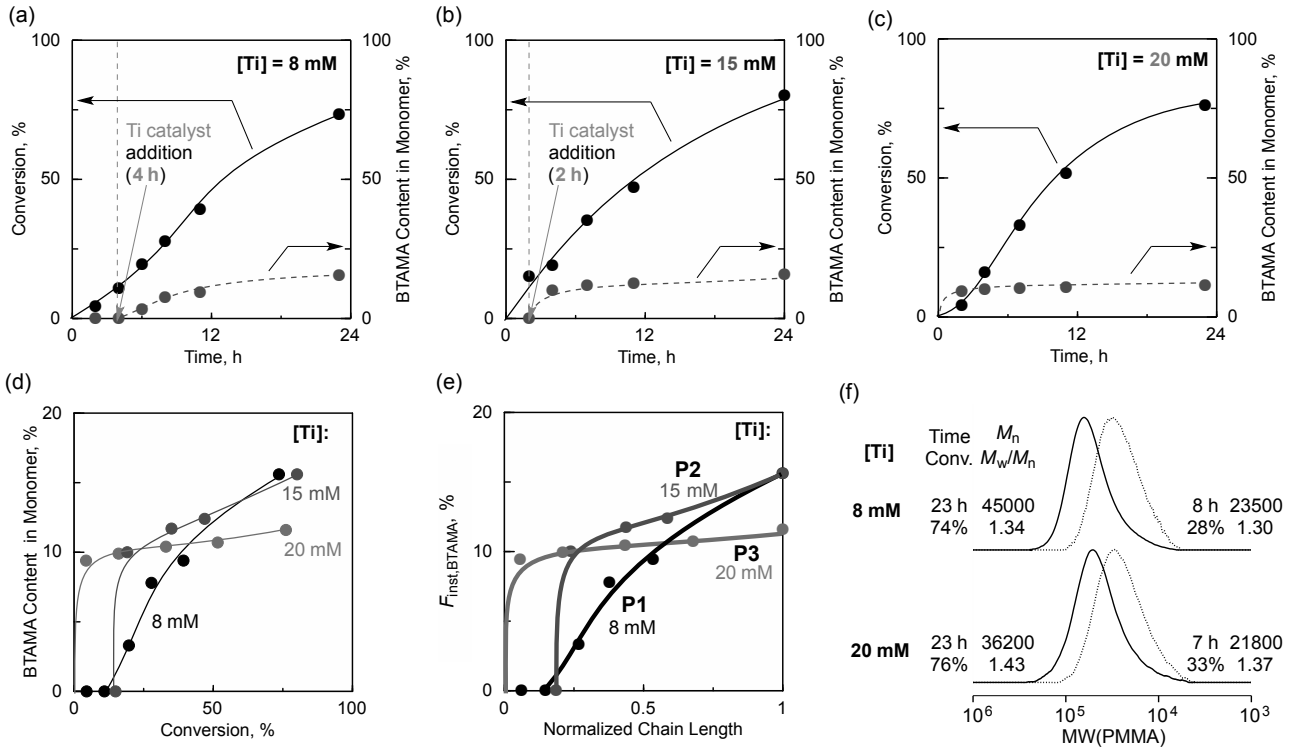

Figure 1. Synthesis of EHMA/BTAMA copolymers (**P1** – **P3**) via concurrent tandem catalysis of LRP and in-situ transesterification: [EHMA]/[ECPA]/[Ru(Ind)Cl(PPh$_3$)$_2$]/[Ti(O*i*-Pr)$_4$]/[*n*-Bu$_3$N]/[BTA-OH] = 1000/5/2/8 (**P1**), 15 (**P2**), and 20 (**P3**)/20/120 mM in 1,4-dioxane at 80 ^{o}C. (a-c) Total monomer conversion and BTAMA content in monomer; (a, b) 1,4-dioxane solutions of Ti(O*i*-Pr)$_4$ catalyst were added to polymerization solutions at (a) 4 h or (b) 2 h under argon. (d) BTAMA content in monomer as a function of total conversion. (e) Instantaneous BTAMA composition in copolymers as a function of normalized chain length. (f) SEC curves of products obtained with 8 or 20 mM Ti.

The author further conducted the tandem polymerization with Ti(O*i*-Pr)$_4$ of 20 mM without the delayed addition of the Ti catalyst; all reagents including the Ti catalyst were charged before the reaction. EHMA was immediately transesterified into BTAMA much faster than copolymerization of EHMA and the generating BTAMA. The content of BTAMA in monomer already saturated at 10% during the induction period of LRP (Figure 1c,d). As a result, this condition provided a EHMA/BTAMA random copolymer (**P3**: M_n = 36200, M_w/M_n = 1.43, by size exclusion chromatography (SEC), Figure 1f); $F_{inst,BTAMA}$ was virtually constant along a chain (Figure 1e). As estimated by ^{1}H NMR measurement of isolated **P3** and the intermediate, the cumulative BTA content in the copolymers was almost constant ($F_{cum,BTAMA}$ = 8 – 9 mol%), and independent of the chain length.

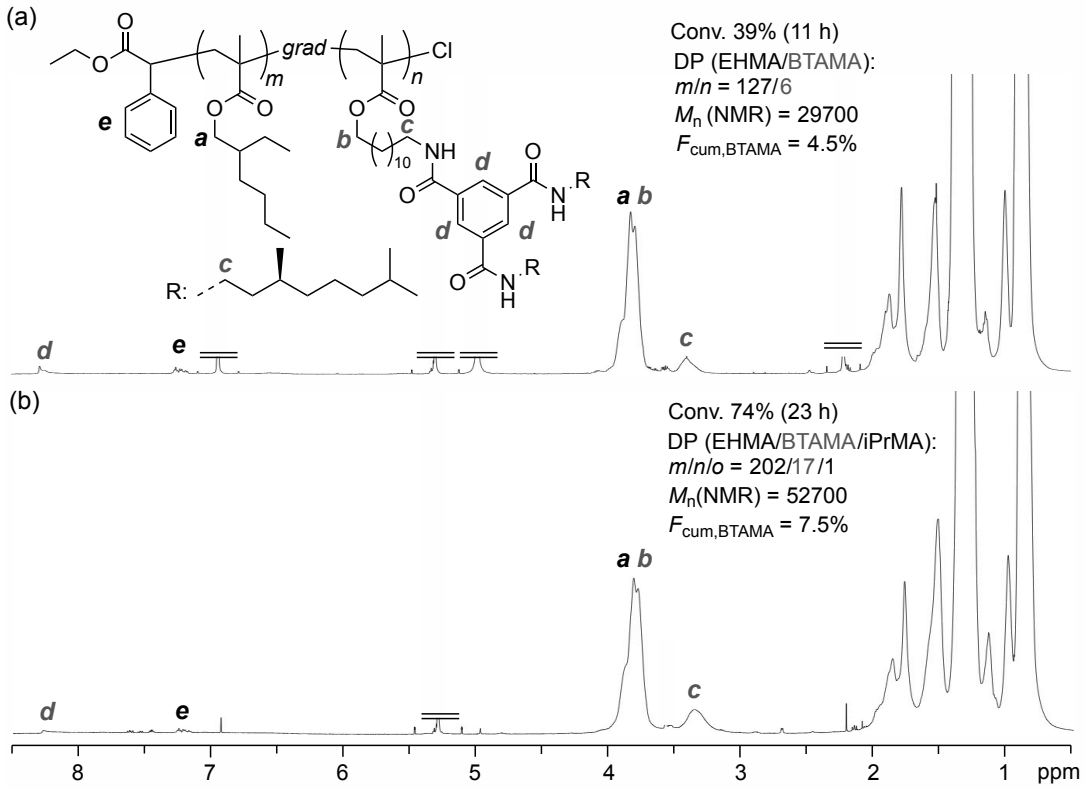

Figure 2. ^{1}H NMR spectra of EHMA/BTAMA copolymers in CD_2Cl_2 at 25 ^oC: (b) **P1** (74% conversion, 23 h); (a) the intermediate at 39% conversion (11 h).

2. Synthesis of Bidirectional EHMA/BTAMA Gradient Copolymers

Performing the tandem catalysis with a bifunctional initiator, dichloroacetophenone (DCAP), instead of monofunctional ECPA is an effective way to obtain bidirectional gradient copolymers, in which the monomer composition gradually changes from the central part of the polymer chains to both terminals.[49] The synthesis of a EHMA/BTAMA bidirectional gradient copolymer was thus examined by tandem living radical polymerization of EHMA with DCAP and BTA-OH in

1,4-dioxane at 80 °C (Figure 3). The author applied the same conditions and Ti(O*i*-Pr)$_4$ addition technique as those optimized for **P1**: Ti(O*i*-Pr)$_4$ (8 mM) was added into LRP solution of EHMA 4 h after starting the polymerization. Synchronized tandem catalysis of transesterification and LRP again took place, and the BTAMA content in the monomer linearly increased with the total monomer conversion (Figure 3a). SEC indicated that a well-controlled EHMA/BTAMA bifunctional gradient copolymer was obtained (**P4**: M_n = 43700, M_w/M_n = 1.35, Figures 3bc). These results demonstrate that this tandem catalysis of LRP and transesterification efficiently affords the sequence control of hydrogen-bonding BTAMA units in copolymers by tuning Ti catalyst concentration, additional timing of Ti catalyst, and initiators.

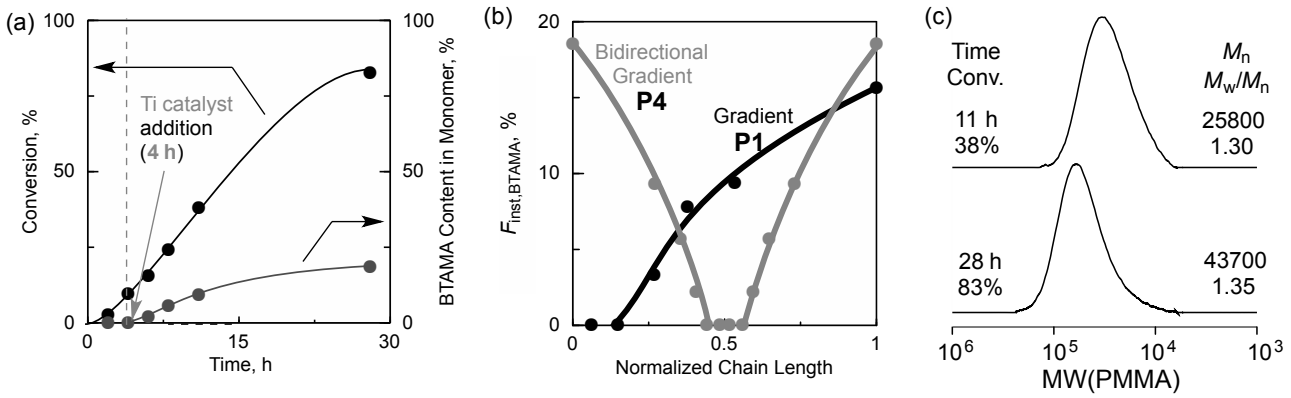

Figure 3. Synthesis of a EHMA/BTAMA bifunctional gradient copolymer (**P4**) via concurrent tandem catalysis: [EHMA]/[DCAP]/[Ru(Ind)Cl(PPh$_3$)$_2$]/[Ti(O*i*-Pr)$_4$]/[*n*-Bu$_3$N]/[BTA-OH] = 1000/5/2/8/20/120 mM in 1,4-dioxane at 80 °C. (a) Total monomer conversion and BTAMA content in monomer; a 1,4-dioxane solution of Ti(O*i*-Pr)$_4$ was added to the polymerization solution at 4 h under argon. (b) Instantaneous BTAMA composition of **P4** or **P1** as a function of normalized chain length. (c) SEC curves of the products.

3. Self-Assembly and Self-Folding of EHMA/BTAMA Sequence-Controlled Copolymers

BTAMA-based copolymers often intramolecularly fold or intermolecularly self-assemble to form single-chain polymeric nanoparticles or multi-chain aggregates, respectively, via the helical self-assembly of the chiral BTA pendants by hydrogen-bonding interaction in halogenated or hydrocarbon solvents.[11-14] It was previously shown that the local BTA content (BTA composition) in the polymers strongly affects the BTA self-assembly and chain-folding/aggregation properties.[11-18] In contrast, the effects of the sequence distribution of the BTA units along a polymer chain on the properties have not yet been explored. The author thus evaluated self-folding/aggregation properties of **P1** – **P4** by using circular dichroism (CD) spectroscopy and dynamic light scattering (DLS) in 1,2-dichloroethane (DCE), methylcyclohexane (MCH), and its mixtures. Importantly, the four polymer samples consist of different monomer sequence distribution

(gradient, random, and bidirectional gradient) but have almost identical BTAMA content ($F_{cum,BTAMA}$ = ~10%) and degree of polymerization. Here, helical self-assembly behavior of the chiral BTA pendants was evaluated by CD spectroscopy, while the size of the resulting single-chain or multi-chain polymeric nanoparticles was determined by DLS.

3-1. ***BTA Self-assembly.*** **P1** – **P4** were analyzed by CD spectroscopy in DCE or MCH at 25 °C ([BTA] = 50 mM). Prior to analysis, the polymers were homogeneously solubilized in their solvents by sonication for 5 hours at room temperature. As typically shown in Figure 4a (sample: **P1**), all of the samples clearly showed negative Cotton effect originating from helical self-assembly of the chiral BTA pendants (λ_{max} = 223 nm) in both DCE and MCH. In all cases, the CD intensity in MCH was larger than that in DCE, indicating that MCH enhanced the self-assembly of the pendant BTA more than DCE.

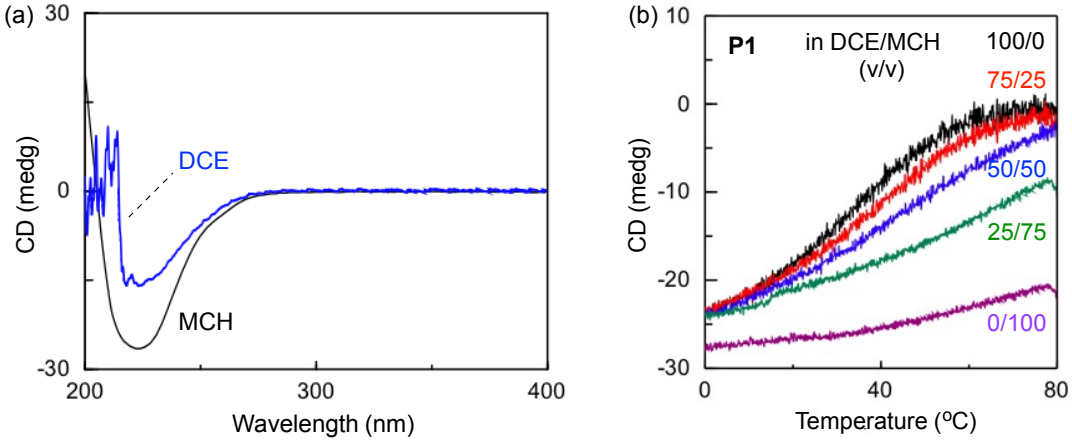

Figure 4. (a) CD spectra of **P1** in 1,2-dichloroethane (blue) or methylcyclohexane (black) at 25 °C: (λ = 200-400 nm, [BTA] = 50 μM, *l* = 0.5 cm). (b) Temperature-dependent CD cooling curves of **P1** in 1,2-dichloroethane (DCE), methylcyclohexane (MCH), and mixed solvents (DCE/MCH = 100/0, 75/25, 50/50, 25/75, 0/100, v/v) at a cooling rate of 60 K h^{-1} on probed at λ = 223 nm: ([BTA] = 50 μM, *l* = 0.5 cm).

To investigate the effects of solvents and temperature on self-assembly of the BTA pendants, temperature-dependent CD measurements of **P1** were conducted in DCE, MCH, and DCE/MCH mixed solvents (75/25, 50/50, 25/75, v/v) by cooling from 80 °C to 0 °C (Figure 4b). In DCE, the solution was CD silent at 80 °C but the CD effect gradually appeared starting from around 60 °C by cooling and finally reached a value of -24 mdeg at 0 °C. Similarly, **P1** showed a gradual increase of negative Cotton effect by cooling in DCE/MCH mixtures and MCH alone. The intensity increased with increasing MCH content in the temperature range between 0 and 80 °C. Interestingly, **P1** still exhibited large negative Cotton effect (-22 mdeg) at 80 °C in MCH, indicating that **P1** can effectively maintain self-assembly of the BTA pendants even at such a high temperature. The molar ellipticity (Δ*e*) for **P1** in DCE, DCE/MCH (75/25, v/v), and MCH at 20 °C was -22, -22, and -32 L

$mol^{-1}cm^{-1}$, respectively. These values are relatively close to those for ABA or ABC random triblock copolymers functionalized with BTA in the B segment and other hydrogen-bonding units in the A segment in similar organic media (Δe = - 23 - -30 L $mol^{-1}cm^{-1}$).[12,14]

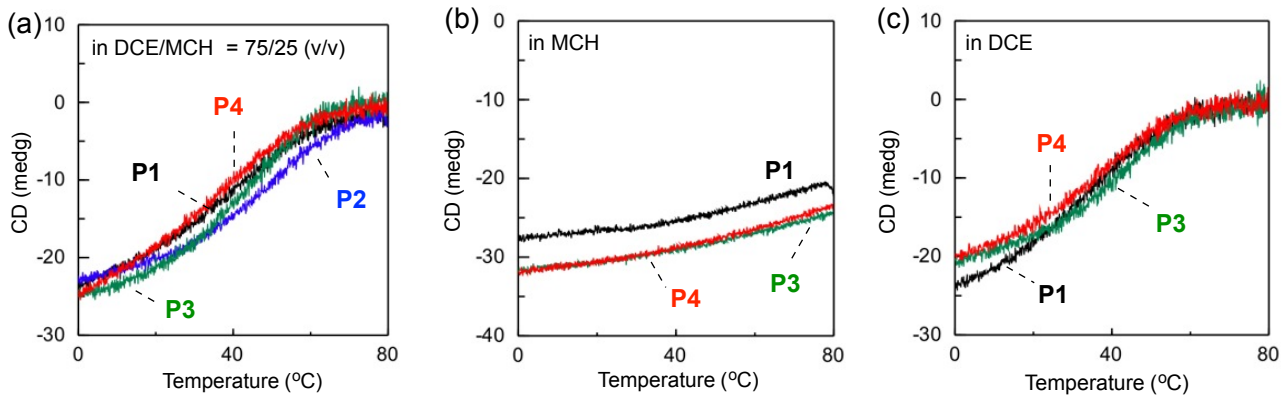

Figure 5. Temperature-dependent CD cooling curves of EHMA/BTAMA copolymers (**P1**-**P4**) in organic solvents ([BTA] = 50 μM, l = 0.5 cm) at a cooling rate of 60 K h^{-1} on probed at λ = 223 nm. (a) **P1**, **P2**, **P3**, and **P4** in DCE/MCH (75/25, v/v). (b, c) **P1**, **P3**, and **P4** in (b) MCH or (c) DCE.

The author further conducted temperature-dependent CD measurement of **P2**, **P3**, and **P4** in DCE, MCH, and a DCE/MCH mixture (75/25, v/v) to clarify the effects of BTA-sequence distribution on self-assembly of the BTA pendants. **P1** (linear gradient), **P3** (random), and **P4** (bidirectional gradient) showed similar shapes of the CD cooling curves and CD intensity in DCE (Figure 5c). The molar ellipticity (Δe) for **P1**, **P3**, and **P4** in DCE at 20 °C was -22, -21, and -19 L $mol^{-1}cm^{-1}$, respectively. The elongation temperature of the BTA pendants into helical self-assembly was about 60 °C, and was independent of the BTA sequence distribution. A similar trend in CD intensity was also observed in MCH or DCE/MCH (75/25) mixture; the intensity in MCH was largest (Figure 5a,b). These results importantly suggest that the total BTA unit number capable of helical self-assembly is in fact independent of the random or gradient sequence of 10 mol% BTAMA. In gradient copolymers (**P1** and **P4**), a BTAMA-rich segment in polymer chain can efficiently induce helical self-assembly of the pendants, while a BTAMA-poor segment in turn can hardly contribute the self-assembly. Additionally, **P1** and **P4** have the instantaneous BTAMA content ($F_{inst,BTAMA}$) of 16 and 19%, respectively, at the most. They further consist of relatively long polymer chain of 200 DP. As a result, **P1** and **P4** of such a BTA-gradient distribution would have almost identical efficiency of BTA-pendant self-assembly to **P3** of homogeneous (random) counterpart. The self-assembly of BTA pendants for gradient copolymers (**P1** and **P4**) did not undergo a cooperative process, similar to that for a random counterpart (**P3**) and several BTA-functionalized random copolymers as already reported.[11-18] In DCE/MCH mixture (75/25,

v/v), **P2** maintained negative Cotton effects at higher temperature than **P3** (Figure 5a). This is because the local BTA concentration in **P2** is higher than that in **P3**.[11-16] The negative Cotton effect of **P2** at 0 °C was, however, almost identical to that of **P1**, **P3**, and **P4** (Figure 5a). Thus, in relatively long polymer chains of 200 DP comprising 10 mol% BTA units, the sequence distribution, random or gradient, does not significantly affect the self-assembly behavior of the BTA pendants.

3-2. ***Aggregation Properties.*** EHMA/BTAMA gradient, random, and bidirectional gradient copolymers (**P1**, **P3**, and **P4**) were further analyzed by DLS in DCE, MCH, and a DCE/MCH (75/25, v/v) mixed solvent at 25 °C (Figure 6, Table 2). In DCE, **P1** and **P3** showed bimodal size distributions comprising particles with a small size (R_h = ~10 nm) and with a larger size (R_h = ~100 nm) (Figure 6a). The former originate from SCPNs or nanoaggregates comprising a small number of polymers, while the latter are attributed to multi-chain aggregates. The small size portion of **P1** (R_h = ~10 nm) increased upon heating to 60 °C. This demonstrates that aggregated polymer chains are dynamically isolated into single polymer chains by disruption of hydrogen-bonding self-assembly of BTA-pendants upon heating. This is consistent with the lack of a Cotton effect of **P1** in DCE at 60 °C (Figure 5c). In a DCE/MCH (75/25, v/v) mixed solvent, **P1** showed a bimodal size distribution, and the volume fraction of the small size portion (R_h = 6.2 nm: 40 %) was larger than that in DCE alone (Table 2). In contrast to the results in DCE, **P1**, **P3**, and **P4** showed a single, monomodal size distribution (R_h = 26 – 55 nm) in MCH at 25 °C, indicating the presence of multi-chain aggregates (Figure 6b). **P1** and **P4** with gradient sequence (**P1**: R_h = 40 nm, **P4**: R_h = 55 nm) formed nanoaggregates larger than those of the corresponding random copolymer (**P3**: R_h = 26 nm). This is probably because locally concentrated BTA pendants of **P1** and **P4** promote intermolecular self-assembly of the polymer chains to provide relatively large aggregates. Therefore, the sequence distribution of BTA units mainly affects the aggregation behavior of the polymer chains and the total size of resulting aggregates.

Table 2. Hydrodynamic Radius of EHMA/BTAMA Copolymers[a]

entry	polymer	solvent	R_h (nm)
1	**P1**	DCE	13 (25%), 111 (75%)
2	**P1**	DCE/MCH (75/25, v/v)	6.2 (40%), 128 (60%)
3	**P1**	MCH	40
4	**P3**	DCE	7.4 (9%), 97 (91%)
5	**P3**	MCH	26
6	**P4**	MCH	55

[a]Determined by DLS in DCE, MCH, and a DCE/MCH (75/25, v/v) mixed solvent at 25 °C: [polymer] = 1 mg/mL.

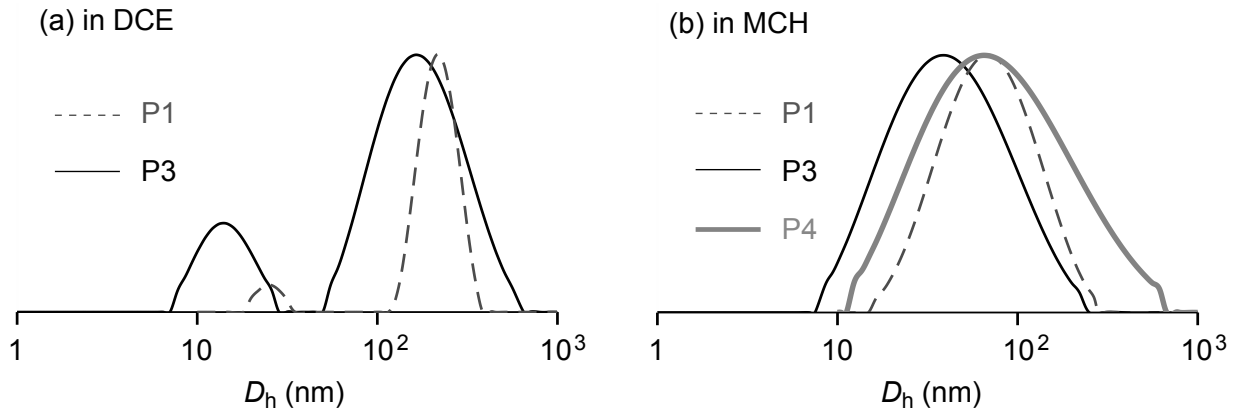

Figure 6. DLS intensity size distribution of EHMA/BTAMA copolymers (**P1**, **P3**, and **P4**) in (a) DCE or (b) MCH at 25 ^{o}C: [Polymer] = 1 mg/mL.

Conclusion

Sequence-controlled copolymers with hydrogen-bonding chiral BTA pendants were successfully synthesized by tandem catalysis of Ru-catalyzed LRP and Ti-mediated transesterification with BTA-OH. Transesterification using Ti(O*i*-Pr)$_4$ was compatible with an amide-functionalized alcohol to afford the catalytic control of introducing a hydrogen-bonding monomer sequence in copolymers. Ti-mediated transesterification of EHMA with BTA-OH was efficiently synchronized with LRP of EHMA and a generating BTAMA by tuning the concentration and addition time of the Ti catalyst, giving a well-controlled EHMA/BTAMA gradient copolymer. Additionally, synchronized tandem catalysis with a bifunctional initiator provided an EHMA/BTAMA bidirectional gradient copolymer, while transesterification faster than LRP resulted in a EHMA/BTAMA random copolymer. A series of BTA sequence-controlled copolymers efficiently formed single-chain polymeric nanoparticles or multi-chain aggregates via the helical self-assembly of the chiral BTA pendants in DCE, MCH, and their mixtures. In all cases, the self-assembly of BTA pendants was enhanced in MCH and maintained up to high temperatures (80 ^{o}C). Importantly, the total size and/or size distribution of single-chain or multi-chain nanoparticles was dependent on BTAMA sequence distribution, although temperature-dependent self-assembly behavior of the chiral BTA pendants was independent of the sequence. Typically, BTAMA gradient or bidirectional gradient copolymers formed nanoaggregates larger than the corresponding random copolymer in MCH, indicating that gradient sequence of BTA pendants would efficiently promote the intermolecular self-assembly of polymer chains. Apparently, a high local concentration of BTAs leads to intermolecular aggregation, a phenomenon observed before with polymers with too many BTAs in the main chain. Thus, the author revealed that gradient incorporation of hydrogen-bonding self-assembly units along chains is also one option to control the structure and size of nanoaggregates in organic media.

References

(1) Mavila, S.; Eivgi, O.; Berkovich, I.; Lemcoff, N. G. *Chem. Rev.* **2016**, *116*, 878-961.

(2) Ouchi, M.; Badi, N.; Lutz, J.-F.; Sawamoto, M. *Nat. Chem.* **2011**, *3*, 917–924.

(3) Li, L.; Raghupathi, K.; Song, C.; Prasad, P.; Thayumanavan, S. *Chem. Commun.* **2014**, *50*, 13417–13432.

(4) Hanlon, A. M. Lyon, C. K. Berda, E. B. *Macromolecules* **2016**, *49*, 2-14.

(5) Altintas, O.; Barner-Kowollik, C. *Macromol. Rapid Commun.* **2016**, *37*, 29–46.

(6) Gonzalez-Burgos, M.; Latorre-Sanchez, A.; Pomposo, J. A. *Chem. Soc. Rev.* **2015**, *44*, 6122-6142.

(7) Artar, M.; Huerta, E.; Meijer, E. W.; Palmans, A. R. A. *ACS Symp. Ser*. **2014**, *1170*, 313–325.

(8) Terashima, T. *Polym. J.* **2014**, *46*, 664-673.

(9) Seo, M.; Beck, B. J.; Paulusse, J. M. J.; Hawker, C. J.; Kim, S. Y. *Macromolecules* **2008**, *41*, 6413–6418.

(10) Foster, E. J.; Berda, E. B.; Meijer, E. W. *J. Am. Chem. Soc.* **2009**, *131*, 6964-6966.

(11) Mes, T.; van der Weegen, R.; Palmans, A. R. A.; Meier, E. W. *Angew. Chem. Int. Ed.* **2011**, *50*, 5085-5089.

(12) Hosono, N.; Gillissen, M. A. J.; Li, Y.; Sheiko, S. S.; Palmans, A. R. A.; Meijer, E. W. *J. Am. Chem. Soc.* **2013**, *135*, 501-510.

(13) Hosono, N.; Palmans, A. R. A.; Meijer E. W. *Chem. Commun.* **2014**, *50*, 7990–7993.

(14) Altintas, O.; Artar, M.; ter Huurne, G.; Voets, I. K.; Palmans, A. R. A.; Barner-Kowollik, C.; Meijer, E. W. *Macromolecules* **2015**, *48*, 8921-8932.

(15) Stals, P. J. M.; Gillissen, M. A. J.; Paffen, T. F. E.; de Greef, T. F. A.; Lindner, P.; Meijer, E. W.; Palmans, A. R. A.; Voets, I. K. *Macromolecules* **2014**, *47*, 2947-2954.

(16) Terashima, T.; Mes, T.; de Greef, T. F. A.; Gillissen, M. A. J.; Besenius, P.; Palmans, A. R. A.; Meijer, E. W. *J. Am. Chem. Soc.* **2011**, *133*, 4742–4745.

(17) Artar, M.; Souren, E. R. J.; Terashima, T.; Meijer, E. W.; Palmans, A. R. A. *ACS Macro Lett.* **2015**, *4*, 1099-1103.

(18) Liu, Y.; Pauloehrl, T.; Presolski, S. I.; Albertazzi, L.; Palmans, A. R. A.; Meijer, E. W. *J. Am. Chem. Soc.* **2015**, *137*, 13096-13105.

(19) Altintas, O.; Lejeune, E.; Gerstel, P.; Barner-Kowollik, C. *Polym. Chem*. **2012**, *3*, 640–651.

(20) Romulus, J.; Weck, M. *Macromol. Rapid Commun.* **2013**, *34*, 1518–1523.

(21) Willenbacher, J.; Altintas, O.; Trouillet, V.; Knöfel, N.; Monteiro, M. J.; Roesky, P. W.; Barner-Kowollik, C. *Polym. Chem.* **2015**, *6*, 4358–4365.

(22) Mavila, S.; Rozenberg, I.; Lemcoff, N. G. *Chem. Sci.* **2014**, *5*, 4196-4203.

(23) Sanchez-Sanchez, A.; Arbe, A.; Kohlbrecher, J.; Colmenero, J.; Pomposo, J. A. *Macromol.*

Rapid. Commun. **2015**, *36*, 1592-1597.

(24) Appel, E. A.; Dyson, J.; del Barrio, J.; Walsh, Z.; Scherman, O. A. *Angew. Chem. Int. Ed.* **2012**, *51*, 4185–4189.

(25) Morishima, Y.; Nomura, S.; Ikeda, T.; Seki, M.; Kamachi, M. *Macromolecules* **1999**, *32*, 7469-7475.

(26) Terashima, T.; Sugita, T.; Fukae, K.; Sawamoto, M. *Macromolecules* **2014**, *47*, 589–600.

(27) Matsumoto, K.; Terashima, T.; Sugita, T.; Takenaka, M.; Sawamoto, M. *Macromolecules* **2016**, *49*, 7917-7927.

(28) Koda, Y.; Terashima, T.; Sawamoto, M. *Macromolecules* **2016**, *49*, 4534-4543.

(29) Hirai, Y.; Terashima, T.; Takenaka, M.; Sawamoto, M. *Macromolecules* **2016**, *49*, 5084-5091.

(30) Croce, T. A.; Hamilton, S. K.; Chen, M. L.; Muchalski, H.; Harth, E. *Macromolecules* **2007**, *40*, 6028–6031.

(31) Cherian, A. E.; Sun, F. C.; Sheiko, S. S.; Coates, G. W. *J. Am. Chem. Soc.* **2007**, *129*, 11350–11351.

(32) Murray, B. S.; Fulton, D. A. *Macromolecules* **2011**, *44*, 7242–7252.

(33) Chao, D.; Jia, X.; Tuten, B.; Wang, C.; Berda, E. B. *Chem. Commun.* **2013**, *49*, 4178–4180.

(34) Song, C.; Li, L.; Dai, L.; Thayumanavan, S. *Polym. Chem.* **2015**, *6*, 4828–4834.

(35) Wong, E. H. H.; Qiao, G. G. *Macromolecules* **2015**, *48*, 1371-1379.

(36) Matsunaga, Y.; Miyajima, N.; Nakayasu, Y.; Sakai, S.; Yonenaga, M. *Bull. Chem. Soc. Jpn.* **1988,** *61,* 207-210

(37) Yasuda, Y.; Iishi, E.; Inada, H.; Shirota, Y. *Chem. Lett.* **1996**, *7,* 575-576.

(38) Sakamoto, A.; Ogata, D.; Shikata, T.; Hanabusa, K. *Macromolecules* **2005**, *38*, 8983-8986.

(39) de Loos, M.; van Esch, J. H.; Kellogg, R. M.; Feringa, B. L. *Tetrahedron* **2007**, *63,* 7285-7301.

(40) Blomenhofer, M.; Ganzleben, S.; Hanft, D.; Schmidt, H.-W.; Kristiansen, M.; Smith, P.; Stoll, K.; Maeder, D.; Hoffmann, K. *Macromolecules* **2005**, *38,* 3688-3695.

(41) van Gorp, J. J.; Vekemans, J. A. J. M.; Meijer, E. W. *J. Am. Chem. Soc.* **2002**, *124*, 14759–14769.

(42) Smulders, M. M. J.; Filot, I. A. W.; Leenders, J. M. A.; van der Schoot, P.; A. R. A. Palmans.; Schenning, A. P. H. J.; E. W. Meijer. *J. Am. Chem. Soc.* **2010**, *132*, 611–619.

(43) Y. Nakano.; T. Hirose.; P. J. M. Stals.; E. W. Meijer.; A. R. A. Palmans. *Chem. Sci.* **2012**, *3*, 148-155.

(44) Ouchi, M.; Terashima, T.; Sawamoto, M. *Chem. Rev.* **2009,** 109, 4963−5050.

(45) Matyjaszewski, K.; Tsarevsky, N. V. *J. Am. Chem. Soc.* **2014**, *136*, 6513-6533.

(46) Nakatani, K.; Terahsima, T.; Sawamoto, M. *J. Am. Chem. Soc.* **2009**, *131*, 13600-13601.

(47) Nakatani, K.; Ogura, Y.; Koda, Y.; Terashima, T.; Sawamoto, M. *J. Am. Chem. Soc.* **2012**, *134*, 4373-4383.

(48) Ogura, Y.; Terashima, T.; Sawamoto, M. *ACS Maco Lett.* **2013**, *2*, 985-989.

(49) Ogura, Y.; Terashima, T.; Sawamoto, M. *Macromolecules* **2017** in press.

(50) Matyjaszewski, K.; Ziegler, M. J.; Arehart, S. V.; Greszta, D.; Pakula, T. *J. Phys. Org. Chem.* **2000**, *13*, 775−786.

(51) Park, J-S.; Kataoka, K. *Macromolecules* **2006**, *39*, 6622-6630.

(52) Kim, J.; Mok, M. M.; Sandoval, R. W.; Woo, D. J.; Torkelson, J. M. *Macromolecules* **2006**, *39*, 6152-6160.

(53) Seno, K.; Tsujimoto, I.; Kanaoka, S.; Aoshima, S. *J. Polym. Sci. Part A: Polym. Chem.* **2008**, *46*, 6444–6454.

(54) Rehwinkel, H.; Steglich, W. *Synthesis* **1982**, 826-827.

(55) Krasik, P. *Tetrahedron Lett.* **1998**, *39*, 4223-4226.

Chapter 4

Fluorinated Gradient Copolymers: Tandem Transesterification with Fluoroalcohols

Abstract

Fluorinated gradient copolymers were successfully synthesized by tandem catalysis of ruthenium-catalyzed living radical polymerization (LRP) and titanium alkoxide-mediated transesterification of methyl methacrylate (MMA) with less nucleophilic fluoroalcohols (R_FOH). For this, various metal catalysts with or without molecular sieves 4A (MS 4A) were investigated for efficient transesterification of MMA using fluroalcohols into fluorinated methacrylates (R_FMA). As a result, Ti(O*i*-Pr)$_4$ (2 – 8 mol%) with MS 4A was effective for transesterification of MMA into R_FMA. The yield of R_FMA increased with increasing the alkyl spacer length between the hydroxyl group and the fluorinated alkyl segment in fluoroalcohols: propyl (4,4,4,5,5-pentafluoro-1-pentanol: 5FPOH) > ethyl (1*H*,1*H*,2*H*,2*H*-nonafluoro-1-hexanol: 9FHOH) > methyl (1*H*,1*H*-heptafluoro-1-butanol). Given that, tandem polymerization of MMA was conducted with a ruthenium catalyst, a chloride initiator, and Ti(O*i*-Pr)$_4$ in toluene/fluoroalcohol mixture (1/1, v/v) at 80 ^oC. Typically, in the presence of 4 mol% Ti and MS 4A, transesterification of MMA with 5FPOH or 9FHOH was synchronized with LRP to produce well-controlled MMA/5FPMA or MMA/9FHMA gradient copolymers in high yield.

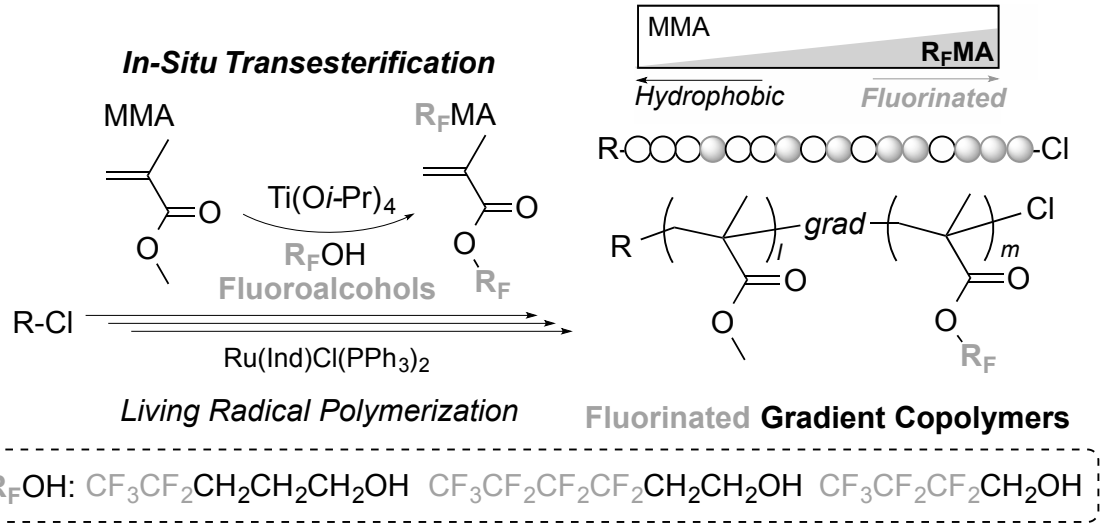

Introduction

Fluorination of polymers is a promising strategy to create functional polymeric materials with characteristic properties distinct from non-fluorinated polymers.[1-10] Perfluorinated polymers are "so called" fluorous, immiscible with organic and aqueous solvents and compounds, to show water/oil repellency.[10-15] In contrast, fluorinated copolymers containing hydrophobic or hydrophilic monomer units are soluble and/or dispersed in organic or aqueous media, while they effectively induce specific self-assembly and modulate physical properties owing to the partially fluorinated segments.[16-20] The properties and functions of fluorinated copolymers certainly depend on the sequence distribution of fluorinated units along a chain. Among sequence-controlled copolymers, gradient copolymers have unique monomer sequence; the instantaneous composition of two monomers gradually changes from one terminal to another.[21,22] Thus, functional gradient copolymers show physical properties (e.g., phase separation, glass transition temperature) distinct form corresponding random or block counterparts.[23-25] In this context, fluorinated gradient copolymers would be intriguing as a new class of functional materials, where the distribution, *i.e.*, local concentration, of fluorinated units gradually changes along a chain. Although several functional gradient copolymers have been already synthesized, the efficient synthetic systems of fluorinated gradient copolymers are hardly developed yet.[15]

As a versatile system for functional gradient copolymers, the author has developed concurrent tandem catalysis combined with metal alkoxide [$Al(O\textit{i}\text{-}Pr)_3$, $Ti(O\textit{i}\text{-}Pr)_4$]-mediated transesterification and ruthenium-catalyzed living radical polymerization (LRP).[26,24d] Here, methacrylate (R_1MA) as a starting monomer is transesterified with alcohol (R_2OH) into different methacrylate (R_2MA) during LRP of both monomers. Importantly, adjusting concentration of the transesterification catalyst enables to control generation of R_2MA and comonomer ratio (R_1MA/R_2MA), resulting in control of monomer sequence and composition in obtained R_1MA/R_2MA gradient copolymers. Full synchronization of LRP and transesterification leads to gradient sequence where instantaneous R_2MA composition linearly increases along polymer chain from the initiating terminal to growing counterpart. Importantly, a wide variety of alcohols such as 1-dodecanol (hydrophobic), poly(ethylene glycol) methyl ether (PEG-OH: hydrophilic), *iso*-propanol (sec-alcohol) are applicable to this system to efficiently functionalize gradient and relating sequence-controlled copolymers.

In this chapter, the author works on the synthesis of fluorinated gradient copolymers via tandem catalysis of LRP and transesterification of methyl methacrylate (MMA) with fluoroalcohols (R_FOH) (Scheme 1). In general, efficiency of transesterification depends on the steric hindrance and/or electronical factors of ester compounds and alcohols.[27] Less nucleophilic alcohols such as fluoroalcohols are recognized to be not so suitable for transesterification because the reverse

reaction between the product and a liberated alcohol is more favored. Owing to electron-withdrawing fluorinated segments, fluoroalcohols actually are more acidic (lower pH) and less nucleophilic than non-fluorinated alcohols (e.g., methanol: pH = 15.5, trifluoroethanol: pH = 12.4).[28-30] Therefore, fluoroalcohols have been hardly utilized for transesterification, whereas the reaction would be potentially effective to produce fluorinated compounds and polymers.

Considering such backgrounds, the author first investigated various metal alkoxides and Lewis Acid as catalyst for transesterification of MMA with fluoroalcohols (R_FOH) into fluorinated methacrylates (R_FMA): Al(O*i*-Pr)$_3$, Ti(O*i*-Pr)$_4$, Sc(OTf)$_3$, Y(OTf)$_3$, $ZrCl_4$, and Yb(OTf)$_3$.[31] In order to examine the effects of nucleophilicity and pH on transesterification, several fluoroalcohols of different fluorine number and/or the alkyl spacer length between hydroxyl group and perfluorinated alkyl segments are employed: 4,4,5,5,5-pentafluoro-1-pentanol (5FPOH), 1*H*,1*H*,2*H*,2*H*-nonafluoro-1-hexanol (9FHOH), 1*H*,1*H*-heptafluoro-1-butanol (7FBOH), and trifluoroethanol (TFEOH). Among various catalysts, Ti(O*i*-Pr)$_4$ (2 – 8 mol%) coupled with molecular sieves 4A (MS 4A) was found to effectively promote transesterification of MMA with all of the fluoroalcohols. The yield of R_FMA increased with increasing the alkyl spacer length between the hydroxyl group and the fluorinated alkyl segment in fluoroalcohols: propyl (5FPOH) > ethyl (9FHOH) > methyl (7FBOH, TFEOH).

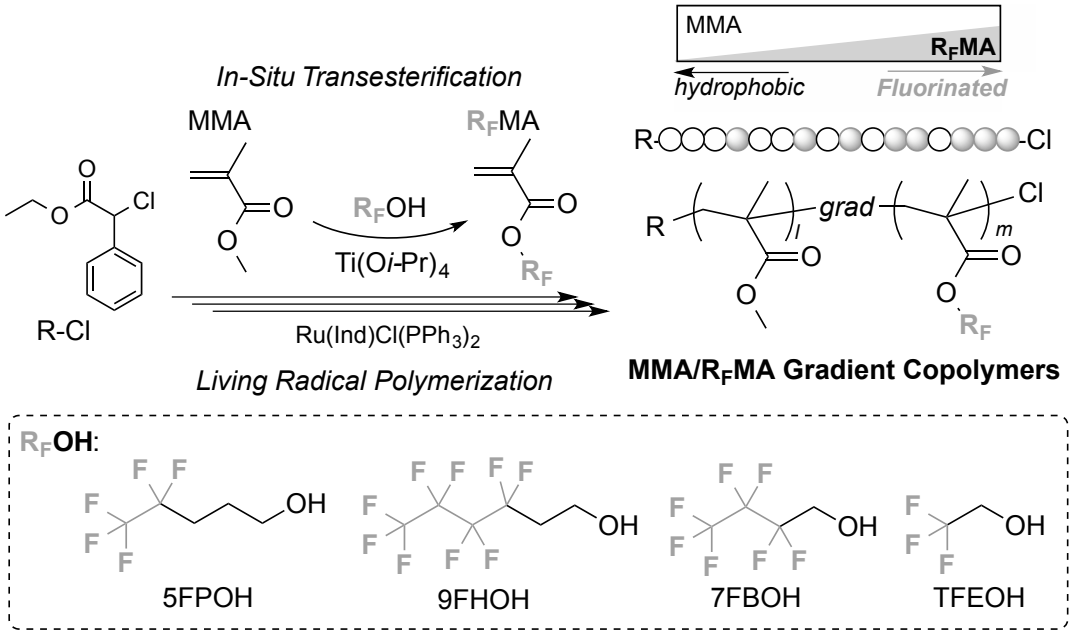

Scheme 1. Synthesis of Fluorinated Gradient Copolymers via Tandem Catalysis of Living Radical Polymerization and Transesterification of MMA with Fluoroalcohols.

Ti(O*i*-Pr)$_4$ was then applied to tandem polymerization of MMA with a ruthenium catalyst, a chloride initiator, and fluoroalcohols. To control the kinetic balance of transesterification and LRP,

the concentration of Ti catalyst and fluoroalcohols, and reaction temperature were systematically varied. As a result, in the presence of 4 mol% Ti and MS 4A, transesterification of MMA with 5FPOH or 9FHOH was fully synchronized with LRP at 80 ^{o}C to produce well-controlled MMA/5FPMA or MMA/9FHMA gradient copolymers with linear gradient sequence distribution. To my best knowledge, this is the first example to use transesterification with fluoroalcohols as efficient and practical synthetic strategy of fluorinated gradient sequence-controlled copolymers with various sequence distribution. This work importantly provided a novel fluorination technique of ester compounds and polymers by transesterification with fluoroalcohols.

Experimental Section

Materials. Methyl methacrylate (MMA: TCI; purity >99.8%) and tetralin (1,2,3,4-tetrahydronaphthalene: Kishida Chemical; purity >98%; an internal standard for ^{1}H NMR analysis) were dried overnight with calcium chloride and distilled from calcium hydride under reduced pressure before use. Methacryloyl chloride (TCI, purity >80.0%) and triethylamine (TCI, purity >99.0%) were purified by distillation before use. 4,4,4,5,5-Pentafluoro-1-pentanol (5FPOH) (TCI, purity >93%), 1*H*,1*H*-heptafluoro-1-butanol (7FBOH) (TCI, purity >95%), 1*H*,1*H*,2*H*,2*H*-nonafluoro-1-hexanol (9FHOH) (TCI, purity >97%), 2,2,2-trifluoroethanol (TFEOH) (TCI, purity >99%), and Ti(O*i*-Pr)$_4$ (Aldrich, purity >97%) were degassed by triple vacuum-argon purge cycles before use. Ethyl 2-chloro-2-phenylacetate (ECPA: Aldrich; purity >97%) was distilled under reduced pressure before use. Ru(Ind)Cl(PPh$_3$)$_2$ (Aldrich), Al(O*i*-Pr)$_3$ (Aldrich, purity >98%), zirconium (IV) chloride ($ZrCl_4$: Aldrich, purity >98%), scandium(III) trifluoromethanesulfonate (Sc(SO$_3$CF$_3$)$_3$: Aldrich, purity >99%), ytterbium (III) trifluoromethanesulfonate (Yb(SO$_3$CF$_3$)$_3$: Aldrich, purity >99.99%) and yttrium (III) trifluoromethanesulfonate (Y(SO$_3$CF$_3$)$_3$: Aldrich, purity >99.99%) were used as received and handled in a glove box under moisture- and oxygen-free argon (H_2O <1 ppm; O_2 <1 ppm). Toluene was purified by pashing it through a purification column (Glass Contour Solvent Systems: SG Water USA). Dry THF (Wako, dehydrated), dry diethyl ether (Wako, dehydrated), hexane (Wako, purity >96%) and ethyl acetate (Wako, purity >99.5%) were used as received. Molecular sieves 4A (Wako) were baked with heat gun under reduced pressure before use.

Characterization. Molecular weight distribution (MWD) curves, M_n, and M_w/M_n ratio of the polymers were measured by SEC in $CHCl_3$ at 40 ^{o}C (flow rate: 1 mL/min) on three linear-type polystyrene gel columns (Shodex K-805L: exclusion limit = 4 × 10^6; particle size = 10 mm; pore size = 5000 Å; 0.8 cm i.d. × 30 cm) that were connected to a Jasco PU-980 precision pump, a Jasco

RI-1530 refractive index detector, and a Jasco UV-980 UV/vis detector set at 250 nm. The columns were calibrated against 10 standard poly(MMA) samples (Polymer Laboratories; M_n = 1000–1200000; M_w/M_n = 1.06–1.22). To remove unreacted monomers and catalyst and fluoroalcohol residues, polymer samples were purified by preparative SEC before characterization [column: Shodex K-5002; particle size = 15 mm; 5.0 cm i.d. × 30 cm; exclusion limit = 5×10^3 g/mol; flow rate = 10 mL/min]. ^{1}H and ^{19}F NMR spectra were recorded in $CDCl_3$ or CD_2Cl_2 at 25 ^{o}C on a JEOL JNM-ECA500 spectrometer operating at 500.16 (^{1}H) or 470.62 (^{19}F) MHz. Differential scanning calorimetry (DSC) measurement of polymers (ca. 5 mg weighed into an aluminum pan) was performed under dry nitrogen flow on a DSC Q200 calorimeter (TA Instruments) equipped with a RCS 90 electric freezing machine. The polymer samples were heated to 150 ^{o}C at the rate of 10 ^{o}C/min and held at the temperature for 10 min to erase thermal history. Then, the samples were cooled to -80 ^{o}C at the rate of -10 ^{o}C/min and held at the temperature for 10 min, and again heated to 150 ^{o}C at the rate of 10 ^{o}C/min. The second heating runs were used for the thermal analysis of polymers.

Synthesis of 5FPMA. In 200 mL round-bottomed flask filled with argon, methacryloyl chloride (77.3 mmol, 7.48 mL) was added to a solution of 5FPOH (51.5 mmol, 6.8 mL) and triethylamine (77.0 mmol, 10.7 mL) in dry THF (36.7 mL) at 0 ^{o}C. The reaction mixture was stirred at 25 ^{o}C for 27 h. The THF solvent was removed in vacuo. Into the condensed mixture, distilled water (50 mL) and diethyl ether (50 mL) were added. The aqueous phase was separated and extracted by diethyl ether (25 mL), and the ether extracts were combined with the organic layer. The combined organic phase was washed with water three times, ammonia-water, and brine, and was dried over anhydrous Na_2SO_4 overnight. After the ether was removed in vacuo, the crude product was purified by silica gel column chromatography with hexane/ethyl acetate (15/1, v/v) to give 5FHMA as a liquid (4.1g, 32% yield). ^{1}H NMR [500 MHz, $CDCl_3$, 25 ^{o}C, δ = 0 TMS]: δ = 6.1, 5.6 ($C\underline{H}_2$=C(CH_3)COO-, 1H, s), 4.2 (-COO$C\underline{H}_2CH_2$-, 2H, t, J = 6.5 Hz), 2.2-2.1 (-$CH_2C\underline{H}_2CF_2$-, 2H, m), 2.0-1.9 (-$CH_2C\underline{H}_2CH_2$-, 2H, quin), 1.9 (CH_2=C($C\underline{H}_3$)COO-, 3H, s). ^{19}F NMR [470 MHz, $CDCl_3$, 25 ^{o}C, δ = -76.5 ppm (CF_3COOH in $CDCl_3$)]: δ -86.4 – -86.6 (-CF_3), -119.1 – -119.4 (-$CH_2C\underline{F}_2CF_3$). ^{13}C NMR [125 MHz, $CDCl_3$, 25 ^{o}C, δ = 77.0 ppm ($CDCl_3$)]: δ = 167.1 (C=O), 136.0 (CH_2=$\underline{C}CH_3$), 125.3 ($\underline{C}H_2$=CCH_3), 119.1 (CF_3, qt, $^1J_{CF}$ =283.8, $^2J_{CF}$ =36.3 Hz), 115.5 (CF_2, tq $^1J_{CF}$ =250.0, $^2J_{CF}$ =38.8 Hz), 63.0 (O$\underline{C}H_2CH_2$), 27.6 ($\underline{C}H_2CF_2$, t, $^2J_{CF}$ =22.5 Hz), 20.1 ($\underline{C}H_3$), 18.2 ($CH_2\underline{C}H_2CH_2$).

Transesterification of MMA with Fluoroalcohols. A typical procedure for transesterification of MMA with 5FPOH (2.9 M) and Ti(O*i*-Pr)$_4$ (40 mM) was given: Into a 30 mL glass tube, toluene (0.30 mL), 5FPOH (2.9 mmol, 0.38 mL), tetralin (0.03 mL), a 500 mM toluene solution of

$Ti(O\textit{i}\text{-}Pr)_4$ (0.08 mL, $Ti(O\textit{i}\text{-}Pr)_4$ = 0.04 mmol), and MMA (2 mmol, 0.21 mL) were added sequentially in that order at 25 °C under argon (the total volume: 1.0 mL). The glass tube was then placed in an oil bath kept at 80 °C. At predetermined intervals, the mixture was sampled with a syringe under argon, and the sampled solutions were cooled to –78 °C to terminate the reaction. Conversion of MMA into 5FPMA was determined by ^{1}H NMR measurement of the solution in $CDCl_3$ at 25 °C with tetralin as an internal standard (48 h, conv. 8%).

Polymerization. The synthesis of fluorinated gradient copolymers was carried out by syringe technique under argon in baked glass tubes equipped with a three-way stopcock.

MMA/5FPMA gradient copolymer (entry 9)**.** MS 4A (1.0 g) was first placed and dried in a 30 mL glass tube under reduced pressure with heat gun. Into the tube, $Ru(Ind)Cl(PPh_3)_2$ (0.006 mmol, 4.66 mg) was charged, and toluene (0.55 mL), 5FPOH (1.14 mL), tetralin (0.08 mL), a 500 mM toluene solution of $Ti(O\textit{i}\text{-}Pr)_4$ (0.48 mL, $Ti(O\textit{i}\text{-}Pr)_4$ = 0.24 mmol), MMA (6 mmol, 0.64 mL), and a 550 mM toluene solution of ECPA (0.11 mL, ECPA = 0.06 mmol) were added sequentially in that order at 25 °C under argon (the total volume: 3.0 mL). The glass tube was then placed in an oil bath kept at 80 °C. At predetermined intervals, the mixture was sampled with a syringe under argon, and the sampled solutions were cooled to –78 °C to terminate the reaction. The total monomer conversion, 5FHMA content in monomer, and cumulative 5FPMA content in polymer ($F_{cum,5FPMA}$) were directly determined by ^{1}H NMR measurement of the terminated reaction solutions in $CDCl_3$ at 25 °C with tetralin as an internal standard. Instantaneous 5FPMA content in polymer ($F_{inst,5FPMA}$) was estimated according to the following equation: $F_{inst,5FPMA} = [Conv._{total,\,\textit{i}} \times F_{cum,5FPMA,\,\textit{i}} - Conv._{total,\,\textit{i-1}} \times F_{cum,5FPMA,\,\textit{i-1}}]/[Conv._{total,\,\textit{i}} - Conv._{total,\,\textit{i-1}}]$, where $Conv._{total}$ is the total conversion of both monomers. The quenched solutions were evaporated to dryness to give the crude product. To remove unreacted monomers, solvents, and catalyst residue, the product was purified by preparative SEC before characterization (^{1}H NMR, thermal properties). SEC ($CHCl_3$, PMMA std.): M_n = 32500, M_w/M_n = 1.17. ^{1}H NMR [500 MHz, CD_2Cl_2, 25 °C, δ = 5.33 $CDHCl_2$] δ 7.3–7.1 (aromatic), 4.9–4.7 (-COOC<u>H</u>$(CH_3)_2$), 4.2–3.9 (-COOC<u>H</u>$_2$$CH_2$-), 3.7–3.40 (-OC<u>H</u>$_3$), 2.3−2.1 (-CH_2C<u>H</u>$_2$$CF_2$-), 2.1−1.4 (-$CH_2$C<u>H</u>$_2$$CH_2$-, -C<u>H</u>$_2C(CH_3)$-), 1.3−0.7 (-COOCH(C<u>H</u>$_3)_2$, -CH_2C(C<u>H</u>$_3$)-). M_n (NMR, α) = 25600; $DP_{MMA}/DP_{5FPMA}/DP_{\textit{i}\text{-}PrMA}$ = 47/81/6; $F_{cum,5FPMA}$ = 61%. ^{19}F NMR [470 MHz, CD_2Cl_2, 25 °C, δ = -76.5 ppm (CF_3COOH in $CDCl_3$)]: δ -86.8 – -87.3 (-CF_3), -119.3 – -120.1 (-CH_2C<u>F</u>$_2$$CF_3$).

MMA/9FHMA gradient copolymer (entry 10)**.** SEC ($CHCl_3$, PMMA std.): M_n = 19600 g/mol; M_w/M_n = 1.27. ^{1}H NMR [500 MHz, CD_2Cl_2, 25 °C, δ = 5.33 $CDHCl_2$] δ 7.3–7.1 (aromatic), 4.9–4.7 (-COOC<u>H</u>$(CH_3)_2$), 4.4–4.1 (-COOC<u>H</u>$_2$$CH_2$-), 3.7–3.4 (-OC<u>H</u>$_3$), 2.6−2.4 (-$CH_2$C<u>H</u>$_2$$CF_2$-), 2.1−1.4 (-C<u>H</u>$_2C(CH_3)$-), 1.30–0.6 (-COOCH(C<u>H</u>$_3)_2$, -CH_2C(C<u>H</u>$_3$)-). M_n (NMR, α) = 17300;

$DP_{MMA}/DP_{9FHMA}/DP_{i\text{-}PrMA}$ = 65/45/3; $F_{cum,9FHMA}$ = 40%. ^{19}F NMR [470 MHz, CD_2Cl_2, 25 °C, δ = -76.5 ppm (CF_3COOH in $CDCl_3$)]: δ -81.8 – -83.1 (-CF_3), -114.0 – -115.7 (-$CH_2C\underline{F}_2CF_2$-), -125.2 – -126.4 (-$CF_2C\underline{F}_2CF_2$-), -126.8 – -127.7 (-$CF_2C\underline{F}_2CF_3$).

MMA/7FBMA gradient copolymer (entry 11)**.** SEC ($CHCl_3$, PMMA std.): M_n = 12400 g/mol; M_w/M_n = 1.43. ^{1}H NMR [500 MHz, CD_2Cl_2, 25 °C, δ = 5.33 $CDHCl_2$] δ 7.3–7.1 (aromatic), 4.9–4.7 (-COOC$\underline{H}(CH_3)_2$), 4.6–4.3 (-COOC$\underline{H}_2CF_2$-), 3.7–3.4 (-OC$\underline{H}_3$), 2.2−1.4 (-C$\underline{H}_2C(CH_3)$-), 1.3–0.6 (-COOCH(C$\underline{H}_3)_2$, -$CH_2C(C\underline{H}_3)$-). M_n (NMR, α) = 16400; $DP_{MMA}/DP_{7FBMA}/DP_{i\text{-}PrMA}$ = 66/27/18; $F_{cum,7FBMA}$ = 25%. ^{19}F NMR [470 MHz, CD_2Cl_2, 25 °C, δ = -76.5 ppm (CF_3COOH in $CDCl_3$)]: δ -81.9 – -82.6 (-CF_3), -120.8 – -121.6 (-$CH_2C\underline{F}_2CF_2$-), -128.2 – -128.8 (-$CF_2C\underline{F}_2CF_3$).

Results and Discussion

1. Transesterification of MMA with Fluoroalcohols

We investigated transesterification of MMA with fluoroalcohols (R_FOH) and various metal catalysts into fluorinated alkyl methacrylates (R_FMA) at 80 °C as model reaction for tandem polymerization (Scheme 2). To produce R_FMA with different pendant units, the author employed four kinds of fluoroalcohols, $CF_3CF_2CH_2CH_2CH_2OH$ (5FPOH), $CF_3CF_2CF_2CF_2CH_2CH_2OH$ (9FHOH), $CF_3CF_2CF_2CH_2OH$ (7FBOH), and CF_3CH_2OH (TFEOH) with different fluorine atom number and alkyl spacer length [R_F-$(CH_2)_n$-OH]. Here, the author testified six kinds of catalysts including Al(O*i*-Pr)$_3$, Ti(O*i*-Pr)$_4$, Sc(OTf)$_3$, Y(OTf)$_3$, $ZrCl_4$, and Yb(OTf)$_3$ that were used as transesterification catalysts for tandem polymerization or well known as active catalysts for transesterification and the related reactions.[31,32] In the model reactions, MMA concentration and volume of alcohols (R_FOH) were kept constant as 2000 mM and 50 vol% [toluene/R_FOH (1/1, v/v)], respectively, while the catalyst concentration was varied ([catalyst] = 40, 80, and 160 mM: 2, 4, and 8 mol%) without or with molecular sieves 4A (MS 4A: 0.33 g/mL). Conversion of MMA into a corresponding R_FMA in 48 h was determined by ^{1}H NMR. The results are depicted in Table 1.

First, using 40 mM of Al(O*i*-Pr)$_3$, Ti(O*i*-Pr)$_4$, Sc(OTf)$_3$, Y(OTf)$_3$, $ZrCl_4$, and Yb(OTf)$_3$, the author examined transesterification of MMA (2000 mM) with 5FPOH of a relatively long alkyl spacer [-$(CH_2)_3$-] between hydroxyl group (OH) and fluorinated alkyl segment (-CF_2CF_3). Sc(OTf)$_3$ efficiently induced transesterification of MMA into a corresponding 5FPMA (conversion 34%), while the other catalysts gave lower yield of the product (0 - 15%). Generally, 5 – 40 mM (0.25 – 2 mol%) of Ti(O*i*-Pr)$_4$ was enough as catalyst to effectively induce transesterification of MMA with alkyl alcohols and poly(ethylene glycol)s in our tandem catalysis: e.g, MMA (2000 mM) was efficiently transformed with dodecanol and 20 mM Ti into dodecyl methacrylate (65%, 42 h).[24d] The low yield of 5FPMA with 40 mM Ti is due to the less nucleophilic character of

5FPOH by the electron-withdrawing fluorinated alkyl segment. To promote the transesterification, the author increased Ti concentration from 40 mM to 80 mM and also used molecular sieves 4A (MS 4A) to remove a generating methanol therefrom. As a result, the yield of 5FPMA reached to 58% (without MS 4A) or 78% (with MS 4A), importantly indicating that the removal of methanol efficiently suppresses the reverse reaction that produces MMA via transesterification of 5FPMA with the methanol.

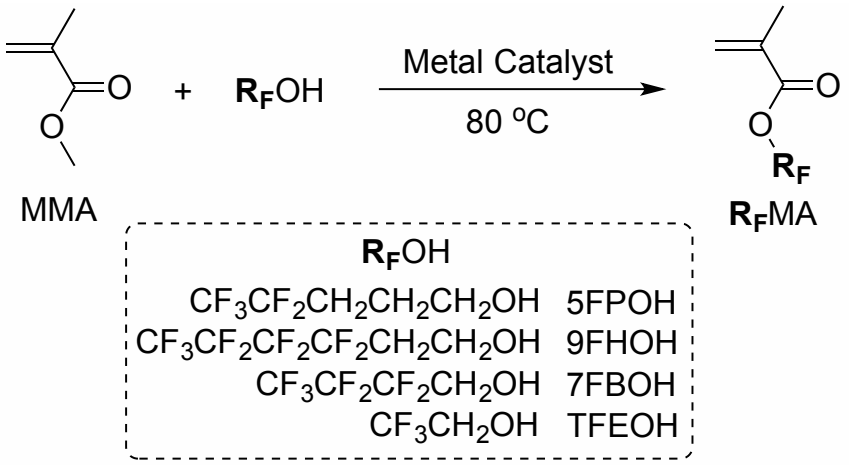

Scheme 2. Transesterification of MMA with fluoroalcohols (R_FOH) into fluorinated methacrylates (R_FMA).

The author further utilized Al(O*i*-Pr)$_3$, Ti(O*i*-Pr)$_4$, $ZrCl_4$, and Sc(OTf)$_3$ for transesterification of MMA with 9FHOH, 7FBOH, and TFEOH. 9FHOH, 7FBOH, and TFEOH are much less nucleophilic than 5FPOH owing to the larger number of fluorine atoms and/or shorter alkyl spacers. In the case of 40 mM catalysts, $ZrCl_4$, and Sc(OTf)$_3$ were effective for transesterification of MMA with 9FHOH. Relatively high concentration of Ti (80 or 160 mM; 4 or 8 mol%) with MS 4A was more effective for transesterification of MMA with TFEOH, 9FHOH and 7FBOH. The yield of products (R_FMA) increased with increasing alkyl spacer length of R_FOH: 5FPOH > 9FHOH > TFEOH > 7FBOH. This tendency is consistent with the nucleophilicity of R_FOH. These results suggest that $ZrCl_4$, Sc(OTf)$_3$, and Ti(O*i*-Pr)$_4$ are effective as catalysts for tandem polymerization of MMA with a series of fluoroalcohols (5FPOH, 9FHOH, 7FBOH, and TFEOH).

To accomplish gradient sequence control by this tandem catalysis, selective transesterification of monomers even in the presence of polymers is essential.[26] Thus, the author also tested the transesterification of a chlorine-capped poly(methyl methacrylate) (PMMA-Cl: M_n = 12000, M_w/M_n = 1.14) with 5FPOH (2.9 M) and Ti(O*i*-Pr)$_4$ (160 mM) at 80 °C for 50 h. Owing to the steric hindrance around pendant carbonyl group,[26b] the polymer pendant methyl esters were not transesterified under this condition at all. Thus, Ti-catalyzed transesterification of MMA with fluroalcohols can be potentially applicable to tandem catalysis for fluorinated gradient copolymers.

Table 1. Transesterification of MMA with Fluoroalcohol[a]

R_FOH	Alkyl Spacer	catalyst	catalyst (mM)	conv.[b] (%)
5FPOH	3	$Al(Oi\text{-}Pr)_3$	40	9
5FPOH	3	$Ti(Oi\text{-}Pr)_4$	40	8
5FPOH	3	$Ti(Oi\text{-}Pr)_4$	80	58
5FPOH	3	$Ti(Oi\text{-}Pr)_4$ + MS 4A[c]	80	78
5FPOH	3	$ZrCl_4$	40	15
5FPOH	3	$Sc(OTf)_3$	40	34
5FPOH	3	$Y(OTf)_3$	40	0
5FPOH	3	$Tb(OTf)_3$	40	0
9FHOH	2	$Al(Oi\text{-}Pr)_3$	40	0
9FHOH	2	$Ti(Oi\text{-}Pr)_4$	40	0
9FHOH	2	$Ti(Oi\text{-}Pr)_4$	80	41
9FHOH	2	$Ti(Oi\text{-}Pr)_4$+ MS 4A[c]	80	66
9FHOH	2	$ZrCl_4$	40	35
9FHOH	2	$Sc(OTf)_3$	40	33
7FBOH	1	$Ti(Oi\text{-}Pr)_4$	40	0
7FBOH	1	$Ti(Oi\text{-}Pr)_4$	80	12
7FBOH	1	$Ti(Oi\text{-}Pr)_4$+ MS 4A[c]	80	34
7FBOH	1	$Ti(Oi\text{-}Pr)_4$+ MS 4A[c]	160	43
7FBOH	1	$ZrCl_4$	40	0
7FBOH	1	$Sc(OTf)_3$	40	0
TFEOH	1	$Ti(Oi\text{-}Pr)_4$	80	14
TFEOH	1	$Ti(Oi\text{-}Pr)_4$+ MS 4A[c]	80	48

[a][MMA]/[catalyst] = 2000/40, 80, and 160 mM in toluene/R_FOH (1/1, v/v) at 80 °C for 48 h. R_FOH: $CF_3CF_2CH_2CH_2CH_2OH$ (5FPOH: 2.9 M), $CF_3CF_2CF_2CF_2CH_2CH_2OH$ (9FHOH: 2.3 M), $CF_3CF_2CF_2CH_2OH$ (7FBOH: 3 M), and CF_3CH_2OH (TFEOH: 5.3 M)]. [b]Determined by ^1H NMR with an internal standard (tetralin). [c]With molecular sieves 4A (MS 4A): [MS 4A] = 0.33 g/mL.

2. Synthesis of MMA/5FPMA Gradient Copolymers via Concurrent Tandem Catalysis

MMA was efficiently transesterified with 5FPOH and $Ti(Oi\text{-}Pr)_4$ even in the absence of MS 4A by tuning the catalyst concentration as described above. Focusing on the compatibility with ruthenium-catalyzed polymerization, the author first employed 5FPOH as an alcohol and $Ti(Oi\text{-}Pr)_4$ as catalyst for concurrent tandem catalysis of living radical polymerization and transesterification of MMA to synthesize MMA/5FPMA gradient copolymers. For this, MMA was polymerized with $Ru(Ind)Cl(PPh_3)_2$, a chloride initiator (ethyl 2-chloro-2-phenylacetate: ECPA), and $Ti(Oi\text{-}Pr)_4$ in

toluene/5FPOH mixed solvents. Concentration of Ti(O*i*-Pr)$_4$ (40, 80, and 160 mM) or 5FPOH (1.5, 2.9, and 4.0 M), and reaction temperature (40, 60, and 80 ^{o}C) were systematically varied without MS 4A (Table 2, entries 1-7). The author especially focused on the kinetic balance of living radical polymerization for chain growth and in-situ transformation of MMA for monomer composition change, because the synchronization of the two reactions is required for the formation of gradient copolymers.

Table 2. Synthesis of MMA/R_FMA Gradient Copolymers via Concurrent Tandem Living Radical Polymerization of MMA with Fluoroalcohols (R_FOH)[a]

entry	R_FOH	[R_FOH] (M)	[Ti(O*i*-Pr)$_4$] (mM)	temperature (^{o}C)	time (h)	conv[c] (%)	M_n[d] (GPC)	M_w/M_n[d]	$F_{cum, RFMA}$[e] (%)
1	5FPOH	2.9	40	80	50	74	12800	1.26	18
2	5FPOH	2.9	80	80	26	88	14700	1.15	39
3	5FPOH	2.9	160	80	26	88	18600	1.15	43
4	5FPOH	1.5	80	80	32	90	14000	1.12	31
5	5FPOH	4.0	80	80	32	93	16100	1.18	35
6	5FPOH	2.9	80	40	97	16	3900	1.27	10
7	5FPOH	2.9	80	60	49	78	18800	1.17	19
8	TFEOH	5.3	80	80	21	86	18500	1.51	15
9[b]	5FPOH	2.9	80	80	20	95	32500	1.17	61
10[b]	9FHOH	2.3	80	80	20	96	25000	1.27	40
11[b]	7FBOH	3.1	160	80	26	83	12400	1.43	25

[a][MMA]/[ECPA]/[Ru(Ind)Cl(PPh$_3$)$_2$]/[Ti(O*i*-Pr)$_4$] = 2000/20/2/40, 80, and 160 mM in toluene/R_FOH (5FPOH, TFEOH, 9FHOH, and 7FBOH) (3/7, 1/1, 3/1, v/v) at 40, 60, and 80 ^{o}C. [b]Entries 9-11: polymerization with MS 4A (0.33 g/mL). [c]Total monomer conversion determined by ^{1}H NMR with an internal standard (tetralin). [d]Determined by SEC in $CHCl_3$ with a PMMA standard calibration. [e]Cumulative R_FMA content ($F_{cum,RFMA}$) determined by ^{1}H NMR (R_FMA: 5FPMA, TFEMA, 9FHMA, and 7FBMA).

First, effects of Ti(O*i*-Pr)$_4$ concentration (40, 80, and 160 mM) on the rate of polymerization and transesterification were examined with 2.9 M 5FPOH (toluene/5FPOH = 1/1, v/v) at 80 ^{o}C (Table 2, entries 1-3). Total conversion of both monomers (MMA, 5FPMA generating from in-situ transesterification) and 5FPMA content in total monomer [5FPMA/(MMA+5FPMA)] were analyzed by ^{1}H NMR measurement of the polymerization solutions that are sampled at predetermined periods (Figure 1a-c). In all cases, transesterification of MMA into 5FPMA proceeded during polymerization. 80 mM Ti catalyst effectively synchronized transesterification with polymerization to give 50 % 5FPMA in monomer. 160 mM Ti, higher concentration of Ti, quickly led to about 50 % 5FPMA in monomer even at the initial stage of polymerization to reach

the equilibrium. 40 mM Ti, lower concentration, just gave about 25% 5FPMA in monomer. Confirmed by size exclusion chromatography in chloroform, all of the copolymers are well controlled with narrow molecular weight distribution (Conv. >74%, M_n = 12800 – 18600, M_w/M_n = 1.1 – 1.3, Table 2 entries 1-3).

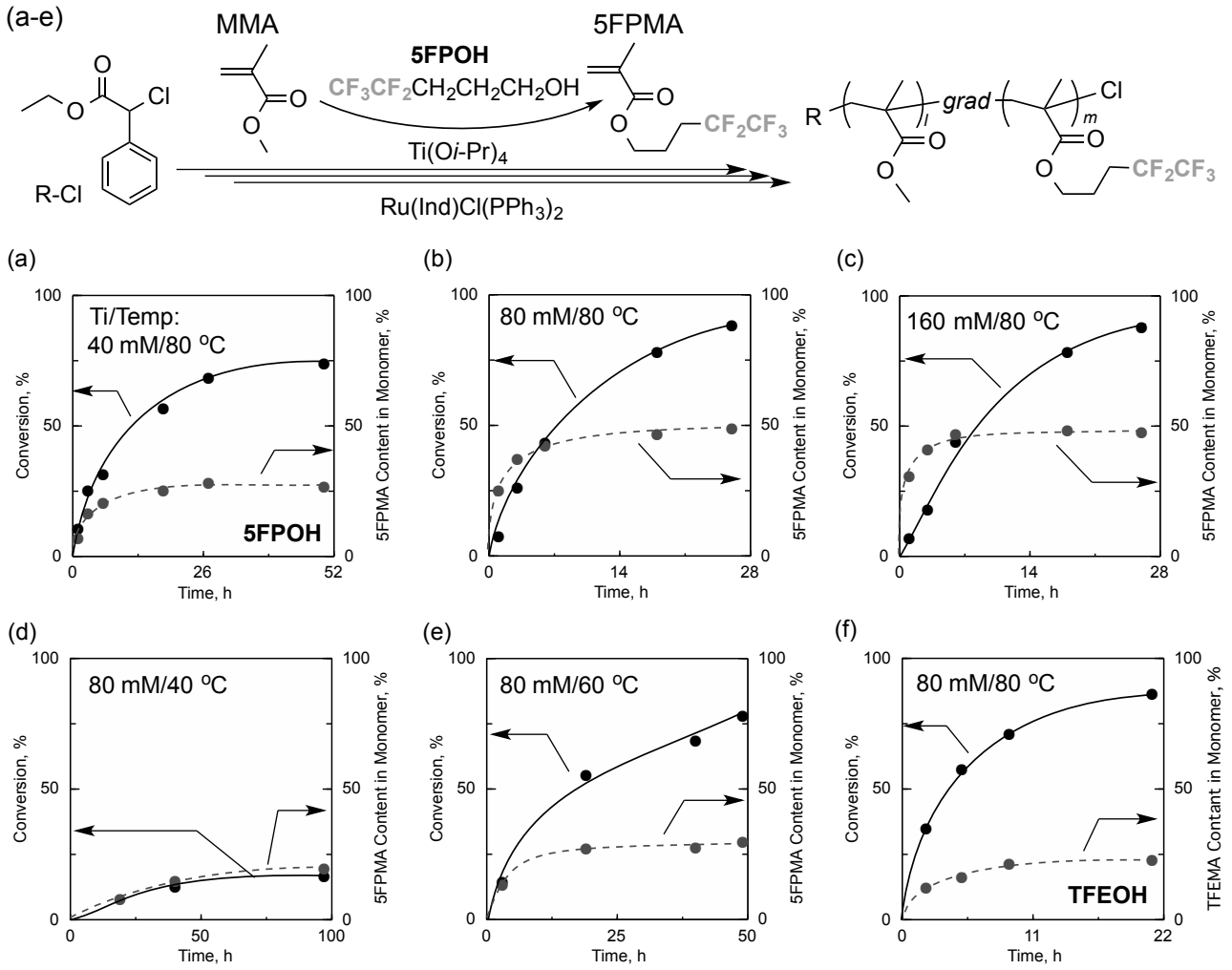

Figure 1. Tandem polymerization of MMA with 5FPOH (a-e) or TFEOH (f) by varying Ti(O*i*-Pr)$_4$ concentration and temperature: [MMA]/[ECPA]/[Ru(Ind)Cl(PPh$_3$)$_2$]/[Ti(O*i*-Pr)$_4$] = 2000/20/2/40-160 mM in toluene/5FPOH or TFE (1/1, v/v) at 40-80 °C ([5FPOH] = 2.9 M, [TFEOH] = 5.3 M) (a-e) Total conversion and 5FPMA content in monomer: [Ti(O*i*-Pr)$_4$]/temperature = (a) 40 mM/80 °C, (b) 80 mM/80 °C, (c) 160 mM/80 °C, (d) 80 mM/40 °C, and (e) 80 mM/60 °C. (f) Total conversion and TFEMA content in monomer: [Ti(O*i*-Pr)$_4$]/temperature = 80 mM/80 °C.

The author further investigated the effects of 5FPOH concentration (1.5 or 4.0 M) at 80 °C or temperature (40 or 60 °C) with 5FPOH (2.9 M); Ti(O*i*-Pr)$_4$ concentration was kept as 80 mM (Table 2, entries 2, 4-7). With 80 mM Ti at 80 °C, MMA was efficiently transesterified into 5FPMA with

5FPOH in the concentration range from 1.5 M to 4.0 M to give 50 % 5FPMA in monomer; i.e. the alcohol concentration was virtually independent of the transesterification. Well-controlled products were obtained in high yield (Conv. ~90%, M_w/M_n = 1.1-1.2). In contrast, both transesterification and polymerization did not so efficiently proceed at low temperature (40 or 60 ^oC) even with 80 mM Ti(O*i*-Pr)$_4$ (Figure 1d,e). The 5FPMA content in monomer and polymerization rate decreased with decreasing temperature.

The author also applied the typical condition of 80 mM Ti(O*i*-Pr)$_4$ in toluene/R_FOH (1/1, v/v) at 80 ^oC to tandem polymerization of MMA with a trifluoroethanol (TFEOH). The TFEMA content in monomer was less than 5FPMA content in monomer (Figure 1b,f). This importantly indicates that in-situ transesterification is dependent on the nucleophilicity and/or pH of alcohols; i.e., TFEOH is less nucleophilic than 5FPOH to lead to lower yield of TFEMA (Table 1).

To analyze sequence distribution of 5FPMA units along a polymer chain, cumulative 5FPMA content in polymer ($F_{cum,5FPMA}$) was further determined by ^{1}H NMR measurement of polymerization mixtures that were sampled at predetermined periods. Figure 2 shows the sequence distribution of copolymers obtained by varying Ti concentration (40, 80, and 160 mM) in 5FPOH (2.9 M) at 80 ^oC or temperature (40 or 60 ^oC) with 80 mM Ti in 5FPOH (2.9 M) or 5FPOH (1.5, 4.0 M) with 80 mM Ti at 80 ^oC. $F_{cum,5FPMA}$ against total monomer conversion was first estimated with the area ratio of the methylene protons of polymerized 5FPMA adjacent to the ester groups (4.1-3.9 ppm) and the methoxy protons of polymerized MMA (3.6-3.5 ppm). $F_{cum,\ 5FPMA}$ values were then plotted as a function of normalized chain length (Figure 2a,b,c). The normalized chain length is defined as DP_t/DP_{final} for living copolymers; DP_t = $[MMA]_0$ × (total conversion/100)/$[ECPA]_0$; DP_{final} = $[MMA]_0$ × (total final conversion/100)/$[ECPA]_0$. Both $F_{cum,5FPMA}$ and the instantaneous 5FPMA content ($F_{inst.5FPMA}$) calculated therefrom (see supporting information)[26] linearly increased with normalized chain length (Figure 2d,e,f), indicating that the composition of 5FPMA incorporated in copolymers gradually increases along a polymer chain to give MMA/5FPMA gradient copolymers.

$F_{cum,5FPMA}$ and the detail $F_{inst.5FPMA}$ profiles were dependent on the reaction conditions. $F_{cum,5FPMA}$ increased with increasing Ti concentration from 40 mM to 160 mM ($F_{cum,5FPMA}$ = 18, 39, and 43%, Table 2 entries 1-3) or temperature [$F_{cum,5FPMA}$ = 10% (40 ^oC), 19% (60 ^oC), and 39% (80 ^oC), Table 2 entries 2,6,7], while $F_{cum,5FPMA}$ was almost constant even by changing 5FPOH concentration (Table 2 entries 2,4,5). $F_{inst.5FPMA}$ smoothly increased along a chain with 80 mM Ti at 80 ^oC, whereas $F_{inst.5FPMA}$ in turn steeply increased around α-end terminal (normalized chain length <0.2) with 160 mM Ti. Therefore, gradient sequence distribution of 5FPMA in copolymer was successfully controlled by adjusting system conditions (Ti concentration and temperature) in tandem polymerization.

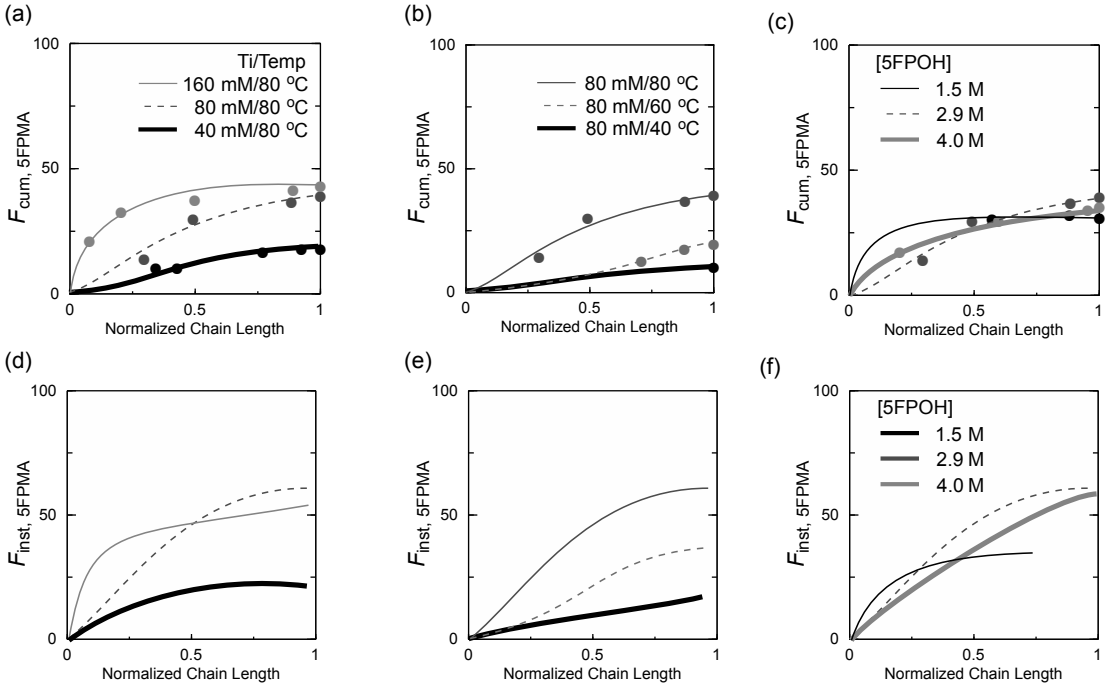

Figure 2. Gradient sequence distribution [a,b: cumulative 5FPMA content ($F_{cum,5FPMA}$); c,d: instantaneous 5FPMA content ($F_{inst,5FPMA}$)] of MMA/5FPMA gradient copolymers via concurrent tandem catalysis: [MMA]/[ECPA]/[Ru(Ind)Cl(PPh_3)$_2$]/[Ti(O*i*-Pr)$_4$] = 2000/20/2/40-160 mM in toluene/5FPOH (1.5-4.0 M) at 40-80 °C. (a, c) [Ti(O*i*-Pr)$_4$] = 40, 80, and 160 mM at 80 °C. (b, d) [Ti(O*i*-Pr)$_4$] = 80 mM at 40, 60, and 80 °C. (c, f) [5FPOH]: 1.5, 2.9 and 4.0 M.

3. Synthesis and Sequence Control of Fluorinated Gradient Copolymers

To synthesize fluorinated gradient copolymers with various fluoroalcohols (5FPOH, 9FHOH, and 7FBOH), the author attempted to utilize Ti(O*i*-Pr)$_4$ with MS 4A or the other metal catalysts [$ZrCl_4$ and Sc(OTf)$_3$]. Though Ti(O*i*-Pr)$_4$ was effective to synthesize MMA/5FPMA gradient copolymers, the instantaneous composition of 5FPMA in copolymer was retarded at about 65% even by tuning the system conditions (e.g., Ti concentration). This is due to the equilibrium of transesterification. So far, the author have already revealed that the removal of methanol with MS 4A is effective to promote in-situ transesterification of MMA with alcohols (ROH) into RMA.[24d]

The author thus employed MS 4A (0.33 g/mL) for the tandem polymerization of MMA with 5FPOH and Ti(O*i*-Pr)$_4$ at 80 °C (Table 2, entry 9). The concentration of Ti and 5FPOH were identical to that of entry 2 without MS 4A. As shown in Figure 3a, transesterification of MMA into 5FPMA was fully synchronized with polymerization of MMA and the generating 5FPMA. As a result, the cumulative and instantaneous composition of 5FPMA almost linearly increased with normalized chain length (Figure 3d), giving well-controlled MMA/5FPMA gradient copolymers with narrow molecular weight distribution in high yield (conv. = 95%, M_n = 32500, M_w/M_n = 1.17, Figure 3g). It should be noted that $F_{inst.5FPMA}$ increased up to about 80% at ω-terminal (Figure 3d,

bold line) and was higher than that without MS4A (Figure 3d, dash line). This result revealed that molecular sieves (MS 4A) were effective to control sequence distribution of fluorinated gradient copolymers.

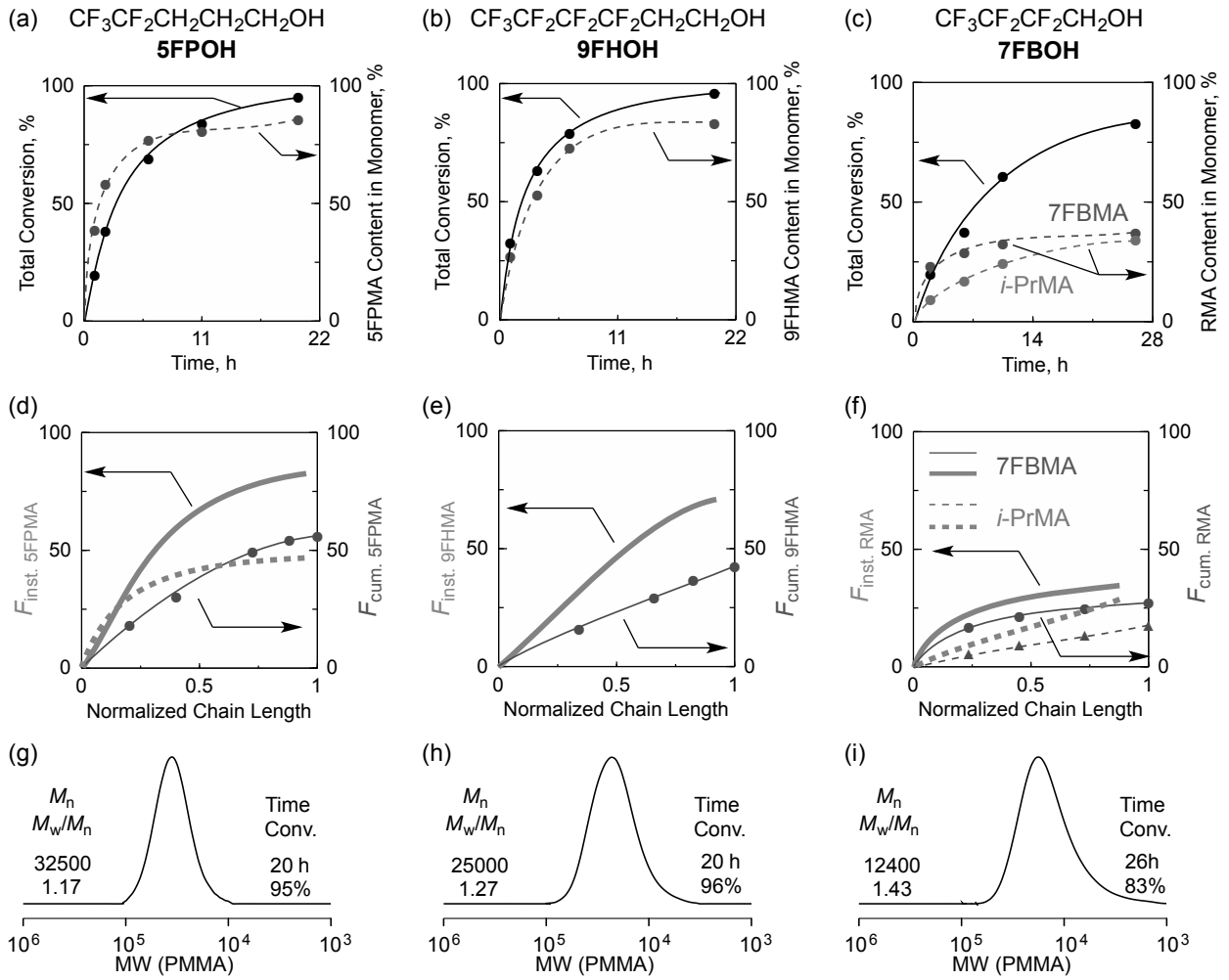

Figure 3. Synthesis of MMA/R_FMA gradient copolymers via concurrent tandem polymerization of MMA with R_FOH (5FPOH, 9FHOH, and 7FBOH) in the presence of molecular sieves (MS 4A): [MMA]/[ECPA]/[Ru(Ind)Cl(PPh_3)$_2$]/[Ti(O*i*-Pr)$_4$] = 2000/20/2/80 (5FPOH, 9FHOH) or 160 (7FBOH) mM in toluene/R_FOH (1/1, v/v) with MS 4A (0.33 g/mL) at 80 °C. (a, b, c) total monomer conversion and R_FMA content in monomer. (d, e, f) cumulative ($F_{cum,\ RMA}$) RMA content and instantaneous ($F_{inst,\ RMA}$) RMA content in products. SEC curves of (g) MMA/5FPMA, (h) MMA/9FHMA, and (i) MMA/7FBMA gradient copolymers.

The obtained MMA/5FPMA gradient copolymer was analyzed by ^{1}H and ^{19}F NMR spectroscopy (Figures 4). The polymer showed methylene protons adjacent to the fluorinated alkyl and ester pendants (b: 4.2–3.9 ppm, c: 2.3−2.1 ppm, d: 2.1−1.7 ppm), methoxy protons (a: 3.7–3.4 ppm), and aromatic protons of the ECPA initiator fragment (e: 7.3–7.1 ppm), in addition to

the methyl and methylene protons of methacrylate backbones (g: 2.1−1.4 ppm, f: 1.3−0.7 ppm) (Figure 4a). The polymer further exhibited small amount of methine and methyl protons (4.8 ppm, 1.3 ppm) of isopropyl groups. This means that small amount of isopropyl methacrylate (~4 mol%) is also formed via in-situ transesterification of MMA with 5FPOH and Ti(O*i*-Pr)$_4$ to be incorporated into MMA/5FPMA gradient copolymers. From the area ratio of the corresponding pendant protons to the initiator aromatic protons, the degree of polymerization ($DP_{MMA}/DP_{5FPMA}/DP_{i\text{-}PrMA}$), number-average molecular weight, and cumulative 5FPMA content were determined: $DP_{MMA}/DP_{5FPMA}/DP_{i\text{-}PrMA}$ = 47/81/6; M_n (NMR, α) = 25600; $F_{cum,5FPMA}$ = 61%. Additionally, the gradient copolymer showed fluorine signals originating from the 5FPMA pendants (Figure 4d).

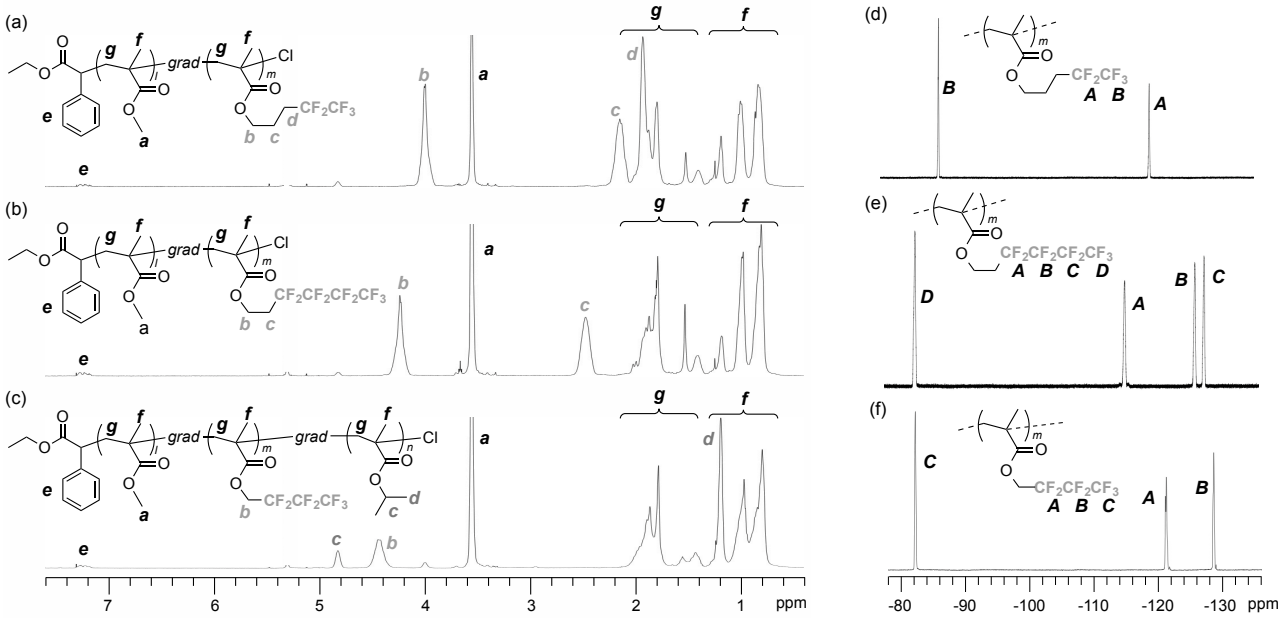

Figure 4. (a-c) ^{1}H and (d-f) ^{19}F NMR spectra of (a)(d) MMA/5FPMA, (b)(e) MMA/9FHMA, and (c)(f) MMA/7FBMA gradient copolymers in CD_2Cl_2 at 25 ^oC.

Ti(O*i*-Pr)$_4$ with MS 4A was further applied to tandem polymerization of MMA with 9FHOH and 7FBOH. Similar to that with 5FPOH, transesterification of MMA with 9FHOH was efficiently synchronized with polymerization using 80 mM Ti catalyst to give a well-controlled MMA/9FHMA gradient copolymer ($DP_{MMA}/DP_{9FHMA}/DP_{i\text{-}PrMA}$ = 65/45/3; M_n (NMR, α) = 17300; $F_{cum,9FHMA}$ = 40%, Figure 3b,h,4b,e). The 9FHMA composition linearly increased with normalized chain length (Figure 3e). In contrast, transesterification of MMA with 7FBOH into 7FBMA was not so fully synchronized with polymerization even using 160 mM Ti and MS 4A (Figure 3c). 7FBMA and isopropyl methacrylate (*i*-PrMA) were simultaneously and gradually formed, both of which were however retarded at about 30 %. As a result, this system produced a unique MMA/7FBMA/*i*-PrMA gradient copolymer ($DP_{MMA}/DP_{7FBMA}/DP_{i\text{-}PrMA}$ = 66/27/18; M_n

(NMR, α) = 16400, $F_{cum,7FBMA}$ = 25%), where the composition of both 7FBMA and *i*-PrMA gradually increased along with a chain (Figure 3f,i,4c,f). Confirmed by ^{1}H NMR, the stereoregularity of the MMA/R_FMA gradient copolymers was close to that of conventional PMMAs similarly obtained without fluoroalcohols: *mm*/*mr*/*rr* (R_FMA) = 3.7/41.9/54.4 (5FPMA), 4.4/36/59.6 (9FHMA), and 5.7/37.8/56.5 (7FBMA).

Focused on the high activity for transesterification (Table 1), $ZrCl_4$ or $Sc(OTf)_3$ (without MS 4A) were also used as catalysts for tandem polymerization of MMA with 9FHOH at 80 °C. Polymerization of MMA was attempted with $Ru(Ind)Cl(PPh_3)_2$, ECPA, and 9FHOH in the presence of $ZrCl_4$ or $Sc(OTf)_3$. In both catalysts, MMA was transesterified into 9FHMA up to about 30 % yield, whereas polymerization did not proceed. This is probably because $ZrCl_4$ or $Sc(OTf)_3$ deactivate the ruthenium catalyst. These results indicate that the combination of $Ti(O$*i*$-Pr)_4$ and fluoroalcohols with MS 4A is effective to synthesize fluorinated methacrylate gradient copolymers.

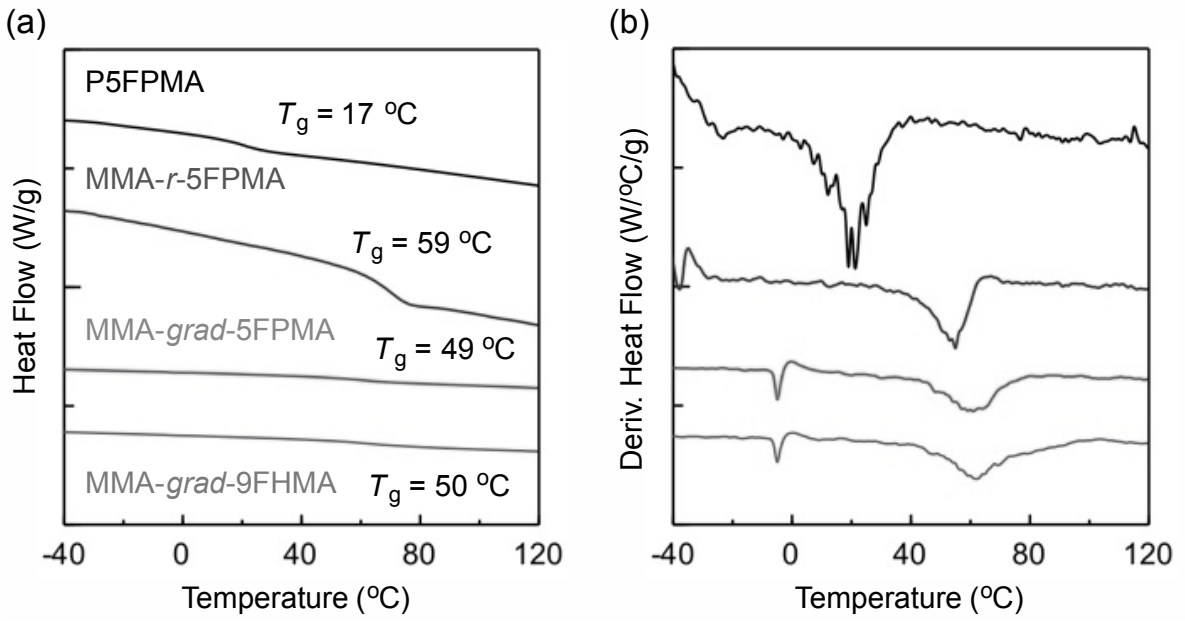

Figure 5. DSC measurements of 5FPMA homopolymer (P5FPMA), MMA/5FPMA copolymers (random, gradient) and MMA/9FHMA gradient copolymer: plot of (a) heat flow and (b) the first derivative of heat flow with temperature as function of temperature; heating = 1 °C/min.

4. Thermal Properties of Fluorinated Gradient Copolymers

Thermal properties of fluorinated gradient copolymers were evaluated by differential scanning calorimetry (DSC) (Figure 5). A MMA/5FPMA gradient copolymer (entry 9 Table 2: M_n = 32500, M_w/M_n = 1.17, $F_{cum,5FPMA}$ = 61%) had glass transition temperature (T_g) at 49 °C. The T_g was between T_g of MMA homopolymer (~ 100 °C) and that of 5FPMA homopolymer (~17 °C, M_n = 9700, M_w/M_n = 1.08). The T_g of the gradient copolymer was further close to that of a

corresponding MMA/5FPMA random copolymer (M_n = 31600, M_w/M_n = 1.08, $F_{cum,5FPMA}$ = 57%, T_g = 59 ^oC) that was prepared by living radical random copolymerization of MMA and 5FPMA. However, the T_g response of the gradient copolymer was much milder than that of the random counterpart, as also confirmed by the derivative of heat flow. Similarly, a MMA/9FHMA gradient copolymer (entry 10 Table 2: M_n = 25000, M_w/M_n = 1.27, $F_{cum,9FHMA}$ = 40%) had T_g at 50 ^oC with broad temperature range (~60 ^oC). Such mild T_g response and/or broad T_g range are properties characteristic of gradient copolymers.[24]

Conclusion

Fluorinated gradient copolymers were efficiently synthesized by tandem catalysis of LRP and in-situ transesterification of MMA with fluoroalcohols. Although transesterifcation with less nucleophilic alcohols such as fluoroalcohols are not so favored generally, the author successfully achieved transesterification of MMA with fluoroalcohols (R_FOH) into fluorinated methacrylates (R_FMA) by using Ti(O*i*-Pr)$_4$ (4-8 mol%). The yield of R_FMA was effectively enhanced by using molecular sieves 4A (MS 4A), where MS 4A effectively removed a generating methanol to suppress the reverse reaction. Various fluoroalcohols were applicable to the transesterification and tandem catalysis: 4,4,4,5,5-pentafluoro-1-pentanol (5FPOH), 1*H*,1*H*,2*H*,2*H*-nonafluoro-1-hexanol (9FHOH), 1*H*,1*H*-heptafluoro-1-butanol (7FBOH), and trifluoroethanol (TFEOH). Tandem polymerization of MMA with Ti(O*i*-Pr)$_4$ and their fluoroalcohols efficiently proceeded to provide well-controlled fluorinated gradient copolymers with different sequence distribution and pendant functionality. Thus, this work opened new vistas to design fluorinated gradient and relating sequence-controlled copolymers by using transesterification with fluoroalcohols.

References

(1) Kendall, J. L.; Canelas, D. A.; Young, J. L.; DeSimone, J. M. *Chem. Rev.* **1999**, *99*, 543-563.

(2) Zhang, Z.; Shi, Z.; Han, X.; Holdcroft, S. *Macromolecules* **2007**, *40*, 2295-2298.

(3) Kurt, I.; Wynne, K. J. *Macromolecules* **2007**, *40*, 9537-9543.

(4) Ding, J.; Jiang, J.; Blanchetière, C.; Callender, C. L. *Macromolecules* **2008**, *41*, 758-763.

(5) Huang, H.; He, L. *RSC Adv*. **2014**, *4*, 13108-13118.

(6) Jin-Kyun Lee, J-K.; Fong, H. H.; Zakhidov, A. A.; McCluskey, G. E.; Taylor, P. G.; Santiago-Berrios, M.; Abruña, H. D.; Holmes, A. B.; Malliaras, G. G.; Ober, C. K. *Macromolecules* **2010**, *43*, 1195-1198.

(7) Wynne, K. J.; Makal. U.; Kurt, P.; Gamble, L. *Langmuir* **2007**, *23,* 10573-10580.

(8) Abouelmagd, A.; Sugiyama, K.; Hirao, A. *Macromolecules* **2011**, *44*, 826-834.

(9) Koda, Y.; Terashima. T.; Sawamoto, M. *Macromolecules* **2015**, *48*, 2901-2908.

(10) Koda, Y.; Terashima. T.; Takenaka, M.; Sawamoto, M. *ACS Macro Lett.* **2015**, *4*, 377-380.

(11) Wu, Y.; Huang, Y.; Ma, H. *J. Am. Chem. Soc.* **2007**, *129*, 7226-7227.

(12) Yamaguchi, H.; Kikuchi, M.; Kobayashi. M.; Ogawa, H.; Masunaga, H.; Sakata, O.; Takahara, A. *Macromolecules* **2012**, *45*, 1509-1516.

(13) Kobayashi. M.; Terayama, Y.; Yamaguchi, H.; Terada, M.; Murakami, D.; Ishihara, K.; Takahara, A. *Langmuir* **2012**, *28,* 7212-7222.

(14) Chen, Z-C.; Zhu, B-C.; Li, J-J.; Zhou, Y-N.; Luo, Z-H. *J. Polym. Sci. Part A: Polym. Chem.* **2016**, *54*, 3868-3877.

(15) Zhang, G.; Jiang, J.; Zhang, Q.; Gao, F.; Zhan. X.; Chen, F. *Langmuir* **2016**, *32,* 1380-1388.

(16) Schadt, K.; Kerscher, B.; Thomann, R.; Mülhaupt, R. *Macromolecules* **2013**, *46*, 4799-4804.

(17) Peng, H.; Thurecht, K. J.; Blakey, I.; Taran, E.; Whittaker, A. K. *Macromolecules* **2012**, *45*, 8681-8690.

(18) Aizhao Pan, Shao Yang and Ling He. *RSC Adv*. **2015**, *5*, 55048-55058.

(19) (a) Koda, Y.; Terashima. T.; Nomura, A.; Ouchi, M.; Sawamoto, M. *Macromolecules* **2011**, *44*, 4574-4578. (b) Koda, Y.; Terashima. T.; Sawamoto, M. *J. Am. Chem. Soc.* **2014**, *136*, 15742-15748.

(20) (a) Hoang, K. C.; Mecozzi, S. *Langmuir* **2004**, *20,* 7347-7350. (b) Koda, Y.; Terashima. T.; Sawamoto, M. *Macromolecules* **2016**, *49*, 4534-4543. (c) Koda, Y.; Terashima. T.; Sawamoto, M.; Maynard, H. D. *Polym. Chem.* **2015**, *6*, 240-247. (d) Koda, Y.; Terashima. T.; Sawamoto, M. *Polym. Chem.* **2015**, *6*, 5663-5674.

(21) Matyjaszewski, K.; Ziegler, M. J.; Arehart, S. V.; Greszta, D.; Pakula, T. *J. Phys. Org. Chem.* **2000**, *13*, 775−786.

(22) Pakula, T. *Macromol. Theory Simul*. **1996**, *5*, 987-1006.

(23) Seno, K.; Tsujimoto, I.; Kanaoka, S.; Aoshima, S. *J. Polym. Sci. Part A: Polym. Chem.* **2008**, *46*, 6444–6454.

(24) (a) Kim, J.; Mok, M. M.; Sandoval, R. W.; Woo, D. J.; Torkelson, J. M. *Macromolecules* **2006**, *39*, 6152-6160. (b) Mok, M. M.; Kim, J.; Wong, C. L. H.; Marrou, S. R.; Woo, D. J.; Dettmer, C. M.; Nguyen, S. T.; Ellison, C. J.; Shull, K. R.; Torkelson, J. M. *Macromolecules* **2009**, *42*, 7863-7876. (c) Zhang, J.; Li, J.; Huang, L.; Liu, Z. *Polym. Chem.* **2013**, *4*, 4639-4647. (d) Ogura, Y.; Terashima, T.; Sawamoto, M. *ACS Macro Lett.* **2013**, *2*, 985−989.

(25) (a) Mok, M. M.; Pujari, S.; Burghardt, W. R.; Dettmer, C. M.; Nguyen, S. T.; Ellison, C. J.; Torkelson, J. M. *Macromolecules* **2008**, *41*, 5818-5829. (b) Mok, M. M.; Ellison, C. J.; Torkelson, J. M. *Macromolecules* **2011**, *44*, 6220-6226.

(26) (a) Nakatani, K.; Terashima, T.; Sawamoto, M. *J. Am. Chem. Soc.* **2009**, *131*, 13600−13601. (b) Nakatani, K.; Ogura, Y.; Koda, Y.; Terashima, T.; Sawamoto, M. *J. Am. Chem. Soc.* **2012**, *134*, 4373−4383.

(27) Krasik, P. *Tetrahedron Lett*. **1998**, *39*, 4223-4226.

(28) (a) Filler, R.; Schure, R. M. *J. Org. Chem*., **1967**, *32 (4)*, 1217-1219. (b) Robinson, J. R.; Matheson L. E. *J. Org. Chem*., **1969**, *34 (11)*, 3630-3633. (c) Dyatkin, B. L.; Mochalina, E. P.; Knunyants, I. L. *Tetrahedron*, **1965**, *21*, 2991-2995.

(29) Bordwell, F. G. *Acc. Chem. Res*. **1988**, *21*, 456-463.

(30) Yamada, K.; Nakano, T.; Okamoto, Y. *Macromolecules* **1998**, *31*, 7598-7605.

(31) (a) Okano, T.; Miyamoto, K.; Kiji, J. *Chem. Letters*, **1995**, 246. (b) Rodger, A.; Johnson, B. F. G. *Inorg. Chem*. **1988**, *27*, 3062- 3064. (c) Ishihara, K.; Nakayama, M.; Ohara, S.; Yamamoto, H. *Tetrahedron*, **2002**, *58*, 8179-8188.

(32) (a) Weidmann, B.; Seebach, D. *Angew. Chem. Int. Ed. Engl.* **1983**, *12*, 31–45. (b) Ishihara, K.; Kubota, M.; Kurihara, H.; Yamamoto, H. *J. Am. Chem. Soc.* **1995**, *117*, 4413−4414. (c) Mei, F. M.; Chen, E. X.; Li, G. X. *Kinetics and Catalysis*, **2009**, 50 (5), 666-670.

Chapter 5

Fluorous, Perfluorinated Gradient Copolymers: Tandem Transesterification with a Perfluoroalkyl Methacrylate and Physical Properties

Abstract

Fluorous, perfluorinated gradient copolymers were synthesized via tandem catalysis of ruthenium-catalyzed living radical polymerization (LRP) and titanium alkoxide-mediated transesterification with a perfluoroalkyl methacrylate and various alcohols. This is one of the most efficient and versatile systems to produce fluorous gradient and their related sequence-controlled copolymers. Typically, *1H,1H,2H,2H*-perfluorooctyl methacrylate (13FOMA) was polymerized as a starting monomer with a ruthenium catalyst and a chloride initiator in the presence of Ti(O*i*-Pr)$_4$ in alcohols (ROH) at 80 ^{o}C. Owing to the electron-withdrawing perfluorinated alkyl unit, 13FOMA was efficiently transesterified into functional methacylates (RMA) during the copolymerization of 13FOMA and the resulting RMA. The synchronized catalysis of the copolymerization and the transesterification afforded 13FOMA/RMA gradient copolymers whose composition linearly changed from the initiating to growing terminal. A wide variety of alcohols [long alkyl alcohols: hydrophobic, poly(ethylene glycol) methyl ether: hydrophilic] was applied to this tandem catalysis, resulting in fluorous/hydrophobic or fluorous/hydrophilic gradient copolymers. Solid and solution properties of a fluorous/hydrophobic 13FOMA/dodecyl methacrylate (DMA) gradient copolymer were investigated, compared with the random or block counterparts. Typically, the gradient copolymer showed a broad range of glass transition temperature and microphase separation distinct from the block counterpart.

Introduction

Fluorinated polymers were widely used to fabricate products like film, rubber and coating materials.[1-4] Introduction of fluorinated groups into polymers has been attempted for creating novel function, focused on the distinguished nature of fluorinated segments.[5-10] In fact, various characters including low wettability,[11] thermostability,[12] strong fluorophilic nature, and immiscibility with both hydrophobic and hydrophilic compounds have been applied to micellization, aggregation in solution,[13] microphase separation,[14, 15] smetic phase,[16] and surfactants.[17]

Despite huge number of researches concerning the synthesis and physical properties of fluorous polymers have been reported so far, few researches have been focused on the sequence distribution of perfluorinated groups in copolymers. Interaction between fluorinated moieties is considered as one of the most important factors for expression of unique properties. Their interaction might be affected by density of fluorinated moieties that can be controlled by distribution of fluorinated part. For example, unimolecular micelles are formed in water via self-folding of random copolymers of fluorous *1H,1H,2H,2H*-perfluorooctyl methacrylate and hydrophilic poly(ethylene glycol) methacrylate (PEGMA) where each segment is uniformly distributed, while large multichain aggregates are dominant for block copolymers in water.[18-20] Furthermore, star polymers bearing densely fluorinated microgel cores realized selective recognition of fluorous compounds.[21, 22]

In previous chapters, the author has developed novel tandem catalysis of living radical polymerization (LRP) and transesterification to produce methacrylate based gradient copolymers.[23-25] In this system, desired properties can be expressed by using suitable agent (monomers, alcohols). In fact, the author succeeded in synthesizing gradient copolymers with unique properties by combining two distinct segments like soft and hard, hydrophobic and hydrophilic in chapter 1 and chapter 2, respectively.[25] Owing to continuous variation from one nature to another opposite nature along chain, these functional gradient copolymers showed remarkable properties in solid and solution states such as extremely broad glass transition temperature and characteristic aggregation state. On the other hand, in chapter 4, gradient copolymers containing perfluoroalkyl chain were synthesized via tandem catalysis where methyl methacrylate (MMA) was transesterified with fluorinated alcohols into perfluoroalkyl methacrylates during polymerization. However, transesterification with fluoroalcohols was difficult due to their high acidity and low nucleophilic nature, resulting in the limitation of available methacrylates with short perfluoroalkyl chain (C_nF_{2n+1}: $n < 5$).

Thus, the authors were focused on a perfluorinated methacrylate (*1H,1H,2H,2H*-Perfluorooctyl methacrylate: 13FOMA) as a starting monomer for fluorous gradient copolymers via tandem transesterification; the monomer is expected to be transesterified with

alcohols (ROH) into other methacrylates (RMA) owing to the less nucleophilic nature of a generating perfluoroalcohol. In fact, Tao and coworkers report that 2,2,2-trifluoroethyl methacrylate is smoothly transesterified into other methacrylates even with enzyme catalyst whose catalytic activity is weaker than that of metal alkoxide catalyst.[26,27] Zhang et al. also synthesized hydrophilic/fluorous gradient copolymers to evaluate its superior oil-fouling resistant properties derived from gradient distribution.[28] However, versatile synthetic systems of fluorous gradient copolymers with tunable gradient sequence and functional groups are not developed yet; the methodology allows to design various fluorous gradient copolymers and lead to the discovery of novel and exquisite characters and functions.

In this chapter, *1H,1H,2H,2H*-Perfluorooctyl methacrylate (13FOMA) was used as a monomer in tandem catalysis because it contains multiple fluorine groups enough to express fluorous nature. First, concurrent tandem catalysis of LRP and transesterification of 13FOMA with ethanol was examined with Ti(O*i*-Pr)$_4$ as a catalyst, compared with other methacrylates. After confirming optimal conditions for synchronization of LRP and transesterification, 13FOMA was polymerized with various alcohols (ROH) to synthesize gradient copolymers of 13FOMA and RMA (in-situ generating from transesterification of 13FOMA with ROH) (Scheme 1). Solid and solution properties (thermo property, phase separation, contact angle and surface tension) of various fluorous gradient copolymers were evaluated, particularly focused on the effects of 13FOMA sequence distribution. Typically, 13FOMA/dodecyl methacrylate (DMA) gradient copolymers showed broad glass transition temperature and phase separation different from corresponding random or block counterparts.

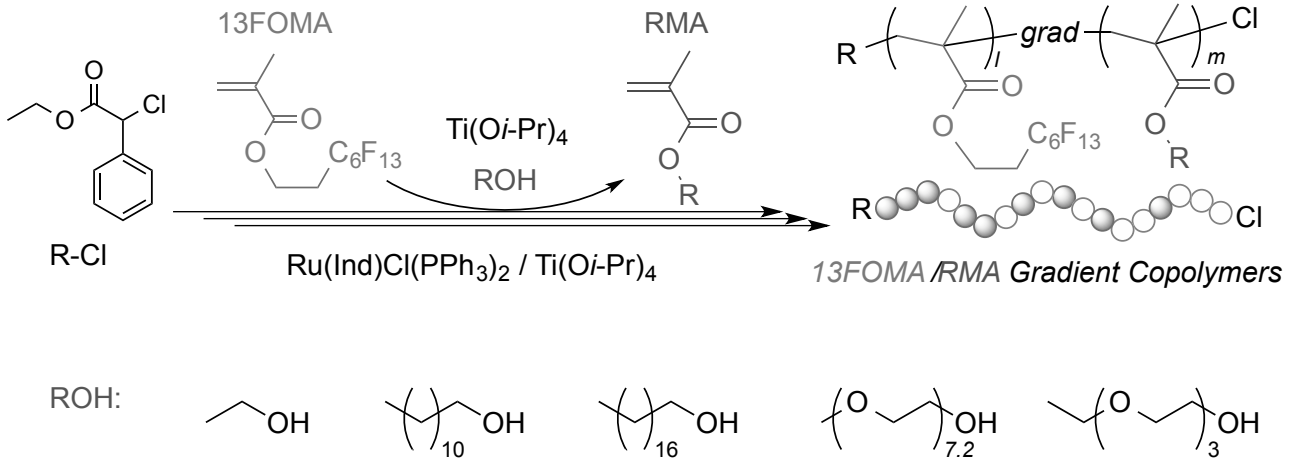

Scheme 1. Synthesis of Fluorous, Perfluorinated Gradient Copolymers via Tandem Catalysis of Living Radical Polymerization and Transesterification of 13FOMA with Various Alcohols

Experimental Section

Materials. Methyl methacrylate (MMA: TCI; purity >99.8%) and tetralin (1,2,3,4-tetrahydronaphthalene: Kishida Chemical; purity >98%; an internal standard for ^{1}H NMR analysis) were dried overnight with calcium chloride and distilled from calcium hydride under reduced pressure before use. Poly(ethylene glycol) methyl ether methacrylate [PEGMA; CH_2=$CMeCO_2(CH_2CH_2O)_n$Me: M_n = 475; n = 9 on average] (Aldrich), dodecyl methacrylate (DMA) (TCI, purity >97%) and *1H,1H,2H,2H*-Perfluorooctyl methacrylate (13FOMA: Wako, purity >95%) was purified by column chromatography charged with inhibitor remover (Aldrich) and purged by argon before use. Polyethylene glycol methyl ether (PEG-OH) (Aldrich, M_n = 350), triethylene glycol monoethyl ether (TEG-OH) (Wako, purity >99%), Ti(O*i*-Pr)$_4$ (Aldrich, purity >90%), and *n*-Bu_3N (TCI, purity >98%) were degassed by triple vacuum-argon purge cycles before use. Dodecyl alcohol (TCI, purity >99%) and octadecyl alcohol (TCI, purity >98%) were used as received. Ethyl 2-chloro-2-phenylacetate (ECPA: Aldrich; purity >97%) was distilled under reduced pressure before use. Ru(Ind)Cl$(PPh_3)_2$ (Aldrich) was used as received and handled in a glove box under moisture- and oxygen-free argon (H_2O <1 ppm; O_2 <1 ppm). Toluene (solvent) was purified by pashing it through a purification column (Glass Contour Solvent Systems: SG Water USA).

Characterization. Molecular weight distribution (MWD) curves, M_n, and M_w/M_n ratio of polymers were measured by SEC in $CHCl_3$ or DMF containing 10 mM LiBr (for polymers containing poly(ethylene) glycol) at 40 ^{o}C (flow rate: 1 mL/min) on three linear-type polystyrene gel columns ($CHCl_3$: Shodex K-805L: exclusion limit = 4×10^6; particle size = 10 mm; pore size = 5000 Å; 0.8 cm i.d. × 30 cm, DMF: Shodex KF-805L: exclusion limit = 4×10^6; particle size = 10 mm; pore size = 5000 Å; 0.8 cm i.d. × 30 cm) that were connected to detectors ($CHCl_3$: a Jasco PU-980 precision pump, a Jasco RI-1530 refractive index detector, and a Jasco UV-980 UV/vis detector set at 250 nm, DMF: a Jasco PU-2080 precision pump, a Jasco RI-2031 refractive index detector, and a Jasco UV-2075 UV/vis detector set at 270 nm). The columns were calibrated against 10 standard poly(MMA) samples (Polymer Laboratories; M_n = 1000–1200000; M_w/M_n = 1.06–1.22). To remove unreacted monomers, alcohols, and catalyst residues, polymer samples for the evaluation of solution/solid properties were fractionated by preparative SEC [TOSOH TSKgel α-3000: particle size = 13 mm; 5.5 cm i.d. × 30 cm; exclusion limit = 9×10^4 g/mol; flow rate = 15 mL/min] connected to a Jasco PU-2086 precision pump, a Jasco RI-2013 refractive index detector, and a Jasco UV-2075 ultraviolet detector. ^{1}H NMR spectra were recorded in $CDCl_3$ and CD_2Cl_2 on a JEOL JNM-ECA500 spectrometer operating at 500.16 MHz. Differential scanning calorimetry (DSC) was performed for samples (ca. 5 mg weighed into an aluminum pan) under dry

nitrogen flow on a DSC Q200 calorimeter (TA Instruments) equipped with a RCS 90 electric freezing machine. The polymer samples were heated to 150 ^{o}C at the rate of 10 ^{o}C/min and held at the temperature for 10 min to erase thermal history. Then, the samples were cooled to -80 ^{o}C at the rate of -10 ^{o}C/min and held at the temperature for 10 min, and again heated to 150 ^{o}C at the rate of 10 ^{o}C/min. The second heating runs were used for the thermal analysis of polymers in Figure 6 in results and discussion.

Polymerization. The synthesis of 13FOMA/DMA copolymers (random, gradient, block) was carried out by syringe technique under argon in baked glass tubes equipped with a three-way stopcock.

13FOMA/DMA gradient copolymer (Table 2)**.** A typical procedure for a gradient copolymer was given: Ru(Ind)Cl(PPh_3)$_2$ (0.015 mmol, 11.6 mg) was charged into the 30mL glass tube. Toluene (4.51 mL), dodecyl alcohol (23.4 mmol, 5.24 mL), tetralin (0.20 mL), a 500 mM toluene solution of Ti(O*i*-Pr)$_4$ (0.45 mL, Ti(O*i*-Pr)$_4$ = 0.23 mmol), 13FOMA (15 mmol, 4.33 mL), and a 274 mM toluene solution of ECPA (0.27 mL, ECPA = 0.075 mmol) were added sequentially in that order at 25 ^{o}C under argon (the total volume of the reaction mixture: 15 mL). The glass tube was then placed in an oil bath kept at 80 ^{o}C. At predetermined intervals, the mixture was sampled with a syringe under argon, and the sampled solutions were cooled to –78 °C to terminate the reaction. The total monomer conversion, DMA content in monomer, and cumulative DMA content in polymer ($F_{cum,DMA}$) were directly determined by ^{1}H NMR measurements of the terminated reaction solution in $CDCl_3$ at 25 ^{o}C with tetralin as an internal standard. Instantaneous DMA content in polymer ($F_{inst,DMA}$) was estimated according to the following equation: $F_{inst,DMA}$ = [Conv.$_{total,\ i}$ x $F_{cum,DMA,\ i}$ - Conv.$_{total,\ i-1}$ x $F_{cum,DMA,\ i-1}$]/[Conv.$_{total,\ i}$ - Conv.$_{total,\ i-1}$], where Conv.$_{total}$ is the total conversion of both monomers. The quenched solutions were evaporated to dryness to give the crude product. To remove unreacted monomers, solvents, and catalyst residue, the product was purified by preparative SEC before characterization (^{1}H NMR, thermal and solution properties). SEC ($CHCl_3$, PMMA std.): M_n = 31000 g/mol; M_w/M_n = 1.33. ^{1}H NMR [500 MHz, CD_2Cl_2, 25 ^{o}C, δ = 5.33 $CDHCl_2$] δ 7.30–7.15 (aromatic), 4.40–4.07 (-COOC$\underline{H}_2$CH$_2$CF$_2$-), 4.02–3.75 (-COOC$\underline{H}_2$CH$_2$-), 2.60–2.32 (-COOCH$_2$C$\underline{H}_2$CF$_2$-), 2.15–1.67 (-C$\underline{H}_2$C(CH$_3$)-), 1.67−1.52 (-COOCH$_2$C$\underline{H}_2$CH$_2$-), 1.43–0.60 (-CH$_2$CH$_2$(C$\underline{H}_2$)$_9$C$\underline{H}_3$, -CH$_2$C(C$\underline{H}_3$)-). M_n (NMR, α) = 58700; DP_{13FOMA}/DP_{DMA} = 76/101; $F_{cum,DMA}$ = 57%. ^{19}F NMR [470 MHz, CD_2Cl_2, 25 ^{o}C, δ = -76.5 ppm (CF_3COOH in $CDCl_3$)]: δ -81.9 – -83.3 (-CF$_3$), -114.4 – -115.7 (-CH$_2$CF$_2$-), -122.8 – -123.8 (-CH$_2$CF$_2$CF$_2$C$\underline{F}_2$-), -123.9 – -124.6 (-C$\underline{F}_2$CF$_2$CF$_3$), -124.6 – -125.6 (-CH$_2$CF$_2$C$\underline{F}_2$-), -127.1 – -128.3 (-C$\underline{F}_2$CF$_3$).

13FOMA/PEGMA gradient copolymer (Table 1, Entry 9)**.** SEC ($CHCl_3$, PMMA std.): M_n = 51800 g/mol; M_w/M_n = 1.19. ^{1}H NMR [500 MHz, CD_2Cl_2, 25 ^oC, δ = 5.33 $CDHCl_2$] δ 7.3–7.1 (aromatic), 4.4–4.1 (-COOC$\underline{H}_2$CH$_2$CF$_2$-), 4.1–4.0 (-COOC$\underline{H}_2$CH$_2$O-), 3.7–3.6 (-COOCH$_2$C$\underline{H}_2$O-), 3.6-3.5 (-OC$\underline{H}_2$C$\underline{H}_2$O-), 3.5–3.4 (-OCH$_2$C$\underline{H}_2$OCH$_3$), 3.4–3.3 (-OC$\underline{H}_3$), 2.6-2.3 (-COOCH$_2$C$\underline{H}_2$CF$_2$-), 2.1−1.6 (-C$\underline{H}_2$C(CH$_3$)-), 1.3–0.8 (-CH$_2$C(C$\underline{H}_3$)-). M_n (NMR, α) = 69600; DP_{13FOMA}/DP_{PEGMA} = 60/104; $F_{cum,PEGMA}$ = 64%. ^{19}F NMR [470 MHz, CD_2Cl_2, 25 ^oC, δ = -76.5 ppm (CF_3COOH in $CDCl_3$)]: δ -81.7 – -82.7 (-CF$_3$), -114.3 – -115.4 (-CH$_2$CF$_2$-), -122.7 – -123.5 (-CH$_2$CF$_2$CF$_2$C$\underline{F}_2$-), -123.7 – -124.5 (-C$\underline{F}_2$CF$_2$CF$_3$), -124.5 – -125.3 (-CH$_2$CF$_2$C$\underline{F}_2$-), -127.1 – -127.9 (-C$\underline{F}_2$CF$_3$).

13FOMA/DMA random copolymer. In a 30 mL glass tube, Ru(Ind)Cl(PPh_3)$_2$ (0.015 mmol, 11.6 mg) was placed. Then, toluene (9.41 mL), tetralin (0.20 mL), a 400 mM toluene solution of *n*-Bu_3N (0.75 mL, *n*-Bu_3N = 0.30 mmol), DMA (8.25 mmol, 2.42 mL), 13FOMA (6.75 mmol, 1.95 mL), and a 274 mM toluene solution of ECPA (0.27 mL, ECPA = 0.075 mmol) were added sequentially in that order into the tube at 25 ^oC under argon (The total volume: 15 mL). The glass tube was placed in an oil bath kept at 80 ^oC. After 72 h, the solution was cooled to –78 °C to terminate the reaction. The conversion of 13FOMA and DMA was determined as 94% and 91%, respectively, by ^{1}H NMR in $CDCl_3$ at r.t. with tetralin as an internal standard. The quenched solution was evaporated to dryness to give the crude product. The product was further fractionated by preparative SEC for analysis. SEC ($CHCl_3$, PMMA std.): M_n = 31,200 g/mol; M_w/M_n = 1.16. ^{1}H NMR [500 MHz, CD_2Cl_2, 25 ^oC, δ = 5.33 CH_2Cl_2] δ 7.30–7.15 (aromatic), 4.41–4.08 (-COOC$\underline{H}_2$CH$_2$CF$_2$-), 4.03–3.73 (-COOC$\underline{H}_2$CH$_2$-), 2.62–2.30 (-COOCH$_2$C$\underline{H}_2$CF$_2$-), 2.13–1.68 (-C$\underline{H}_2$C(CH$_3$)-), 1.68−1.48 (-COOCH$_2$C$\underline{H}_2$CH$_2$-), 1.48–0.61 (-CH$_2$CH$_2$(C$\underline{H}_2$)$_9$C$\underline{H}_3$, -CH$_2$C(C$\underline{H}_3$)-). M_n (NMR, α) = 57700; DP_{13FOMA}/DP_{DMA} = 80/90; $F_{cum,DMA}$ = 53%. ^{19}F NMR [470 MHz, CD_2Cl_2, 25 ^oC, δ = -76.5 ppm (CF_3COOH in $CDCl_3$)]: δ -81.7 – -82.7 (-CF$_3$), -114.3 – -115.4 (-CH$_2$CF$_2$-), -122.7 – -123.5 (-CH$_2$CF$_2$CF$_2$C$\underline{F}_2$-), -123.7 – -124.5 (-C$\underline{F}_2$CF$_2$CF$_3$), -124.5 – -125.3 (-CH$_2$CF$_2$C$\underline{F}_2$-), -127.1 – -127.9 (-C$\underline{F}_2$CF$_3$).

13FOMA/DMA block copolymer. In a 30 mL glass tube, Ru(Ind)Cl(PPh_3)$_2$ (0.0025 mmol, 1.94 mg) was placed. Then, toluene (4.23 mL), tetralin (0.20 mL), a 400 mM toluene solution of *n*-Bu_3N (0.38 mL, *n*-Bu_3N = 0.15 mmol), DMA (8.25 mmol, 2.42 mL), and a 274 mM toluene solution of ECPA (0.27 mL, ECPA = 0.075 mmol) were added sequentially in that order into the tube at 25 ^oC under argon (The total volume: 7.5 mL). The glass tube was placed in an oil bath kept at 80 ^oC. After 75 h, the polymerization reached 84% conversion (determined by ^{1}H NMR) to give PDMA-Cl (M_n = 17600 g/mol; M_w/M_n = 1.21, by SEC in $CHCl_3$ with PMMA std.). Into the polymerization mixture, toluene (5.55 mL) and 13FOMA (6.75 mmol, 1.95 mL) were directly

added under argon. After 74 h, the reaction solution was cooled to –78 °C to terminate the reaction (91% (13FOMA), 89% (DMA) conversion: determined by ^{1}H NMR). The quenched reaction solution was evaporated to dryness and the resulting crude product was fractionated by preparative SEC for analysis. SEC ($CHCl_3$, PMMA std.): M_n = 33,900 g/mol; M_w/M_n = 1.31. ^{1}H NMR [500 MHz, CD_2Cl_2, 25 ^oC, δ = 5.33 CH_2Cl_2]: δ 7.32–7.16 (aromatic), 4.62–3.63 (-COOC<u>H</u>$_2$CH$_2$CF$_2$-), 4.02–3.75 (-COOC<u>H</u>$_2$CH$_2$-), 2.70–2.18 (-COOCH$_2$C<u>H</u>$_2$CF$_2$-), 2.17–1.69 (-C<u>H</u>$_2$C(CH$_3$)-), 1.68−1.49 (-COOCH$_2$C<u>H</u>$_2$CH$_2$-), 1.49–0.58 (-CH$_2$CH$_2$(C<u>H</u>$_2$)$_9$C<u>H</u>$_3$, -CH$_2$C(C<u>H</u>$_3$)-). M_n (NMR, α) = 56400: DP_{13FOMA}/DP_{DMA} = 73/97; $F_{cum,DMA}$ = 57%. ^{19}F NMR [470 MHz, CD_2Cl_2, 25 ^oC, δ = -76.5 ppm (CF_3COOH in $CDCl_3$)]: δ -82.1 – -83.8 (-CF$_3$), -114.3 – -116.5 (-CH$_2$CF$_2$-), -123.0 – -124.1 (-CH$_2$CF$_2$CF$_2$C<u>F</u>$_2$-), -124.2 – -125.0 (-C<u>F</u>$_2$CF$_2$CF$_3$), -125.0 – -125.9 (-CH$_2$CF$_2$C<u>F</u>$_2$-), -127.4 – -128.9 (-C<u>F</u>$_2$CF$_3$).

Results and Discussion

1. Tandem Catalysis of LRP and Transesterification with 13FOMA as a Starting Monomer

In order to synthesize fluorous, perfluorinated gradient copolymers in tandem catalysis of LRP and transesterification, the author attempted to use a perfluoroalkyl methacrylate, 13FOMA, as a fluorinated source instead of fluoroalcohols ($C_nF_{2n+1}OH$) reported in Chapter 4. The author first evaluated the potential of 13FOMA as a starting monomer in tandem LRP with transesterification, compared with other methacrylates [RMA: methyl methacrylate (MMA), dodecyl methacrylate (DMA), poly(ethylene glycol) methyl ether methacrylate (PEGMA)]. All four methacrylates (MMA, DMA, 13FOMA: 2M, PEGMA: 1M) were polymerized respectively with a Ru(Ind)Cl(PPh$_3$)$_2$ catalyst and a chloride initiator (ethyl 2-chloro-2-phenylacetate: ECPA) in the presence of Ti(O*i*-Pr)$_4$ (20 mM) in a toluene/ethanol (EtOH) (1/1, v/v) mixture at 80 ^oC (Table 1, entry 1-4, Figure 1). The ratio of ethyl methacrylate (EMA) in monomer [EMA/(RMA+EMA)] and the total conversion (olefin consumption) of RMA and EMA by copolymerization were estimated with the ^{1}H NMR measurements of the reaction solutions sampled at predetermined time (Figure 1a-d).

The three RMA monomers except for PEGMA were smoothly copolymerized with EMA, accompanied by in-situ generation of EMA from the transesterification of RMA with EtOH (Figure 1a-c). Similar to MMA, 13FOMA was transesterified into EMA quickly although the EtOH amount was smaller than that for MMA. As a result, transesterification of 13FOMA to EMA was fully synchronized with copolymerization of 13FOMA and the resulting EMA. In contrast, PEGMA was not transformed into EMA at all to result in homopolymerization of PEGMA (Figure 1d).

Table 1. Synthesis of Gradient Copolymers via Concurrent Tandem Living Radical Polymerization[a]

Entry	Monomer	Alcohol	[Alcohol] (M)	Time (h)	Conv[b] (%)	M_n[c] (GPC)	M_w/M_n[c]	$F_{cum,\ RMA}$[d] (%)
1	MMA	EtOH	6.5	42	90	9900	1.37	68
2	DMA	EtOH	3.3	29	96	17800	1.26	39
3	13FOMA	EtOH	3.4	22	97	16700	1.23	64
4	PEGMA	EtOH	4.4	9.0	98	75900	2.10	0
5	TFEMA	EtOH	5.9	18	37	7200	1.24	71
6	13FOMA	DOH	1.5	20	95	28200	1.17	55
7	13FOMA	ODOH	1.5	25	90	27000	1.56	53
8	13FOMA	TEGOH	1.2	24	90	5800	1.11	36
9	13FOMA	PEGOH	1.1	49	77	51800	1.19	47

[a][Monomer (MMA, DMA, 13FOMA, PEGMA, TFEMA)]/[ECPA]/[Ru(Ind)Cl(PPh_3)$_2$]/[Ti(O*i*-Pr)$_4$] = 1000 (entry 4, 9) or 2000/10 (entry 4, 9) or 20/2/20 mM in toluene/ROH [ROH: EtOH (CH_3CH_2OH), DOH ($CH_3(CH_2)_{11}OH$), ODOH ($CH_3(CH_2)_{17}OH$), TEGOH ($CH_3CH_2(OCH_2CH_2)_3OH$), PEG-OH ($CH_3(OCH_2CH_2)_nOH$; n = 7.2 (average); M_n = 350)] (1/1, v/v) at 80 °C. [b]Total monomer conversion determined by ^{1}H NMR with an internal standard (tetralin). [c]Determined by SEC in $CHCl_3$ with a PMMA standard calibration. [d]Cumulative RMA content ($F_{cum,RMA}$) of copolymers determined by ^{1}H NMR.

Cumulative EMA content in polymers ($F_{cum,EMA}$) was further directly estimated from ^{1}H NMR measurements of the polymerization solutions that were sampled at predetermined periods. $F_{cum,EMA}$ against total monomer conversion was first determined with methylene protons of polymerized EMA adjacent to the ester units (4.1 – 3.9 ppm). To express variation of $F_{cum,EMA}$ along polymer chain, $F_{cum,EMA}$ values were then plotted as a function of normalized chain length. The normalized chain length is defined as DP_t/DP_{final} for living copolymers; DP_t = [RMA]$_0$ × (total conversion/100)/[ECPA]$_0$; DP_{final} = [RMA]$_0$ × (total final conversion/100)/[ECPA]$_0$. Instantaneous EMA content ($F_{inst.EMA}$) of the 13FOMA/EMA copolymer calculated therefrom[23] increased with normalized chain length (Figure 1f), as well as that of MMA/EMA or DMA/EMA copolymers. Analyzed by SEC, 13FOMA/EMA copolymers was well controlled (M_n = 16700, M_w/M_n = 1.23), similar to MMA/EMA (M_n = 9900, M_w/M_n = 1.37) and DMA/EMA (M_n = 17800, M_w/M_n = 1.26) copolymers (Figure 2a-c). Broad molecular weight distribution of poly(PEGMA) (M_n = 75900, M_w/M_n = 2.10) (Figure 2d) is attributed to higher concentration of PEGMA (1000 mM) than that is generally employed for PEGMA polymerization ([PEGMA]: 500 mM). These results support that 13FOMA is effective as a fluorinated source and starting monomer to synthesize fluorous gradient copolymers via tandem catalysis with alcohols.

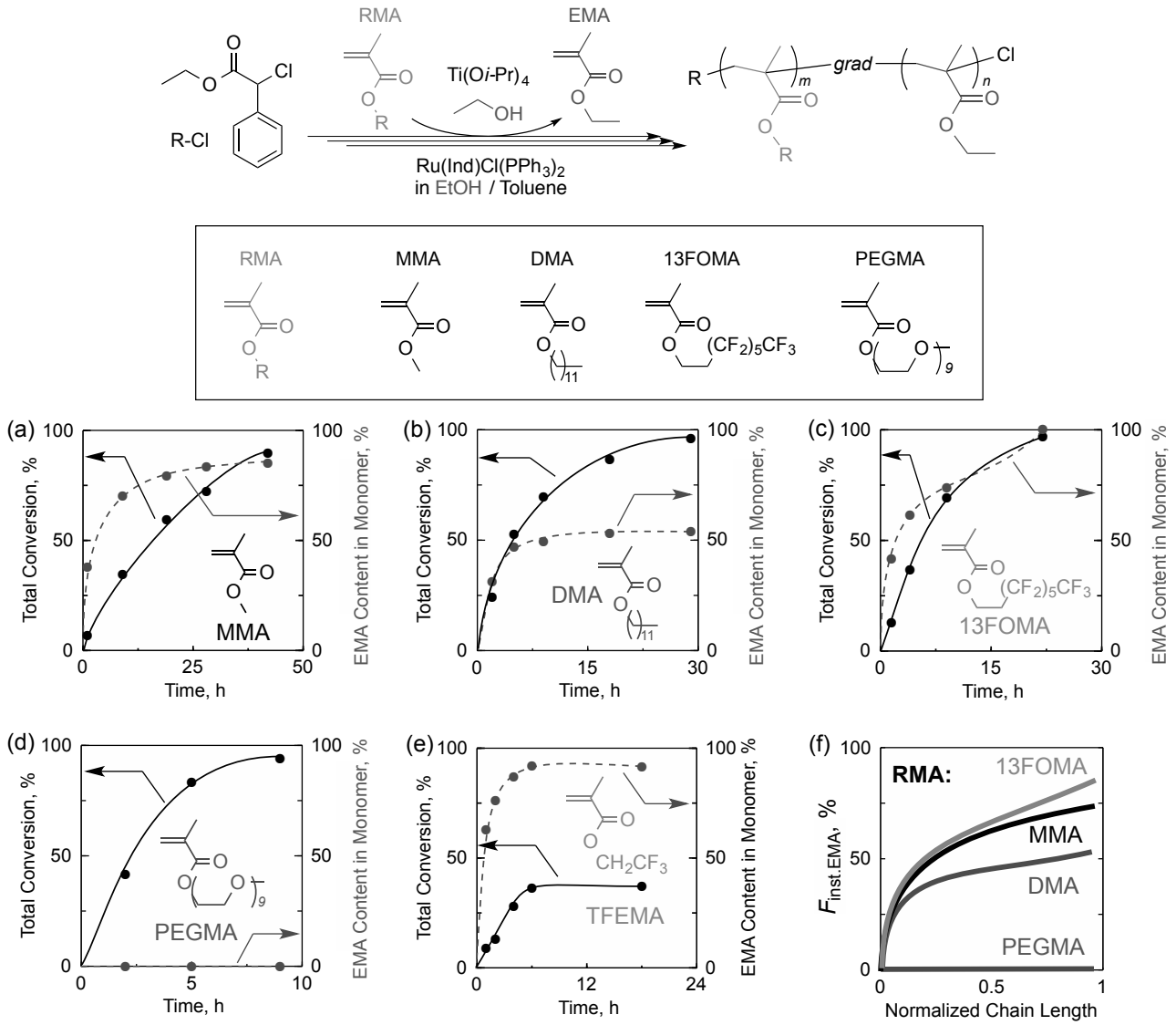

Figure 1. Concurrent tandem living radical polymerization of various methacrylates (RMA: MMA, DMA, 13FOMA, PEGMA, TFEMA) with Ti(O*i*-Pr)$_4$ and ethanol: [RMA]/[ECPA]/[Ru(Ind)Cl(PPh$_3$)$_2$]/[Ti(O*i*-Pr)$_4$] = 1000 (PEGMA) or 2000/10 (PEGMA) or 20/2/20 mM in toluene/EtOH (1/1, v/v) at 80 °C. (a-e) total monomer conversion and EMA (ethyl methacrylate) content in monomer. (f) instantaneous ($F_{inst,EMA}$) EMA content in products as a function of normalized chain length.

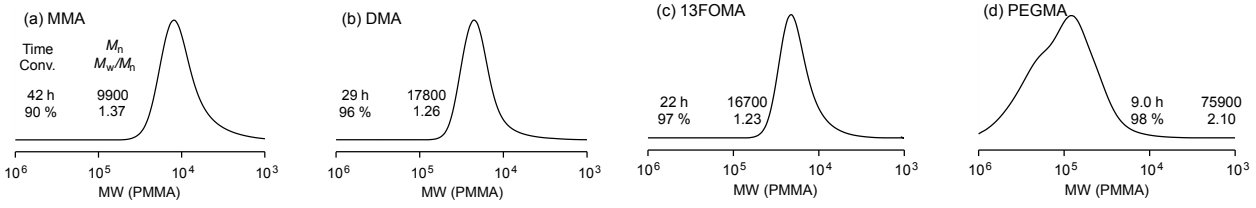

Figure 2. SEC curves of (a) MMA/EMA, (b) DMA/EMA, and (c) 13FOMA/EMA gradient copolymers and (d) a PEGMA homopolymer.

To guarantee gradient sequence, transesterification should be selective for 13FOMA (monomer) and not occur for the resulting polymers. Thus, the transesterification of a 13FOMA/MMA random copolymer (13FOMA/MMA = 20/40), prepared via ruthenium catalyzed living radical copolymerization (M_n = 20400, M_w/M_n = 1.25) of 13FOMA and MMA, was examined with Ti(O*i*-Pr)$_4$ (160 mM) and ethanol. No structure change was confirmed by ^{1}H NMR, indicating that the perfluoroalkyl ester pendants built in the copolymer were not transesterified.

To investigate the effects of the fluorine number and alkyl spacer in fluorinated methacrylates on transesterification, 2,2,2-trifluoroethyl methacrylate (TFEMA) bearing a methylene spacer was applied to tandem polymerization under the same conditions as the former experiments (Table 1, entry 5). TFEMA was transesterified with EtOH much faster than 13FOMA (Figure 1c,e), although TFEMA has less number of fluorine atoms than 13FOMA. The high reactivity of TFEMA is attributed to more acidic and less nucleophilic character of trifluoroethanol that is generating from TFEMA. Thus, 13FOMA bearing an ethylene spacer between methacrylate and a perfluorinated alklyl group is one of the best fluorinated monomers to design fluorous gradient copolymers.

2. Synthesis of Fluorous Gradient Copolymers with Various Functionalities

Various alcohols were combined with 13FOMA in tandem catalysis to synthesize fluorous gradient copolymers whose sequence distribution gradually changes from perfluorinated units to other functional groups with different properties. Here, the authors used long alkyl alcohols (1-dodecanol: DOH, 1-octadecyl alcohol: ODOH) and hydrophilic alcohols (triethylene glycol monoethyl ether: TEGOH, poly(ethylene glycol) methyl ether: PEG-OH [$CH_3(OCH_2CH_2)_nOH$; n = 7.2 (average); M_n = 350]) (Table 1, entry 6-9). Polymerization was conducted under catalytic systems and conditions similar to those applied to 13FOMA/EMA copolymers. Keeping target degree of polymerization as 100, 13FOMA concentration was adjusted as follows: 2000 mM for DOH, ODOH, and TEGOH; 1000 mM for PEGPH. As a result, transesterification concurrently took place with polymerization in all cases (Figure 3), while the kinetic balances of the two catalysis was dependent on the alcohols. Polymerization with ODOH was slower than that in DOH probably because of the high viscosity of polymerization solutions with ODOH (Figure 3a,b). PEG-OH induced transesterification faster than polymerization because the polymerization turned slower than that with the other alcohols owing to the low concentration of a originally fed 13FOMA (i.e., total monomer concentration: 1000 mM) (Figure 3e). Higher transesterification yield of 13FOMA with PEG-OH than that with TEGOH is attributed to excess amount of PEG-OH against 13FOMA (Figure 3d,e).

Confirmed by SEC, molecular weight of all of the copolymers was well controlled. $F_{cum,RMA}$ and $F_{inst,RMA}$ (RMA: DMA, ODMA, TEGMA, PEGMA) were also determined by ^{1}H NMR and plotted as a function of normalized chain length (Figure 3c,f). In all cases, both $F_{cum,RMA}$ and $F_{inst,RMA}$ gradually increased with normalized chain length. In the case of PEG-OH, $F_{cum,RMA}$ and $F_{inst,RMA}$ linearly increased up to the latter stage of polymerization although transesterification of 13FOMA into PEGMA almost turned to be equilibrium state at around 50% monomer conversion. This result suggests that the 13FOMA has slightly higher reactivity than PEGMA in copolymerization of the two monomers. As a result, rather fortunately, this system produced a 13FOMA/PEGMA gradient copolymer whose hydrophilic PEGMA composition ($F_{cum,PEGMA}$, $F_{inst,PEGMA}$) linearly increased from α-end to ω-end.

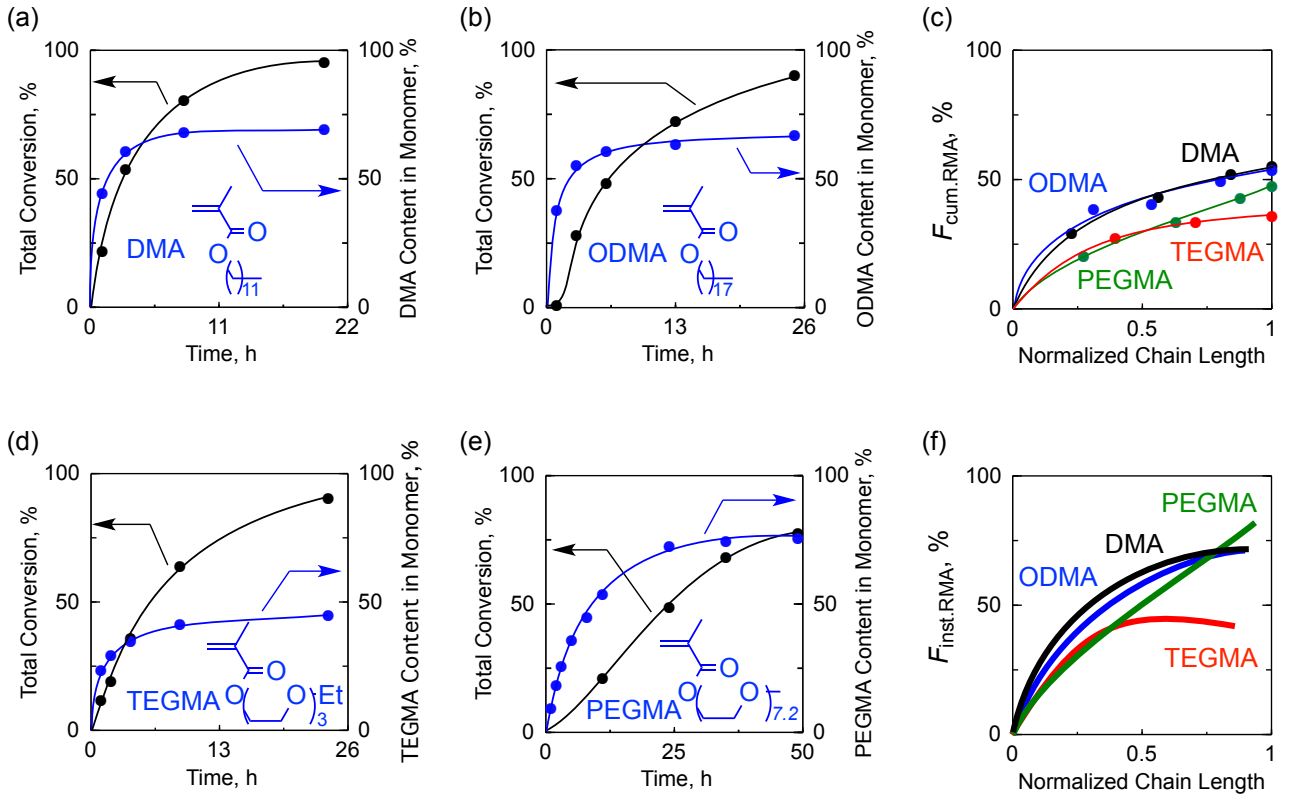

Figure 3. Synthesis of 13FOMA/RMA [RMA: DMA, ODMA, TEGMA, and PEGMA (M_n = 350)] gradient copolymers via concurrent tandem catalysis with 13FOMA and various alcohols: [MMA]/[ECPA]/[Ru(Ind)Cl(PPh_3)$_2$]/[Ti(O*i*-Pr)$_4$] = 1000 (PEGOH) or 2000/10 (PEGOH) or 20/2/20 mM in toluene/ROH (ROH: DOH, ODOH, TEGOH, PEGOH) (1/1, v/v) at 80 °C. (a)(b)(d)(e) total monomer conversion and RMA content in monomer. (c) $F_{cum,RMA}$ of products as a function of normalized chain length. (f) $F_{inst,RMA}$ of products as a function of normalized chain length.

Fluorous/hydrophobic 13FOMA/DMA random, gradient, and block copolymers with about 200 of degree of polymerization were prepared to investigate sequence-dependent physical properties (Table 3). The random and block copolymers were synthesized via living radical copolymerization of 13FOMA and DMA, while the gradient copolymer was synthesized via tandem catalysis based on in-situ transesterification of 13FOMA with DOH. The sequence distribution of three copolymers was depicted in Figure 4a. To reveal the effect of the sequence distribution, the composition ($F_{cum,DMA}$ = 53 - 57) and molecular weight (target DP = 200, M_n = 29700~38600) of the copolymers were adjusted to be similar (Figure 4).

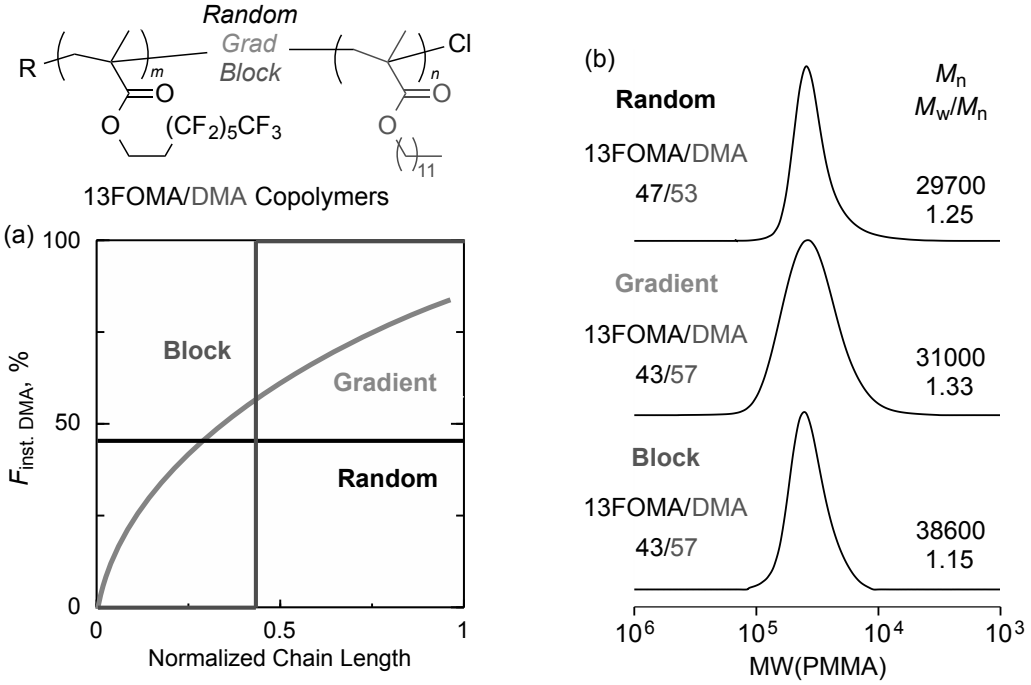

Figure 4. (a) $F_{inst,RMA}$ of products as a function of normalized chain length (b) SEC curves of 13FOMA/DMA random, gradient, and block copolymers.

3. Physical Properties of 13FOMA/DMA Copolymers: Effects of Sequence Distribution

Thermal Properties. Thermal properties of 13FOMA/DMA random, gradient, and block copolymers (Figure 4) were examined by DSC (Figure 5a). The block copolymer clearly showed two peaks originating from T_g of poly(DMA) (-46 ^oC) and poly(13FOMA) (18.3 ^oC) segments, while the random copolymer exhibited a single T_g at -4.2 ^oC between the two T_g's observed in the block copolymer. The gradient copolymer in turn showed a broad T_g signal at around -11 ^oC, where the temperature was close to that of the random counterpart. To see the difference of their heat flow curves clearly, first derivative of the heat flow curves as a function of temperature was evaluated for the three copolymers (Figure 5b). This definitely indicates the broad T_g range of the gradient copolymer spreading from -35 to 25 ^oC, compared with the random counterpart. This

result corresponds to an unique phenomenon for glass transition temperature that is revealed in Chapter 1 and relating previous researches. 13FOMA/DMA copolymers were also examined with thermogravimetric analysis (TGA) (Table 2). All samples showed weight loss at similar temperature (216~218 ^{o}C). This result indicated that heat degradation temperature is independent on distribution of fluorinated parts.

Table 2. Synthesis and Characterization of 13FOMA/DMA Random, Gradient, and Block Copolymers

Sample	13FOMA/DMA[d] (^{1}H NMR)	M_n[d] (^{1}H NMR)	M_n[e] ($CHCl_3$ GPC)	M_w/M_n[e] ($CHCl_3$ GPC)	M_n[f] (GPC)	M_w/M_n[f] (GPC)	TGA
Random[a]	47/53	57700	31200	1.16	30400	1.08	218.1
Gradient[b]	43/57	58700	31000	1.33	29000	1.23	216.4
Block[c]	43/57	56400	33900	1.31	22100	1.15	217.8

[a][13FOMA]/[DMA]/[ECPA]/[Ru(Ind)Cl(PPh_3)$_2$]/[nBu$_3$N] = 450/550/5/1/20 mM in toluene at 80 ^{o}C. [b][13FOMA]/[ECPA]/[Ru(Ind)Cl(PPh_3)$_2$]/[Ti(Oi-Pr)$_4$] = 1000/5/1/15 mM in toluene/1-dodecanol (1/1, v/v) at 80 ^{o}C. [c]1st block: [DMA]/[ECPA]/[Ru(Ind)Cl(PPh_3)$_2$]/[nBu$_3$N] = 1100/10/2/20 mM in toluene at 80 ^{o}C. 2nd block: [13FOMA]/[PDMA-Cl]/[Ru(Ind)Cl(PPh_3)$_2$]/[nBu$_3$N] = 450/5/1/10 mM in toluene at 80 ^{o}C. [d]Composition and number-average molecular weight of copolymers determined by ^{1}H NMR. [e]Determined by SEC in $CHCl_3$ with a PMMA standard calibration. [f]Determined by SEC in HFCl225/HFIP = 90/10 (wt%) with a PMMA standard calibration.

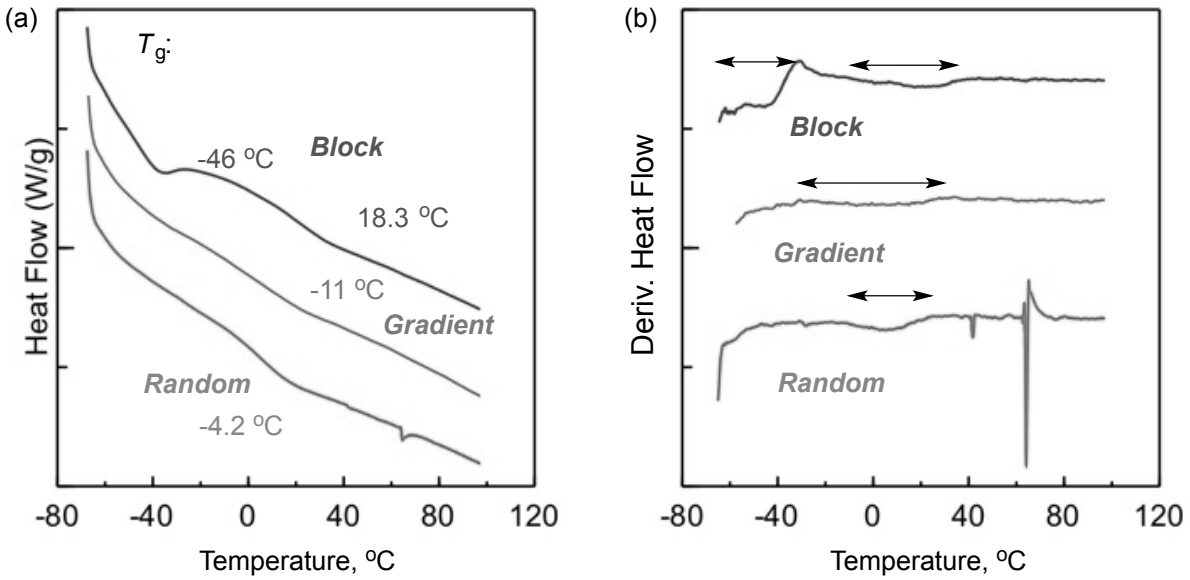

Figure 5. DSC measurements of 13FOMA/DMA random, gradient, block copolymers: (a) heat flow and (b) first derivative heat flow; heating = 1 ^{o}C/min.

Phase Separation Behavior. Owing to the unclear boundary between the 13FOMA-rich segment and the DMA-rich counterpart, the 13FOMA/DMA gradient copolymer would show phase separation phase separation behavior different from the random or block counterparts. Thus, the 13FOMA/DMA copolymers with different sequences (random, gradient, and block) were analyzed

by small angle X-ray scattering (SAXS) (Figure 6a). Interestingly, SAXS profiles of three kinds of copolymer were clearly different. The gradient copolymer showed a single scattering intensity maximum (q_m) at 0.27 nm^{-1}, while the random copolymer showed no such peak and the block copolymer in turn clearly exhibited four peaks with constant interval (1:2:3:4) (Figure 6a). This result importantly indicates that the 13FOMA/DMA gradient copolymer induces the microphase separation in contrast to the random counterpart. The phase separation structure of the gradient copolymer consists of the broad interface between poly(13FOMA)-rich segment and poly(DMA)-rich counterpart and is not so clear, though the block counterpart clearly forms lamella structure (domain spacing: D = 34 nm). These results suggest that the gradient monomer sequence of ambiguous boundary is one option to create unique microstructure in solid state.

Surface Tension of Toluene Solutions. To elucidate the solution properties of the 13FOMA/DMA gradient copolymer, surface tension of the toluene solution of the gradient copolymers was examined, compared with that of random or block counterparts (Figure 6b). All copolymers reduced surface tension of the toluene solutions. In particular, both block and gradient copolymers reduced the surface tension more than the random counterpart. This result indicated that the poly(13FOMA)-rich segment of the gradient copolymer would be also placed and arranged on the surface of the solutions, similarly to that of block counterpart. This is probably due to the strong segregation effect of the fluorous poly(13FOMA)-rich segment to the hydrophobic poly(DMA)-rich counterpart.

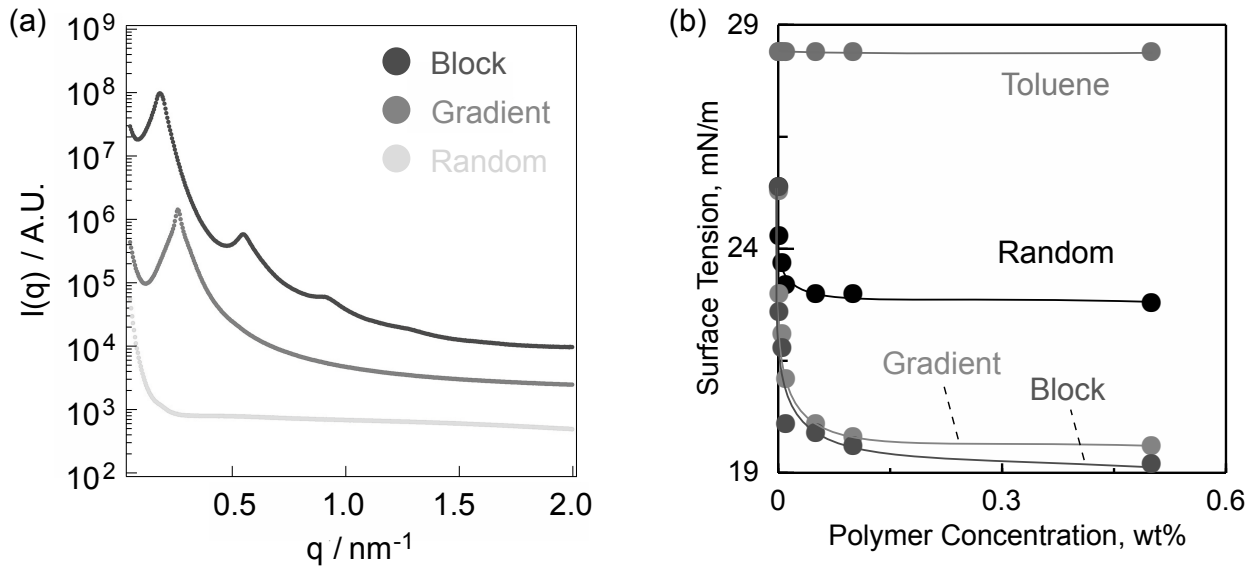

Figure 6. (a) SAXS profiles of 13FOMA/DMA random, gradient, and block copolymers. (b) Surface tension of the toluene solutions of 13FOMA/DMA random, gradient, and block copolymers: [Polymer] = 0-0.5 mg/mL.

Table 3. Water/Oil Repellency of 13FOMA/DMA Copolymers[a]

Sample	Immediate (H_2O)	After 30s (H_2O)	Immediate (*n*HD)	After 30s (*n*HD)
Random	111	103	67	54
Gradient	116	114	70	70
Block	117	107	72	70

Sample (H_2O)	Slope (^{o})	Forward Contact Angle	Backward Contact Angle	$\Delta\theta$
Random	80	120	69	51
Gradient	80	125	75	50
Block	80	106	62	44

Sample (*n*HD)	Slope (^{o})	Forward Contact Angle	Backward Contact Angle	$\Delta\theta$
Random	80	68	26	42
Gradient	80	90	54	36
Block	80	90	53	27

[a]Contact angle of H_2O or *n*-hexadecane (*n*HD) on 13FOMA/DMA random, gradient, and block copolymer surfaces cast on silicon wafers from the HFC225/$CHCl_3$ (75/25, v/v) solutions (10 mg/mL).

Contact Angle. Water/oil repellency was one of the most important properties of fluorinated polymers. Contact angle of water or *n*-hexadecane (*n*-HD) on the 13FOMA/DMA copolymers (random, gradient, block) cast on silicon wafers was evaluated, focused on the effects of the sequence distribution of the perfluorinated segments (Figure 7, Table 3). All copolymers almost showed similar contact angles against both water and *n*-HD at both 0^o and 80^o angles of the wafers (polymer surfaces). Thought clear differences dependent on the monomer sequence was not observed in these experiments, detail experiments typically changing temperature or aging times may reveal the effects of the sequence distribution on water/oil repellency.

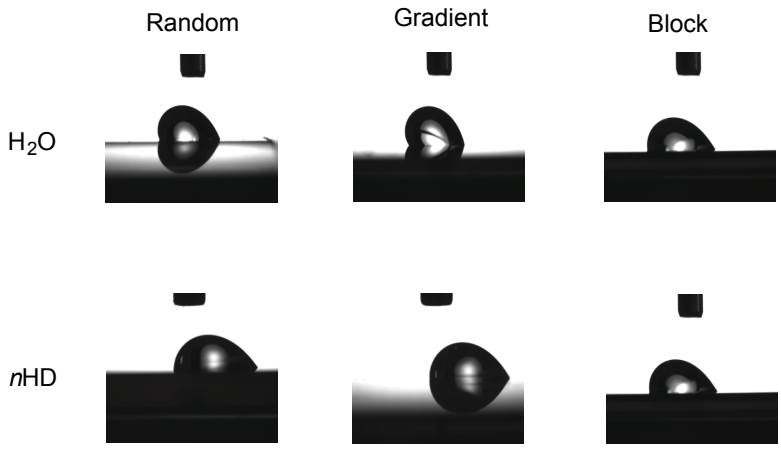

Figure 7. Pictures of H_2O or *n*-hexadecane (*n*HD) droplets on 13FOMA/DMA random, gradient, and block copolymer surfaces cast on silicon wafers at 80^o angle.

Conclusion

Fluorous, perfluorinated gradient copolymers were successfully synthesized via concurrent tandem catalysis of LRP with in-situ transesterification of a perfluoroalkyl methacrylate (13FOMA) with as a starting monomer. Owing to the electron-withdrawing perfluoroalkyl segment, 13FOMA allows efficient transesterification with various alcohols including 1-dodecanol (hydrophobic), 1-octadecanol (crystalline), and poly(ethylene glycol) methyl ether (hydrophilic). As a result, the tandem catalysis gave fluorous/hydrophobic or fluorous/hydrophilic gradient copolymers. A fluorous/hydrophobic 13FOMA/DMA gradient copolymer exhibited unique physical properties dependent on the sequence distribution of perfluorinated units. Typically, the gradient copolymer showed broad range of T_g and phase separation different from the corresponding random or block copolymers. In toluene, the gradient copolymer effectively reduced the surface tension of the toluene solution as well as the block copolymer.

References

(1) Boschet, F.; Ameduri, B. *Chem. Rev.* **2014**, *114*, 927-980.

(2) Mao, Z.; Vakhshouri, K.; Jaye, C.; Fischer, D. A.; Fernando, R.; DeLongchamp, D. M.; Gomez, E. D.; Sauvé, G. *Macromolecules* **2013**, *46*, 103-112.

(3) Dhara, M. G.; Banerjee, S. *Prog. Polym. Sci*. **2010**, *35*, 1022-1077.

(4) Souzy, R.; Ameduri, B. *Prog. Polym. Sci.* **2005**, *30*, 644-687.

(5) Vitale, A.; Bongiovanni, R.; Ameduri, B. *Chem. Rev.* **2015**, *115*, 8835-8866.

(6) Asandei, A. D. *Chem. Rev.* **2016**, *116*, 2244-2274.

(7) Reisinger, J. J.; Hillmyer, M. A. *Prog. Polym. Sci.* **2002**, *27*, 971-1005.

(8) Olvera, L. I.; Guzmán-Gutiérrez, M. T.; Zolotukhin, M. G.; Fomine, S.; Cárdenas, J.; Ruiz-Trevino, F. A.; Villers, D.; Ezquerra, T. A.; Prokhorov, E. *Macromolecules* **2013**, *46*, 7245-7256.

(9) Dessipri, E.; Tirrell, D. A.; Atkins, E. D. T. *Macromolecules* **1996**, *29*, 3545-3551.

(10) Wisian-Neilson, P.; Xu, G-F.; Wang, T. *Macromolecules* **1995**, *28*, 8657-8661.

(11) Martinelli, E.; Paoli, F.; Gallot, B.; Galli, G. *J. Polym. Sci. Part A: Polym. Chem.* **2010**, *48*, 4128-4139.

(12) Doi, T.; Sakurai, Y.; Tamatani, A.; Takenaka, S.; Kusabayashi, S.; Nishihata, Y.; Terauchi, H. *J. Mater. Chem.* **1991**, *1*, 169-173.

(13) Peng, H.; Thurecht, K. J.; Blakey, I.; Taran, E.; Whittaker, A. K. *Macromolecules* **2012**, *45*, 8681-8690.

(14) Ishige, R.; Ohta, N.; Ogawa, H.; Tokita, M.; Takahara. A. *Macromolecules* **2016**, *49*, 6061-6074.

(15) Dong, X-H.; Ni, B.; Huang, M.; Hsu, C-H.; Chen, Z.; Lin, Z.; Zhang, W-B.; Shi, A-C.; Cheng, S. Z. D. *Macromolecules* **2015**, *48*, 7172-7179.

(16) Ishige, R.; Shinohara, T.; White, K. L.; Meskini, A.; Raihane, M.; Takahara, A.; Ameduri, B. *Macromolecules* **2014**, *47*, 3860-3870.

(17) Zaggia, A.; Ameduri, B. *Curr. Opin. Colloid Interface Sci.* **2012**, *17*, 188-195.

(18) Koda, Y.; Terashima, T.; Sawamoto, M. *Macromolecules* **2016**, *49*, 4534-4543.

(19) Koda, Y.; Terashima, T.; Sawamoto, M. *Polym. Chem.* **2015**, *6*, 5663-5674.

(20) Koda, Y.; Terashima, T.; Sawamoto, M.; Maynard, H. D. *Polym. Chem.* **2015**, *6*, 240-247.

(21) Koda, Y.; Terashima, T.; Nomura, A.; Ouchi, M.; Sawamoto, M. *Macromolecules* **2011**, *44*, 4574-4578.

(22) Koda, Y.; Terashima, T.; Sawamoto, M. *J. Am. Chem. Soc.* **2014**, *136*, 15742−15748.

(23) Nakatani, K.; Terashima, T.; Sawamoto, M. *J. Am. Chem. Soc.* **2009**, *131*, 13600−13601.

(24) Nakatani, K.; Ogura, Y.; Koda, Y.; Terashima, T.; Sawamoto, M. *J. Am. Chem. Soc.* **2012**, *134*, 4373−4383.

(25) Ogura, Y.; Terashima, T.; Sawamoto, M. *ACS Macro Lett.* **2013**, *2*, 985−989.

(26) Wang, S.; Fu, C.; Zhang, Y.; Tao, L.; Li, S.; Wei, Y. *ACS Macro Lett.* **2012**, *1*, 1224−1227.

(27) Fu, C.; Xu, J.; Tao, L.; Boyer, C. *ACS Macro Lett.* **2014**, *3*, 633−638.

(28) Zhang, G.; Jiang, J.; Zhang, Q.; Gao, F.; Zhan. X.; Chen, F. *Langmuir* **2016**, *32,* 1380-1388.

PART II

Sequential/Iterative Tandem Catalysis and Functionalization with Terminal and Acrylate-Selective Transesterification for Telechelic or Pinpoint-Functionalized Polymers

Chapter 6

Telechelic and Pinpoint-Functionalized Polymers via Terminal-Selective Transesterifcation of Chlorine-Capped Poly(methyl methacrylate)s

Abstract

Terminal-selective transesterification of chlorine-capped poly(methyl methacrylate)s (PMMA-Cl) with alcohols was developed as a modular approach to create telechelic and pinpoint-functionalized polymers. Sterically less hindered, both α-end ethyl ester and ω-end methyl ester of PMMA-Cl were efficiently and selectively transesterified with diverse alcohols in the presence of a titanium alkoxide catalyst, while retaining the pendent esters intact, to almost quantitatively give various chlorine-capped telechelic PMMAs. In sharp contrast to conventional telechelic counterparts, the telechelic polymers obtained in this chapter yet carry a chlorine atom at the ω-terminal to further work as macroinitiator in living radical polymerization. The iterative process of living radical polymerization and terminal-selective transesterification successfully afforded unique pinpoint-functionalized polymers where a single functional monomer unit was introduced into the desired site of the polymer chains.

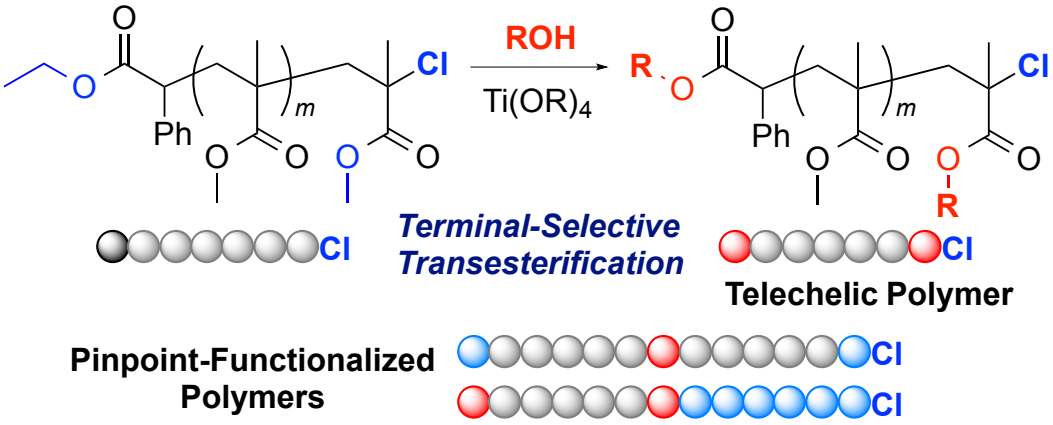

Introduction

Precision functionalization of synthetic macromolecules is a key to create unique and selective functions therefrom.[1] Recent advances in precision polymerization including living radical polymerization[2-4] has allowed the synthesis of various functional polymers with precision primary structure (e.g., molecular weight, terminal structure) and three-dimensional architectures (e.g., star and folding polymers). In particular, selective and pinpoint functionalization of the desired positions and the sequence control of monomers (functional groups) are important to create functional materials with unique properties.[1,5] For these, the combination of selective and efficient organic reactions and precision polymerization would be promising, since they can play different roles as follows: the former may selectively modify the target segments and/or compounds, while the latter can indeed control the molecular weight and terminal structure.[6-10]

In fact, the authors have originally developed concurrent tandem catalysis of living radical polymerization and metal alkoxide-mediated transesterification of methacrylates (e.g., methyl methacrylate: MMA) with alcohols (ROH) as a versatile synthetic strategy of gradient copolymers and their related sequence-regulated copolymers.[10] The key is the transesterification selective for the monomer (e.g., MMA) into RMA; uniquely, the resulting polymethacrylates with quarternary carbons in main chains are hardly transesterified though polyacrylates with tertiary carbons (without α-methyl groups) are transesterifed.[10a] This importantly suggests that the steric hindrance around esters by adjacent substituents hinders metal alkoxide catalysts from activating the carbonyl groups.[10a,11]

Given these features, in this chapter, the author herein focuses on terminal-selective transesterification of chlorine-capped poly(MMA)s (Et-PMMA-Cl) with a titanium alkoxide catalyst and alcohols; this serves as a novel modular approach to synthesize telechelic and pinpoint-functionalized polymers (Scheme 1). The selective functionalization is achieved without any specific functional units (e.g., activated esters or protecting groups),[12,13] thanks to that these terminals are far less sterically hindered than the pendent esters and ω-end terminal would be also electronically activated by chlorine atom. It should be noted that the transesterification of Et-PMMA-Cl almost quantitatively provides "chlorine-capped" telechelic poly(MMA)s (R-PMMA-RMA-Cl), in sharp contrast to the conventional telechelic polymers obtained from the transformation of an active polymer terminal via living polymerization.[14-17] Thus, the chlorine-capped telechelic polymers work as macroinitiator in living radical polymerization. The iterative process of living radical polymerization and terminal-selective transesterification thereby affords "pinpoint-functionalized" polymers, where a single functionality may precisely be introduced into a specific site (terminal, center, mid-chain unit, etc.) in a macromolecule.

Obviously, such a precision "pinpoint" (or position-specific) functionalization is generally difficult in radical polymerization.[1] This strategy would be further applicable to the design of various functional polymers with precise and complex repeat-unit and functionality sequence such as periodic sequence-regulated copolymers.

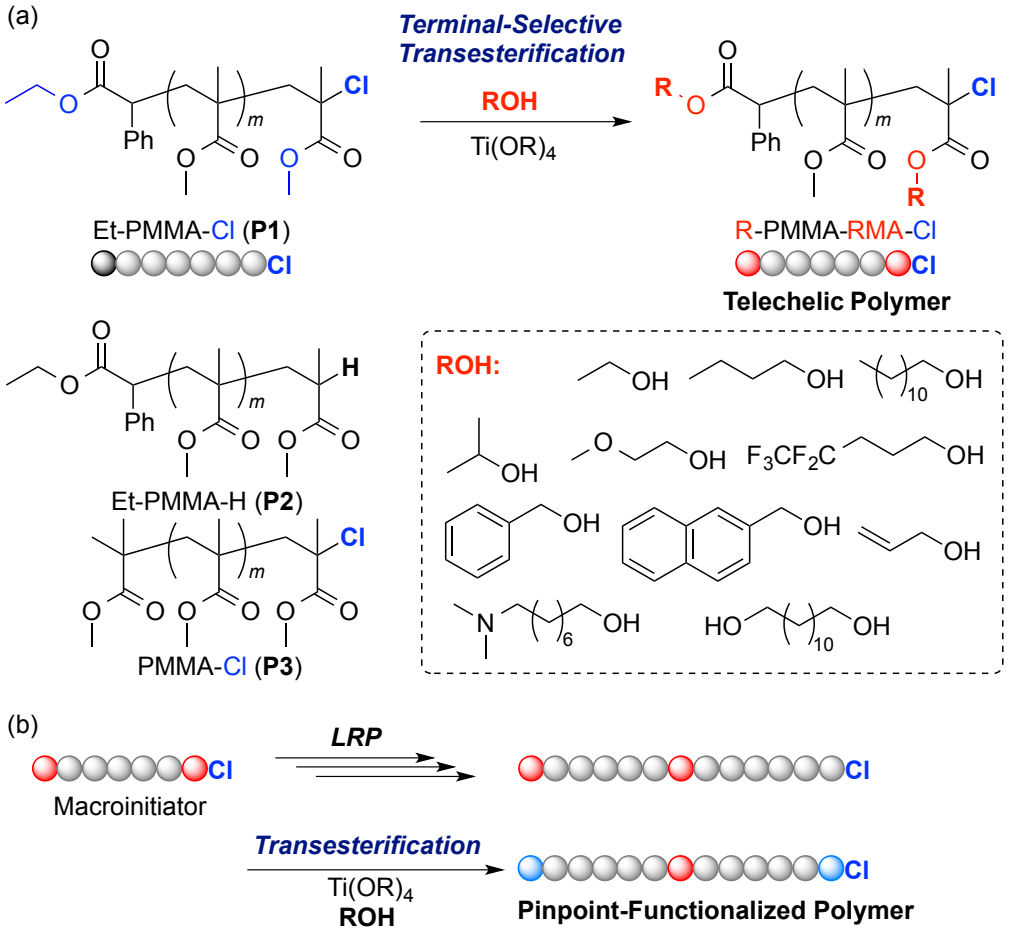

Scheme 1. (a) Chlorine-Capped Telechelic and (b) Pinpoint-Functionalized Polymers via Terminal-Selective Transesterification of Chlorine-Capped PMMAs with Living Radical Polymerization (LRP)

Experimental Section

Materials

Methyl methacrylate (MMA: TCI; purity >99.8%) and tetralin (1,2,3,4-tetrahydronaphthalene: Kishida Chemical; purity >98%; an internal standard for ^{1}H NMR analysis) were dried overnight over calcium chloride and distilled from calcium hydride under reduced pressure before use. Dodecyl methacrylate (DMA) (Wako, purity >95%), poly(ethylene glycol) methyl ether methacrylate [PEGMA: CH_2=C(CH_3)CO_2(CH_2CH_2O)$_l$$CH_3$, Aldrich, 500 ($l$ =

9)] and 1*H*,1*H*,2*H*,2*H*-perfluorooctyl methacrylate (13FOMA: Wako, purity >95%) were purified by column chromatography charged with inhibitor remover (Aldrich) and degassed by triple vacuum-argon purge cycles before use. Ethanol (Wako, purity 99.5%), isopropanol (Wako, dehydrated), 1-butanol (Wako, purity >99%), benzyl alcohol (Wako, purity >99%), 1-dodecanol (TCI, purity >99%), 4,4,5,5,5-pentafluoro-1-pentanol (TCI, purity >93%), 2-methoxyethanol (Wako, purity >99%), 2-naphthalene methanol (TCI, purity >98%), 8-dimethylamino-1-octanol (TCI, purity >92%), 1,12-dodecanediol (TCI, purity >97%), Ti(O*i*-Pr)$_4$ (Aldrich, purity >97%), and *n*-Bu_3N (TCI, purity >98%) was degassed by triple vacuum-argon purge cycles before use. Ethyl 2-chloro-2-phenylacetate (ECPA: Aldrich; purity >97%) and H-(MMA)$_2$-Cl (H-(CH_2CMeCO_2Me)$_2$-Cl: prepared according to the literature[19]) were distilled under reduced pressure before use. Ru(Ind)Cl(PPh_3)$_2$ (Aldrich) were used as received and handled in a glove box under moisture- and oxygen-free argon (H_2O <1 ppm; O_2 <1 ppm). Toluene (solvent) was purified before use; pashing it through a purification column (Glass Contour Solvent Systems: SG Water USA).

Characterization

The molecular weight distribution (MWD) curves, M_n and M_w/M_n ratio of the polymers were measured by SEC at 40 °C in THF as an eluent on three polystyrene-gel columns (Shodex LF-404: exclusion limit = 2 × 10^6 g/mol; particle size = 6 μm; pore size = 3000 Å; 0.46 cm i.d. × 25 cm; flow rate, 0.3 mL/min) connected to a DU-H2000 pump, a RI-74S refractive index detector, and a UV-41 ultraviolet detector (all from Shodex; Shodex GPC-104). The columns were calibrated against 13 standard poly(MMA) samples (Polymer Laboratories; M_n = 620−1200000; M_w/M_n = 1.06−1.22). MWD, M_n, and M_w/M_n ratios of an amine-functionalized polymer and a PEGMA-based polymer were measured by SEC in DMF containing 10 mM LiBr at 40 °C (flow rate: 1 mL/min) on three linear-type polystyrene gel columns (Shodex KF-805L: exclusion limit = 4 × 10^6 g/mol; particle size = 6 μm; pore size = 5000 Å; 0.8 cm i.d. × 30 cm) that were connected to a Jasco PU-2080 precision pump, a Jasco RI-2031 refractive index detector, and a Jasco UV-2075 UV/vis detector set at 270 nm. The columns were calibrated against 10 standard samples of poly(MMA) samples (Polymer Laboratories; M_n = 1000 – 1200000; M_w/M_n = 1.06–1.22). ^{1}H NMR spectra were recorded in $CDCl_3$ and CD_2Cl_2 on a JEOL JNM-ECA500 spectrometer operating at 500.16 MHz. MALDI-TOF-MS analysis was performed on a Shimadzu AXIMA-CFR instrument equipped with 1.2 m linear flight tubes and a 337 nm nitrogen laser (matrix: dithranol; cationizing agent: sodium trifluoroacetate). Polymer samples for structure analysis were fractionated by preparative SEC at r.t. in $CHCl_3$ or DMF (for polymer containing amino group or PEGMA) as eluents on a polystyrene-gel column (in $CHCl_3$: Shodex K-5002;

particle size = 15 mm; 5.0 cm i.d. × 30 cm; exclusion limit = 5×10^3 g/mol; flow rate = 10 mL/min, in DMF: TOSOH TSKgel α-3000: particle size = 13 mm; 5.5 cm i.d. × 30 cm; exclusion limit = 9×10^4 g/mol; flow rate = 15 mL/min) connected to a Jasco PU-2086 precision pump, a Jasco RI-2013 refractive index detector, and a Jasco UV-2075 ultraviolet detector.

Polymerization

The synthesis of poly(MMA)s was carried out by syringe technique under argon in baked glass tubes equipped with a three-way stopcock.

Et-PMMA-Cl (P1): Into the 30 mL glass tube, Ru(Ind)Cl(PPh_3)$_2$ (0.03 mmol, 23.3 mg) was charged, and then toluene (9.54 mL), tetralin (0.20 mL), MMA (30 mmol, 3.20 mL), a 400 mM toluene solution of *n*-Bu_3N (0.75 mL, *n*-Bu_3N = 0.3 mmol), and a 229 mM toluene solution of ECPA (1.31 mL, ECPA = 0.3 mmol) were added sequentially at 25 °C under argon. The total volume of the reaction mixture was thus 15.0 mL. The glass tube was placed in an oil bath kept at 80 °C for 7 h and then cooled to –78 °C to terminate the reaction. The monomer conversion was determined as 33% by ^{1}H NMR measurement of the terminated reaction solution in $CDCl_3$ at r.t. with tetralin as an internal standard. The quenched solution was evaporated to dryness to give crude Et-PMMA-Cl. To remove the ruthenium catalyst, the product was purified by preparative SEC. SEC (THF, PMMA std.): M_n = 4700 g/mol; M_w/M_n = 1.13. ^{1}H NMR [500 MHz, CD_2Cl_2, 25 °C, δ = 5.33 ($CHDCl_2$)]: M_n (NMR, α) = 3800 g/mol; M_n (NMR, ω) = 4000 g/mol.

Et-PMMA-H (P2): Et-PMMA-H was synthesized by $RuCl_2(PPh_3)_3$/*n*-Bu_3N-catalyzed living radical polymerization of MMA and the sequential hydrogenation with K_2CO_3 and 2-propanol.[7] SEC (THF, PMMA std.): M_n = 6200 g/mol; M_w/M_n = 1.27. ^{1}H NMR [500 MHz, CD_2Cl_2, 25 °C, δ = 5.33 ($CHDCl_2$)]: M_n (NMR, α) = 5500 g/mol.

PMMA-Cl (P3): Into the 30 mL glass tube, Ru(Ind)Cl(PPh_3)$_2$ (0.006 mmol, 4.66 mg) was charged, and then toluene (2.02 mL), tetralin (0.08 mL), MMA (6 mmol, 0.64 mL), a 400 mM toluene solution of *n*-Bu_3N (0.15 mL, *n*-Bu_3N = 0.06 mmol), and a 545 mM toluene solution of H-$(MMA)_2$-Cl (0.11 mL, H-$(MMA)_2$-Cl = 0.06 mmol) were added sequentially at 25 °C under argon. The total volume of the reaction mixture was thus 3.0 mL. The glass tube was placed in an oil bath kept at 80 °C for 7 h and then cooled to –78 °C to terminate the reaction. The monomer conversion was determined as 18% by ^{1}H NMR measurement of the reaction solution in $CDCl_3$ at r.t. with tetralin as an internal standard. The quenched solution was evaporated to dryness to give crude PMMA-Cl. To remove the ruthenium catalyst, the product was purified by preparative SEC. SEC (THF, PMMA std.): M_n = 4100 g/mol; M_w/M_n = 1.11. ^{1}H NMR [500 MHz, CD_2Cl_2, 25 °C, δ = 5.33 ($CHDCl_2$)]: M_n (NMR, ω) = 3800 g/mol.

Et-PMMA-EMA-PMMA-Cl: Into the 30 mL glass tube, Ru(Ind)Cl(PPh_3)$_2$ (0.002 mmol, 1.56 mg) and Et-PMMA-EMA-Cl (M_n = 2900, 0.02 mmol, 58 mg) was charged, and toluene (1.46 mL), tetralin (0.06 mL), MMA (4 mmol, 0.43 mL) and a toluene solution of *n*-Bu_3N (400 mM, 0.05 mL, *n*-Bu_3N = 0.02 mmol) were added sequentially in that order at 25 °C under argon. The total volume of the reaction mixture was thus 2 mL. The glass tube was placed in an oil bath kept at 80 °C for 3 h and then cooled to –78 °C to terminate the reaction. The monomer conversion (11%) was determined by ^{1}H NMR measurement of the terminated reaction solution in $CDCl_3$ at r.t. with tetralin as an internal standard. The quenched reaction solution was evaporated to dryness to give a crude product. To remove the ruthenium catalyst, the product was purified by preparative SEC. SEC (THF, PMMA std.): M_n = 5800 g/mol; M_w/M_n = 1.08. ^{1}H NMR [500 MHz, CD_2Cl_2, 25 °C, δ = 5.33 ($CHDCl_2$)]: M_n (NMR, α) = 6200 g/mol; M_n (NMR, ω) = 6200 g/mol (Figure 3b). Pinpoint-functionalized block copolymers were similarly synthesized by ruthenium-catalyzed living radical polymerization of DMA, PEGMA, and 13FOMA with *i*Pr-PMMA-*i*PrMA-Cl.

Transesterification of PMMAs

The reaction was carried out by the syringe technique under dry argon in baked glass tubes equipped with a three-way stopcock.

***i*Pr-PMMA-*i*PrMA-Cl**: Into a glass tube, Et-PMMA-Cl (M_n = 4200, M_w/M_n = 1.13, 0.03 mmol, 12.6 mg), toluene (0.74 mL), a 500 mM toluene solution of Ti(O*i*-Pr)$_4$ (0.16 mL, Ti(O*i*-Pr)$_4$ = 0.08 mmol) and isopropanol (0.1 mL) were added at room temperature under dry argon (total volume: 1 mL). The glass tube was placed in an oil bath kept at 80 °C for 47 h and cooled to –78 °C to terminate the reaction. The quenched reaction solutions were evaporated to dryness to give the crude product. To remove the Ti catalyst, the product was fractionated by preparative SEC. By ^{1}H NMR, the yields of α- and ω-end transesterification were determined from the area ratio of the corresponding methine protons to α-end phenyl protons of ECPA (initiator). Characterization: Figure 1 in results and discussion.

R-PMMA-RMA-Cl with ethanol, 1-butanol, allyl alcohol, and 2-methoxy ethanol.

A typical procedure with allyl alcohol was given: Into a glass tube, toluene (0.24 mL), a 500 mM toluene solution of Ti(O*i*-Pr)$_4$ (0.16 mL, Ti(O*i*-Pr)$_4$ = 0.08 mmol) and allyl alcohol (ROH: 0.1 mL) were added at room temperature under dry argon (total volume: 0.5 mL). The glass tube was placed in an oil bath kept at 80 °C for 1 h to in-situ give Ti(OR)$_n$, and then cooled to –78 °C. The solution was evaporated at r.t. to remove isopropanol generating from Ti(O*i*-Pr)$_4$. Into the glass tube, Et-PMMA-Cl (M_n = 2700, M_w/M_n = 1.18, 0.03 mmol, 81 mg), toluene (0.9 mL), and allyl alcohol (0.1 mL) were again added at r.t. under dry argon. The glass tube was placed in an oil

bath kept at 80 °C for 24 h and cooled to –78 °C to terminate the reaction. The quenched reaction solutions were evaporated to dryness to give the crude product. To remove the Ti catalyst and non-volatile alcohols, the product was fractionated by preparative SEC. By ^{1}H NMR, the yields of α- and ω-end transesterification were determined from the area ratio of the corresponding methylene protons adjacent to esters to α-end phenyl protons of ECPA. Characterization: Figure 5, 6 in results and discussion.

R-PMMA-RMA-Cl with 1-dodecanol, 4,4,5,5,5-pentafluoro-1-pentanol, benzyl alcohol, 2-naphthalene methanol, 8-dimethylamino-1-octanol, and 1,12-dodecanediol.

A typical procedure with benzyl alcohol was given: Into a glass tube, toluene (0.24 mL), a 500 mM toluene solution of Ti(O*i*-Pr)$_4$ (0.16 mL, Ti(O*i*-Pr)$_4$ = 0.08 mmol) and benzyl alcohol (ROH: 0.1 mL) were added at room temperature under dry argon (total volume: 0.5 mL). Molecular sieves 4A (0.33 g/mL) were also added for transesterification with 8-dimethylamino-1-octanol and 1,12-dodecanediol. The glass tube was placed in an oil bath kept at 80 °C for 1 h to in-situ give Ti(OR)$_n$, and then cooled to –78 °C. The solution was evaporated at r.t. to remove isopropanol generating from Ti(O*i*-Pr)$_4$. Into the glass tube, Et-PMMA-Cl (M_n = 2700, M_w/M_n = 1.18, 0.03 mmol, 81 mg) and toluene (0.9 mL) were again added at r.t. under dry argon. The glass tube was placed in an oil bath kept at 80 °C for 47 h and cooled to –78 °C to terminate the reaction. The quenched solutions were evaporated to dryness to give the crude product. To remove the Ti catalyst and non-volatile alcohols, the product was fractionated by preparative SEC. By ^{1}H NMR, the yields of α- and ω-end transesterification were determined from the area ratio of the corresponding methylene protons adjacent to esters to α-end phenyl protons of ECPA. For 1,12-dodecanediol, the conversion of ω-end ester was determined from the area ratio of the methoxy protons adjacent to chlorine to α-end phenyl protons of ECPA. Characterization: Figure 5, 6 in results and discussion.

Results and Discussion

1. Terminal selective Transesterification of PMMA-Cl

A chlorine-capped PMMA [Et-PMMA-Cl (**P1**): M_n = 4200, M_w/M_n = 1.13 by size exclusion chromatography (SEC)] was first synthesized by Ru-catalyzed living radical polymerization of MMA with a ruthenium catalytic system [Ru(Ind)Cl(PPh$_3$)$_2$/*n*-Bu$_3$N] and a chloride initiator [ethyl 2-chloro-2-phenylacetate (ECPA)] in toluene at 80 °C. Confirmed by proton nuclear magnetic resonance (^{1}H NMR, Figure 1a), the PMMA almost quantitatively has a α-end ethyl group (*d*: 4.1 – 3.9 ppm) and a ω-end chlorine (*c'*: 3.7 ppm), originating from the initiator [M_n (NMR, α) = 3800, M_n (NMR, ω) = 4000].

Then, transesterification of Et-PMMA-Cl was examined with Ti(O*i*-Pr)$_4$ in isopropanol (*i*-PrOH)/toluene (1/9, v/v) mixture at 80 ^{o}C ([Et-PMMA-Cl]$_0$/[Ti(O*i*-Pr)$_4$]$_0$ = 30/80 mM). After 47 h, the product was analyzed by ^{1}H NMR spectroscopy and matrix assisted laser desorption/ionization time of flight mass spectrometry (MALDI-TOF-MS) (Figure 1). As shown in Figure 1b, both the α-end methylene protons (*a*) and the ω-end methoxy protons adjacent to the chlorine terminal (*b'*) completely disappeared, while two kinds of isopropyl methine protons (*d*, *e*: 5.0 – 4.8 ppm) newly appeared. The signal intensity ratio of the isopropyl protons (*d*, *e*) to the α-end aromatic protons (7.15-7.3 ppm) was close to the calculated values, assuming that a single isopropyl unit was incorporated into both α and ω-terminals of the PMMA chain [Yield (α-end/ω-end) = 95%/96%].

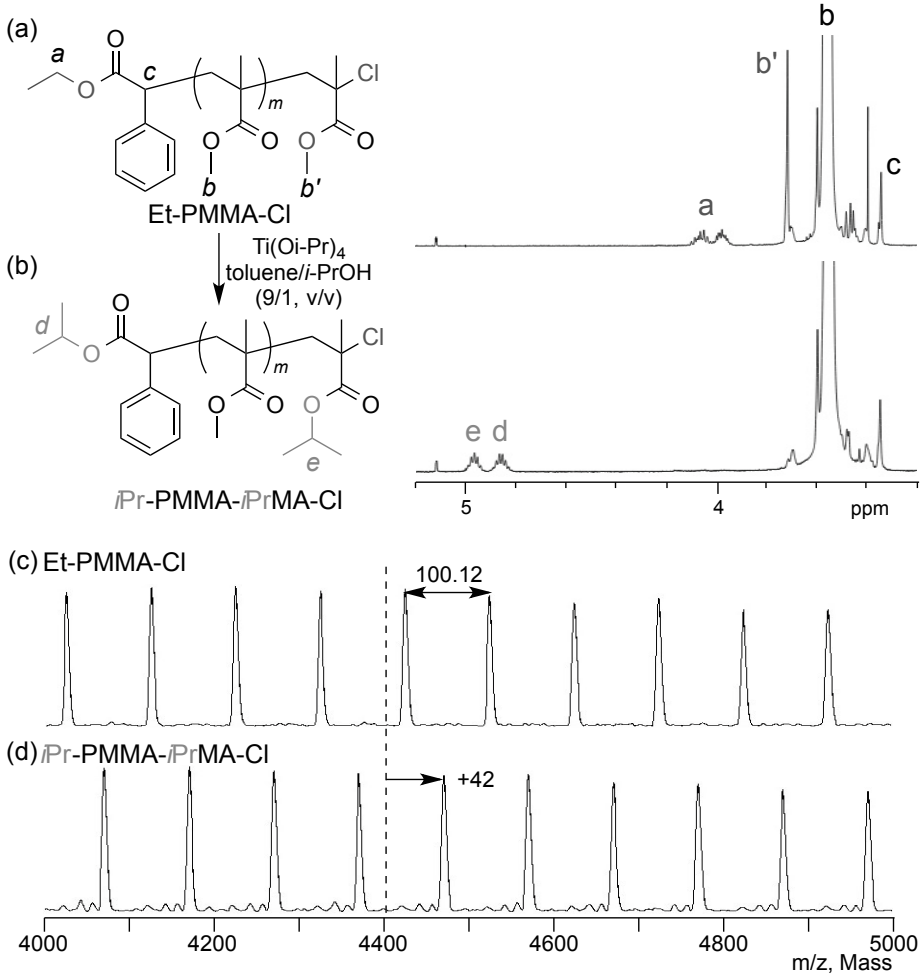

Figure 1. Terminal-selective transesterification of Et-PMMA-Cl with Ti(O*i*-Pr)$_4$ and isopropanol (*i*-PrOH): [Et-PMMA-Cl]/[Ti(O*i*-Pr)$_4$] = 30/80 mM in toluene/isopropanol (9/1, v/v) at 80 ^{o}C. ^{1}H NMR (a, b, in CD_2Cl_2 at r.t.) and MALDI-TOF-MS (c, d) spectra of Et-PMMA-Cl (a, c) and the product (b, d) obtained after the transesterification.

Confirmed by MALDI-TOF-MS, the product exhibited single series signals, regularly separated by the molar mass of MMA (100.12) (Figure 1d). The absolute mass of each peak was equal to that expected for the PMMA bearing an isopropyl ester at the α-end and an isopropyl methacrylate unit capped with one chlorine atom at the ω-end (*i*-Pr-PMMA-*i*-PrMA-Cl), plus a sodium ion from externally added salt for ionization. It should be noted that the product yet quantitatively carries a chlorine terminal. The mass difference between Et-PMMA-Cl (Figure 1c) and the product (Figure 1d) was 42, fully consistent with the selective transformation of *a*-end ethyl and ω-end methyl groups into two isopropyl groups [mass increase: +14 (Et→*i*-Pr); +28 (MMA-Cl→*i*-PrMA-Cl)]. These results demonstrate that both α and ω-terminal esters of Et-PMMA-Cl can be selectively transesterified to yield a chlorine-capped telechelic polymer.

Table 1. Terminal Transesterification with Various Alcohols[a]

entry	PMMA	alcohol	alcohol (mM)	time (h)	α-end yield.[b] (%)	ω-end yield.[b] (%)
1	P1	isopropanol	1300	47	95	96
2	P1	isopropanol	3900	47	>99	>99 (11)
3	P1	isopropanol	6500	47	>99	>99 (22)
4	P1	isopropanol	9100	47	>99	>99 (33)
5	P2	isopropanol	1300	47	91	94
6	P3	isopropanol	1300	47	22	90
7	P1	ethanol	1720	24	n.d.	>99
8	P1	1-butanol	1090	24	>99	>99
9	P1	1-dodecanol	450	24	>99	>99
10	P1	2-methoxy ethanol	1270	47	95	96
11	P1	4,4,5,5,5-pentafluoro-1-pentanol	760	47	97	98
12	P1	benzyl alcohol	970	47	91	92
13	P1	2-naphthalene methanol	1000	47	94	96
14	P1	allyl alcohol	1460	24	97	>99
15[c]	P1	8-dimethylamino-1-octanol	500	60	58	>99
16[c]	P1	1,12-dodecanediol	1000	60	n.d.	83

[a] $[PMMA]_0/[Ti(OR)_4]_0$ = 30/80 (entries 1-10, 12, 14) or 160 (entries 11,13,15,16) mM in toluene/alcohol at 80 °C: Et-PMMA-Cl (**P1**); Et-PMMA-H (**P2**); PMMA-Cl (**P3**). [b] Yield or conversion (Entries 16) determined by ^{1}H NMR. The value in parentheses: cyclized terminal. n.d.: not determined. [c] Reactions were conducted with molecular sieves 4A (0.33 g/mL in solution).

For such efficient and selective terminal transesterification, it was quite important to control isopropanol content in the mixed solvents (*i*-PrOH/toluene). Over 30 vol.% isopropanol mixtures with Ti(O*i*-Pr)$_4$ induced terminal cyclization via the elimination of chlorine terminal,[18] in addition to terminal-selective transesterification, to give *i*-Pr-PMMA-*i*-PrMA with a five-membered ring terminal as a byproduct (Figure 2). The byproduct increased with increasing the content of isopropanol (*i*-PrOH/toluene = 3/7, 5/5, 7/3, v/v, Table 1, entry 2-4).

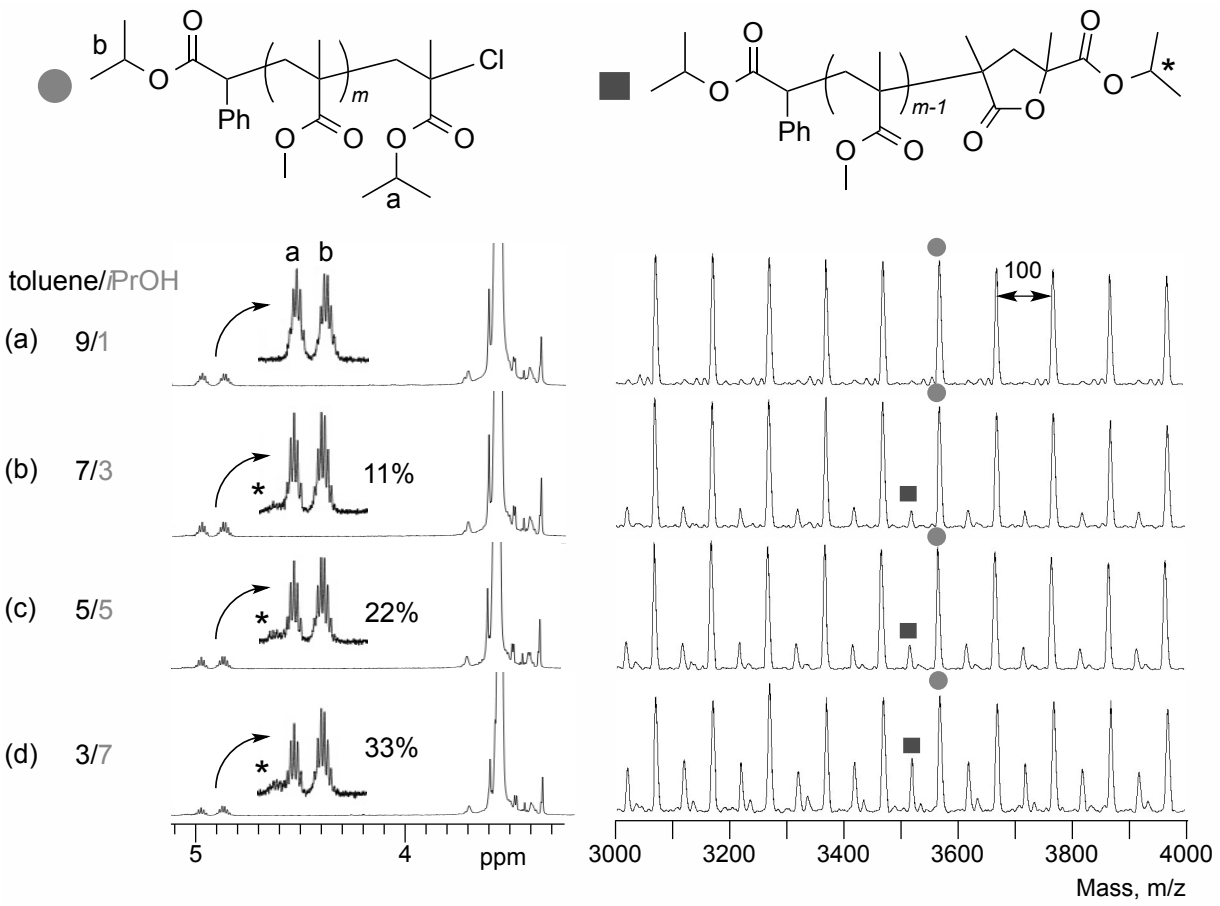

Figure 2. Effects of isopropanol content on terminal-selective transesterification of Et-PMMA-Cl: [Et-PMMA-Cl]$_0$/[Ti(O*i*-Pr)$_4$]$_0$ = 30/80 mM in toluene/isopropanol (a: 9/1; b: 7/3; c: 5/5; d: 3/7, v/v) at 80 °C for 48h. ^{1}H NMR spectra (in CD_2Cl_2 at 25 °C) and MALDI-TOF-MS spectra of obtained polymers.

2. Effects of Polymer Structure on Transesterification

Effects of the terminal structures of PMMAs on Ti(O*i*-Pr)$_4$-mediated transesterification with isopropanol were investigated with three kinds of poly(MMA)s with different terminal structures: Et-PMMA-Cl (**P1**), terminal-hydrogenated Et-PMMA-H (**P2**: M_n = 6200, M_w/M_n = 1.27),[7] and PMMA-Cl with a MMA-type methyl ester α-end (**P3**: M_n = 4100, M_w/M_n = 1.11). Monitored by ^{1}H NMR, Et-PMMA-Cl and Et-PMMA-H underwent simultaneous and almost quantitative

transesterification of both α-end ethyl ester and ω-end methyl ester to give corresponding telechelic PMMAs (Figures 3, Table 1, entries 1 and 5); all of the terminal units were transesterified at equal speed. However, PMMA-Cl underwent much slower transesterification of the α-end methyl ester adjacent to non-chlorinated quarternary carbon atom [ester-$C(CH_3)_2CH_2$-: 22% in 47h] than that of the ω-end methyl ester (Figure 3, Table 1, entry 6). This result suggests that the efficient and selective terminal-unit transesterification of **P1** and **P2** is due to both the less steric hindrance around α- and ω-end esters by adjacent tertiary carbons and the activation of ω-end ester by chlorine atom. For α-end methyl ester in **P3**, an adjacent quarternary carbon substituent would sterically hinder Ti(O*i*-Pr)$_4$ catalyst from activating the carbonyl oxygen, thereby reducing the reactivity of the transesterification. Such a steric effect has been also reported for tertiary butyl esters:[11] *e.g.*, *tert*-butyl methacrylate is not transesterfied with Al(O*i*-Pr)$_3$,[10b] while the activation effect was also in turn observed for a MMA dimer carrying one chlorine atom [H-$(MMA)_2$-Cl] (Figure 4).

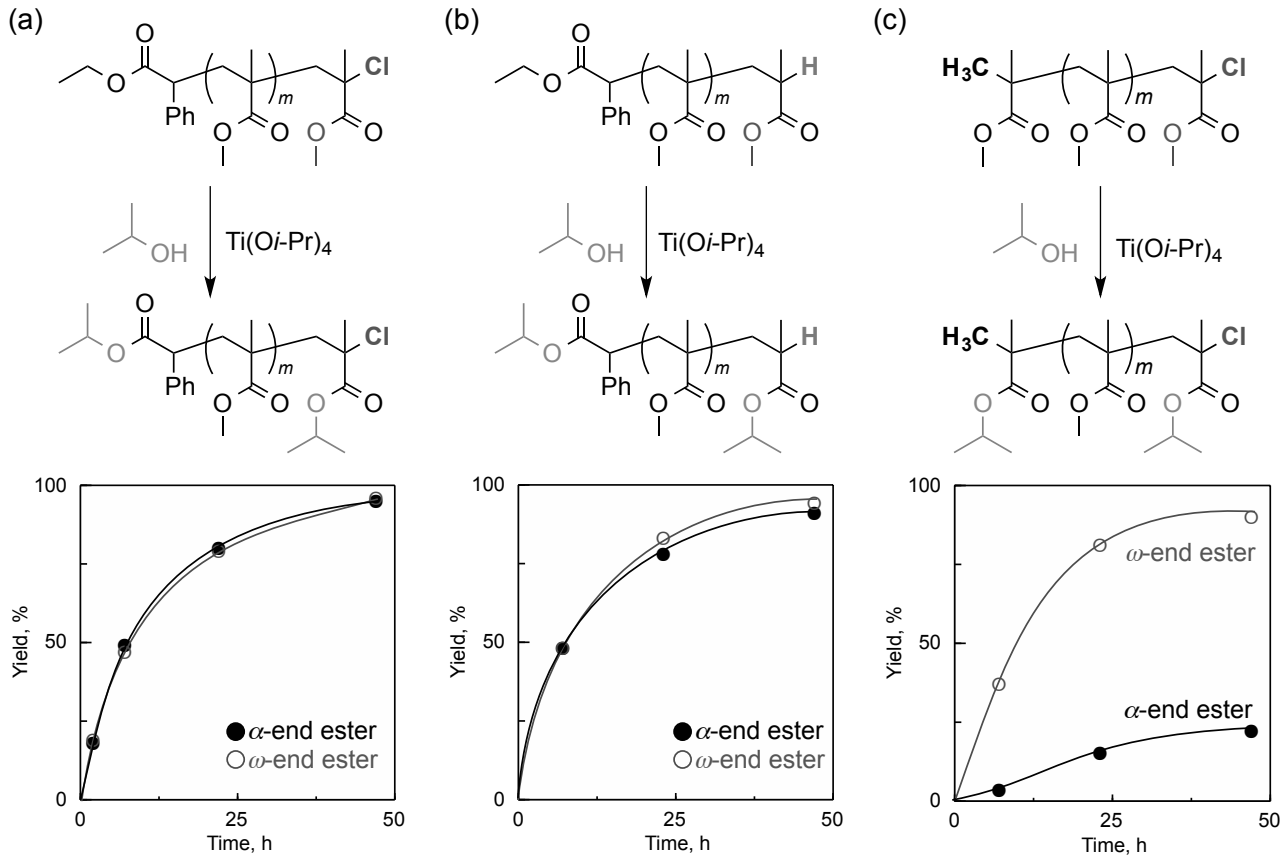

Figure 3. Effects of the terminal structures of PMMAs [(a) Et-PMMA-Cl, (b) Et-PMMA-H, and (c) PMMA-Cl] on the terminal-selective transesterification: [PMMA]/[Ti(O*i*-Pr)$_4$] = 30/80 mM in toluene/isopropanol (9/1, v/v) at 80 ^{o}C. The yield for transesterification was determined by ^{1}H NMR.

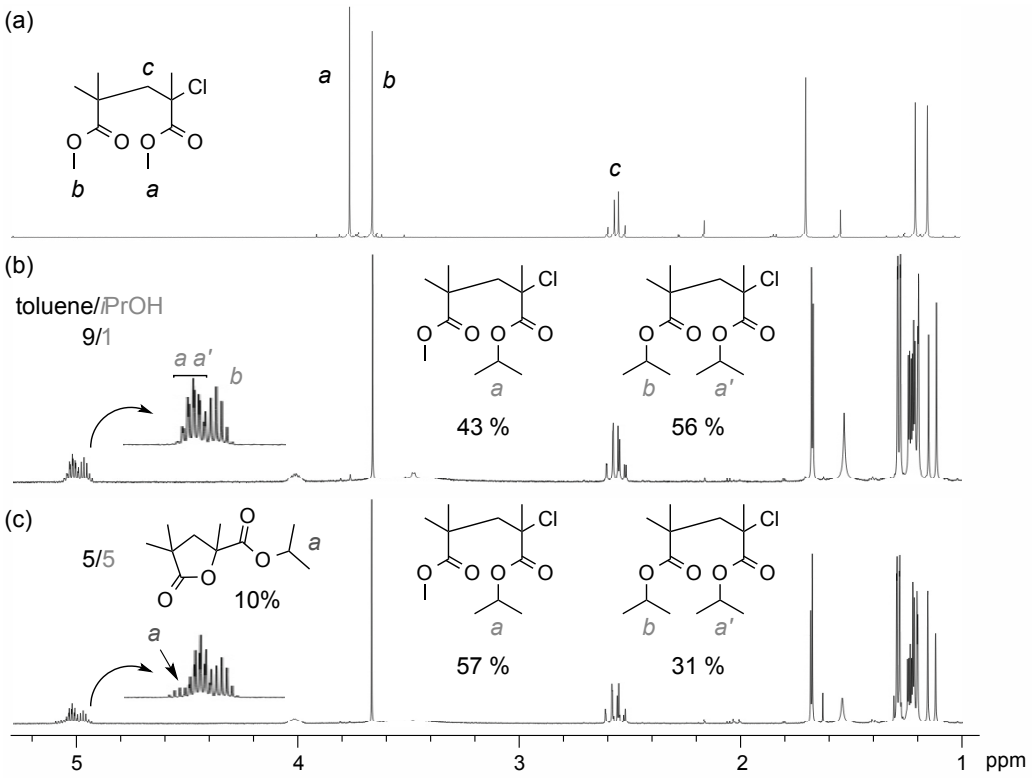

Figure 4. Ti(O*i*-Pr)$_4$-mediated transesterification of (a) H-(MMA)$_2$-Cl into H-(*i*PrMA)$_2$-Cl or H-MMA-*i*PrMA-Cl with isopropanol: [H-(MMA)$_2$-Cl]$_0$/[Ti(O*i*-Pr)$_4$]$_0$ = 30/80 mM in toluene/isopropanol (b: 9/1 or c: 5/5, v/v) at 80 ^{o}C. Product yield with toluene/isopropanol (9/1, v/v) at 48 h: H-MMA-*i*PrMA-Cl 43%, H-(*i*PrMA)$_2$-Cl 56%. Product yield with toluene/isopropanol (5/5, v/v) at 48 h: H-MMA-*i*PrMA-Cl 57%, H-(*i*PrMA)$_2$-Cl 31%, a byproduct with five-membered ring 10%.

3. Variously Functionalized Telechelic Polymer

The author further applied various alcohols (ROH: ethanol, 1-butanol, 1-dodecanol, benzyl alcohol, 2-naphthalene methanol, 4,4,5,5,5-pentafluoro-1-pentanol, 2-methoxy ethanol, allyl alcohol, 8-dimethylamino-1-octanol, 1,12-dodecanediol) to the terminal-selective transesterification of Et-PMMA-Cl to synthesize corresponding chlorine-capped telechelic polymers (Table 1, entries 7-16, Figures 5, 6). Here, prior to the transesterification, Ti(O*i*-Pr)$_4$ was first mixed with the alcohols (ROH) at 80 ^{o}C for 1 h and the mixture was evaporated to in-situ form corresponding Ti(OR)$_n$. The Ti(OR)$_n$ (80 – 160 mM) was utilized for the transesterification of Et-PMMA-Cl in ROH/toluene (1/9, v/v) at 80 ^{o}C.

Confirmed by ^{1}H NMR and MALDI-TOF-MS, ethanol, 1-butanol, 1-dodecanol, benzyl alcohol, 2-naphthalene methanol, 4,4,5,5,5-pentafluoro-1-pentanol, 2-methoxy ethanol, and allyl alcohol efficiently gave the corresponding chlorine-capped telechelic PMMAs (R-PMMA-RMA-Cl) in high yield (>90%). 8-Dimethylamino-1-octanol and 1,12-dodecanediol

also induced terminal-selective transesterification, though the yield of the telechelic PMMAs was lower than that of the others probably owing to the interaction of the amino group to Ti catalyst and low solubility of alcohol (1,12-dodecanediol). The preferential *ω*-end transesterification with these alcohols would be due to the activation by the terminal chlorine. The titanium-catalyzed transesterification of Et-PMMA-Cl is thus quite efficient and versatile to produce chlorine-capped telechelic polymers.

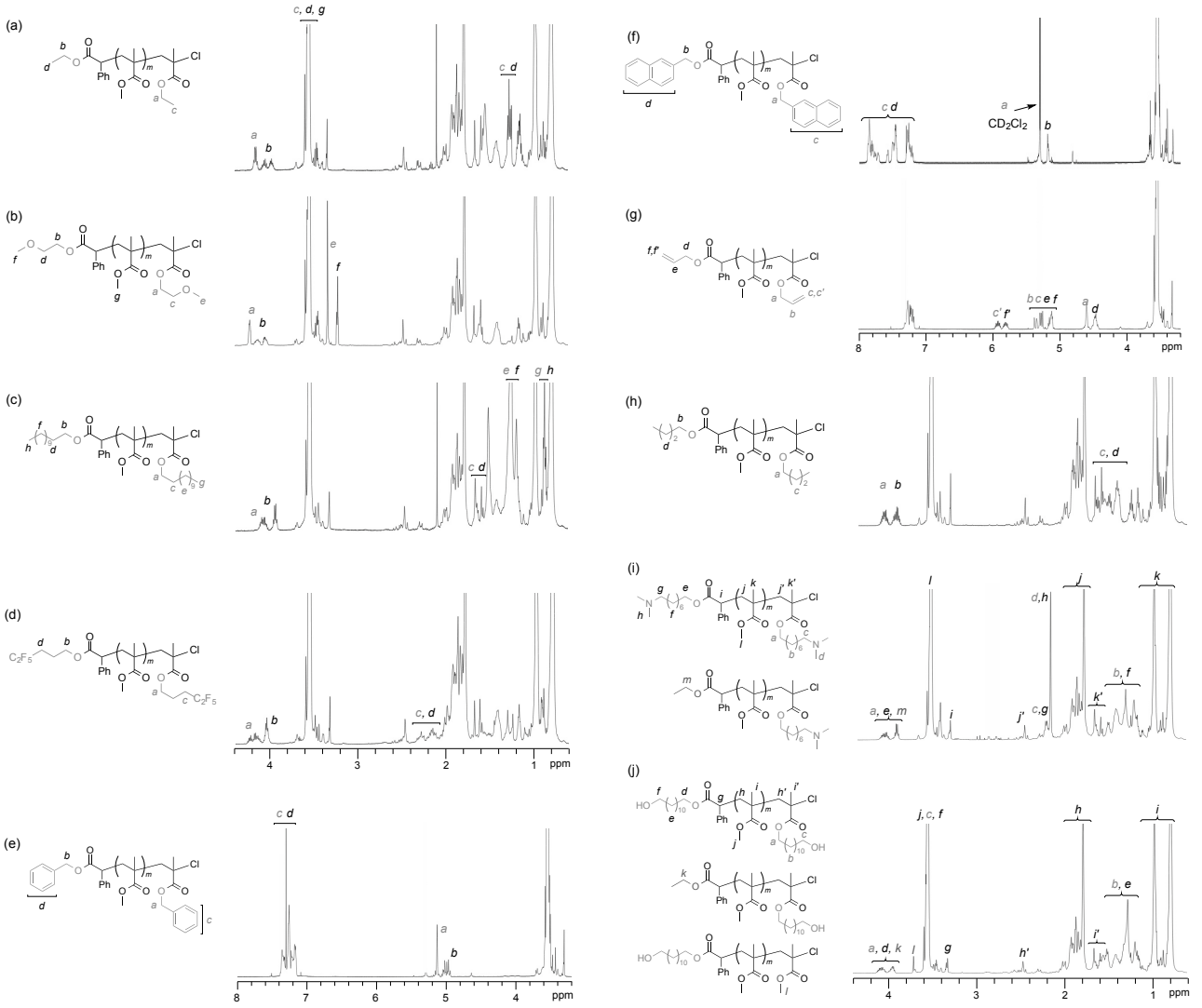

Figure 5. ^{1}H NMR spectra of chlorine-capped telechelic polymers (R-PMMA-RMA-Cl) obtained from the transesterification of Et-PMMA-Cl with alcohols [ROH: (a) EtOH; (b) methoxy ethanol; (c) 1-dodecanol; (d) 4,4,5,5,5-pentafluoro-1-pentanol; (e) benzyl alcohol; (f) 2-naphthalene methanol; (g) allyl alcohol; (h) butanol; (i) 8-dimethylamino-1-octanol; (j) 1,12-dodecanediol]: [Et-PMMA-Cl]/[$Ti(OR)_4$] = 30/80 or 160 (d, f, i, j) mM in toluene/ROH (9/1, v/v) at 80 ^{o}C.

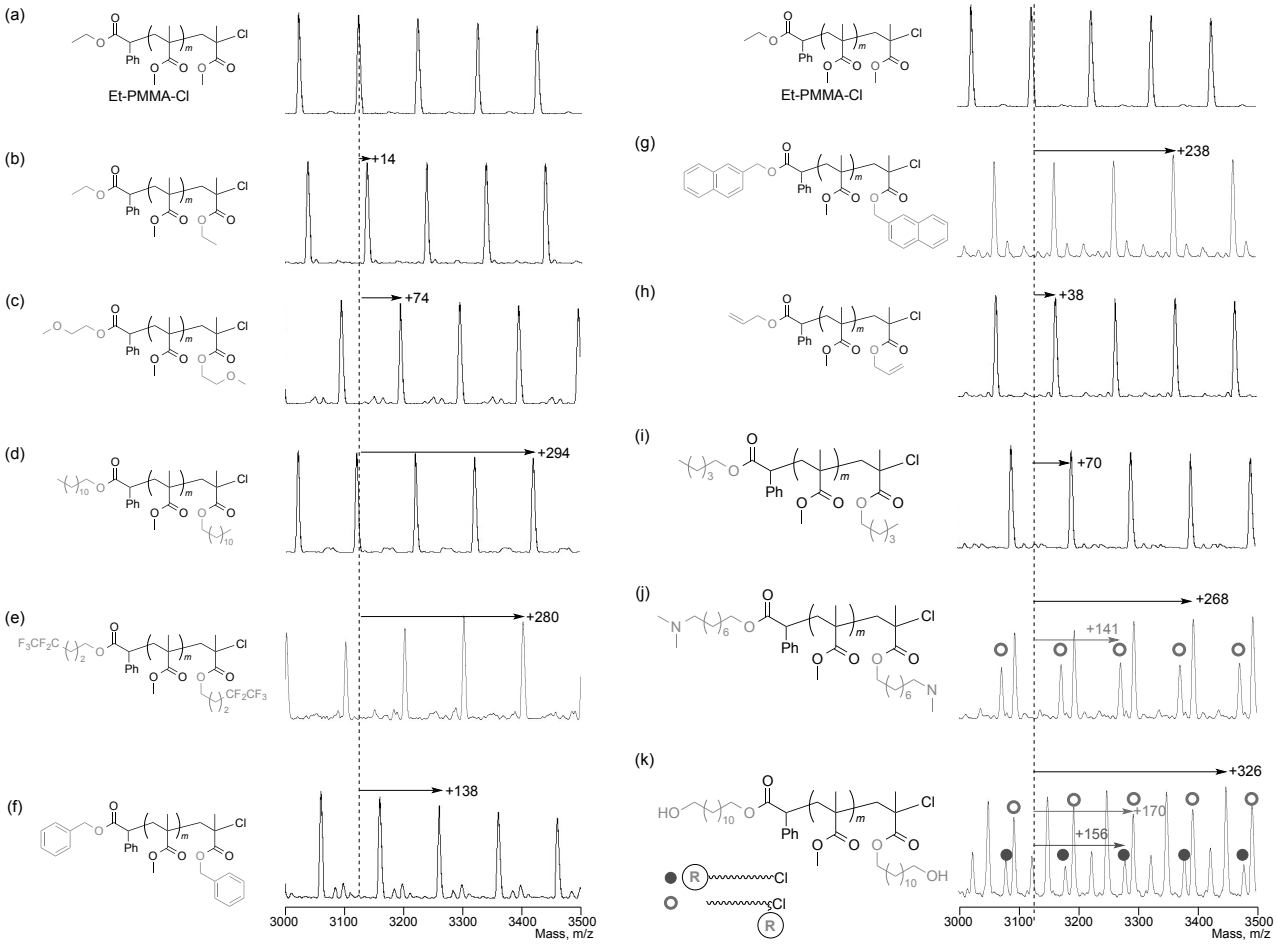

Figure 6. MALDI-TOF-MS spectra of chlorine-capped telechelic polymers (R-PMMA-RMA-Cl) obtained from the transesterification of Et-PMMA-Cl (a) with alcohols [ROH: (b) EtOH; (c) methoxy ethanol; (d) 1-dodecanol; (e) 4,4,5,5,5-pentafluoro-1-pentanol; (f) benzyl alcohol; (g) 2-naphthalene methanol; (h) allyl alcohol; (i) butanol; (j) 8-dimethylamino-1-octanol; (k) 1,12-dodecanediol]: [Et-PMMA-Cl]/[$Ti(OR)_4$] = 30/80 or 160 (d, f) mM in toluene/ROH (9/1, v/v) at 80 ^oC.

3. Pinpoint Functionalization with Iterative LRP and Transesterification

Pinpoint-functionalized polymers can be obtained with chlorine-capped telechelic PMMAs. Typically, Et-PMMA-EMA-Cl (M_n = 2700, M_w/M_n = 1.14), obtained from the transesterification of Et-PMMA-Cl with ethanol, was employed as a macroinitiator for $Ru(Ind)Cl(PPh_3)_2$/ *n*-Bu_3N-catalyzed living radical polymerization of MMA to give well-controlled Et-PMMA-EMA-PMMA-Cl (M_n = 5800, M_w/M_n = 1.08, Figure 5a, 6b). The ^1H NMR spectrum of the product clearly showed the ω-end methyl ester protons (c') adjacent to chlorine atom (Figure 7b). The subsequent titanium-mediated transesterification of the product with allyl alcohol successfully yielded the pinpoint-functionalized telechelic polymers carrying an olefin at the α-end,

a single ethyl pendant at the middle point, and a chlorine-capped allyl methacrylate unit (olefin) at the ω-end (olefin-PMMA-EMA-PMMA-Allyl MA-Cl: M_n = 5900, M_w/M_n = 1.09, Figures 7).

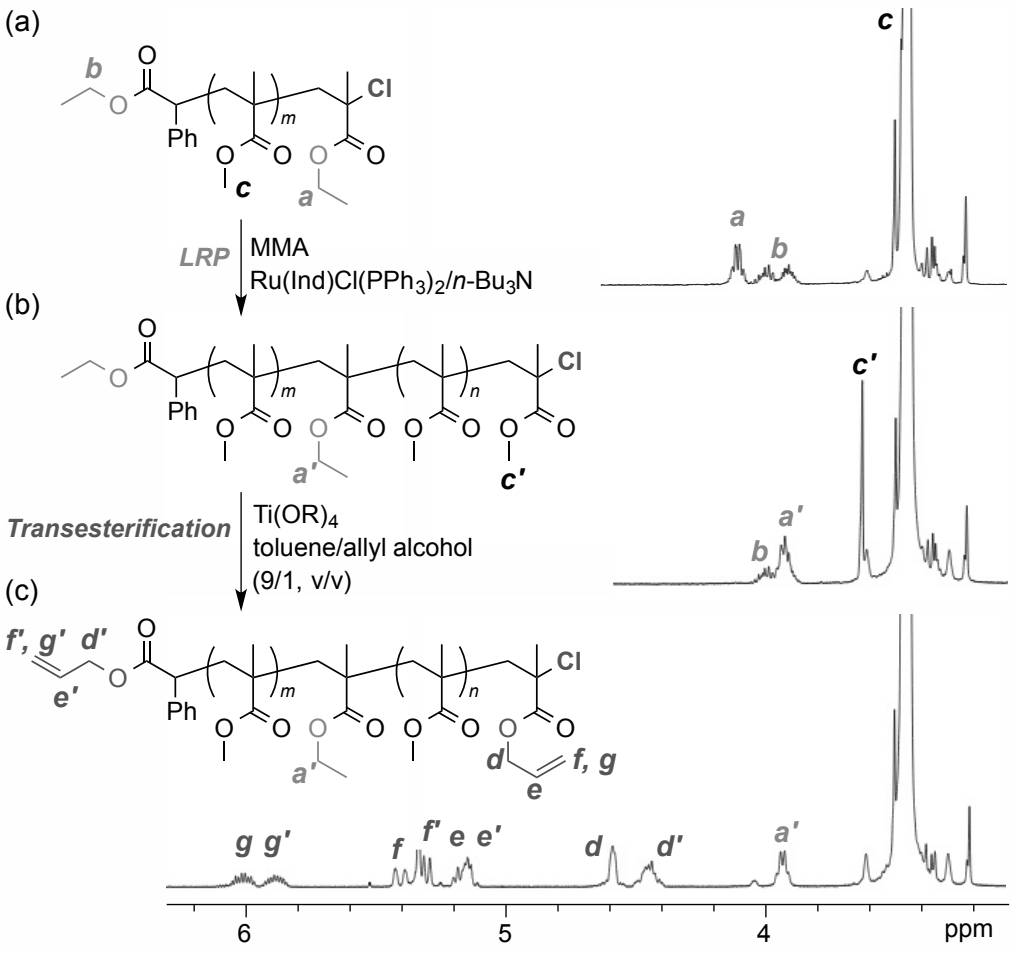

Figure 7. A pinpoint-functionalized telechelic polymer (olefin-PMMA-EMA-PMMA-Allyl MA-Cl) via the iterative process of living radical polymerization (LRP) and terminal-selective transesterification. LRP: [MMA]/[Et-PMMA-EMA-Cl]/[Ru(Ind)Cl(PPh_3)$_2$]/[*n*-Bu_3N] = 2000/10/1/10 mM in toluene at 80 ^oC. Transesterification: [Et-PMMA-EMA-PMMA-Cl]/[Ti(O*i*-Pr)$_4$] = 10/80 mM in toluene/allyl alcohol (9/1, v/v) at 80 ^oC.

In addition, various pinpoint-functionalized block copolymers were also efficiently obtained from polymerization of dodecyl methacrylate (DMA), poly(ethylene glycol) methyl ether methacrylate (PEGMA), and a perfluoroalkyl methacrylate (13FOMA) with a chlorine-capped telechelic PMMA (*i*-Pr-PMMA-*i*-PrMA-Cl, Figure 8). Such block copolymers would be quite useful for the selective interface functionalization of the micro phase-separated materials and core-shell nanocapsules.

This iterative strategy developed herein is applicable to the design of many kinds of pinpoint-functionalized and periodic sequence-regulated polymers with the following advantages: 1) versatile and easy design of functional units with diverse alcohols; 2) precision, on-demand, and site-specific functionalization of polymer chains via living radical polymerization.

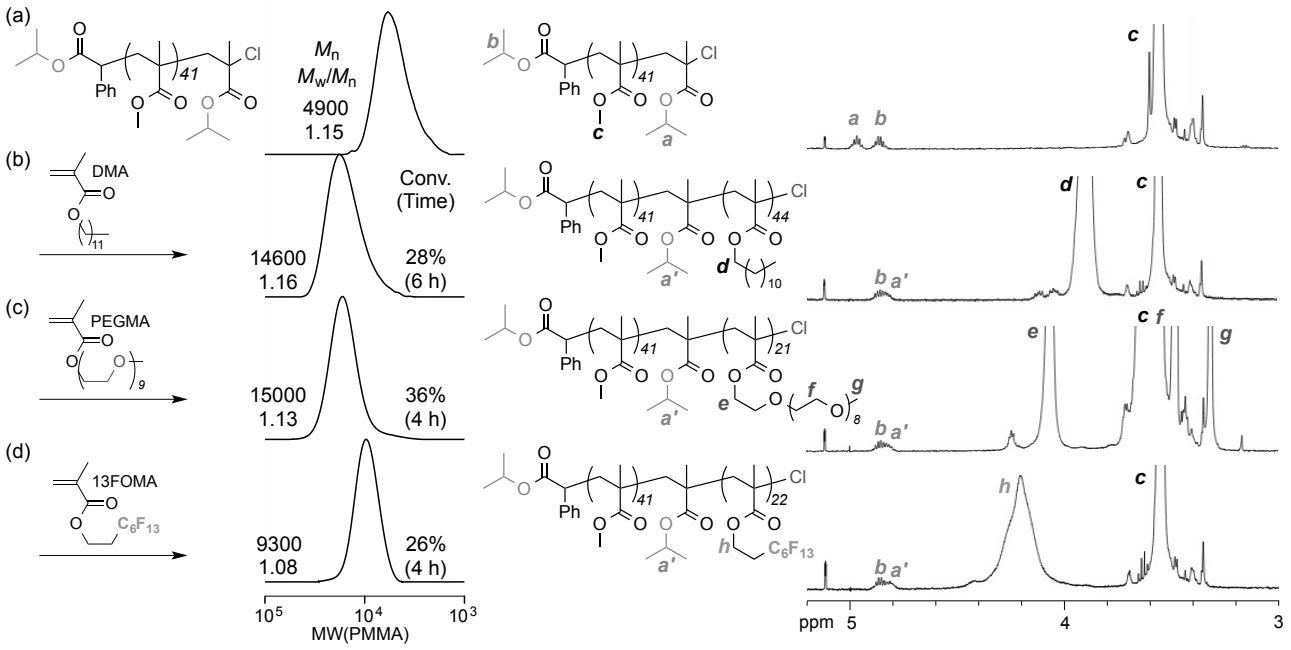

Figure 8. Synthesis of pinpoint-functionalized block copolymers via living radical polymerization of (b) dodecyl methacrylate (DMA), (c) poly(ethylene glycol) methyl ether methacrylate (PEGMA), and (d) a perfluoroalkyl methacrylate (13FOMA) with (a) *i*Pr-PMMA-*i*PrMA-Cl: [RMA]/[*i*Pr-PMMA-*i*PrMA-Cl]/[Ru(Ind)Cl(PPh_2)$_3$]/[*n*-Bu_3N] = 1000 or 500 (PEGMA)/10/1/10 mM in toluene at 80 °C. ^{1}H NMR: in CD_2Cl_2 at 25 °C.

Conclusion

In this chapter, the author developed a modular approach to synthesize chlorine-capped telechelic and pinpoint-functionalized polymers via the Ti-mediated terminal-selective transesterification of chlorine-capped PMMAs in conjunction with ruthenium-catalyzed living radical polymerization. With common and diverse alcohols, various functional groups can be efficiently and easily introduced into the desired position of poly(methacrylate)s. Importantly, chlorine-capped telechelic polymers worked as a macroinitiator in living radical polymerization, opening the new avenue to pinpoint-functionalized polymers. Therefore, the terminal-selective transesterification developed herein would be one of the most innovative strategies to design functional polymeric materials with precision primary structure toward intriguing functions.

References

(1) (a) Lutz, J.-F.; Ouchi, M.; Liu, D. R.; Sawamoto, M. *Science* **2013,** *341,* 628. (b) Ouchi, M.; Badi, N.; Lutz, J.-F.; Sawamoto, M. *Nat. Chem.* **2011,** *3*, 917−924. (c) Lutz, J.-F. *Acc. Chem. Res.* **2013**, *46*, 2696-2705.

(2) (a) Ouchi, M.; Terashima, T.; Sawamoto, M. *Chem. Rev.* **2009,** *109*, 4963−5050. (b) Terashima, T. *Polym. J.* **2014**, *46*, 664-673.

(3) (a) Matyjaszewski, K.; Tsarevsky, N. V. *Nat. Chem.* **2009,** *1*, 276−288. (b) Matyjaszewski, K.; Tsarevsky, N. V. *J. Am. Chem. Soc.* **2014**, *136*, 6513-6533.

(4) Rosen, B. M.; Percec, V. *Chem. Rev.* **2009,** *109*, 5069−5119.

(5) (a) Al Ouahabi, A.; Charles, L.; Lutz, J.-F. *J. Am. Chem. Soc.* **2015,** *137*, 5629−5635. (b) Soejima, T.; Satoh, K.; Kamigaito, M. *J. Am. Chem. Soc.* **2016,** *138*, 944−954.

(6) Geng, J.; Lindqvist, J.; Mantovani, G.; Haddleton, D. M. *Angew. Chem., Int. Ed.* **2008,** *47*, 4180−4183.

(7) Terashima, T.; Ouchi, M.; Ando, T.; Sawamoto, M. *J. Am. Chem. Soc.* **2006,** *128,* 11014–11015.

(8) Van As, B. A. C.; Van Buijtenen, J.; Heise, A.; Broxterman, Q. B.; Verzijl, G. K. M.; Palmans, A. R. A.; Meijer, E. W. *J. Am. Chem. Soc.* **2005,** *127*, 9964−9965.

(9) Doran, S.; Yilmaz, G.; Yagci, Y. *Macromolecules* **2015,** *48*, 7446−7452.

(10) (a) Nakatani, K.; Ogura, Y.; Koda, Y.; Terashima, T.; Sawamoto, M. *J. Am. Chem. Soc.* **2012,** *134*, 4373−4383. (b) Ogura, Y.; Terashima, T.; Sawamoto, M. *ACS Macro Lett.* **2013,** *2*, 985−989.

(11) (a) Otera, J. *Chem. Rev.* **1993**, *93*, 1449-1470. (b) Seebach, D.; Hungerbühler, E.; Naef, R.; Schnurrenberger, P.; Weidmann, B.; Züger, M. *Synthesis* **1982**, 138-141.

(12) (a) Theato, P. J. *Polym. Sci., Part A: Polym. Chem.* **2008,** *46*, 6677–6687. (b) Roth, P. J.; Jochum, F. D.; Forst, F. R.; Zentel, R.; Theato, P. *Macromolecules* **2010**, *43*, 4638-4645.

(13) Malkoch, M.; Thibault, R. J.; Drockenmuller, E.; Messerschmidt, M.; Voit, B.; Russell, T. P.; Hawker, C. J. *J. Am. Chem. Soc.* **2005**, *127*, 14942-14949.

(14) Tokuchi, K.; Ando, T.; Kamigaito, M.; Sawamoto, M. *J. Polym. Sci., Part A: Polym. Chem.* **2000,** *38*, 4735-4748.

(15) Nakatani, K.; Terashima, T.; Ouchi, M.; Sawamoto, M. *Macromolecules* **2010,** *43*, 8910–8916.

(16) Snijder, A.; Klumperman, B.; Van der Linde, R. *J. Polym. Sci., Part A: Polym. Chem.* **2002,** *40*, 2350−2359.

(17) Bon, S. A. F.; Steward, A. G.; Haddleton, D. M. *J. Polym. Sci., Part A: Polym. Chem.* **2000,** *38*, 2678−2686.

(18) (a) Kimura, T.; Hamashima, M. *Polym. J.* **1986,** *18*, 21−30. (b) Kimura, T.; Tasaka, H.; Hamashima, M. *Polym. J.* **1987,** *19*, 305−314.

(19) Ando, T.; Kamigaito, M.; Sawamoto, M. *Macromolecules* **1998,** 31, 6708-6711.

Chapter 7

Telechelic Polymers from Bromine-Capped Poly(methyl methacrylate)s via Terminal-Selective Transesterification and Cyclization

Abstract

Halogen-free telechelic poly(methyl methacrylate)s (R-PMMA-RMAs) bearing a five-membered lactone at ω-end were synthesized by concurrent tandem terminal-selective transesterification and cyclization of bromine-capped PMMA-Br with Ti(O*i*-Pr)$_4$ and alcohols. The cyclization process was investigated by model reactions using a bromine-capped methacrylate dimer [H-(MMA)$_2$-Br]. The model experiments revealed that alcohols are crucial to promote the cyclization. By treating Et-PMMA-Br with Ti(O*i*-Pr)$_4$ and 2-propanol at 80 ^{o}C, both α-end ethyl ester and ω-end methyl ester were selectively transesterified into isopropyl esters, while the ω-end bromine was concurrently eliminated via the cyclization with the preterminal ester. As a result, *i*Pr-PMMA-*i*PrMA-lactone was selectively obtained, confirmed by proton nuclear magnetic resonance (^{1}H NMR) and matrix-assisted laser desorption (MALDI-TOF-MS). Furthermore, sequential tandem catalysis of iron-catalyzed LRP of MMA, followed by the terminal-selective cyclization of the resulting PMMA-Br with ethanol, directly afford a ω-end-cyclized PMMA.

Introduction

Terminal structures of polymers are one of the most significant factors on primary structure to create desired properties and functions.[1-4] There are many examples of functional polymeric materials whose physical properties are improved by modifying the terminal groups with end-capping agents.[5-7] In a history of synthetic polymer chemistry, emergence of various living polymerization systems typically via anionic, cationic, and radical mechanisms has allowed to control the terminal structures of polymers precisely.[8-13] Among many kinds of living polymerizations, metal-catalyzed living radical polymerization (Mt-LRP) including atom transfer radical polymerization (ATRP) is superior in terms of versatile availability of monomers and initiators owing to high tolerance to functional groups.[14,15]

In this system, initiator fragments directly turn to be the α-end functional group of resulting polymers: *i.e.*, desired functional groups can be attached to the terminal by using designed initiators. However, initiators employed for Mt-LRP consist of a carbon-halogen (C-X) bond (X: Cl. Br, and I), which is reversibly activated by metal catalysts (Ru, Cu, Fe) to generate carbon radical species for propagation. Though Mt-LRP gives polymers bearing a halogen-terminal at ω-end, transformation of the halogen into stable substituents is often required in because the halogen may cause unexpected side reactions in final products by chemical or external stimuli. Thus, hydrogenation of the ω-end halogen was established as a method to prepare stable-terminal polymers.[16] In addition, the transformation of the terminal halogen into functional groups is also quite important to create end-functionalized polymers.[17] But most of them, developed so far, often require expensive metal catalysts or multiple step procedures. Thus, development of more convenient and versatile systems to modify the polymer terminals is demanded.

In contrast, Kimura et al. reported intramolecular cyclization of bromine-capped methyl methacrylate (MMA) dimer and trimer [H-(MMA)$_n$-Br: n = 2~3].[18] This reaction not only eliminates bromine but also forms stable five-membered ring structure like lactone. Cyclization is induced by the reaction between bromide terminal and methyl ester next to bromine-capped MMA [-MMA-MMA-Br]. This cyclization is mainly utilized to synthesize monomers containing lactone rings with unique properties.[19,20] The author also reported that such cyclization took place for chlorine-capped poly(methyl methacrylate)s (PMMA-Cls) in the presence of alcohols at 80 ^{o}C, as shown in Chapter 6.[21] In this case, cyclization efficiency is limited up to about 33% that means that chloride terminal (-Cl) is less reactive than bromine terminal (-Br). These results encouraged the author to develop terminal cyclization of a bromine-capped poly(methyl methacrylate) (PMMA-Br) as an efficient elimination technique of the terminal halogen. This procedure has several advantages compared with conventional methods: 1) metal catalyst is not necessary. 2) One step reaction proceeds without complicated operation, bothersome recovery and purification.

3) Introduction of lactone structure is effective to improve thermal stability and gives hydrophilic group via hydrolysis.[22,23] In addition to these profits, a methyl ester is further attached to the *ω*-end lactone ring of polymers. As indicated in previous Chapter 6, terminal esters of poly(MMA)s can be selectively transesterified with Ti(O*i*-Pr)$_4$ and alcohols.[21]

Given these backgrounds, in this chapter, the author developed the concurrent tandem terminal-selective transesterification and *ω*-end cyclization by treating PMMA-Br with Ti(O*i*-Pr)$_4$ and alcohols (Scheme 1). This is a new tandem catalysis to efficiently synthesize "halogen-free" telechelic PMMAs with a *ω*-end lactone ring. For this, model reactions were first investigated with bromine-capped methyl methacrylate dimer [H-(MMA)$_2$-Br]. Then, concurrent tandem catalysis of terminal-selective transesterification and *ω*-end cyclization of PMMA-Br was examined with Ti(O*i*-Pr)$_4$ and 2-propanol; the products were analyzed by SEC, ^{1}H NMR, and MALDI-TOF-MS. End-cyclized PMMAs were further obtained from sequential tandem catalysis of iron-catalyzed living radical polymerization (LRP) of MMA, followed by *ω*-end cyclization via the direct addition of ethanol.

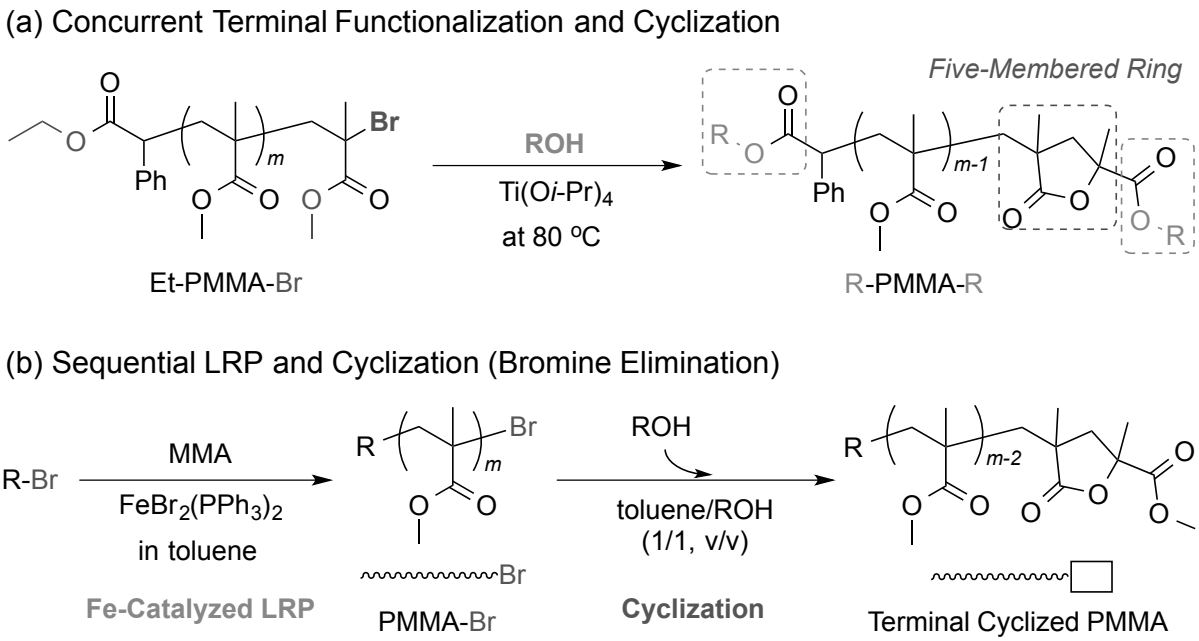

Scheme 1. (a) Concurrent and terminal-selective transesterification and intramolecular cyclization of Et-PMMA-Br with alcohols and a Ti catalyst. (b) Sequential tandem catalysis of Fe-catalyzed LRP of MMA and terminal-selective cyclization for end-cyclized PMMAs.

Experimental Section

Materials. Methyl methacrylate (MMA: TCI; purity >99.8%), butyl methacrylate (BMA: TCI; purity >99%), methyl acrylate (MA: TCI; purity >99%) and tetralin (1,2,3,4-tetrahydronaphthalene:

Kishida Chemical; purity >98%; an internal standard for ^{1}H NMR analysis) were dried overnight with calcium chloride and distilled from calcium hydride under reduced pressure before use. Ti(O*i*-Pr)$_4$ (Aldrich, purity >97%) and Ethyl 2-bromo-2-phenylacetate (EBPA: Aldrich; purity >97%) were degassed by triple vacuum-argon purge cycles before use. Ethyl 2-chloro-2-phenylacetate (ECPA: Aldrich; purity >97%) was distilled under reduced pressure before use. The H(MMA)$_2$Br [H(CH$_2$CMeCO$_2$Me)$_2$Br; a MMA dimer bromide] was prepared according to the literature. Ethanol (Wako, super dehydrated) and 2-Propanol (Wako, super dehydrated) were used as received. Ru(Ind)Cl(PPh$_3$)$_2$ (Aldrich), FeBr$_2$ (Aldrich) and triphenylphosphine (PPh$_3$, Aldrich) were used as received and handled in a glove box under moisture- and oxygen-free argon (H_2O <1 ppm; O_2 <1 ppm). Toluene was purified by pashing it through a purification column (Glass Contour Solvent Systems: SG Water USA). Molecular sieves 4A (Wako) were baked with heat gun under reduced pressure before use.

Characterization. The molecular weight distribution (MWD) curves, M_n and M_w/M_n ratio of the polymers were measured by SEC at 40 °C in THF as an eluent on three polystyrene-gel columns (Shodex LF-404: exclusion limit = 2×10^6 g/mol; particle size = 6 μm; pore size = 3000 Å; 0.46 cm i.d. × 25 cm; flow rate, 0.3 mL/min) connected to a DU-H2000 pump, a RI-74S refractive index detector, and a UV-41 ultraviolet detector (all from Shodex; Shodex GPC-104). The columns were calibrated against 13 standard poly(MMA) samples (Polymer Laboratories; M_n = 620−1200000; M_w/M_n = 1.06−1.22). To remove unreacted monomers and catalyst, polymer samples were purified by preparative SEC before characterization [column: Shodex K-5002; particle size = 15 mm; 5.0 cm i.d. × 30 cm; exclusion limit = 5×10^3 g/mol; flow rate = 10 mL/min]. ^{1}H NMR spectra were recorded in $CDCl_3$ or CD_2Cl_2 at 25 ^{o}C on a JEOL JNM-ECA500 spectrometer operating at 500.16 MHz. MALDI-TOF-MS analysis was performed on a Shimadzu AXIMA-CFR instrument equipped with 1.2 m linear flight tubes and a 337 nm nitrogen laser (matrix: dithranol; cationizing agent: sodium trifluoroacetate).

Model reaction of H-(MMA)$_2$-Br with Ti(O*i*-Pr)$_4$ and 2-Propanol. A typical procedure for reaction of H-(MMA)$_2$-Br (20 mM) with Ti(O*i*-Pr)$_4$ (40 mM) and 2-Propanol was given: Into a 30 mL glass tube, toluene (0.75 mL), 2-propanol (13 mmol, 1.0 mL), a 500 mM toluene solution of Ti(O*i*-Pr)$_4$ (0.16 mL, Ti(O*i*-Pr)$_4$ = 0.08 mmol), and a 446 mM toluene solution of H-(MMA)$_2$-Br (0.09 mL, H-(MMA)$_2$-Br = 0.04 mmol) were added sequentially in that order at 25 ^{o}C under argon (the total volume: 2.0 mL). The glass tube was then placed in an oil bath kept at 80 ^{o}C for 16h. Then, the glass tube was cooled to –78 °C to terminate the reaction. The reaction solution was evaporated to remove toluene and 2-propanol. Residual sample was analyzed by ^{1}H NMR

measurement of the solution in $CDCl_3$ at 25 °C. ^{1}H NMR spectrum of product: Figure 1 in results and discussion.

Concurrent transesterification and cyclization of Et-PMMA-Br. Into a glass tube, Et-PMMA-Br (M_n = 2100, M_w/M_n = 1.11, 0.02 mmol, 42.0 mg), toluene (0.42 mL), a 500 mM toluene solution of Ti(O*i*-Pr)$_4$ (0.08 mL, Ti(O*i*-Pr)$_4$ = 0.04 mmol) and 2-propanol (6.5 mmol, 0.5 mL) were added at room temperature under dry argon (total volume: 1.0 mL). The glass tube was placed in an oil bath kept at 80 °C for 24 h and cooled to –78 °C to terminate the reaction. The quenched reaction solutions were evaporated to dryness to give the crude product. The product was fractionated by preparative SEC for ^{1}H NMR and MALDI-TOF-MS analysis. SEC (THF, PMMA std.): M_n = 2400 g/mol; M_w/M_n = 1.05. ^{1}H NMR and MALDI-TOF-MS spectra of product: Figure 3 in results and discussion.

Polymerization. The synthesis of all polymers was carried out by syringe technique under argon in baked glass tubes equipped with a three-way stopcock.

Et-PMMA-Br for precursor. Into the 30 mL glass tube, Ru(Ind)Cl(PPh$_3$)$_2$ (0.0025 mmol, 1.94 mg) was charged, and then toluene (3.43 mL), tetralin (0.10 mL), MMA (10 mmol, 1.06 mL), a 400 mM toluene solution of *n*-Bu$_3$N (0.06 mL, *n*-Bu$_3$N = 0.024 mmol), and a 287 mM toluene solution of EBPA (0.35 mL, EBPA = 0.1 mmol) were added sequentially at 25 °C under argon. The total volume of the reaction mixture was thus 5.0 mL. The glass tube was placed in an oil bath kept at 80 °C for 2.5 h and then cooled to –78 °C to terminate the reaction. The monomer conversion was determined as 36% by ^{1}H NMR measurements of the terminated reaction solution in $CDCl_3$ at r.t. with tetralin as an internal standard. The quenched reaction solutions were evaporated to dryness to give the crude Et-PMMA-Cl. The product was fractionated by preparative SEC. SEC (THF, PMMA std.): M_n = 2100 g/mol; M_w/M_n = 1.11. ^{1}H NMR [500 MHz, CD_2Cl_2, 25 °C, δ = 5.33 ($CHDCl_2$)]: M_n (NMR, α) = 2100 g/mol; M_n (NMR, ω) = 2200 g/mol. δ 7.3–7.1 (aromatic), 4.1–3.9 (-COOC$\underline{H}_2$CH$_3$), 3.7–3.5 (-OC$\underline{H}_3$), 2.1—1.7 (-C$\underline{H}_2$C(CH$_3$)-), 1.2−0.7 (-CH$_2$C(C$\underline{H}_3$)-).

Polymerization with mixture of PMMA-Cl (P1) and terminal cyclized PMMA (P2). A typical procedure for polymerization of MMA with mixed P1 and P2 (P1/P2 = 67/33) as a macroinitiator was given: Into the 30 mL glass tube, Ru(Ind)Cl(PPh$_3$)$_2$ (0.002 mmol, 1.55 mg) and P1 and P2 mixture (obtained in chapter 6: M_n = 4200, 0.02 mmol, 84 mg) was charged, and toluene (1.82 mL), tetralin (0.02 mL), MMA (1 mmol, 0.11 mL) and a toluene solution of *n*-Bu$_3$N (400 mM, 0.05 mL, *n*-Bu$_3$N = 0.02 mmol) were added sequentially in that order at 25 °C under argon. The

total volume of the reaction mixture was thus 2 mL. The glass tube was placed in an oil bath kept at 80 °C for 23 h and then cooled to –78 °C to terminate the reaction. The monomer conversion (44%) was determined by ^{1}H NMR measurements of the terminated reaction solution in $CDCl_3$ at r.t. with tetralin as an internal standard. The quenched reaction solutions were evaporated to dryness to give the crude product. The product was fractionated by preparative SEC. SEC (THF, PMMA std.): M_n = 6500 g/mol; M_w/M_n = 1.18. ^{1}H NMR spectrum of product: Figure 4f in results and discussion.

Sequential Fe catalyzed polymerization and cyclization. Into the 30 mL glass tube, $FeBr_2$ (0.0075 mmol, 1.60 mg) and PPh_3 (0.015 mmol, 4.0 mg) were charged, and toluene (2.53 mL) was added at 25 °C under argon. And then, the glass tube was placed in an oil bath kept at 80 °C for 13 h. After cooling the glass tube to –78 °C, tetralin (0.04 mL), MMA (3 mmol, 0.32 mL) and a toluene solution of EBPA (287 mM, 0.11 mL, EBPA = 0.03 mmol) were added sequentially in that order at 25 °C under argon. The total volume of the reaction mixture was thus 3 mL. The glass tube was placed in an oil bath kept at 80 °C for 9 h. The monomer conversion (51%) was determined by ^{1}H NMR measurements of the terminated reaction solution in $CDCl_3$ at r.t. with tetralin as an internal standard. Then, ethanol (3 mL) was added directly to polymerization solution at 80 °C under argon (total volume; 6.0 mL). The glass tube was kept in an oil bath at 80 °C for 24 h and then cooled to –78 °C to terminate the reaction. The quenched reaction solutions were evaporated to dryness to give the crude product. The product was fractionated by preparative SEC. SEC (THF, PMMA std.): M_n = 5700 g/mol; M_w/M_n = 1.12. ^{1}H NMR spectrum of product: Figure 6a in results and discussion.

Results and Discussion

1. Concurrent Transesterification and Cyclization of H-(MMA)$_2$-Br

To develop concurrent terminal-selective transesterification/cyclization systems of bromine-capped poly(methyl methacrylate) [(MMA)$_n$-Br], the transesterification and cyclization of methyl methacrylate dimer [(MMA)$_2$-Br] were first investigated with 2-propanol (*i*PrOH) and Ti(O*i*-Pr)$_4$ at 80 °C. The methacrylate dimer is selected as a reactant because the chemical structure can be analyzed more facilely and precisely by ^{1}H NMR. The reaction was conducted for 46 h, and the product was obtained by evaporating volatile *i*PrOH and toluene (toluene/*i*PrOH = 1/1, v/v). Confirmed by ^{1}H NMR spectroscopy (Figure 1), the peaks (a, b) assigned to two methyl esters of (MMA)$_2$-Br perfectly disappeared, while new peaks (g, h) appeared. A peak **g** is derived from an isopropyl ester and a peak **h** originates from five-membered lactone structure. Product

yield was over 99 %. This result indicates that Ti-mediated transesterification and cyclization proceeded quantitatively and concurrently in the model reaction.

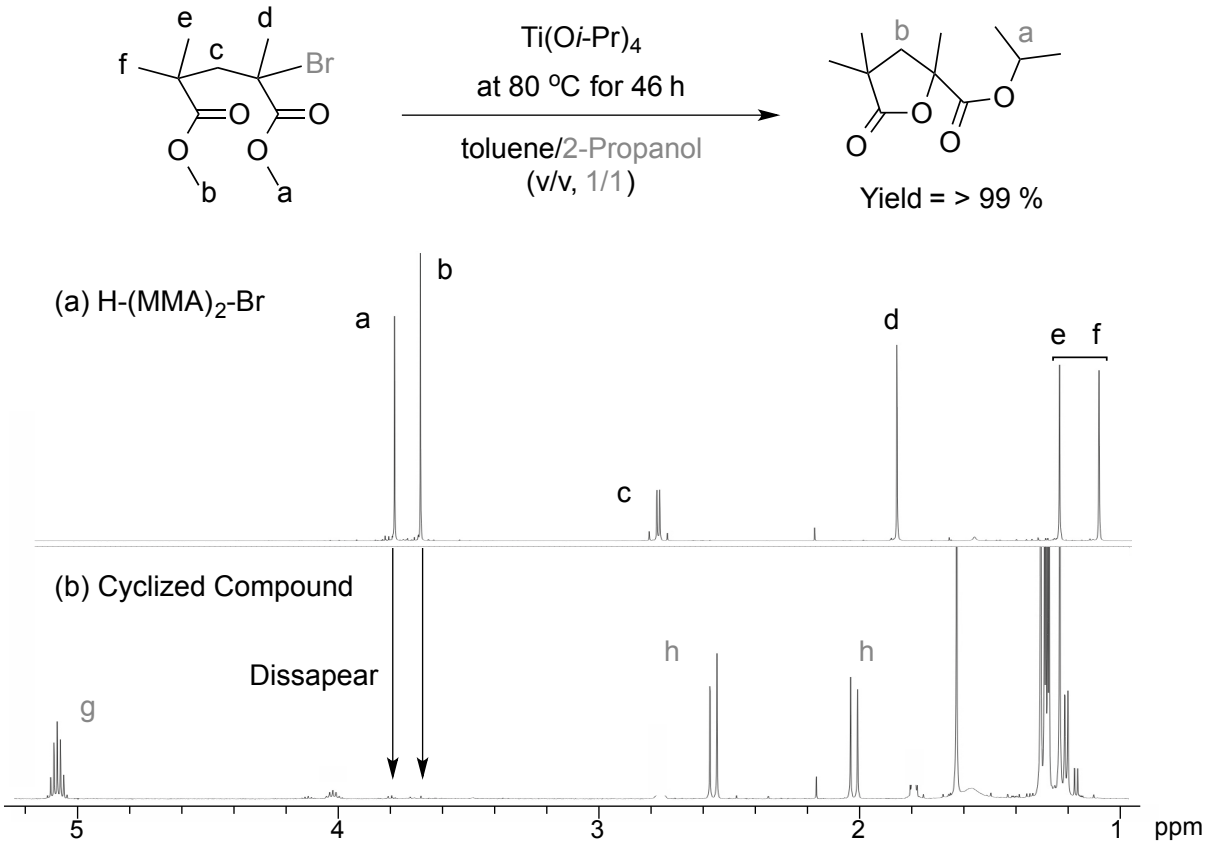

Figure 1. Model reaction with H-$(MMA)_2$-Br for cyclization and transesterification: [H-$(MMA)_2$-Br]/[Ti(O*i*-Pr)$_4$] = 20/40 mM in toluene/*i*PrOH (1/1, v/v) at 80 °C for 46h. ^{1}H NMR spectra of (a) H-$(MMA)_2$-Br and (b) the product in $CDCl_3$ at 25 °C.

Cyclization mechanism was not elucidated adequately in contrast to transesterification. To clarify it, the effect of Ti and *i*PrOH on cyclization was also examined by comparing the products obtained in several conditions. Here, four different conditions focusing on the existence of Ti(O*i*-Pr)$_4$ and *i*PrOH [(1) Ti(O*i*-Pr)$_4$ + *i*PrOH (2) Ti(O*i*-Pr)$_4$ (3) *i*PrOH (4) None] were applied to $(MMA)_2$-Br. In all cases, reactions were conducted for 46 h at 80 °C and obtained products were analyzed with ^{1}H NMR (Figure 2). A reaction with *i*PrOH caused cyclization to mainly give a lactone ring-bearing product, regardless of the use of Ti(O*i*-Pr)$_4$ (Figure 2a, c). In contrast, an unreacted $(MMA)_2$-Br was a major product in the absence of *i*PrOH (Figure 2b, d). A reaction with Ti(O*i*-Pr)$_4$ in toluene slightly induced cyclization and transesterification owing to small amount of *i*PrOH attached in Ti(O*i*-Pr)$_4$ (Figure 2b). These results support that the cyclization was promoted by *i*PrOH.

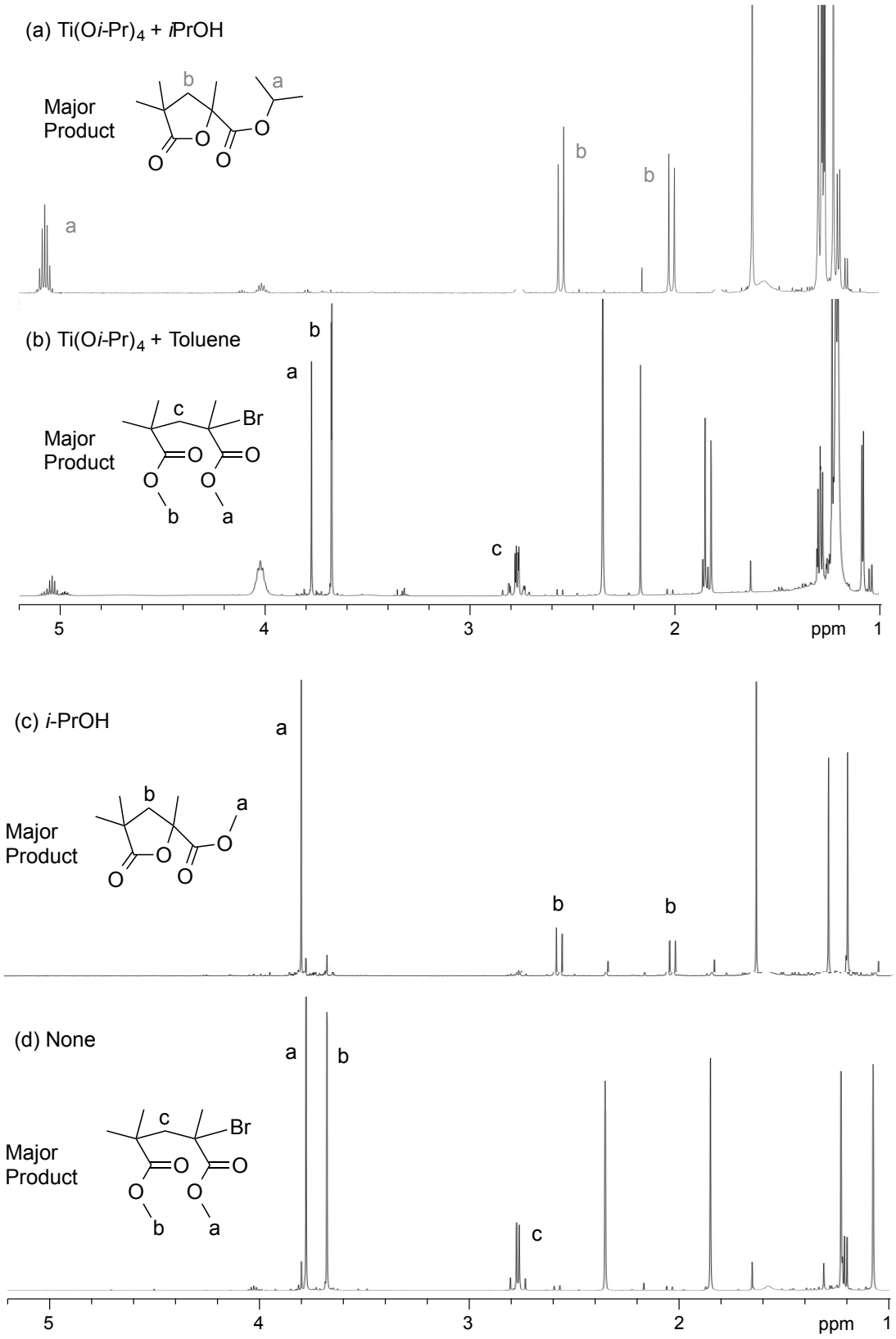

Figure 2. Effects of Ti catalyst and *i*PrOH on cyclization of H-(MMA)$_2$-Br: [H-(MMA)$_2$-Br]/[Ti(O*i*-Pr)$_4$] = 20/0 (c,d) or 40 (a,b) mM in toluene/*i*PrOH (1/1, v/v) (a,c) or toluene (b,d) at 80 ^{o}C for 46h. ^{1}H NMR spectra of their products in $CDCl_3$ at 25 ^{o}C.

2. Concurrent Cyclization and Transesterification of PMMA-Br

Bromine-capped poly(methyl methacrylate) (PMMA-Br) with high end-functionality was prepared by Ru-catalyzed living radical polymerization of MMA with a bromide initiator (EBPA: ethyl 2-bromo-2-phenylacetate) [M_n = 2100, M_w/M_n = 1.11, $F(\omega)$ = 95 %]. The PMMA-Br was treated with Ti(O*i*-Pr)$_4$ in *i*PrOH/toluene mixture (1/1, v/v) at 80 ^oC for 48 h. The products were analyzed with ^1H NMR and MALDI-TOF-MS (Figure 3). The MALDI-TOF-MS spectrum of PMMA-Br shows bimodal peaks at constant interval corresponding to the molecular weight of MMA (100.18). A split bimodal peak is attributed to isotope of bromine (^{79}Br, ^{81}Br). After the reaction, the peaks were shifted and turned to be unimodal, which is an evidence of elimination of the bromine terminal (Figure 3a). Additionally, the mass values of the main peak series (marked as filled circle) were good agreement with those for PMMA bearing two isopropyl esters and a single lactone ring, while the minor peak series (marked as open circle) correspond to the products containing a α-end ethyl ester. ^1H NMR spectra also support the concurrent cyclization and transesterification of PMMA-Br. After the reaction, a peak **a'** of the ω-end methyl ester disappeared and a peak **b** of the α-end ethyl ester decreased, while two isopropyl peaks newly emerged (Figure 3b). These results also proved that PMMA-Br was directly transformed into an isopropyl-functionalized telechelic PMMA with a ω-end lactone ring via concurrent cyclization and transesterification.

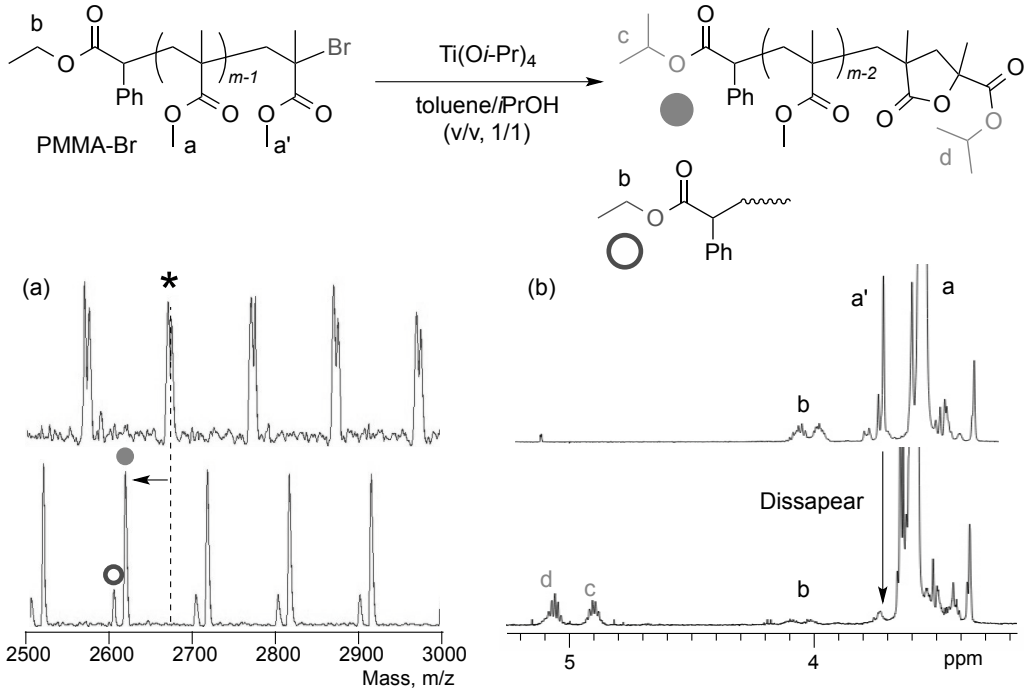

Figure 3. Concurrent cyclization and transesterification of Et-PMMA-Br: [Et-PMMA-Br]/[Ti(O*i*-Pr)$_4$] = 20/40 mM in toluene/*i*PrOH (1/1, v/v) at 80 ^oC for 48h: (a) MALDI-TOF-MS and (b) ^1H NMR ([Polymer] = 10 mg in CD_2Cl_2 at 25 ^oC) spectra of PMMA-Br (upper) and the product (lower).

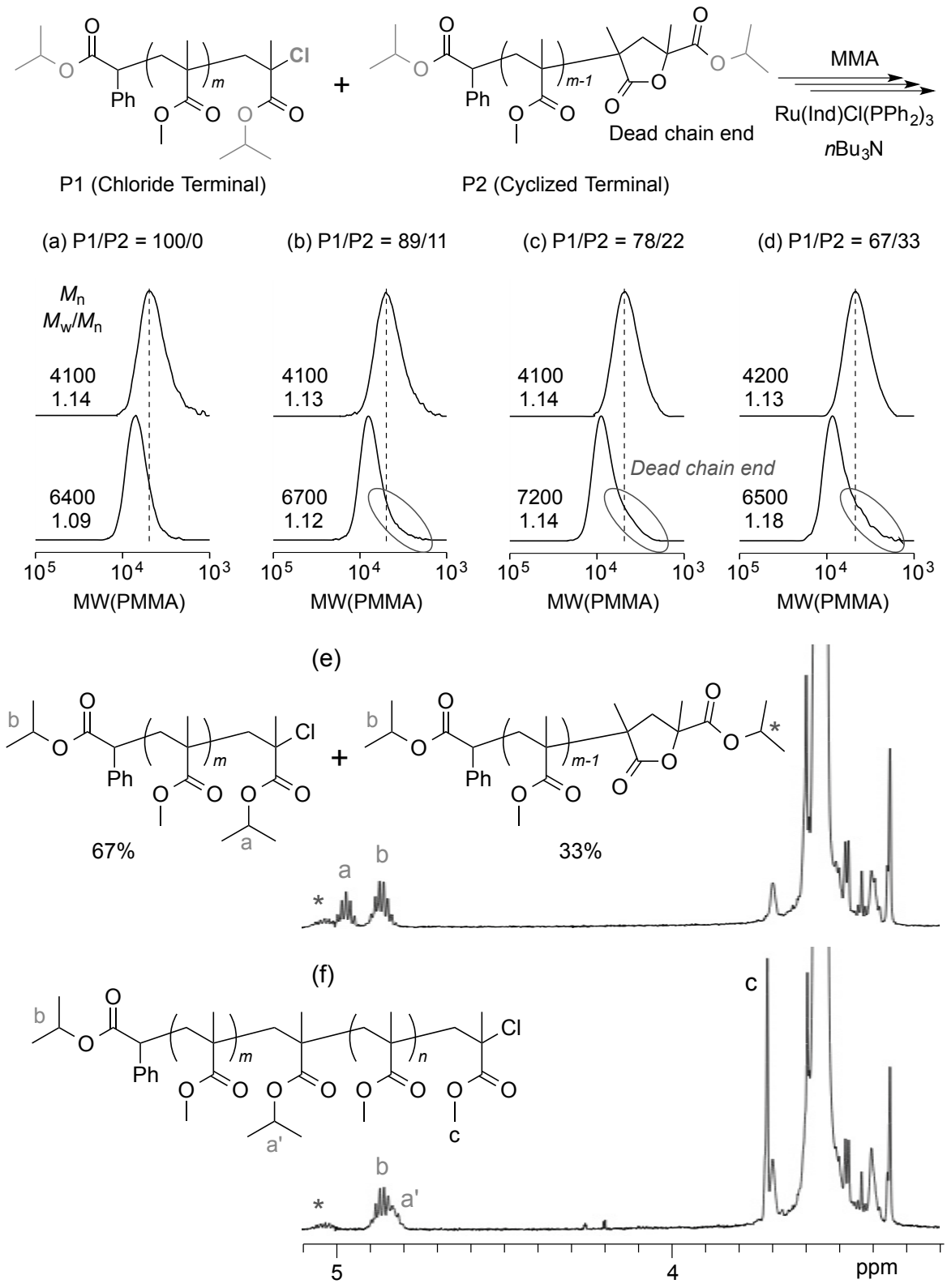

Figure 4. Chain extension from P1/P2 mixture via LRP of MMA: [MMA]/[P1+P2]/[Ru(Ind)Cl(PPh_3)$_2$]/[*n*-Bu_3N] = 500/10/1/10 mM in toluene at 80 °C. SEC curves of products obtained from (a) P1/P2 =100/0 (b) 89/11 (c) 78/22 (d) 67/33. ^{1}H NMR spectra of (e) P1/P2 mixture and (f) the product: [polymer] = 10 mg/mL in CD_2Cl_2 at 25 °C.

A terminal-cyclized PMMA obtained from PMMA-Br was utilized as a macroinitiator to verify the removal of a *ω*-end bromine, whereas polymerization of MMA did not proceed from the macroinitator with a Ru catalyst. As comparison, four samples containing mixture of chlorine-capped PMMA-*i*PrMA-Cl (P1) and terminal cyclized polymer (P2) (P1/P2 = 100/0, 89/11, 78/22, 67/33) were used as macroinitiator for LRP. These samples were prepared by transesterification of P1 by changing alcohol (2-propanol) volume terminal-selective transesterification of PMMA-Cl as described in Chapter 6. Ru-catalyzed LRP of MMA was conducted with P1/P2 mixed sample. In all cases, polymerization smoothly proceeded (Figure 4a-d). Though peak top of SEC curves shifted to higher molecular weight, tailing in low molecular weight region was clearly observed in except for pure P1. The tailing part becomes larger as the ratio of P2 increases. To investigate it in detail, polymer obtained from mixture containing 33% of P2 was analyzed with ^{1}H NMR (Figure 4e). A peak (marked with asterisk) originating from the isopropyl ester of P2 did not change at all, while a peak (marked with **a**) assigned to the isopropyl ester of P1 clearly shifted by reflecting the environmental change.

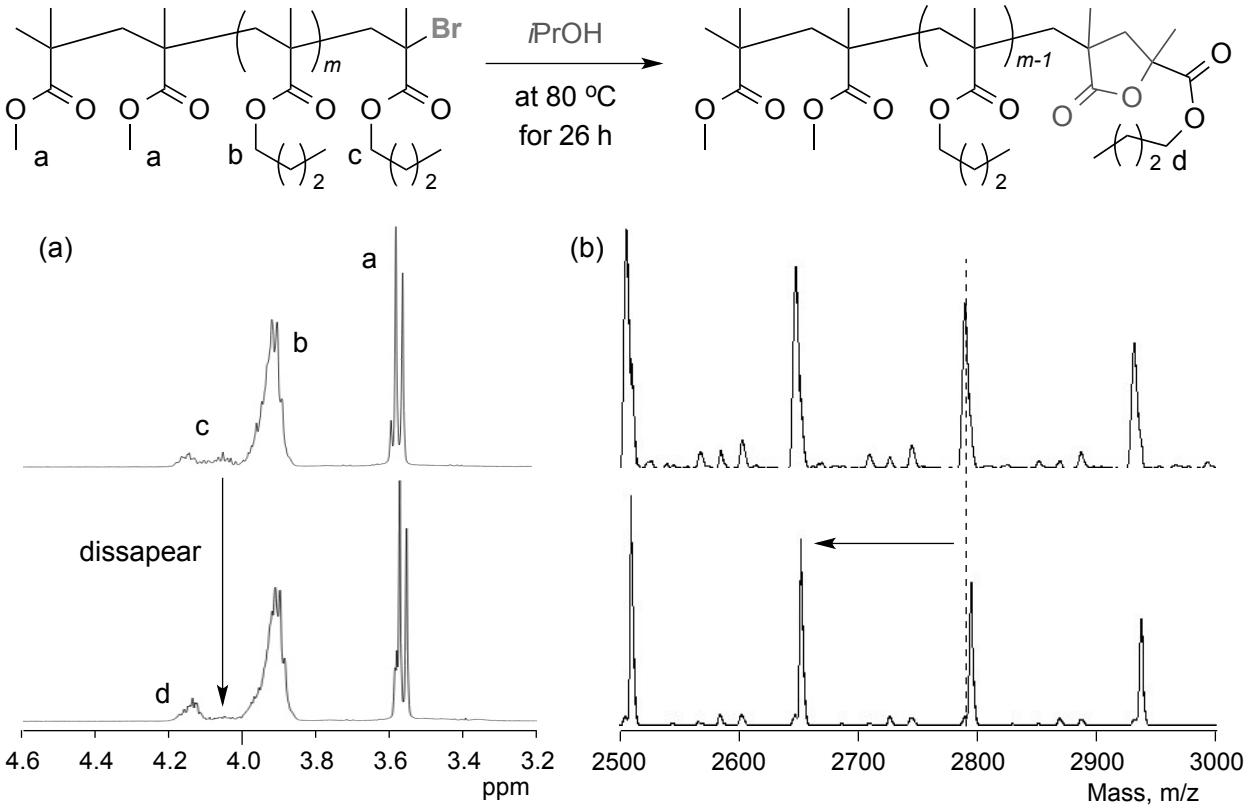

Figure 5. Intramolecular cyclization of PBMA-Br: [PBMA-Br] = 20 mM in toluene/*i*PrOH (1/1, v/v) at 80 °C for 48h. (a) ^{1}H NMR ([polymer] = 10 mg in CD_2Cl_2 at 25 °C) and (b) MALDI-TOF-MS spectra of PBMA-Br (upper) and the product (lower).

3. Effects of Polymer Structure on Cyclization

To further reveal the relation between polymer structure and *ω*-end cyclization, a bromine-capped poly(butyl methacrylate) (PBMA-Br) and poly(methyl acrylate) (PMA-Br) were compared with PMMA-Br. Both polymers were heated in toluene/*i*PrOH (1/1, v/v) mixture at 80 ^{o}C for 46 h. Quantitative cyclization of PBMA-Br was confirmed with ^{1}H NMR and MALDI-TOF-MS; the peak changes agreed with the elimination of the terminal bromine via cyclization (Figure 5a,b). In ^{1}H NMR spectra, a peak derived from bromine-capped terminal butyl ester (denoted **c**: 4.0 - 4.2 ppm) turned into a different peak assigned to butyl ester that is attached to the terminal lactone (denoted **d**: 4.1 - 4.2 ppm) (Figure 5a). MALDI-TOF-MS indicated decreased mass of approximately 95 whose value corresponds to the formation of a lactone ring (Figure 5b). The same reaction was applied to PMA-Br. ^{1}H NMR and MALDI-TOF-MS spectra of PMA-Br after the reaction showed the same signals as those before the reaction. This importantly indicates that no cyclization took place for polyacrylate.

4. Sequential LRP and Terminal Cyclization of MMA with Bromide Initiator

Efficient cyclization of PMMA-Br with alcohol encouraged the author to develop sequential tandem catalysis of LRP of MMA with a bromide initiator and the terminal cyclization of the resulting PMMA-Br. Here, an alcohol was directly added into the solutions of $FeBr_2(PPh_3)_2$-catalyzed LRP of MMA under inert atmosphere, because the iron catalyst is easily deactivated by alcohol and thereby polymerization is also quenched is well known to deactivate Fe catalyst to terminate LRP.

MMA was polymerized with $FeBr_2(PPh_3)_2$ and EBPA in toluene at 80 ^{o}C. When conversion of MMA reached 51% (9 h), ethanol (volume: equal to polymerization solution) was directly added to the polymerization solution at 80 ^{o}C. After 24 h, the product was purified and analyzed by ^{1}H NMR spectroscopy. A characteristic signal of the methyl ester adjacent to the *ω*-end bromine (3.7 ppm, a' in Figure 3b) was not observed, whereas a peak derived from the methyl ester attached to terminal lactone was observed at 3.7-3.8 ppm (Figure 6a). This result demonstrated that end-cyclized PMMA was directly synthesized in one-pot via sequential tandem catalysis of Fe-catalyzed LRP and in-situ *ω*-end cyclization. Confirmed by SEC, the product had almost identical molecular weight and narrow molecular weight distribution (MWD) (M_n = 5700, M_w/M_n = 1.12) to the PMMA-Br precursor (M_n = 5500, M_w/M_n = 1.11) (Figure 6b). This indicates that Fe-catalyzed LRP was immediately quenched with ethanol.

Sequential tandem *ω*-end cyclization via direct addition of ethanol was further applied to $Ru(Ind)Cl(PPh_3)_2$-catalzyed LRP of MMA with a bromide initiator. The product mainly showed

similar ^{1}H NMR signals to that obtained with a Fe catalyst (Figure 6a,c), whereas it included terminal olefins generated from disproportionation (6.2, 5.5 ppm). The olefin content was estimated as 5.7 %. The product treated with ethanol had slightly higher molecular weight (M_n = 5600, M_w/M_n = 1.13) than a PMMA-Br precursor, though the molecular weight distribution is narrow (Figure 6d). This result indicates that the termination of LRP of MMA is achieved by the transformation of ω-end bromine into a cyclized structure via ethanol addition; i.e., polymerization of MMA still proceeds until the completion of cyclization. Instead of ethanol, *i*PrOH was also effective for sequential tandem ω-end cyclization. However, the molecular weight distribution of the product turned broader than that with ethanol; this would be attributed to slower cyclization with *i*PrOH than EtOH.

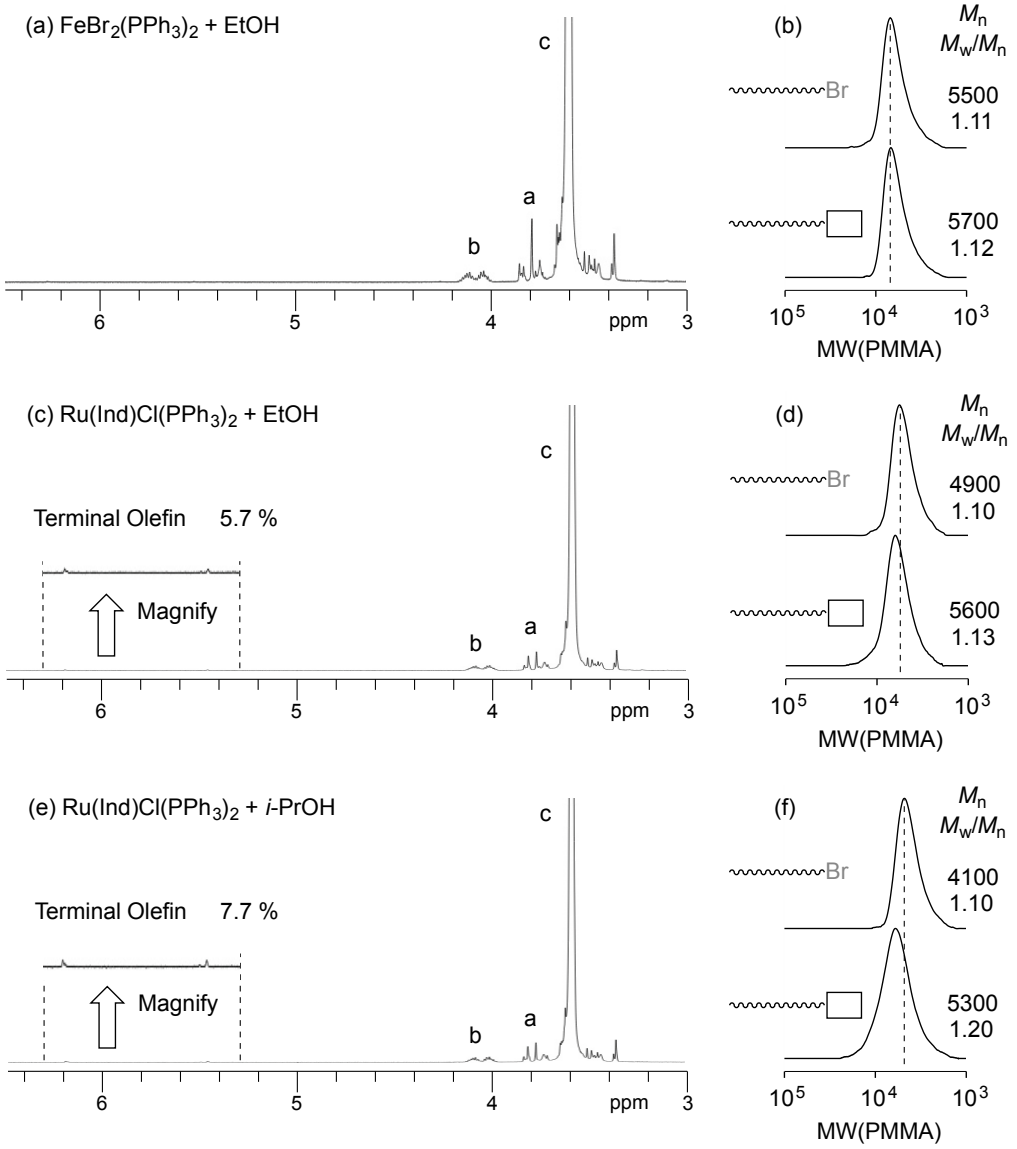

Figure 6. One-pot LRP of MMA and Cyclization of PBMA-Br: [MMA]/[ECPA]/[$FeBr_2$]/[PPh_3] = 2000/20/5/10 mM in toluene/*i*PrOH (1/1, v/v) at 80 ^oC for 48h. (a)(c)(e) ^{1}H NMR ([polymer] = 10 mg in CD_2Cl_2 at 25 ^oC) and (b) SEC curves of PBMA-Br and the products.

Conclusion

Concurrent tandem terminal-selective transesterification and ω-end cyclization of PMMA-Br was developed as a novel strategy to prepare "halogen-free" telechelic PMMAs. The formation of a ω-end lactone ring in PMMAs is triggered with alcohols. The dual use of Ti(O*i*-Pr)$_4$ and alcohols (ROH) allows to synthesize telechelic PMMAs bearing the alcohol-based esters at α- and ω-ends. Such ω-end cyclization also occurred for a bromine-capped poly(butyl methacrylate)s (PBMA-Br), but it did not in turn take place for a bromine-capped poly(metyl acrylate) (PMA-Br). ω-End-cyclized PMMAs were efficiently obtained from the sequential tandem catalysis of Fe-catalyzed LRP of MMA with a bromide initiator and subsequent ω-end cyclization via the direct addition of ethanol into the polymerization solution. Here, the efficient deactivation of the iron catalyst by ethanol is also important to suppress subsequent LRP of MMA and induce efficient ω-end cyclization.

References

(1) Yamago, S.; Yamada, T.; Togai, M.; Ukai, Y.; Kayahara, E.; Pan, N. *Chem. Eur. J.* **2009**, *15*, 1018-1029.

(2) Gody, G.; Rossner, C.; Moraes, J.; Vana, P.; Maschmeyer, T.; Perrier, S. *J. Am. Chem. Soc.* **2012**, *134*, 12596−12603.

(3) Sudo, A.; Endo, T. *J. Polym. Sci. Part A: Polym. Chem.* **2002**, *40*, 3103–3111.

(4) (a) Tokuchi, K.; Ando, T.; Kamigaito, M.; Sawamoto, M. *J. Polym. Sci. Part A: Polym. Chem.* **2000**, *38*, 4735–4748. (b) Ando, T.; Kamigaito, M.; Sawamoto, M. *Macromolecules* **1998**, *31*, 6708-6711.

(5) Wang, Q.; Zhang, B.; Liu, L.; Chen, Y.; Qu, Y.; Zhang, X.; Yang, J.; Xie, Z.; Geng, Y.; Wang, L.; Wang, F. *J. Phys. Chem. C* **2012**, *116*, 21727-21733.

(6) Park, J. K.; Jo, J.; Seo, J. H.; Moon, J. S.; Park, Y. D.; Lee, K.; Heeger, A. J.; Bazan, G. C. *Adv. Mater*. **2011**, *23*, 2430-2435.

(7) Robb, M. J.; Montarnal, D.; Nancy D. Eisenmenger, N. D.; Ku, S-Y.; Chabinyc, M. L.; Hawker, C. J. *Macromolecules* **2013**, *46*, 6431-6438.

(8) Aoshima, S.; Kanaoka, S. *Chem. Rev.* **2009**, *109*, 5245-5287.

(9) Hawker, C. J.; Bosman, A. W.; Harth, E. *Chem. Rev.* **2001**, *101*, 3661-3688.

(10) Kamigaito, M.; Ando, T.; Sawamoto, M. *Chem. Rev.* **2001**, *101*, 3689-3745.

(11) Matyjaszewski, K.; Tsarevsky, N. V. *J. Am. Chem. Soc.* **2014**, *136*, 6513-6533.

(12) Moad, G.; Rizzardo, E.; Thang, S. H. *Aust. J. Chem*. **2012**, *65*, 985-1076.

(13) Yamago, S. *Chem. Rev.* **2009**, *109*, 5051-5068.

(14) Ouchi, M.; Terashima, T.; Sawamoto, M. *Chem. Rev.* **2009**, *109*, 4963-5050.

(15) Matyjaszewski, K. *Macromolecules* **2012**, *45*, 4015-4039.

(16) Terashima, T.; Ouchi, M.; Ando, T.; Sawamoto, M. *J. Am. Chem. Soc.* **2006**, *128*, 11014−11015.

(17) (a) Nakatani, K.; Ouchi, M.; Sawamoto, M. *Macromolecules* **2008**, *41*, 4579-4581. (b) Nakatani, K.; Terashima, T.; Ouchi, M.; Sawamoto, M. *Macromolecules* **2010**, *43*, 8910-8916.

(18) (a) Kimura, T.; Hamashima, M. *Polym. J.* **1986**, *18*, 21-30. (b) Kimura, T.; Tasaka, H.; Hamashima, M. *Polym. J.* **1987**, *19*, 305-314. (c) Kimura, T.; Ezura, H.; Hamashima, M. *Polym. J.* **1992**, *24*, 187-197.

(19) Li, Z-L.; Li, L.; Deng, X-X.; Zhang, L-J.; Dong, B-T.; Du, F-S.; Li, Z-C. *Macromolecules* **2012**, *45*, 4590-4598.

(20) (a) Kimura, T.; Morimoto, H.; Sasaki, E.; Tanji, K.; Hamashima, M. *Polym. J.* **1990**, *22*, 1015-1021. (b) Kimura, T.; Tanji, K.; Sasaki, R.; Sato, D.; Minabe, M. *Polym. J.* **1993**, *25*, 267-273.

(21) Ogura, Y.; Terashima, T.; Sawamoto, M. *J. Am. Chem. Soc.* **2016**, *138*, 5012−5015.

(22) Ho, H. T.; Levere, M. E.; Fournier, D.; Montembault, V.; Pascual, S.; Fontaine, L. *Aust. J. Chem*. **2012**, *65*, 970-977.

(23) Li, Z-L.; Lv, A.; Du, F-S.; Li, Z-C. *Macromolecules* **2014**, *47*, 5942-5951.

Chapter 8

Post-Functionalization of Methacrylate/Acrylate Copolymers via Acrylate-Selective Transesterification: A New Avenue in Polymer Reactions

Abstract

Acrylate-selective transesterification of methacrylate and methyl acrylate (MA) copolymers was developed as a site-selective post-functionalization technique. Importantly, a common methyl acrylate works as transformable units via transesterification with a Ti catalyst and alcohols, without using specific monomers such as activated ester methacrylates. The key is less steric hindrance of acrylate carbonyl groups than methacrylate counterparts; the carbonyl group of the acrylate units is attached to the secondary carbon of the main chain [-C<u>H</u>(COOCH$_3$)CH$_2$-], while that of methacrylate is anchored to the tertiary carbon [-C<u>C</u>H$_3$(COOCH$_3$)CH$_2$-]. In fact, a poly(methyl acrylate) (PMA) was efficiently transesterified with 1-dodecanol (*n*-CH$_2$(CH$_2$)$_{10}$CH$_3$), Ti(O*i*-Pr)$_4$, and molecular sieves into a poly(dodecyl acrylate) (PDA) up to 96% conversion at 130 ^{o}C, in sharp contrast to low conversion of a poly(methyl methacrylate) (PMMA) into a poly(dodecyl methacrylate) (PDMA: ~4%). Owing to the high reactivity, the acrylate units of a DMA/MA random copolymer (DMA/MA = 64/36) was selectively transesterified with benzyl alcohol (BzOH), resulting in a DMA/BzA/MA random copolymers (DMA/BzA/MA = 50/44/6).

Introduction

Polymer reaction and post-functionalization are indispensable techniques to modulate physical properties and functions of synthetic polymer materials in laboratory and industrial production.[1] Site-selective post-functionalization is attractive to introduce functional groups into polymers, since designed precursors allow position-selective functionalization (e.g., side chain, terminal) and identical precursors can be also employed to design wide variety of functional polymers.[2-5] This method is particularly useful for the case: e.g., desired functional groups are incompatible to polymerization systems. The key to develop such efficient post-functionalization is to find active but selective organic reactions. So far, several efficient reactions, so called click reactions, using azide and alkyn,[6,7] thiol-ene,[8-11] alcohol and isocyanate have been applied as post-functionalization of polymers. These post-functionalization systems provided various functional polymers bearing hydrogen bonding unit,[12,13] olefin for crosslinking,[14,15] and initiators for graft polymerization.[16,17]

Among organic reactions, transesterification with alcohols draws much attention as one of the most efficient synthetic strategies of ester compounds and derivatives owing to wide applicability of their starting materials into diverse ester products. Transesterification is also important in polymer chemistry. Transesterification is not only industrially employed to produce monomers (e.g., acrylate and methacrylate) but also play important roles in step growth polymerization,[18] ring opening polymerization,[19] and functionalization of acrylate or methacrylate.[20] Efficient post-functionalization of poly(meth)acrylates generally requires activated ester (meth)acrylates as monomers. For example, Theato and coworkers reported that pentafluorophenyl (meth)acrylate is effective as an activated monomer for post-functionalization via transesterification or amidation.[21] 2-Hydroxyethyl methacrylate also serves as a site-selectively functional unit of polymers, where the hydroxyl group is effectively transformed with isocyanate derivatives.

In previous chapters, the authors revealed that Ti(O*i*-Pr)$_4$-catalyzed transesterification with alcohols showed unique selectivity dependent on the steric hindrance around the carbonyl groups of ester compounds.[21] For example, in Chapters 6 and 7, the authors find that the terminal esters of poly(methacrylate)s are selectively transesterified with alcohols and the Ti catalyst owing to the less steric hindrance of the carbonyl groups. Given this finding, the authors further noticed the possibility that polyacrylate pendants would be efficiently transesterified because of the less steric hinderance of the carbonyl groups.

In this chapter, the author thus aimed to develop a novel site-selective post-functionalization of methacrylate/acrylate random copolymers via Ti(O*i*-Pr)$_4$-catalyzed acrylate-selective transesterification. This system allows efficient and site-selective transformation of copolymers using a common methyl acrylate as a selective transforming site, although efficient

post-functionalization of poly(meth)acrylates generally requires activated esters monomers such as [pentafluorophenyl (meth)acrylate, *N*-hydroxysuccinimide methacrylate]. The diverse alcohols potentially afford unlimited design and functionalization of copolymers.[15] Thus, simple but versatile Ti-mediated transesterification would open new vistas in post-functionalization and polymer reactions applicable to various research fields.

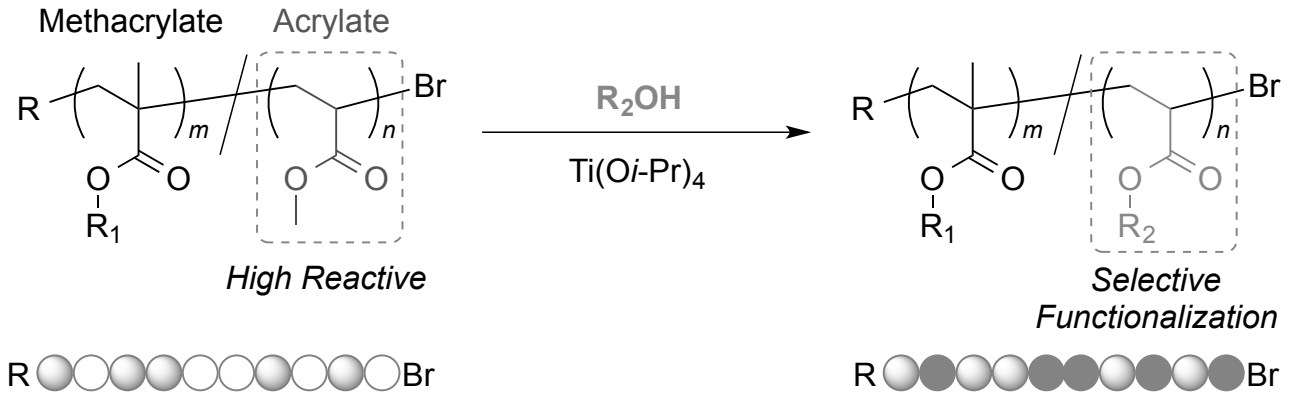

Scheme 1. Acrylate-Selective Transesterification of Methacrylate/Methyl Acrylate (R_1MA/MA) Random Copolymers with Alcohols (R_2OH) into R_1MA/R_2A Random Copolymers

Experimental Section

Materials. Methyl methacrylate (MMA: TCI; purity >99.8%), methyl acrylate (MA: TCI; purity >99%) and tetralin (1,2,3,4-tetrahydronaphthalene: Kishida Chemical; purity >98%; an internal standard for ^{1}H NMR analysis) were dried overnight with calcium chloride and distilled from calcium hydride under reduced pressure before use. Dodecyl methacrylate (DMA) (TCI, purity >97%) was purified by column chromatography charged with inhibitor remover (Aldrich) and purged by argon before use. Ti(O*i*-Pr)$_4$ (Aldrich, purity >97%) was degassed by triple vacuum-argon purge cycles before use. The H(MMA)$_2$Br [H(CH_2CMeCO_2Me)$_2$Br; a MMA dimer bromide] was prepared according to the literature. Ru(Ind)Cl(PPh_3)$_2$ (Aldrich) was used as received and handled in a glove box under moisture- and oxygen-free argon (H_2O <1 ppm; O_2 <1 ppm). Toluene was purified by pashing it through a purification column (Glass Contour Solvent Systems: SG Water USA). Ethanol (Wako, purity 99.5%), 1-dodecanol (Wako, purity >99%) benzyl alcohol (Wako, purity >99%), and Anisole (Wako, purity >99%) were used as received. Molecular sieves 4A (Wako) were baked with heat gun under reduced pressure before use.

Characterization. The molecular weight distribution (MWD) curves, M_n and M_w/M_n ratio of the polymers were measured by SEC at 40 °C in THF as an eluent on three polystyrene-gel columns (Shodex LF-404: exclusion limit = 2×10^6 g/mol; particle size = 6 μm; pore size = 3000 Å; 0.46 cm

i.d. × 25 cm; flow rate, 0.3 mL/min) connected to a DU-H2000 pump, a RI-74S refractive index detector, and a UV-41 ultraviolet detector (all from Shodex; Shodex GPC-104). The columns were calibrated against 13 standard poly(MMA) samples (Polymer Laboratories; M_n = 620−1200000; M_w/M_n = 1.06−1.22). To remove unreacted monomers and catalyst, polymer samples were purified by preparative SEC before characterization [column: Shodex K-5002; particle size = 15 mm; 5.0 cm i.d. × 30 cm; exclusion limit = 5×10^3 g/mol; flow rate = 10 mL/min]. ^{1}H NMR spectra were recorded in $CDCl_3$ at 25 ^{o}C on a JEOL JNM-ECA500 spectrometer operating at 500.16 MHz.

Transesterification. Transesterification of all polymers was carried out by syringe technique under argon in baked glass tubes equipped with a three-way stopcock.

Transesterification of MMA/MA copolymer with 1-dodecanol (Table 1, entry 2). A typical procedure for transesterification of MMA/MA copolymer with 1-dodecanol, Ti(O*i*-Pr)$_4$ and MS (4A) was given: MS 4A (0.33 g) was first placed and dried in a 30 mL glass tube under reduced pressure with heat gun. Into the tube, MMA-*r*-MA (M_n = 9200, M_w/M_n = 1.23, 0.005 mmol, 46 mg) and a 500 mM toluene solution of Ti(O*i*-Pr)$_4$ (0.08 mL, Ti(O*i*-Pr)$_4$ = 0.04 mmol) added into glass tube. The toluene solution was evaporated by vacuum pump to remove toluene. And then, anisole (0.25 mL), and 1-dodecanol (0.25 mL) were added at room temperature under dry argon (total volume: 0.5 mL). The glass tube was placed in an oil bath kept at 80 ^{o}C for 48 h and cooled to –78 °C to terminate the reaction. The quenched reaction solutions were evaporated to dryness to give the crude product. The product was fractionated by preparative SEC for ^{1}H NMR analysis. Characterization: Figure 2 in results and discussion.

Polymerization. The synthesis of all polymers was carried out by syringe technique under argon in baked glass tubes equipped with a three-way stopcock.

PMMA. Into a 30 mL glass tube, Ru(Ind)Cl(PPh$_3$)$_2$ (0.006 mmol, 4.66 mg) was charged, and toluene (1.31 mL), tetralin (0.08 mL), a 400 mM toluene solution of *n*-Bu$_3$N (0.15 mL, *n*-Bu$_3$N = 0.06 mmol), MMA (12 mmol, 1.28 mL), and a 330 mM toluene solution of ECPA (0.18 mL, ECPA = 0.06 mmol) were added sequentially in that order at 25 ^{o}C under argon (the total volume: 3.0 mL). The glass tube was placed in an oil bath kept at 80 ^{o}C for 20 h and then cooled to –78 °C to terminate the reaction. The monomer conversion was determined as 51% by ^{1}H NMR measurements of the terminated reaction solution in $CDCl_3$ at r.t. with tetralin as an internal standard. The quenched reaction solutions were evaporated to dryness to give the crude PMMA. The product was fractionated by preparative SEC. SEC (THF, PMMA std.): M_n = 11500 g/mol; M_w/M_n = 1.20. ^{1}H NMR [500 MHz, $CDCl_3$, 25 ^{o}C, δ = 7.26 ($CDCl_3$)]: M_n (NMR, α) = 11600. δ

7.3–7.1 (aromatic), 4.2–4.0 (-COOC$\underline{H}_2$CH$_3$), 3.8–3.4 (-OC$\underline{H}_3$), 2.1−1.4 (-C$\underline{H}_2$C(CH$_3$)-), 1.3−0.7 (-CH$_2$C(C$\underline{H}_3$)-).

PMA. Into a 30 mL glass tube, RuCp*Cl(PPh$_3$)$_2$ (0.004 mmol, 3.22 mg) was charged, and toluene (0.98 mL), tetralin (0.08 mL), a 400 mM toluene solution of *n*-Bu$_3$N (0.10 mL, *n*-Bu$_3$N = 0.04 mmol), MA (8 mmol, 0.72 mL), and a 342 mM toluene solution of H(MMA)$_2$Br (0.12 mL, H(MMA)$_2$Br = 0.04 mmol) were added sequentially in that order at 25 ^{o}C under argon (the total volume: 2.0 mL). Following procedures were same as in the case of PMMA (Time: 92h, Conversion: 59%). SEC (THF, PMMA std.): M_n = 9800 g/mol; M_w/M_n = 1.21. ^{1}H NMR [500 MHz, CDCl$_3$, 25 ^{o}C, δ = 7.26 (CDCl$_3$)]: δ 3.7–3.6 (-OC$\underline{H}_3$), 2.4–2.2 (-CH$_2$C$\underline{H}$(COO)-), 2.0–1.4 (-C$\underline{H}_2$CH(COO)-).

MMA-*r*-MA. Into a 30 mL glass tube, RuCp*Cl(PPh$_3$)$_2$ (0.004 mmol, 3.22 mg) was charged, and toluene (0.94 mL), tetralin (0.08 mL), a 400 mM toluene solution of *n*-Bu$_3$N (0.10 mL, *n*-Bu$_3$N = 0.04 mmol), MA (5.6 mmol, 0.50 mL), MMA (2.4 mmol, 0.26 mL), and a 550 mM toluene solution of H(MMA)$_2$Br (0.12 mL, H(MMA)$_2$Br = 0.04 mmol) were added sequentially in that order at 25 ^{o}C under argon (the total volume: 2.0 mL). Following procedures were same as in the case of PMMA [Time: 29h, Conversion: 68% (MA), 82% (MMA)]. SEC (THF, PMMA std.): M_n = 9200 g/mol; M_w/M_n = 1.23. ^{1}H NMR [500 MHz, CDCl$_3$, 25 ^{o}C, δ = 7.26 (CDCl$_3$)]: δ 3.7–3.5 (-OC$\underline{H}_3$), 2.5–0.8 (-CH$_2$C$\underline{H}$(COO)-, -C$\underline{H}_2$CH(COO)-, -C$\underline{H}_2$C(CH$_3$)-, -CH$_2$C(C$\underline{H}_3$)-).

DMA-*r*-MA. Into a 30 mL glass tube, RuCp*Cl(PPh$_3$)$_2$ (0.004 mmol, 3.18 mg) was charged, and toluene (0.17 mL), tetralin (0.08 mL), a 400 mM toluene solution of *n*-Bu$_3$N (0.1 mL, *n*-Bu$_3$N = 0.04 mmol), DMA (4 mmol, 1.17 mL), MA (4 mmol, 0.36 mL), and a 342 mM toluene solution of H(MMA)$_2$Br (0.12 mL, H(MMA)$_2$Br = 0.04 mmol) were added sequentially in that order at 25 ^{o}C under argon (the total volume: 2.0 mL). Following procedures were same as in the case of PMMA [Time: 16h, Conversion: 39% (MA), 84% (DMA)]. SEC (THF, PMMA std.): M_n = 21900 g/mol; M_w/M_n = 1.22. ^{1}H NMR [500 MHz, CDCl$_3$, 25 ^{o}C, δ 4.1-3.8 (-COOC$\underline{H}_2$(CH$_2$)$_{10}$CH$_3$), 3.7–3.5 (-OC$\underline{H}_3$), 2.5–0.8 (-CH$_2$C$\underline{H}$(COO)-, -C$\underline{H}_2$CH(COO)-, -C$\underline{H}_2$C(CH$_3$)-, -CH$_2$C(C$\underline{H}_3$)-), 1.4–1.2 (-COOCH$_2$(C$\underline{H}_2$)$_{10}$CH$_3$), 0.9–0.8 (-COOCH$_2$(CH$_2$)$_{10}$C$\underline{H}_3$).

Results and Discussion

1. Transesterification of PMA with Ethanol

Transesterification of poly(methyl acrylate) (PMMA) was demonstrated in previous chapters. Reactivity of acrylate pendant esters in polymers was examined with the reaction of poly(methyl acrylate) (PMA) and ethanol with Ti(O*i*-Pr)$_4$. PMA with well-controlled molecular weight (M_n = 9800, M_w/M_n = 1.21) was prepared as a reactant for transesterification. First, transesterification of

PMA (10 mM) into poly(ethyl acrylate) (PEA) was conducted with Ti(O*i*-Pr)$_4$ (80 mM) and ethanol at 80 °C. The products obtained in different ethanol concentration (2.2 M, 8.5 M) were analyzed by ^{1}H NMR. The product obtained with a large amount of ethanol (8.5 M) showed a broad peak denoted **b** at 4.0-4.2 ppm that is assigned to ethyl ester pendants (Figure 1a). Conversion of the methyl esters into ethyl esters was estimated as 66% from the area ratio of peak **b** and methyl ester peak **a**. On the other hand, the transesterification of PEA was not so effective with a small amount of ethanol (2.2 M: 2.8 % conversion). Confirmed by SEC, the product efficiently transesterifed with ethanol (8.5 M: M_n = 12100, M_w/M_n = 1.14) had larger molecular weight than the original PMA (M_n = 9800, M_w/M_n = 1.21), while the product obtained with 2.2M ethanol had virtually identical peak-top molecular weight to the PMA (Figure 1b). These results indicate that high concentration of alcohols ia required to efficiently promote transesterification of PMA.

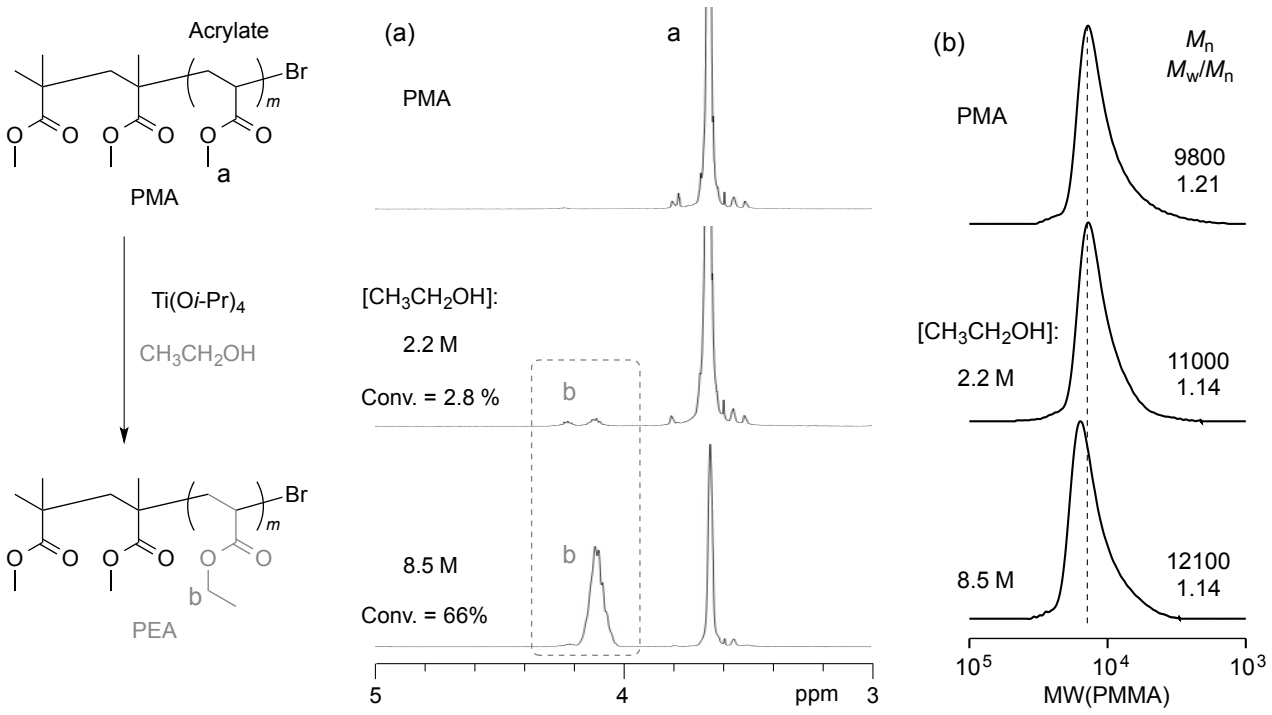

Figure 1. Transesterification of PMA with Ti(O*i*-Pr)$_4$ and ethanol: $[PMA]_0/[Ti(O\textit{i}\text{-Pr})_4]_0$ = 10/80 mM in toluene/EtOH (2.2 or 8.5 M) at 80 °C. (a) ^{1}H NMR spectra of PMA and the products in $CDCl_3$ at 25 °C: [polymer] = 10 mg/mL. (b) SEC curves of PMA and the products.

2. Transesterification of MMA/MA Random Copolymers

For quantitative transesterification of PMA, high temperature (> 80 °C) or adding molecular sieves (MS) were effective. However, ethanol cannot be used under such conditions due to its low boiling point (bp = 78 °C). To achieve quantitative but selective transformation of polyacrylate segments, transesterification of MMA/MA random copolymers was investigated with Ti(O*i*-Pr)$_4$,

1-dodecanol (bp = 259 °C), and molecular sieves 4A. For this, two kinds of MMA/MA random copolymers with different composition were prepared via $Ru(Ind)Cl(PPh_3)_2$-catalyzed living radical copolymerization of MMA and MA with a bromide initiator [H-$(MMA)_2$-Br]: P1 (MMA/MA = 37/63, M_n = 9200, M_w/M_n = 1.23) and P2 (MMA/MA = 18/82, M_n = 7400, M_w/M_n = 1.17). Transesterification was conducted by varying temperature (90 - 130 °C), with constant concentration of 1-dodecanol (2.2 M). The conversion of the methyl esters into dodecyl esters was analyzed by ^{1}H NMR spectroscopy (Table 1, entries 1-6).

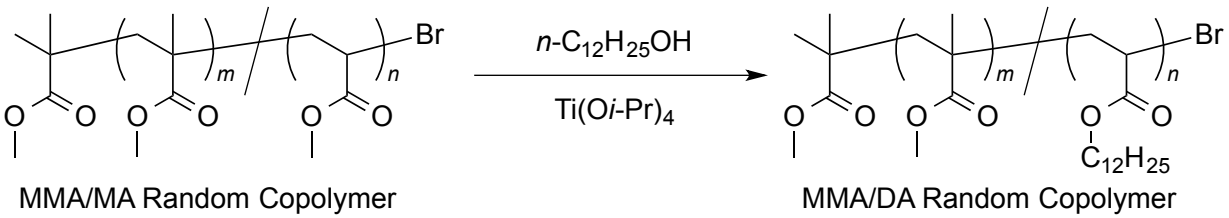

MMA/MA Random Copolymer MMA/DA Random Copolymer

P1: MMA/MA = 37/63, M_n = 9200, M_w/M_n = 1.23 P3: MMA/MA = 0/100, M_n = 9800, M_w/M_n = 1.21

P2: MMA/MA = 18/82, M_n = 7400, M_w/M_n = 1.17 P4: MMA/MA = 100/0, M_n = 11500, M_w/M_n = 1.20

Table 1. Transesterification of MMA/MA Random Copolymers and MMA or MA Homopolymers with Ti(O*i*-Pr)$_4$ and *n*-$C_{12}H_{25}OH$[a]

Entry	Polymer	MS (g/mL)	Temperature (°C)	Conversion[b] (%)	M_n[c]	M_w/M_n[c]
1	P1	0.33	130	76	19300	1.15
2	P1	0.33	110	64	18100	1.15
3	P1	0.33	90	50	15300	1.24
4	P1	None	110	13	13500	1.10
5	P1	None	90	4	11100	1.15
6	P2	0.33	130	93	18000	1.14
7	P3	0.33	130	96	19900	1.24
8	P4	0.33	130	5	14400	1.14

[a][Polymer (P1-P4)]$_0$/[Ti(O*i*-Pr)$_4$]$_0$ = 10/80 mM with or without MS 4A in anisole/*n*-$C_{12}H_{25}OH$ (1/1, v/v) at 90-130 °C. [b]Conversion of the pendant methyl esters into isopropyl ester: determined by ^{1}H NMR with an internal standard. [c]Determined by SEC in THF with a PMMA standard calibration.

The reaction at 110 °C with MS (0.33 g/mL) was most suitable for acrylate-selective and quantitative transesterification (Table 1, entry 2) because the conversion (64%) was very close to the content of methyl acrylate in the copolymer (63%). The introduction of dodecyl esters into the

copolymers was confirmed by the appearance of the corresponding new peak (denoted **b**, Figure 2a) in ^{1}H NMR. The product had larger molecular weight than the original MMA/MA random copolymer (Figure 4a). In contrast, higher temperature condition (130 ^{o}C) with MS induced conversion higher than the original acrylate composition of P1 and P2 precursors (Table 1, entry 1, 6), indicating that methacrylate units were also transesterified into dodecyl esters. Lower temperature condition (90 ^{o}C) or no use of MS were not so effective for transesterification of P1 (Table 1, entry 3-5). In particular, MS influenced the yield of the transesterification more strongly than Ti catalyst concentration.

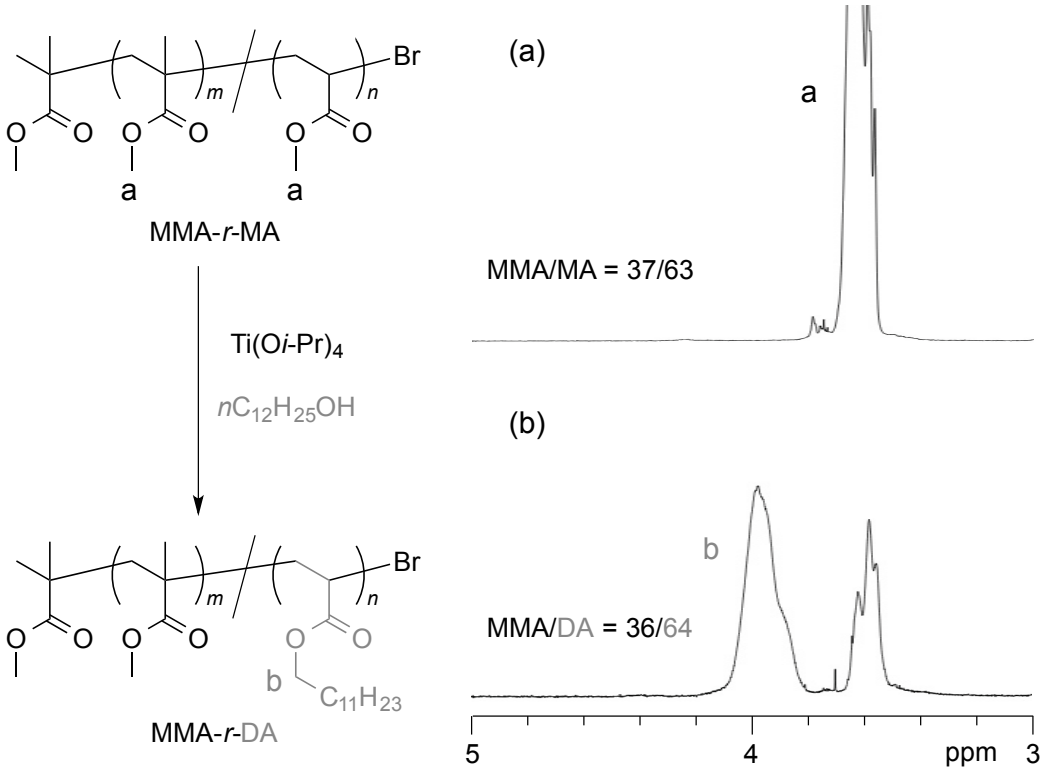

Figure 2. Transesterification of MMA/MA random copolymers with Ti(O*i*-Pr)$_4$ and *n*-$C_{12}H_{25}OH$: [MMA-*r*-MA]/[Ti(O*i*-Pr)$_4$] = 10/80 mM with MS 4A (0.33 g/mL) in anisole/*n*-$C_{12}H_{25}OH$ (1/1, v/v) at 110 ^{o}C. ^{1}H NMR spectra of (a) MMA-*r*-MA and (b) the product: [polymer] = 10 mg/mL in $CDCl_3$ at 25 ^{o}C.

3. Effects of Polymer Structures on Transesterification

Transesterification of PMA (denoted P3 in Table 1) was compared with that of PMMA (denoted P4 in Table 1), to investigate the effect of α-methyl groups of the polymer backbones on transesterification of the pendant esters. P3 was efficiently transesterified with 1-dodecanol, Ti(O*i*-Pr)$_4$, and MS 4A at 130 ^{o}C to reach 96 % conversion, while P4 was hardly transesterified (5%) under the identical conditions (Table 1, entry 7, 8, Figure 3). The product obtained from P3

had larger molecular weight than P3, while the product from P4 had slightly larger molecular weight than P4 (Figure 4). These results strongly support that Ti-catalyzed transesterification is effective as a post-functionalization system for the pendant esters of polyacrylates.

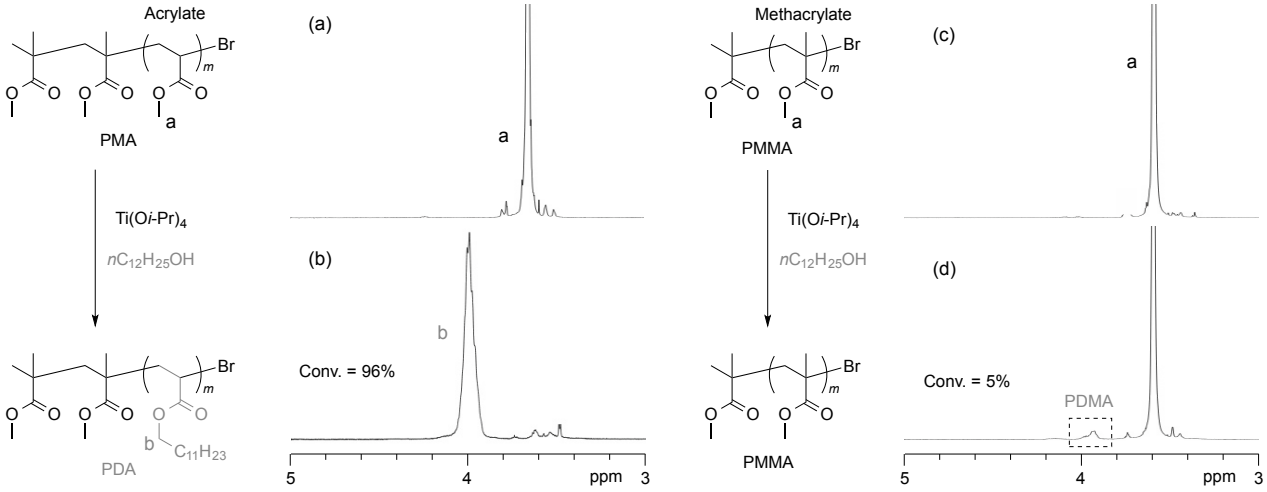

Figure 3. Transesterification of MMA and MA homopolymers with Ti(O*i*-Pr)$_4$ and *n*-$C_{12}H_{25}OH$: [PMA or PMMA]/[Ti(O*i*-Pr)$_4$] = 10/80 mM with MS 4A (0.33 g/mL) in anisole/*n*-$C_{12}H_{25}OH$ (1/1, v/v) at 130 °C. ^{1}H NMR spectra of (a) PMA, (b) the transesterified product, (c) PMMA, and (d) the transesterifed product: [polymer] = 10 mg/mL in $CDCl_3$ at 25 °C.

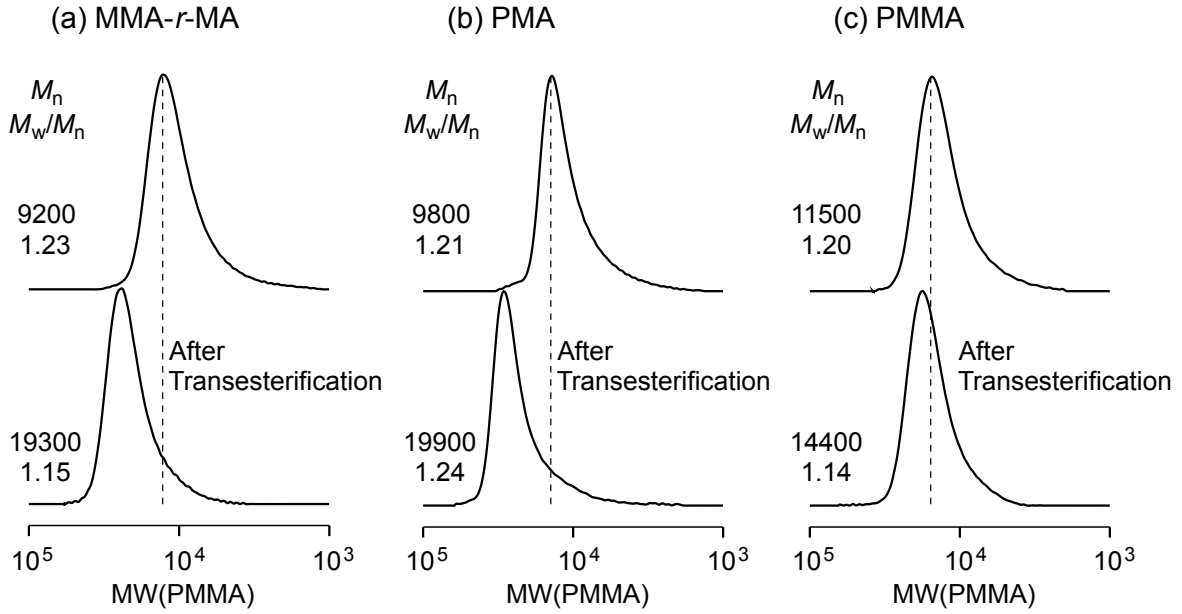

Figure 4. SEC curves of the products obtained via transesterification of (a) MMA-*r*-MA, (b) PMA and (c) PMMA with Ti(O*i*-Pr)$_4$ and *n*-$C_{12}H_{25}OH$: Reaction condition is shown in Figures 2 and 3.

4. Acrylate-Selective Transesterification of DMA/MA Random Copolymers

Given the effective transesterification of the pendant esters of polyacrylates, transesterification of a DMA/MA random copolymer was investigated with Ti(O*i*-Pr)$_4$ and benzyl alcohol (BzOH) (Figure 5). A DMA/MA random copolymer (DMA/MA = 64/36, M_n = 21900, M_w/M_n = 1.22) was prepared by Ru-catalyzed LRP of DMA and MA with a bromide initiator.

Transesterification of the copolymer was conducted with Ti(O*i*-Pr)$_4$ (160 mM) and BzOH (4.8 M) at 130 ^oC. The product was analyzed by ^1H NMR and SEC. After the reaction, a peak **b** derived from the methyl ester decreased, while a peak **a** originating from dodecyl methacrylate was maintained and new peaks **c** and **d** from benzyl acrylate (BzA) or methacrylate (BzMA) further appeared (Figure 4a). The composition in copolymer was determined from the area ratio of their signals: DMA/BzMA+BzA/MA = 50/44/6. This result is fully consistent with the fact that transesterification preferentially occurs for the methyl acrylate units. The product still maintained narrow molecular weight distribution (M_n = 21600, M_w/M_n = 1.27) after transesterification. Thus, acrylate-selective transesterification of a DMA/MA random copolymer was successfully achieved with Ti(O*i*-Pr)$_4$ and BzOH.

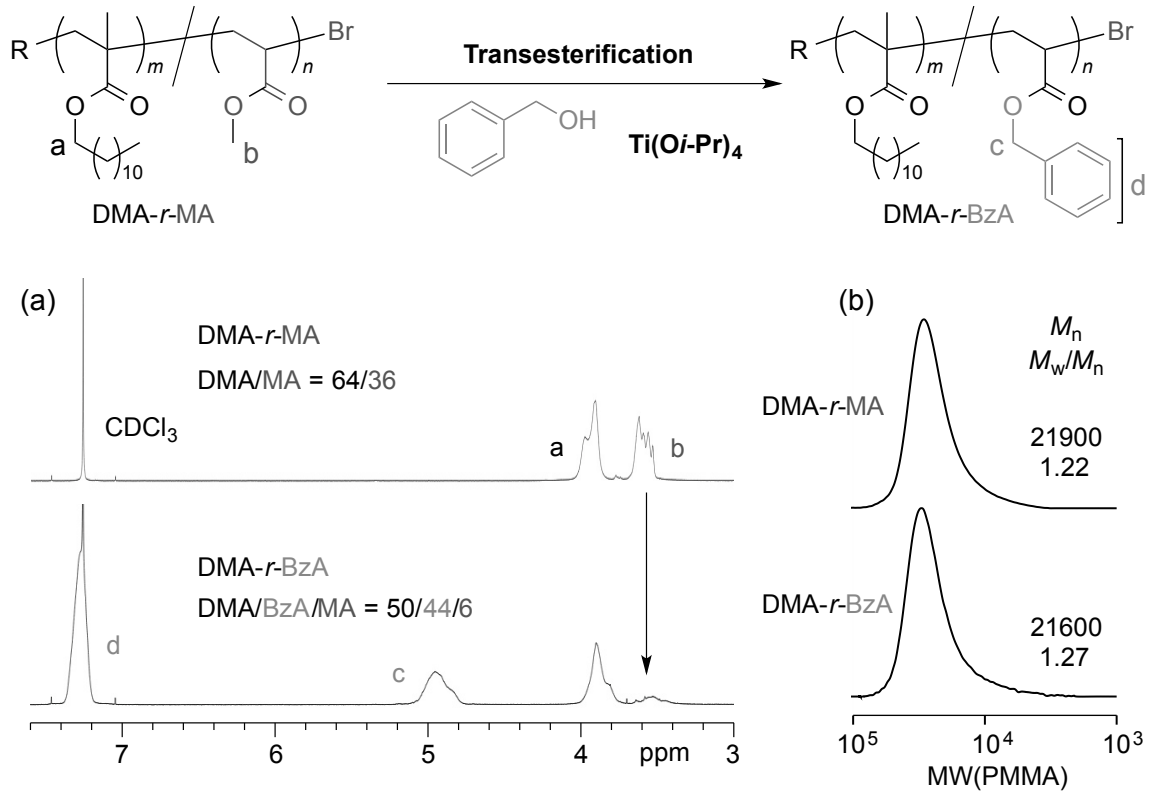

Figure 5. Transesterification of DMA/MA random copolymer with Ti(O*i*-Pr)$_4$ and benzyl alcohol: [MMA-*r*-MA]/[Ti(O*i*-Pr)$_4$] = 10/160 mM with MS 4A (0.33 g/mL) in anisole/benzyl alcohol (1/1, v/v) at 130 ^oC. (a) ^1H NMR spectra ([polymer] = 10 mg/mL in $CDCl_3$ at 25 ^oC) and (b) SEC curves of DMA-*r*-MA and the product.

Conclusion

Acrylate-selective transesterification of methacrylate/methyl acrylate random copolymers were developed as a novel post-functionalization technique. Importantly, this system allows efficient and site-selective transformation of copolymers just using a common methyl acrylate as a selective transforming site though efficient post-functionalization of poly(meth)acrylates often requires activated esters as monomers. This acrylate-selective transesterification no doubt opens new avenue to design and synthesize various functional polymers with diverse alcohols, far more efficiently and conveniently than conventional post-functionalization methodologies.

References

(1) Iha, R. K.; Wooley, K. L.; Nyström, A. M.; Burke, D. J.; Kade, M. J.; Hawker, C. J. *Chem. Rev.* **2009**, *109*, 5620-5686.

(2) Lyu, S-P.; Cernohous, J. J.; Bates, F. S.; Macosko, C. W. *Macromolecules* **1999**, *32*, 106-110.

(3) Kessler, D.; Theato, P. *Langmuir* **2009**, *25,* 14200-14206.

(4) Roth, P. J.; Jochum, F. D.; Romina Forst, F.; Zentel, R.; Theato, P. *Macromolecules* **2010**, *43*, 4638-4645.

(5) Bobade, S.; Wang, Y.; Mays, J.; Baskaran, D. *Macromolecules* **2014**, *47*, 5040-5050.

(6) Munteanu, M.; Choi, S.; Ritter, H. *Macromolecules* **2008**, *41*, 9619-9623.

(7) Huang, J.; Habraken, G.; Audouin, F.; Heise, A. *Macromolecules* **2010**, *43*, 6050-6057.

(8) Xu, L. Q.; Pranantyo, D.; Neoh, K-G.; Kang, E-T. *ACS Sustainable Chem. Eng*. **2016**, *4*, 4264-4272

(9) Han Shih, H.; Greene, T.; Korc, M.; Lin, C-C. *Biomacromolecules* **2016**, *17*, 3872-3882.

(10) Delaittre, G.; Pauloehrl, T.; Bastmeyer, M.; Barner-Kowollik, C. *Macromolecules* **2012**, *45*, 1792-1802.

(11) Xu, J.; Boyer, C. *Macromolecules* **2015**, *48*, 520-529.

(12) Altintas, O.; Barner-Kowollik, C. *Macromol. Rapid. Commun.* **2012**, *33*, 958-971.

(13) Hosono, N.; Gillissen, M. A. J.; Li, Y.; Sheiko, S. S.; Palmans, A. R. A.; Meijer, E. W. *J. Am. Chem. Soc.* **2013**, *135*, 501-510.

(14) Mavila, S.; Eivgi, O.; Berkovich, I.; Lemcoff, N. G. *Chem. Rev.* **2016**, *116*, 878-961.

(15) Terashima, T. *Polym. J.* **2014**, *46*, 664-673.

(16) Cheng, G.; Bo1ker, A.; Zhang, M.; Krausch, G. Müller, A. H. E. *Macromolecules* **2001**, *34*, 6883-6888.

(17) Miura, Y.; Satoh, K.; Kamigaito, M.; Okamoto, Y.; Kaneko, T.; Jinnai, H.; Kobukuta, S. *Macromolecules* **2007**, *40*, 465-473.

(18) Collins, S.; Peace, S. K.; Richards, R. W.; MacDonald, W. A.; Mills, P.; King, S. M. *Macromolecules* **2000**, *33*, 2981-2988.

(19) Kamber, N. E.; Jeong, W.; Waymouth, R. M.; Pratt, R. C.; Lohmeijer, B. G. G.; Hedrick, J. L. *Chem. Rev.* **2007**, *107*, 5813-5840.

(20) Alvès, M-H.; Riondel, A.; Paul, J-M.; Birot, M.; Deleuze, H. C. R. Chimie. **2010**, *13*, 1301-1307.

(21) (a) Das, A.; Theato, P. *Chem. Rev.* **2016**, *116*, 1434-1495. (b) Theato, P. *J. Polym. Sci. Part A: Polym. Chem.* **2008**, *46*, 6677–6687. (c) Das, A.; Theato, P. *Macromolecules* **2015**, *48*, 8695-8707. (d) Théato, P.; Zentel, R. *Langmuir* **2000**, *16,* 1801-1805.

(22) (a) Nakatani, K.; Ogura, Y.; Koda, Y.; Terashima, T.; Sawamoto, M. *J. Am. Chem. Soc.* **2012**, *134*, 4373−4383. (b) Ogura, Y.; Terashima, T.; Sawamoto, M. *J. Am. Chem. Soc.* **2016**, *138*, 5012−5015.

(23) Otera, J. *Chem. Rev.* **1993**, *93*, 1449-1470.

LIST OF PUBLICATIONS

Part I

Chapter 1

Ogura, Y.; Terashima, T.; Sawamoto, M.

Synchronized Tandem Catalysis of Living Radical Polymerization and Transesterification: Methacrylate Gradient Copolymers with Extremely Broad Glass Transition Temperature.

ACS Macro Lett. **2013**, *2*, 985−989.

Chapter 2

Ogura, Y.; Terashima, T.; Sawamoto, M.

Amphiphilic PEG-Functionalized Gradient Copolymers via Tandem Catalysis of Living Radical Polymerization and Transesterification.

Macromolecules **2017** *in press.*

Chapter 3

Ogura, Y.; Artar, M.; Palmans, A. R. A.; Sawamoto, M.; Meijer, E. W.; Terashima, T.

Self-Assembly of Hydrogen-Bonding Gradient Copolymers: Sequence Control via Tandem Living Radical Polymerization with Transesterification

Macromolecules submitted.

Chapter 4

Ogura, Y.; Terashima, T.; Sawamoto, M.

Synthesis of Fluorinated Gradient Copolymers via In-Situ Transesterification with Fluoroalcohols in Tandem Living Radical Polymerization

Polym. Chem., submitted.

(Chapter 4 is the unedited Author's version of a Submitted Work that will be accepted for publication after peer review.)

Chapter 5

Ogura, Y.; Terashima, T.; Sawamoto, M.

Fluorous Gradient Copolymers via Tandem Living Radical Polymerization with In-Situ Transesterification of a Perfluoroalkyl Methacrylate

to be submitted.

(Chapter 5 is the Author's version of an Unsubmitted Work that will be submitted for publication.)

PART II

Chapter 6

Ogura, Y.; Terashima, T.; Sawamoto, M.

Terminal-Selective Transesterification of Chlorine-Capped Poly(Methyl Methacrylate)s: A Modular Approach to Telechelic and Pinpoint-Functionalized Polymers

J. Am. Chem. Soc. **2016**, *138*, 5012−5015.

(Chapter 6 is the unedited Author's version of a Submitted Work that was subsequently accepted for publication in *J. Am. Chem. Soc.*, copyright © American Chemical Society after peer review. To access the final edited and published work see the following website: http://pubs.acs.org/doi/abs/10.1021/jacs.6b01239)

Chapter 7

Ogura, Y.; Terashima, T.; Sawamoto, M.

Tandem Terminal-Selective Transesterification and Cyclization of Bromine-Capped Polymethacrylates for Halogen-Free Telechelic Polymers

to be submitted.

(Chapter 7 is the Author's version of an Unsubmitted Work that will be submitted for publication.)

Chapter 8

Ogura, Y.; Terashima, T.; Sawamoto, M.

Acrylate-Selective Transesterification of Methacrylate/Acrylate Copolymers: A New Avenue in Post-Functionalization

to be submitted.

(Chapter 8 is the Author's version of an Unsubmitted Work that will be submitted for publication.)

Other Publications

1 "Sequence-Regulated Copolymers via Tandem Catalysts of Living Radical Polymerization and In Situ Transesterification"

Kazuhiro Nakatani, Yusuke Ogura, Yuta Koda, Takaya Terashima, and Mitsuo Sawamoto

J. Am. Chem. Soc. **2012**, *134*, 4373–4383.

ACKNOWLEDGMENTS

This thesis presents the research that the author carried out from 2011 to 2017 at the Department of Polymer Chemistry, Graduate School of Engineering, Kyoto University under the direction of Professor Mitsuo Sawamoto and Assistant Professor Takaya Terashima.

First of all, the author would like to express his sincere gratitude to Professor Mitsuo Sawamoto, Assistant Professor Takaya Terashima and Associate Professor Makoto Ouchi for their continuous guidance, support and encouragement through this work.

The author also acknowledges his appreciation to Professor Yoshiki Chujo and Professor Mikihito Takenaka for careful reviews of this thesis and valuable comments.

The author would like to offer sincere thanks to Dr. Yusuke Hibi (Tokyo Institute of Technology), Dr. Yuta Koda (Kyoto University) for their kind support and significant discussion in this research.

Most importantly, the author greatly appreciates the kind hosting, support and valuable suggestion from Professor E. W. Meijer (Eindhoven University of Technology, Netherlands) for his studies in *Chapter 3*. During his precious ten-week stay at Eindhoven (October to December, 2014), Dr. Müge Artar, Dr. Anja R. A. Palmans and all members in Meijer group also kindly supported the author for daily life as well as his research, so that the author also wishes to express his thank to them for their kindness and friendship.

Furthermore, the author is particularly grateful to Dr. Keita Nishizawa, Dr. Kojiro Fujimura, Mr. Sho Kitagawa, Mr. Takanori Sugita and Mr. Hajime Kammiyada for their encouragement. The author also wishes to his thanks to his colleagues for useful suggestion and the pleasant days in Sawamoto group: Dr. Sang-Ho Lee, Ms. Minami Kawabe, Mr. Akito Konishi, Ms. Natsuki Naruse, Mr. Shunsuke Konoike, Mr. Tomoya Nakanishi, Ms. Saki, Nishimura, Mr. Tadashi Miyazaki, Mr. Hirotomo Ono, Mr. Kohei Kuraoka, Mr. Sinya Tsuji, Mr. Songyuan Tian, Mr. Kazuma Matsumoto, Mr. Yuichiro Miyabara, Mr. Takahiro Konishi, Ms. Ayaka Suzuki, Ms. Chitose Nagao, Ms. Marina Nakano, Mr. Yuji Hirai, Ms. Xiaonan Liang, Mr. Yusuke Azuma, Mr. Dong-Young Oh, Mr. Yoshihiko Kimura, Ms. Kana Nishimori, Ms. Mayuko Matsumoto, Mr. Taizo Yamamoto, Mr. Shota Imai, Mr. Yuki Kametani, Ms. Reina Kojima, Ms. Yuki Sano, Mr. Goki Hattori, Mr. Daiki Ito, Mr. Sho Kambayashi, Mr. Motoki Shibata, Mr. Masaya Murata, Mr. Sho Yoshida, Dr. Tomohiro Seki, Mr. Shingo Okuno, Dr. Kiyomi Fuchigami, Dr. Paul Philip Brooks, Dr. Elijah Baruch Bültz and all friends. The author is also obliged to Ms. Miro Takayama for her kind assistance during the author's school life.

The author also would like to express his appreciation to Professor Yoshio Okamoto (Harbin Engineering University), Professor Eiji Yashima (Nagoya University), Professor Sadahito Aoshima (Osaka University), Professor Masami Kamigaito (Nagoya University), Professor Shokyoku Kanaoka (the University of Shiga Prefecture), Associate Professor Kotaro Satoh (Nagoya University), Associate Professor Tsuyoshi Ando (Nara Institute of Science and Technology), Assistant Professor Arihiro Kanazawa (Osaka University), Assistant Professor Shohei Ida (the University of Shiga Prefecture), Assistant Professor Mineto Uchiyama (Nagoya University), Dr. Takamasa Soejima, Dr. Ryohei Saitoh, Dr. Tomoya Yoshizaki and all "ORION" members for their meaningful discussion and kind encouragement.

The author also appreciates Dr. Takayuki Nakamura and Mr. Ikuo Yamamoto (Daikin Industries, Ltd.) for measurement, analysis, and precious discussion about fluorous gradient copolymers in *Chapter 5*.

The author is grateful to the Japan Society for the Promotion of Sciences (JSPS) for JSPS Research Fellowships and a Grant-in-Aid for JSPS Fellows (DC2: 26-2677) from April 2014 to March 2016.

Finally, the author would like to express his deep appreciation to his parents Mr. Tetsuzo Ogura, Mrs. Sumiko Ogura, his brother Mr. Tomoki Ogura and all other his family members for their constant care and encouragement.

March, 2017

Yusuke Ogura

Department of Polymer Chemistry
Graduate School of Engineering
Kyoto University